ABSTRACT

Title of dissertation:	CYCLIC PURSUIT: SYMMETRY, REDUCTION AND NONLINEAR DYNAMICS
	Kevin Galloway, Doctor of Philosophy, 2011
Dissertation directed by:	Professor P.S. Krishnaprasad Department of Electrical and Computer Engineering Dr. Eric W. Justh Naval Research Laboratory

In this dissertation, we explore the use of pursuit interactions as a building block for collective behavior, primarily in the context of constant bearing (CB) cyclic pursuit. Pursuit phenomena are observed throughout the natural environment and also play an important role in technological contexts, such as missile-aircraft encounters and interactions between unmanned vehicles. While pursuit is typically regarded as adversarial, we demonstrate that pursuit interactions within a cyclic pursuit framework give rise to seemingly coordinated group maneuvers.

We model a system of agents (e.g. birds, vehicles) as particles tracing out curves in the plane, and illustrate reduction to the shape space of relative positions and velocities. Introducing the CB pursuit strategy and associated pursuit law, we consider the case for which agent i pursues agent $i+1$ (modulo n) with the CB pursuit law. After deriving closed-loop cyclic pursuit dynamics, we demonstrate asymptotic convergence to an invariant submanifold (corresponding to each agent attaining the CB pursuit strategy), and proceed by analysis of the reduced dynamics

restricted to the submanifold. For the general setting, we derive existence conditions for relative equilibria (circling and rectilinear) as well as for system trajectories which preserve the shape of the collective (up to similarity), which we refer to as pure shape equilibria. For two illustrative low-dimensional cases, we provide a more comprehensive analysis, deriving explicit trajectory solutions for the two-particle "mutual pursuit" case, and detailing the stability properties of three-particle relative equilibria and pure shape equilibria. For the three-particle case, we show that a particular choice of CB pursuit parameters gives rise to remarkable almost-periodic trajectories in the physical space. We also extend our study to consider CB pursuit in three dimensions, deriving a feedback law for executing the CB pursuit strategy, and providing a detailed analysis of the two-particle mutual pursuit case.

We complete the work by considering evasive strategies to counter the motion camouflage (MC) pursuit law. After demonstrating that a stochastically steering evader is unable to thwart the MC pursuit strategy, we propose a (deterministic) feedback law for the evader and demonstrate the existence of circling equilibria for the closed-loop pursuer-evader dynamics.

CYCLIC PURSUIT: SYMMETRY, REDUCTION AND NONLINEAR DYNAMICS

by

Kevin Galloway

Dissertation submitted to the Faculty of the Graduate School of the
University of Maryland, College Park in partial fulfillment
of the requirements for the degree of
Doctor of Philosophy
2011

Advisory Committee:
Professor P.S. Krishnaprasad, Chair/Advisor
Dr. Eric W. Justh, Co-Advisor
Professor André Tits
Professor Nuno Martins
Professor Derek Paley
Professor Raymond Adomaitis

© Copyright by
Kevin Galloway
2011

Dedication

To my parents,

whose faithful prayers and encouragement

have been a constant source of strength

Acknowledgments

First, I am very grateful to my advisor Professor P.S. Krishnaprasad, who has served as a role model and mentor in the truest meaning of the words. His enjoyment of teaching and scientific discovery has inspired me and proven rather infectious, and I have learned from him that you can whistle while "working in the salt mines". I am also deeply indebted to my co-advisor Dr. Eric Justh, who sacrificed every Friday evening to listen to my research ideas and provide invaluable feedback. I'm grateful for his painstaking review of many laborious trigonometric calculations and his remarkable ability to locate even the smallest of errors.

I would like to thank Professor André Tits, Professor Nuno Martins, Professor Derek Paley, and Professor Raymond Adomaitis for serving on my dissertation committee and providing constructive feedback and comments.

The staff of the Institute for Systems Research has provided outstanding support, and I would particularly like to acknowledge Ms. Pam White, Ms. Alexis Jenkins, Ms. Regina King and Ms. Beverly Dennis.

I would like to thank the many friends and colleagues who have provided encouragement along the way and made the journey enjoyable. Special thanks are in order for the fellow members of the Intelligent Servosystems Laboratory, who supplied feedback, engaged in stimulating discussion, and enjoyed talking over cups of (sometimes free) coffee. I'm particularly thankful to Matteo Mischiati, Biswadip Dey, Ben Flom and Viswa Reddy, who shared significant portions of my trek.

I gratefully acknowledge the financial support I received during my graduate studies from the Air Force Office of Scientific Research under AFOSR Grant Nos. FA95500410130, FA9550710446 and FA95501010250; from the Army Research Office under ARO Grant No. W911NF0610325; from the Army Research Office under ODDR&E MURI01 Program Grant No. DAAD19-01-1-0465 to the Center for Communicating Networked Control Systems (through Boston University); from NIH-NIBIB grant 1 R01 EB004750-01, as part of the NSF/NIH Collaborative Research in Computational Neuroscience Program; from the ODDR&E MURI2007 Program Grant N000140710734 (through the Office of Naval Research); from L-3 Communications; and from the Office of Naval Research.

Finally, thank you to my Savior, the fount of joy and the lifter of my head.

Table of Contents

List of Figures

List of Abbreviations and Notation

Pursuit Strategies

CB	Constant Bearing
α_i	CB Pursuit Angle (planar version) for agent i
a_i	CB Pursuit Parameter (3-D version) for agent i
Λ_i	CB Pursuit cost function for agent i
CP	Classical Pursuit
MC	Motion Camouflage

System Model

$\mathbf{r}_i$	Position of agent i
$\mathbf{r}_{i,i+1}$	$\mathbf{r}_i - \mathbf{r}_{i+1}$ (with index addition modulo n)
$\{\mathbf{x}_i, \mathbf{y}_i\}$	(planar) Natural Frenet Frame for agent i
$\{\mathbf{x}_i, \mathbf{y}_i, \mathbf{z}_i\}$	(3-D) Natural Frenet Frame for agent i
ν_i	Speed of agent i

Lie Groups and Manifolds

$SE(n)$	Special Euclidean group
$SO(n)$	Special Orthogonal group
S^1	Circle group
$\mathfrak{se}(n)$	Lie Algebra of Special Euclidean group $SE(n)$
M_{state}	State manifold
M_{shape}	Shape manifold ($\cong M_{state}/SE(2)$)
$\tilde{M}_{shape}$	Pure Shape manifold ($\cong M_{shape}/\mathbb{R}^+$)
$M_{CB(\boldsymbol{\alpha})}$	CB Pursuit manifold (planar version)
$\tilde{M}_{CB(\boldsymbol{\alpha})}$	CB Pursuit Pure Shape manifold ($\cong M_{CB(\boldsymbol{\alpha})}/\mathbb{R}^+$)
$M_{CB(\mathbf{a})}$	CB Pursuit manifold (3-D version)

Miscellaneous

CW	Clockwise
CCW	Counter-clockwise
$R(\theta)$	CCW rotation by θ radians in the plane
$\mathbf{a}^\perp$	the vector $\mathbf{a}$ rotated CCW by $\pi/2$ radians

Chapter 1

Introduction

1.1 Background

Nature abounds with the phenomenon of pursuit and evasion. In some instances pursuit and evasion is a matter of survival, as the predator seeks to capture its next meal and the quarry attempts to avoid such a fate by maneuver, stealth, or defense. In some cases, pursuit and evasion is part of a mating ritual in which reproduction, not sustenance, is the pursuer's goal. And in other cases, pursuit and evasion is simply a part of animal play behavior, often serving as a training ground for more perilous encounters.

Pursuit also plays a significant role in the vehicular setting, as in military encounters between planes and missiles or between adversarial unmanned vehicles. This context presents compelling reasons to develop control strategies which optimize certain aspects of the pursuit-evasion encounter. For instance, a pursuer may want to minimize capture time or steering requirements (i.e. fuel expenditure); an evader may seek to maneuver in such a way as to maximize time to capture (or evade capture altogether) or to maximize the effective coverage area of some type of defensive weapon.

The study of pursuit and evasion has fascinated mathematicians for centuries. While the study of pursuit may date as far back as Leonardo Da Vinci, it was the French hydrographer and mathematician Pierre Bouguer (1698-1758) who ignited modern interest in the subject by solving for the "pursuit curve" traced out by a naval vessel pursuing an evader which flees in a straight line[2]. Interest in the subject continued as various mathematicians proposed variations on this theme, mostly focused on deriving pursuit curves for more complex evader trajectories. While most of these problems could best be described as pursuer-pursuee engagements, a rather original game-theoretic approach was developed by Isaacs in the 1960's, which addressed adversarial pursuer-evader encounters[23]. This differential games approach described "optimal" strategies for each player as well as the curves traced out under optimal play. Military applications have also driven the development of an extensive literature on missile guidance in a pursuit-evasion context [51, 44].

In considering a control-theoretic study of pursuit, it is important to distinguish between *pursuit strategies* and the particular feedback control laws used to execute those strategies. Pursuit strategies are specifications of a desired geometry for the encounter, usually expressed in terms of relative velocities, headings, and ranges. These strategies then lend themselves to the construction of pursuit manifolds which are characterized by the specified geometry, and the effectiveness of an associated *pursuit law* can then be assessed in terms of the properties of the associated pursuit manifold (such as invariance, accessibility, stability) under the closed-loop system dynamics. In [57], the authors describe the *classical pursuit (CP) strategy* and the *constant bearing (CB) pursuit strategy*, and derive biologically plausible CP and CB pursuit laws (in the plane) which serve as a basis for much of the work in this thesis. The CP strategy corresponds to our most intuitive notion of pursuit, and prescribes that the pursuer should always move directly toward the current position of the evader. The CB strategy extends CP by prescribing a fixed, possibly non-zero angular offset between the pursuer's heading and the direction to the evader. We present a more precise definition of these strategies and associated pursuit laws in section 2.3. The *motion camouflage (MC) pursuit strategy* is a stealthy pursuit strategy observed in nature, in which the pursuer attempts to maneuver so as to minimize the perceived relative motion from the standpoint of the pursuee. A pursuit law for attainment of the MC strategy is developed in [27] and figures prominently in chapters 5 and 6.

Though pursuit is often thought of as a competitive or adversarial phenomenon, we will demonstrate that pursuit can also serve as a building block for collective behavior. The last twenty years has seen a surge of research interest in the analysis and synthesis of collective behavior, in biological fields as well as in engineering. With regards to analysis, researchers have attempted to identify the mechanisms underlying various exhibits of collective behavior observed in nature, such as the remarkable flocking maneuvers of starlings [13], the schooling behaviors exhibited in marine environments [45], and the swarming of insects such as locusts [9]. Typically, it is hypothesized that relatively simple local interactions between nearest neighbors (with respect to some metric) are responsible for generating the observed emergent global behavior. As an example, Bruckstein showed that a trail of ants can iteratively straighten a path between an anthill and a food source by the simple strategy of following directly toward the immediate leader ant on the path [7].

In regards to synthesis of collective behavior, researchers in the controls and robotics communities have developed a number of methods for designing and implementing “cooperative control” [43, 32, 25, 24]. With applications including search and rescue, military surveillance, highway automation, and air traffic control, cooperative control provides a promising approach to developing robust and scalable solutions.

A major contribution of this thesis is to demonstrate that relatively simple unidirectional CB pursuit interactions executed in a cyclic pursuit framework give rise to a remarkably rich display of group trajectories, supporting the claim that pursuit can serve as an effective building block for collective behavior. *Cyclic pursuit* refers to the phenomenon in which agent i pursues agent $i+1$, modulo n, where n denotes the total number of agents. On one hand, our study falls primarily under the analytical approach to collective behavior, as we consider the closed-loop dynamics associated with a cyclic CB pursuit system and employ tools of symmetry, reduction, and nonlinear analysis to characterize the existence and stability properties of particular emergent behaviors such as relative equilibria and shape-preserving spiral motions. On the other hand, cyclic CB pursuit presents the designer with n CB angle parameters which can be used to select a desired steady-state system behavior, and therefore our work also provides a tool for synthesizing collective behavior.

Original studies of cyclic pursuit were driven primarily by mathematical curiosity, beginning with the question Edouard Lucas posed in 1877, which asked what trajectories would be traced out by three "dogs" which started at the vertices of an equilateral triangle and pursued one another at a constant speed. (See [50] for a historical summary of the cyclic pursuit problem.) From Brocard's original answer (the dogs trace out logarithmic spirals and meet at a common point) to the variations that have been proposed (three dogs – or "bugs" – on a non-equilateral triangle, n bugs on a regular polygon, etc.), the problem has traced out its own interesting history [30, 50, 8]. More recently, there has been a growing interest in the occurrence of *network motifs* in biological systems (e.g. gene regulation, food webs, etc.), of which the *cycle motif* (or *feedback motif*) serves as an example [38, 58, 1]. One such illustration of the cycle motif is provided by [12], where the authors demonstrate that the cycle motif can be used at the biomolecular level to engineer an oscillatory network, which they term the *repressilator*. A current discussion surrounding network motifs centers on the question of whether the characterization of network architecture in terms of the statistical description of motif occurrence can truly provide significant insights into system behavior apart from an understanding of the relevant parameters and dynamics which govern the interactions across the network [22]. *Thus it is of interest that in the current work a single motif (the cycle motif) gives rise to a wide array of diverse system behaviors, strongly dependent on the choice of CB angle parameters.*

More recent work on cyclic pursuit from a control-theoretic perspective has been spurred by an interest in synthesizing collective behavior for a group of autonomous agents. An initial formulation in terms of linear dynamics was presented by Lin, Broucke and Francis in [33]. Marshall, Broucke and Francis then presented a subsequent formulation in terms of wheeled vehicles (modeled as kinematic unicycles) engaged in cyclic (classical) pursuit, with steering control governed by linear feedback on the heading error[36]. The authors classified the possible equilibrium formations (which are all regular polygons) and provided a local stability analysis based on linearization of the relative dynamics. In [37], the same authors extended their analysis to the case where vehicle speeds were also variable and governed by linear feedback on the intervehicle range, once again characterizing the stability of equilibrium formations in terms of the ratio of the two control gains (i.e. speed and steering). In [52], Sinha and Ghose generalized these results to heterogeneous formations of agents with differing speeds and controller gains. A novel hierarchical approach to cyclic pursuit was also presented by Smith, Broucke and Francis in [53], in which subgroups of agents engaged in cyclic pursuit within group, pursue other subgroups in a cyclic fashion.

While the previous references all dealt with cyclic *classical* pursuit, Pavone and Frazzoli introduced a formulation of cyclic constant bearing pursuit in [46], in which Hilare-type mobile robots employ CB pursuit with a *common* CB angle parameter. After using output feedback linearization about a "hand" position to transform the system into normal form, the authors prove global stability of certain equilibrium formations. Ramirez-Riberos, Pavone and Frazzoli also present a three-dimensional formulation of cyclic CB pursuit in terms of single-integrator and double-integrator linear dynamics in [47].

1.2 Overview

Chapter 2 begins with a general development of our framework for modeling n particles (agents) interacting in the plane, in terms of the natural Frenet frame equations as well as the corresponding Lie group formulation. We then outline a symmetry reduction to the $3n - 3$ dimensional shape space, the space of relative positions and velocities, and present a particular parametrization of the shape space in terms of $3n$ scalar variables with three algebraic constraint equations. Having described the general formulation, we proceed by prescribing a particular pursuit strategy (CB pursuit), a pursuit law (2.60), and a pursuit graph (cycle), which combine to yield the cyclic CB pursuit dynamics (2.61) that form the basis for the subsequent analysis. Key results are then presented in **Propositions 2.3.2, 2.4.1**, and **2.4.2**, where we first prove asymptotic convergence to an invariant submanifold and then derive existence conditions for relative equilibria and "pure shape equilibria" in terms of the reduced dynamics on the submanifold.

In chapter 3, we present a characterization and stability analysis for two illuminating low-dimensional cases: the $n = 2$ "mutual pursuit" case, and three-particle cyclic CB pursuit. These low-dimensional examples permit tractable analysis while providing helpful insights into the behavior of cyclic pursuit systems. In the two-particle case, a change of variables renders the shape dynamics integrable, and we derive closed-form expressions which describe system evolution on the full shape space. We also solve the reconstruction problem on the invariant submanifold by deriving a closed-form expression for the motion of the center of mass. In the three-particle case, a further reduction to two-dimensional "pure shape" dynamics enables phase portrait analysis and a subsequent characterization of stability properties for rectilinear equilibria, circling equilibria, and "pure shape equilibria" on the invariant submanifold. In the course of studying three-particle rectilinear equilibria, we show that a particular choice of constant bearing angle parameters results in a conservative system, with corresponding trajectories in the physical space which display remarkable quasi-periodic precessing behavior. The chapter ends with a full characterization of the three-particle symmetric case, in which each agent employs the CB pursuit law with the same CB angle parameter α.

In chapter 4, we extend the concept of the constant bearing pursuit strategy to the three-dimensional setting, and propose a new three-dimensional CB pursuit law for executing the strategy. The three-dimensional CB pursuit strategy is fundamentally different from the planar strategy, in that the planar strategy prescribes both a constant bearing angular offset and a particular direction (i.e. counterclockwise), while the 3-D strategy prescribes only the angular offset. In the context of cyclic CB pursuit, we prove asymptotic convergence to an invariant submanifold and derive the associated reduced dynamics (4.21) on the submanifold. We then provide a complete characterization of the two-particle mutual CB pursuit system, deriving closed-form expressions for the particle trajectories in $\mathbb{R}^3$, and present existence conditions for relative equilibria for the general n-particle case.

Chapter 5 signals a shift from examining cyclic pursuit to studying pursuit in its more traditional adversarial setting. Here we consider motion camouflage in the stochastic setting, considering the case for which the evader employs a stochastic steering process[14]. After reviewing a mathematical formulation for motion camouflage and an associated feedback law (from [27]), we then develop the associated stochastic differential equations (SDEs) for the system with stochastically steering evader, and prove a proposition (**5.3.2**) concerning accessibility of motion camouflage (for the pursuer) under appropriate assumptions. This result, which is analogous to the finite-time accessibility result from the deterministic case (see Proposition 3.3 in [27]), demonstrates that the motion camouflage pursuit law proves effective even when the evader uses a randomized steering control. We complete the chapter by considering families of admissible stochastic evader controls, and present a method (based on Poisson counters) for emulating the "run-and-tumble" stochastic steering process of bacterial chemotaxis.

Having demonstrated certain aspects of the effectiveness of the motion camouflage pursuit law, we turn in chapter 6 to the question of how an evader might best counter the strategy. A proposed cost function provides the intuition for deriving a suitable "Anti-MC" feedback law for the evader, which is designed to increase pursuer-evader separation and force rotation of the "baseline vector" which relates the pursuer and evader positions. The rest of the chapter is spent analyzing the closed-loop "MC vs. Anti-MC" pursuer-evader dynamics, which yield both rectilinear and circling relative equilibria. We present existence conditions and stability characterization for the relative equilibria, and demonstrate that asymptotically stable circling equilibria exist even in some cases for which the pursuer has a speed advantage and a higher control gain. Since circling equilibria can be viewed as a "stand-off" condition and thus advantageous to the evader, we suggest that the

"Anti-MC" evasion law may serve as an effective counter-strategy to motion camouflage pursuit.

1.3 Preliminaries

1.3.1 Notions of invariance

Here we define several notions of invariance that will be used in this thesis. The first notion of invariance is used in section 2.2.2 in the context of reduction from the state space to the "shape space", and can be found in [35].

Definition 1.3.1 Given a Lie group G, let $L_g : G \longrightarrow G,\ h \longmapsto g \cdot h$ denote the left translation by g, for any $g, h \in G$, and let $T_h L_g : T_h G \longrightarrow T_{gh} G$ denote the linearization of the translation map L_g. Then a vector field X on G is a *left-invariant vector field* if

$$(T_h L_g)(X(h)) = X(gh) \tag{1.1}$$

for every $h \in G$. If a vector field is defined in terms of a feedback control law $u(t)$, we say that *the control law is G-invariant* if it renders the closed-loop vector field left-invariant.

The following notion of invariance figures prominently in the description of the CB Pursuit Manifold in section 2.3.

Definition 1.3.2 Given a manifold M and a vector field X on M, we say that *the manifold M is invariant under the vector field X* if X is tangent to M.

This definition implies that trajectories of the dynamics $\dot{m} = X(m)$ which start on M at time t_0 will remain on M for all times $t > t_0$.

1.3.2 Rotations and rigid motions in the plane

Throughout this thesis we will work with rotations and rigid motions in the plane. For any $\theta \in [0, 2\pi)$, we let $R(\theta)$ denote the 2×2 *rotation matrix* defined by

$$R(\theta) = \begin{pmatrix} \cos(\theta) & -\sin(\theta) \\ \sin(\theta) & \cos(\theta) \end{pmatrix}, \tag{1.2}$$

which acts on two-vectors by rotating them counter-clockwise in the plane through an angle of θ radians. One can readily verify that the group of 2×2 rotation matrices is isomorphic to $SO(2)$, abelian (but $SO(n)$ is not abelian for $n > 2$), and satisfies the following properties:

$$R(\theta_1)R(\theta_2) = R(\theta_1 + \theta_2), \tag{1.3}$$

$$R^{-1}(\theta) = R^T(\theta) = R(-\theta), \tag{1.4}$$

$$R(\theta \pm \pi) = -R(\theta), \tag{1.5}$$

$$|R(\theta)\mathbf{a}| = |\mathbf{a}|\,,\ \forall \mathbf{a} \in \mathbb{R}^2, \tag{1.6}$$

$$R(\theta) + R(-\theta) = 2\cos(\theta)\mathbb{1}. \tag{1.7}$$

(The proof of properties (1.3)-(1.7) follows in a straightforward fashion from (1.2).) In addition, the following are equivalent:

i. The null space of the matrix $[R(2\theta) - I]$ is nontrivial,

ii. $R(2\theta) = I$

iii. $\sin(\theta) = 0.$ (1.8)

(The proof of (1.8) is given in appendix A.) If the rotation angle $\theta = \theta(t)$ is time-varying, then the derivative of the corresponding rotation matrix is given by

$$
\begin{aligned}
\frac{d}{dt}\Big(R(\theta)\Big) &= \frac{d}{dt}\begin{pmatrix} \cos(\theta) & -\sin(\theta) \\ \sin(\theta) & \cos(\theta) \end{pmatrix} \\
&= \dot{\theta}\begin{pmatrix} -\sin(\theta) & -\cos(\theta) \\ \cos(\theta) & -\sin(\theta) \end{pmatrix} \\
&= \dot{\theta}\begin{pmatrix} \cos(\theta+\pi/2) & -\sin(\theta+\pi/2) \\ \sin(\theta+\pi/2) & \cos(\theta+\pi/2) \end{pmatrix} \\
&= \dot{\theta}R(\theta+\pi/2).
\end{aligned} \tag{1.9}
$$

It is frequently necessary to use the counterclockwise rotation by $\pi/2$ radians, and therefore for any $\mathbf{a} \in \mathbb{R}^2$ we define the notation

$$\mathbf{a}^{\perp} \triangleq R(\pi/2)\mathbf{a}. \tag{1.10}$$

Application of (1.3), (1.4), and (1.5) yields the inner product identity (for any

$\mathbf{a}, \mathbf{b} \in \mathbb{R}^2$)

$$\mathbf{a}^{\perp} \cdot \mathbf{b} = \mathbf{a}^T R^T(\pi/2)\mathbf{b} = \mathbf{a}^T R(-\pi/2)\mathbf{b} = \mathbf{a}^T R(\pi/2 - \pi)\mathbf{b} = -\mathbf{a}^T R(\pi/2)\mathbf{b} = -\mathbf{a} \cdot \mathbf{b}^{\perp}. \tag{1.11}$$

The rigid motion group $SE(2)$ describes rotations and translations in the plane, with elements of the form

$$h_i = \begin{pmatrix} B_i & \mathbf{q}_i \\ 0\,0 & 1 \end{pmatrix}, \tag{1.12}$$

where $B_i \in SO(2)$ and $\mathbf{q}_i \in \mathbb{R}^2$. For $h_1, h_2, \ldots, h_k \in SE(2)$, we let $\prod_{i=1}^{k} h_i = h_1 h_2 \cdots h_k$ denote the *ordered* product of $SE(2)$ elements, which simplifies to

$$\prod_{i=1}^{k} h_i = \begin{pmatrix} \prod_{j=1}^{k} B_j & \mathbf{q}_1 + \sum_{i=1}^{k-1} \left(\prod_{j=1}^{i} B_j \right) \mathbf{q}_{i+1} \\ 0 \quad 0 & 1 \end{pmatrix}, \; k \geq 2. \tag{1.13}$$

(See appendix A for a proof of (1.13).)

Chapter 2

Planar cyclic CB pursuit for n agents

2.1 Introduction

We begin our discussion of cyclic pursuit[1] by formulating a model to describe the movement of n agents interacting in the plane. Previous work on cyclic pursuit, such as that presented in [33, 53], was based on a single-integrator model

$$\dot{\mathbf{r}}_i = \mathbf{u}_i, \; i = 1, 2, \ldots, n, \tag{2.1}$$

where the vector $\mathbf{r}_i$ denotes the position (in the plane) of agent i, and $\mathbf{u}_i$ is a velocity control. Cyclic (classical) pursuit can then be implemented with controls of the form $\mathbf{u}_i = k(\mathbf{r}_{i+1} - \mathbf{r}_i)$, where k is a positive control gain and $\mathbf{u}_n = k(\mathbf{r}_1 - \mathbf{r}_n)$. This formulation yields linear closed-loop dynamics characterized by a circulant matrix, and it can be shown (see [36]) that the centroid of the formation is stationary and all agents converge to the centroid. Since "rendezvous" is not always a desired outcome, variations on the control law (such as $\mathbf{u}_i = k[(\mathbf{r}_{i+1} + c_i) - \mathbf{r}_i]$ for some $c_i \in \mathbb{R}^2$, as in

[1]The work in chapters 2 and 3 was originally developed with Justh and Krishnaprasad and presented in [15, 17].

[33]) are used to cause convergence to a desired formation. A version of cyclic CB pursuit (with common pursuit angles) is also implemented in the single-integrator model in [46].

Nonlinear models such as the kinematic unicycle model or the related Hilare-type mobile robot model were used in the cyclic pursuit analysis of [36] and [46] respectively. These models are related to our formulation (see section 2.2.1), but the constant bearing pursuit law that we employ (see section 2.3) is quite different from the control laws used in either of these referenced works. We will provide a more detailed comparison in section 2.3.1.

2.2 Modeling interactions

2.2.1 Description of the state space

We describe the movement of agents in our system as unit-mass particles tracing out twice continuously-differentiable curves in $\mathbb{R}^2$, deriving our dynamics from the natural Frenet frame equations (see, e.g., [25] for details). As depicted in figure 2.1, we let $\mathbf{r}_i$ denote the position of the i^{th} particle (with respect to a fixed inertial frame), $\mathbf{x}_i$ denote the unit tangent vector to the curve, and $\mathbf{y}_i$ the unit vector normal to $\mathbf{x}_i$ (i.e., $\mathbf{y}_i = \mathbf{x}_i^{\perp}$). An n-agent system then evolves according to the particle dynamics given by

$$\begin{aligned}
\dot{\mathbf{r}}_i &= \nu_i \mathbf{x}_i, \\
\dot{\mathbf{x}}_i &= \nu_i \mathbf{y}_i u_i, \\
\dot{\mathbf{y}}_i &= -\nu_i \mathbf{x}_i u_i,\ i = 1, 2, \ldots, n,
\end{aligned} \tag{2.2}$$

Note that ν_i, the speed of particle i, could possibly be given by a time-varying function, but in chapters 2 and 3 we assume that it is constant and equal to 1. Our controls, u_i, can be viewed as curvature controls or steering controls in the planar setting. We also define the "baseline vectors" $\mathbf{r}_{i,i+1}$ by $\mathbf{r}_{i,i+1} = \mathbf{r}_i - \mathbf{r}_{i+1}$, $i = 1, 2, ..., n$ (interpreted modulo n throughout this work).

System (2.2) evolves on the manifold M_{state} defined by

$$\begin{aligned}
M_{state} = \Big\{ (\mathbf{r}_1, \mathbf{x}_1, \mathbf{y}_1, \ldots, \mathbf{r}_n, \mathbf{x}_n, \mathbf{y}_n) \in \mathbb{R}^{6n} \ \Big| \ & \mathbf{r}_i \neq \mathbf{r}_{i+1}, \\
& |\mathbf{x}_i| = 1,\ \mathbf{y}_i = \mathbf{x}_i^{\perp},\ i = 1, 2, \ldots, n \Big\}.
\end{aligned} \tag{2.3}$$

Note that we have only disallowed "sequential collocation", i.e. the state manifold does not include states for which $\mathbf{r}_i = \mathbf{r}_{i+1}$. This means that we restrict our analysis away from the point of actual capture/rendezvous, allowing well-posedness of the feedback laws of section 2.3 and in chapter 5.

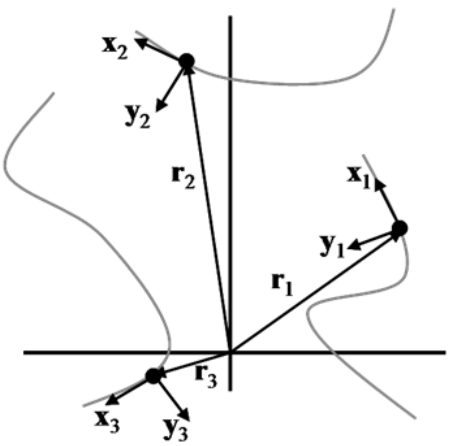

Figure 2.1: Illustration of particle positions and corresponding natural Frenet frames for three particles in the plane.

2.2.2 Reduction from state space to shape space

We can also provide an equivalent representation of the state space in terms of the rigid motion group $G = SE(2)$ by defining $g_i \in SE(2)$ as

$$g_i = \begin{pmatrix} \mathbf{x}_i & \mathbf{y}_i & \mathbf{r}_i \\ 0 & 0 & 1 \end{pmatrix}, \tag{2.4}$$

and therefore our system can be thought of as evolving on the cartesian product of n copies of the Lie group $SE(2)$, i.e.

$$M_{state} = \Big\{ (g_1, g_2, \ldots, g_n) \in \underbrace{SE(2) \times SE(2) \times \cdots \times SE(2)}_{n \text{ times}} \Big| \\ g_i \mathbf{e}_3 \neq g_{i+1} \mathbf{e}_3,\ i = 1, 2, \ldots, n \Big\}, \tag{2.5}$$

where $\mathbf{e}_3 = (0\ 0\ 1)^T$. This takes the form of a *G-snake* (see [31]) with the additional prohibition on sequential colocation. Our dynamics in terms of the Lie group formulation can then be expressed as

$$\dot{g}_i = g_i \xi_i = g_i (A_1 + A_2 u_i), \tag{2.6}$$

where $\xi_i \in \mathfrak{se}(2)$, the Lie algebra of $SE(2)$, and

$$A_1 = \begin{pmatrix} 0 & 0 & 1 \\ 0 & 0 & 0 \\ 0 & 0 & 0 \end{pmatrix}, \; A_2 = \begin{pmatrix} 0 & -1 & 0 \\ 1 & 0 & 0 \\ 0 & 0 & 0 \end{pmatrix} \tag{2.7}$$

generate the Lie algebra under bracketing.

In anticipation of implementing a cyclic pursuit framework (i.e. agent i pursues agent $i+1$ modulo n), it is necessary to define the target of agent n's pursuit. We do this by introducing an additional element $g_{n+1} \in SE(2)$ to our system state and imposing the constraint $g_{n+1} = g_1$. Therefore we have the equivalent representation of M_{state} given by

$$\begin{aligned} M_{state} = \Big\{ (g_1, g_2, \ldots, g_n, g_{n+1}) \in \underbrace{SE(2) \times SE(2) \times \cdots \times SE(2)}_{n+1 \text{ times}} \; \Big| \; g_{n+1} = g_1; \\ g_i \mathbf{e}_3 \neq g_{i+1} \mathbf{e}_3, \; i = 1, 2, \ldots, n+1 \Big\}. \end{aligned} \tag{2.8}$$

In this sense, we can think of our system as a G-snake which "bites its tail".

We are interested in steering laws u_i which leave our system dynamics (2.2) invariant under the action of the special Euclidean group SE(2), in the sense described by Definition 1.3.1. (Particular pursuit laws of this form will be discussed in section 2.3 and chapter 5.) Steering laws of this type (and the resultant closed-loop dynamics) permit reduction to the *shape* *space*, a $(3n-3)$-dimensional quotient manifold $M_{state}/SE(2)$ of relative positions and velocities of the agents. We can parametrize the shape space with n elements of $SE(2)$ by defining $\tilde{g}_i \in SE(2)$ as

$$\tilde{g}_i = g_i^{-1} g_{i+1} = \begin{pmatrix} \mathbf{x}_i \cdot \mathbf{x}_{i+1} & \mathbf{x}_i \cdot \mathbf{y}_{i+1} & -\mathbf{x}_i \cdot \mathbf{r}_{i,i+1} \\ \mathbf{x}_{i+1} \cdot \mathbf{y}_i & \mathbf{y}_i \cdot \mathbf{y}_{i+1} & -\mathbf{y}_i \cdot \mathbf{r}_{i,i+1} \\ 0 & 0 & 1 \end{pmatrix}, \ i = 1, 2, \ldots, n. \tag{2.9}$$

The state space constraint $g_{n+1} = g_1$ can be exhibited in the shape space representation as

$$\prod_{i=1}^{n} \tilde{g}_i = \mathbb{1}, \tag{2.10}$$

where the product notation is understood to imply the *ordered* multiplication of the group elements, i.e. $\prod_{i=1}^{n} \tilde{g}_i = \tilde{g}_1 \tilde{g}_1 \ldots \tilde{g}_n$. We can therefore represent the shape space (which we denote as M_{shape}) as

$$M_{shape} \triangleq M_{state}/SE(2) = \Big\{ (\tilde{g}_1, \tilde{g}_2, \ldots, \tilde{g}_n) \in \underbrace{SE(2) \times SE(2) \times \cdots \times SE(2)}_{n \text{ times}} \Big| \prod_{i=1}^{n} \tilde{g}_i = \mathbb{1};\ (\tilde{g}_i)_{13}^2 + (\tilde{g}_i)_{23}^2 \neq 0,\ i = 1, 2, \ldots, n \Big\}, \tag{2.11}$$

where the two-digit subscripts indicate indices of matrix elements.

It can be shown (see [25]) that for each i, $\tilde{g}_i$ satisfies the dynamics

$$\dot{\tilde{g}}_i = \tilde{g}_i \tilde{\xi}_i, \tag{2.12}$$

where

$$\tilde{\xi}_i = \xi_{i+1} - Ad_{\tilde{g}_i^{-1}} \xi_i = \xi_{i+1} - \tilde{g}_i^{-1} \xi_i \tilde{g}_i. \tag{2.13}$$

Proposition 2.2.1. *The constraint $\prod_{i=1}^{n} \tilde{g}_i = \mathbb{1}$ is preserved by the shape dynamics (2.12).*

Proof: Making use of (2.12) and (2.13), we have

$$
\begin{aligned}
\frac{d}{dt}\left(\prod_{i=1}^{n}\tilde{g}_i\right) &= \dot{\tilde{g}}_1\left(\prod_{j=2}^{n}\tilde{g}_j\right) + \left(\prod_{j=1}^{n-1}\tilde{g}_j\right)\dot{\tilde{g}}_n + \sum_{i=2}^{n-1}\left[\left(\prod_{j=1}^{i-1}\tilde{g}_j\right)\dot{\tilde{g}}_i\left(\prod_{j=i+1}^{n}\tilde{g}_j\right)\right] \\
&= \tilde{g}_1\tilde{\xi}_1\left(\prod_{j=2}^{n}\tilde{g}_j\right) + \left(\prod_{j=1}^{n-1}\tilde{g}_j\right)\tilde{g}_n\tilde{\xi}_n + \sum_{i=2}^{n-1}\left[\left(\prod_{j=1}^{i-1}\tilde{g}_j\right)\tilde{g}_i\tilde{\xi}_i\left(\prod_{j=i+1}^{n}\tilde{g}_j\right)\right] \\
&= \tilde{g}_1\left[\xi_2 - \tilde{g}_1^{-1}\xi_1\tilde{g}_1\right]\left(\prod_{j=2}^{n}\tilde{g}_j\right) + \left(\prod_{j=1}^{n-1}\tilde{g}_j\right)\tilde{g}_n\left[\xi_1 - \tilde{g}_n^{-1}\xi_n\tilde{g}_n\right] \\
&\quad + \sum_{i=2}^{n-1}\left[\left(\prod_{j=1}^{i-1}\tilde{g}_j\right)\tilde{g}_i\left[\xi_{i+1} - \tilde{g}_i^{-1}\xi_i\tilde{g}_i\right]\left(\prod_{j=i+1}^{n}\tilde{g}_j\right)\right] \\
&= \tilde{g}_1\xi_2\left(\prod_{j=2}^{n}\tilde{g}_j\right) - \xi_1\left(\prod_{j=1}^{n}\tilde{g}_j\right) + \left(\prod_{j=1}^{n}\tilde{g}_j\right)\xi_1 - \left(\prod_{j=1}^{n-1}\tilde{g}_j\right)\xi_n\tilde{g}_n \\
&\quad + \sum_{i=2}^{n-1}\left[\left(\prod_{j=1}^{i}\tilde{g}_j\right)\xi_{i+1}\left(\prod_{j=i+1}^{n}\tilde{g}_j\right) - \left(\prod_{j=1}^{i-1}\tilde{g}_j\right)\xi_i\left(\prod_{j=i}^{n}\tilde{g}_j\right)\right].
\end{aligned}
\tag{2.14}
$$

Pairwise cancellation of terms in the summation leaves us with

$$
\begin{aligned}
\frac{d}{dt}\left(\prod_{i=1}^{n}\tilde{g}_i\right) &= \tilde{g}_1\xi_2\left(\prod_{j=2}^{n}\tilde{g}_j\right) - \xi_1\left(\prod_{j=1}^{n}\tilde{g}_j\right) + \left(\prod_{j=1}^{n}\tilde{g}_j\right)\xi_1 - \left(\prod_{j=1}^{n-1}\tilde{g}_j\right)\xi_n\tilde{g}_n \\
&\quad + \left(\prod_{j=1}^{n-1}\tilde{g}_j\right)\xi_n\tilde{g}_n - \tilde{g}_1\xi_2\left(\prod_{j=2}^{n}\tilde{g}_j\right) \\
&= \left(\prod_{j=1}^{n}\tilde{g}_j\right)\xi_1 - \xi_1\left(\prod_{j=1}^{n}\tilde{g}_j\right),
\end{aligned}
\tag{2.15}
$$

and therefore $\left(\prod_{i=1}^{n}\tilde{g}_i\right) = \mathbb{1}$ is an equilibrium point for the $\frac{d}{dt}\left(\prod_{i=1}^{n}\tilde{g}_i\right)$ dynamics. □

Remark 2.2.2 As a result of **Proposition 2.2.1**, we can analyze the system $\dot{\tilde{g}}_i,\ i = 1, 2, \ldots, n$ as a full $3n$-dimensional system of unconstrained dynamics with the closure constraint (2.10) viewed as a constraint on the initial conditions.

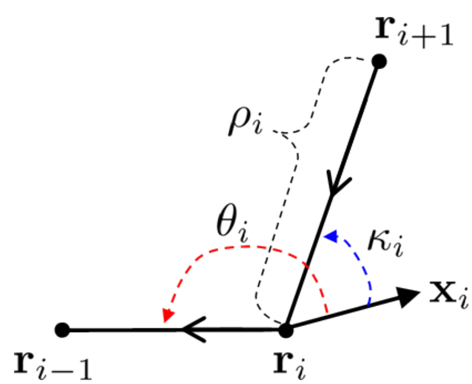

Figure 2.2: Illustration of the shape variables used to parametrize the shape space M_{shape}.

2.2.3 A scalar parametrization of the shape space

The following proposition prescribes a system of shape variables for parametrization of M_{shape}.

Proposition 2.2.3. *If we define $\kappa_i, \theta_i \in [0, 2\pi)$ and $\rho_i \in \mathbb{R}^+$ by*

$$R(\kappa_i)\mathbf{x}_i \cdot \frac{\mathbf{r}_{i,i+1}}{|\mathbf{r}_{i,i+1}|} = -1, \tag{2.16}$$

$$R(\theta_i)\mathbf{x}_i \cdot \frac{\mathbf{r}_{i-1,i}}{|\mathbf{r}_{i-1,i}|} = 1, \tag{2.17}$$

$$\rho_i = |\mathbf{r}_{i,i+1}|\,,\ i = 1, 2, \ldots, n, \tag{2.18}$$

(see figure 2.2), then M_{shape} can be parametrized by $\{(\kappa_i, \theta_i, \rho_i),\ i = 1, 2, \ldots, n\}$, subject to $\rho_i > 0,\ i = 1, 2, \ldots, n$ and the constraint equations

$$R\left(\sum_{i=1}^{n}(\pi + \kappa_i - \theta_i)\right) = \mathbb{1}, \tag{2.19}$$

$$\sum_{i=1}^{n}\rho_i R\left(\sum_{j=1}^{i}(\pi + \kappa_j - \theta_j)\right) = 0. \tag{2.20}$$

Prior to proving **Proposition 2.2.3**, we will state and prove the following lemma which is applicable to sums of $SO(2)$ elements.

Lemma 2.2.4. *Let $a, b \in \mathbb{R}$ and let X_1, X_2 be real-valued two-by-two matrices of the form*

$$X_i = \begin{pmatrix} x_i & -y_i \\ y_i & x_i \end{pmatrix}, \; i = 1, 2. \tag{2.21}$$

Then the matrix $aX_1 + bX_2$ is singular if and only if it is the zero matrix.

Proof of Lemma 2.2.4: Observe that

$$\det\left(aX_1 + bX_2\right) = \det \begin{pmatrix} ax_1 + bx_2 & -(ay_1 + by_2) \\ ay_1 + by_2 & ax_1 + bx_2 \end{pmatrix}$$
$$= (ax_1 + bx_2)^2 + (ay_1 + by_2)^2, \tag{2.22}$$

and therefore $aX_1 + bX_2$ is singular if and only if $ax_1 + bx_2 = 0$ and $ay_1 + by_2 = 0$, i.e. if and only if $aX_1 + bX_2 = 0$. $\square$

Proof of Proposition 2.2.3: Since $\mathbf{x}_i$ is a unit vector, (2.16)-(2.17) implies that

$$R(\kappa_i)\mathbf{x}_i = -\frac{\mathbf{r}_{i,i+1}}{|\mathbf{r}_{i,i+1}|},$$
$$R(\theta_i)\mathbf{x}_i = \frac{\mathbf{r}_{i-1,i}}{|\mathbf{r}_{i-1,i}|}, \tag{2.23}$$

and therefore

$$\cos(\kappa_i) = R(\kappa_i)\mathbf{x}_i \cdot \mathbf{x}_i = -\frac{\mathbf{r}_{i,i+1}}{|\mathbf{r}_{i,i+1}|} \cdot \mathbf{x}_i,$$
$$\sin(\kappa_i) = R(\kappa_i)\mathbf{x}_i \cdot \mathbf{x}_i^{\perp} = -\frac{\mathbf{r}_{i,i+1}}{|\mathbf{r}_{i,i+1}|} \cdot \mathbf{y}_i,$$
$$\cos(\theta_i) = R(\theta_i)\mathbf{x}_i \cdot \mathbf{x}_i = \frac{\mathbf{r}_{i-1,i}}{|\mathbf{r}_{i-1,i}|} \cdot \mathbf{x}_i,$$
$$\sin(\theta_i) = R(\theta_i)\mathbf{x}_i \cdot \mathbf{x}_i^{\perp} = \frac{\mathbf{r}_{i-1,i}}{|\mathbf{r}_{i-1,i}|} \cdot \mathbf{y}_i. \tag{2.24}$$

Thus

$$\begin{aligned}
\mathbf{x}_i \cdot \mathbf{x}_{i+1} &= \left(\mathbf{x}_i \cdot \frac{\mathbf{r}_{i,i+1}}{|\mathbf{r}_{i,i+1}|}\right)\left(\mathbf{x}_{i+1} \cdot \frac{\mathbf{r}_{i,i+1}}{|\mathbf{r}_{i,i+1}|}\right) + \left(\mathbf{x}_i \cdot \frac{\mathbf{r}_{i,i+1}}{|\mathbf{r}_{i,i+1}|}^{\perp}\right)\left(\mathbf{x}_{i+1} \cdot \frac{\mathbf{r}_{i,i+1}}{|\mathbf{r}_{i,i+1}|}^{\perp}\right) \\
&= \left(\mathbf{x}_i \cdot \frac{\mathbf{r}_{i,i+1}}{|\mathbf{r}_{i,i+1}|}\right)\left(\mathbf{x}_{i+1} \cdot \frac{\mathbf{r}_{i,i+1}}{|\mathbf{r}_{i,i+1}|}\right) + \left(\mathbf{y}_i \cdot \frac{\mathbf{r}_{i,i+1}}{|\mathbf{r}_{i,i+1}|}\right)\left(\mathbf{y}_{i+1} \cdot \frac{\mathbf{r}_{i,i+1}}{|\mathbf{r}_{i,i+1}|}\right) \\
&= -\cos(\kappa_i)\cos(\theta_{i+1}) - \sin(\kappa_i)\sin(\theta_{i+1}) \\
&= -\cos(\kappa_i - \theta_{i+1}) \\
&= \cos(\pi + \kappa_i - \theta_{i+1})
\end{aligned} \tag{2.25}$$

and

$$\begin{aligned}
\mathbf{y}_i \cdot \mathbf{x}_{i+1} &= \left(\mathbf{y}_i \cdot \frac{\mathbf{r}_{i,i+1}}{|\mathbf{r}_{i,i+1}|}\right)\left(\mathbf{x}_{i+1} \cdot \frac{\mathbf{r}_{i,i+1}}{|\mathbf{r}_{i,i+1}|}\right) + \left(\mathbf{y}_i \cdot \frac{\mathbf{r}_{i,i+1}}{|\mathbf{r}_{i,i+1}|}^{\perp}\right)\left(\mathbf{x}_{i+1} \cdot \frac{\mathbf{r}_{i,i+1}}{|\mathbf{r}_{i,i+1}|}^{\perp}\right) \\
&= \left(\mathbf{y}_i \cdot \frac{\mathbf{r}_{i,i+1}}{|\mathbf{r}_{i,i+1}|}\right)\left(\mathbf{x}_{i+1} \cdot \frac{\mathbf{r}_{i,i+1}}{|\mathbf{r}_{i,i+1}|}\right) - \left(\mathbf{x}_i \cdot \frac{\mathbf{r}_{i,i+1}}{|\mathbf{r}_{i,i+1}|}\right)\left(\mathbf{y}_{i+1} \cdot \frac{\mathbf{r}_{i,i+1}}{|\mathbf{r}_{i,i+1}|}\right) \\
&= -\sin(\kappa_i)\cos(\theta_{i+1}) + \cos(\kappa_i)\sin(\theta_{i+1}) \\
&= -\sin(\kappa_i - \theta_{i+1}) \\
&= \sin(\pi + \kappa_i - \theta_{i+1}),
\end{aligned} \tag{2.26}$$

and therefore by (2.9) our $\tilde{g}_i$ matrices can be expressed in terms of the new scalar shape variables as

$$\tilde{g}_i = \begin{pmatrix} \cos(\pi + \kappa_i - \theta_{i+1}) & -\sin(\pi + \kappa_i - \theta_{i+1}) & \rho_i \cos(\kappa_i) \\ \sin(\pi + \kappa_i - \theta_{i+1}) & \cos(\pi + \kappa_i - \theta_{i+1}) & \rho_i \sin(\kappa_i) \\ 0 & 0 & 1 \end{pmatrix}$$

$$= \begin{pmatrix} R(\pi + \kappa_i - \theta_{i+1}) & \rho_i R(\kappa_i)\mathbf{e}_1 \\ 0 \quad 0 & 1 \end{pmatrix}, \tag{2.27}$$

where $\mathbf{e}_1 = (1\ 0)^T$. Thus $\tilde{g}_i \mapsto (\kappa_i, \theta_{i+1}, \rho_i)$, and consequently we can parametrize M_{shape} in terms of the scalar shape variables as long as we define the appropriate corresponding form of the closure constraint (2.10). We proceed as follows.

Observe that (2.10) is equivalent to the condition $\tilde{g}_n \tilde{g}_1 \ldots \tilde{g}_{n-1} = \mathbb{1}$. Letting $B_i = R(\pi + \kappa_i - \theta_{i+1})$ and $\mathbf{q}_i = \rho_i R(\kappa_i)\mathbf{e}_1$, by (1.13) and (2.27) we have

$$\tilde{g}_n \prod_{i=1}^{n-1} \tilde{g}_i = \begin{pmatrix} B_n & \mathbf{q}_n \\ 0 \quad 0 & 1 \end{pmatrix} \begin{pmatrix} \prod_{j=1}^{n-1} B_j & \mathbf{q}_1 + \sum_{i=1}^{n-2} \left(\prod_{j=1}^{i} B_j \right) \mathbf{q}_{i+1} \\ 0 \quad 0 & 1 \end{pmatrix}$$

$$= \begin{pmatrix} \prod_{j=1}^{n} B_j & \mathbf{q}_n + B_n \mathbf{q}_1 + B_n \sum_{i=1}^{n-2} \left(\prod_{j=1}^{i} B_j \right) \mathbf{q}_{i+1} \\ 0 \quad 0 & 1 \end{pmatrix}. \tag{2.28}$$

Noting that

$$B_n \mathbf{q}_1 = \rho_1 R(\pi + \kappa_n - \theta_1) R(\kappa_1)\mathbf{e}_1 = \rho_1 R(\pi + \kappa_1 - \theta_1) R(\kappa_n)\mathbf{e}_1 \tag{2.29}$$

and, by application of (1.3),

$$
\begin{aligned}
B_n \sum_{i=1}^{n-2} \left(\prod_{j=1}^{i} B_j \right) \mathbf{q}_{i+1} &= R(\pi + \kappa_n - \theta_1) \sum_{i=1}^{n-2} R \left(\sum_{j=1}^{i} \pi + \kappa_j - \theta_{j+1} \right) \rho_{i+1} R(\kappa_{i+1}) \mathbf{e}_1 \\
&= \sum_{i=1}^{n-2} \rho_{i+1} R(\kappa_n) R \left(\pi + \kappa_{i+1} - \theta_1 + \sum_{j=1}^{i} (\pi + \kappa_j - \theta_{j+1}) \right) \mathbf{e}_1 \\
&= \sum_{i=1}^{n-2} \rho_{i+1} R \left(\sum_{j=1}^{i+1} \pi + \kappa_j - \theta_j \right) R(\kappa_n) \mathbf{e}_1 \\
&= \sum_{i=2}^{n-1} \rho_i R \left(\sum_{j=1}^{i} \pi + \kappa_j - \theta_j \right) R(\kappa_n) \mathbf{e}_1, \qquad (2.30)
\end{aligned}
$$

we can express the $(1, 2)$ element of (2.28) as

$$
\begin{aligned}
&\mathbf{q}_n + B_n \mathbf{q}_1 + B_n \sum_{i=1}^{n-2} \left(\prod_{j=1}^{i} B_j \right) \mathbf{q}_{i+1} \\
&\quad = \rho_n R(\kappa_n) \mathbf{e}_1 + \rho_1 R(\pi + \kappa_1 - \theta_1) R(\kappa_n) \mathbf{e}_1 + \sum_{i=2}^{n-1} \rho_i R \left(\sum_{j=1}^{i} \pi + \kappa_j - \theta_j \right) R(\kappa_n) \mathbf{e}_1 \\
&\quad = \left[\rho_n \mathbb{1} + \sum_{i=1}^{n-1} \rho_i R \left(\sum_{j=1}^{i} (\pi + \kappa_j - \theta_j) \right) \right] R(\kappa_n) \mathbf{e}_1. \qquad (2.31)
\end{aligned}
$$

Thus (2.28) simplifies to

$$
\begin{pmatrix}
R \left(\sum_{j=1}^{n} (\pi + \kappa_{j-1} - \theta_j) \right) & \left[\rho_n \mathbb{1} + \sum_{i=1}^{n-1} \rho_i R \left(\sum_{j=1}^{i} (\pi + \kappa_j - \theta_j) \right) \right] R(\kappa_n) \mathbf{e}_1 \\
0 \quad 0 & 1
\end{pmatrix}, \qquad (2.32)
$$

and our closure constraint (2.10) requires

$$
R \left(\sum_{j=1}^{n} (\pi + \kappa_{j-1} - \theta_j) \right) = \mathbb{1}, \qquad (2.33)
$$

$$
\left[\rho_n \mathbb{1} + \sum_{i=1}^{n-1} \rho_i R \left(\sum_{j=1}^{i} (\pi + \kappa_j - \theta_j) \right) \right] R(\kappa_n) \mathbf{e}_1 = \mathbf{0}. \qquad (2.34)
$$

Hence (2.19) follows directly from (2.33), since our convention regarding summation of indices modulo n implies $\sum_{j=1}^{n} \kappa_{j-1} = \sum_{j=1}^{n} \kappa_j$. Furthermore, (2.20) follows from

(2.34) by application of **Lemma 2.2.4** (note that $R(\kappa_n)\mathbf{e}_1 \neq \mathbf{0}$) and by substituting in the expression for $\mathbb{1}$ from (2.33). $\square$

Remark 2.2.5 It is useful to note that (2.23) implies

$$\begin{aligned}\mathbf{x}_i &= -R(-\kappa_i)\frac{\mathbf{r}_{i,i+1}}{|\mathbf{r}_{i,i+1}|} \\ &= -\frac{1}{\rho_i}R(-\kappa_i)(\mathbf{r}_i - \mathbf{r}_{i+1}),\ i = 1, 2, \ldots, n, \qquad (2.35)\end{aligned}$$

and

$$\begin{aligned}\mathbf{x}_i &= R(-\theta_i)\frac{\mathbf{r}_{i-1,i}}{|\mathbf{r}_{i-1,i}|} \\ &= \frac{1}{\rho_{i-1}}R(-\theta_i)(\mathbf{r}_{i-1} - \mathbf{r}_i),\ i = 1, 2, \ldots, n. \qquad (2.36)\end{aligned}$$

2.2.4 Derivation of shape dynamics

We can derive the $\kappa_i, \theta_i, \rho_i$ shape dynamics as follows. First, we make the preliminary calculation

$$\begin{aligned}\frac{d}{dt}\left(\frac{\mathbf{r}_{i,i+1}}{|\mathbf{r}_{i,i+1}|}\right) &= \frac{1}{|\mathbf{r}_{i,i+1}|}\left[\dot{\mathbf{r}}_{i,i+1} - \left(\dot{\mathbf{r}}_{i,i+1} \cdot \frac{\mathbf{r}_{i,i+1}}{|\mathbf{r}_{i,i+1}|}\right)\frac{\mathbf{r}_{i,i+1}}{|\mathbf{r}_{i,i+1}|}\right] \\ &= \frac{1}{|\mathbf{r}_{i,i+1}|}\left(\dot{\mathbf{r}}_{i,i+1} \cdot \frac{\mathbf{r}_{i,i+1}}{|\mathbf{r}_{i,i+1}|}^{\perp}\right)\frac{\mathbf{r}_{i,i+1}}{|\mathbf{r}_{i,i+1}|}^{\perp} \\ &= -\frac{1}{|\mathbf{r}_{i,i+1}|}\left[(\mathbf{y}_i - \mathbf{y}_{i+1}) \cdot \frac{\mathbf{r}_{i,i+1}}{|\mathbf{r}_{i,i+1}|}\right]\frac{\mathbf{r}_{i,i+1}}{|\mathbf{r}_{i,i+1}|}^{\perp} \\ &= \frac{1}{\rho_i}\left[\sin(\kappa_i) + \sin(\theta_{i+1})\right]\frac{\mathbf{r}_{i,i+1}}{|\mathbf{r}_{i,i+1}|}^{\perp}, \qquad (2.37)\end{aligned}$$

which will prove useful in the following calculations. Note that (2.16) and (2.17) imply that

$$R(\kappa_i)\mathbf{y}_i \cdot \frac{\mathbf{r}_{i,i+1}}{|\mathbf{r}_{i,i+1}|} = 0, \tag{2.38}$$

$$R(\theta_i)\mathbf{y}_i \cdot \frac{\mathbf{r}_{i-1,i}}{|\mathbf{r}_{i-1,i}|} = 0,\ i = 1, 2, \ldots, n, \tag{2.39}$$

and differentiating both sides of (2.38) by means of (1.9) yields

$$\begin{aligned}
0 &= \frac{d}{dt}\left(R(\kappa_i)\mathbf{y}_i\right) \cdot \frac{\mathbf{r}_{i,i+1}}{|\mathbf{r}_{i,i+1}|} + R(\kappa_i)\mathbf{y}_i \cdot \frac{d}{dt}\left(\frac{\mathbf{r}_{i,i+1}}{|\mathbf{r}_{i,i+1}|}\right) \\
&= \left(\dot{\kappa}_i R(\kappa_i + \pi/2)\mathbf{y}_i - u_i R(\kappa_i)\mathbf{x}_i\right) \cdot \frac{\mathbf{r}_{i,i+1}}{|\mathbf{r}_{i,i+1}|} \\
&\qquad + \frac{1}{\rho_i}\left[\sin(\kappa_i) + \sin(\theta_{i+1})\right] R(\kappa_i)\mathbf{y}_i \cdot \frac{\mathbf{r}_{i,i+1}}{|\mathbf{r}_{i,i+1}|}^{\perp} \\
&= \left(-\dot{\kappa}_i R(\kappa_i)\mathbf{x}_i - u_i R(\kappa_i)\mathbf{x}_i\right) \cdot \frac{\mathbf{r}_{i,i+1}}{|\mathbf{r}_{i,i+1}|} \\
&\qquad - \frac{1}{\rho_i}\left[\sin(\kappa_i) + \sin(\theta_{i+1})\right] R(\kappa_i)\mathbf{y}_i^{\perp} \cdot \frac{\mathbf{r}_{i,i+1}}{|\mathbf{r}_{i,i+1}|} \\
&= \left(-\dot{\kappa}_i - u_i + \frac{1}{\rho_i}\left[\sin(\kappa_i) + \sin(\theta_{i+1})\right]\right) R(\kappa_i)\mathbf{x}_i \cdot \frac{\mathbf{r}_{i,i+1}}{|\mathbf{r}_{i,i+1}|}.
\end{aligned} \tag{2.40}$$

By (2.16) we have $R(\kappa_i)\mathbf{x}_i \cdot \frac{\mathbf{r}_{i,i+1}}{|\mathbf{r}_{i,i+1}|} = -1$, and therefore (2.40) implies

$$\dot{\kappa}_i = -u_i + \frac{1}{\rho_i}\left[\sin(\kappa_i) + \sin(\theta_{i+1})\right]. \tag{2.41}$$

Similarly, differentiating both sides of (2.39) yields

$$
\begin{aligned}
0 &= \frac{d}{dt}\left(R(\theta_i)\mathbf{y}_i\right) \cdot \frac{\mathbf{r}_{i-1,i}}{|\mathbf{r}_{i-1,i}|} + R(\theta_i)\mathbf{y}_i \cdot \frac{d}{dt}\left(\frac{\mathbf{r}_{i-1,i}}{|\mathbf{r}_{i-1,i}|}\right) \\
&= \left(\dot{\theta}_i R(\theta_i + \pi/2)\mathbf{y}_i - u_i R(\theta_i)\mathbf{x}_i\right) \cdot \frac{\mathbf{r}_{i-1,i}}{|\mathbf{r}_{i-1,i}|} \\
&\quad + \frac{1}{\rho_{i-1}}\left[\sin(\kappa_{i-1}) + \sin(\theta_i)\right] R(\theta_i)\mathbf{y}_i \cdot \frac{\mathbf{r}_{i-1,i}}{|\mathbf{r}_{i-1,i}|}^{\perp} \\
&= \left(-\dot{\theta}_i R(\theta_i)\mathbf{x}_i - u_i R(\theta_i)\mathbf{x}_i\right) \cdot \frac{\mathbf{r}_{i-1,i}}{|\mathbf{r}_{i-1,i}|} \\
&\quad - \frac{1}{\rho_{i-1}}\left[\sin(\kappa_{i-1}) + \sin(\theta_i)\right] R(\theta_i)\mathbf{y}_i^{\perp} \cdot \frac{\mathbf{r}_{i-1,i}}{|\mathbf{r}_{i-1,i}|} \\
&= \left(-\dot{\theta}_i - u_i + \frac{1}{\rho_{i-1}}\left[\sin(\kappa_{i-1}) + \sin(\theta_i)\right]\right) R(\theta_i)\mathbf{x}_i \cdot \frac{\mathbf{r}_{i-1,i}}{|\mathbf{r}_{i-1,i}|},
\end{aligned}
\tag{2.42}
$$

from which it follows that

$$
\dot{\theta}_i = -u_i + \frac{1}{\rho_{i-1}}\left[\sin(\kappa_{i-1}) + \sin(\theta_i)\right]. \tag{2.43}
$$

Finally, we calculate the derivative of ρ_i by

$$
\begin{aligned}
\dot{\rho}_i &= \frac{d}{dt}|\mathbf{r}_{i,i+1}| \\
&= \dot{\mathbf{r}}_{i,i+1} \cdot \frac{\mathbf{r}_{i,i+1}}{|\mathbf{r}_{i,i+1}|} \\
&= (\mathbf{x}_i - \mathbf{x}_{i+1}) \cdot \frac{\mathbf{r}_{i,i+1}}{|\mathbf{r}_{i,i+1}|} \\
&= -\cos(\kappa_i) - \cos(\theta_{i+1}).
\end{aligned}
\tag{2.44}
$$

In summary, for *any* $SE(2)$ invariant control law u_i, the associated shape dynamics on M_{shape} are given by

$$
\begin{aligned}
\dot{\kappa}_i &= -u_i + \frac{1}{\rho_i}\left[\sin(\kappa_i) + \sin(\theta_{i+1})\right], \\
\dot{\theta}_i &= -u_i + \frac{1}{\rho_{i-1}}\left[\sin(\kappa_{i-1}) + \sin(\theta_i)\right], \\
\dot{\rho}_i &= -\cos(\kappa_i) - \cos(\theta_{i+1}),\ i = 1, 2, \ldots, n
\end{aligned}
\tag{2.45}
$$

with initial conditions subject to the closure constraints (2.19) and (2.20).

2.2.5 The global scaling action

Proposition 2.2.3 implies that $M_{shape} \subset \mathbb{T}^{2n} \times \mathbb{R}^n$ is a differentiable manifold of dimension $3n-3$, where $\mathbb{T}^{2n}$ denotes the $2n$-torus. We define $\tilde{M}_{shape} \subset M_{shape}$ by

$$\tilde{M}_{shape} = \left\{ (\kappa_1, \theta_1, \tilde{\rho}_1, \ldots, \kappa_n, \theta_n, \tilde{\rho}_n) \in M_{shape} \middle| \tilde{\rho}_1 \equiv 1;\ \tilde{\rho}_2, \ldots, \tilde{\rho}_n \in \mathbb{R}^+ \right\}, \tag{2.46}$$

and note that $\tilde{M}_{shape}$ is a $(3n-4)$-dimensional submanifold of M_{shape}. Also, we let the (smooth) map $\Psi : M_{shape} \longrightarrow \tilde{M}_{shape}$ be defined by

$$\Psi(\kappa_1, \theta_1, \rho_1, \ldots, \kappa_n, \theta_n, \rho_n) = \left(\left(\kappa_1, \theta_1, \frac{\rho_1}{\rho_1} \right), \left(\kappa_2, \theta_2, \frac{\rho_2}{\rho_1} \right) \ldots, \left(\kappa_1, \theta_1, \frac{\rho_n}{\rho_1} \right) \right). \tag{2.47}$$

Then letting $G = (\mathbb{R}^+, \times)$, we define the *global scaling action of* G *on* M_{shape} by

$$\begin{aligned} \Phi : G \times M_{shape} &\longrightarrow M_{shape} \\ \Big(\xi, (\kappa_1, \theta_1, \rho_1, \ldots, \kappa_n, \theta_n, \rho_n) \Big) &\longmapsto (\kappa_1, \theta_1, \xi\rho_1, \ldots, \kappa_n, \theta_n, \xi\rho_n), \end{aligned} \tag{2.48}$$

and note that

$$\tilde{M}_{shape} \cong M_{shape}/G. \tag{2.49}$$

Note that G acts freely on M_{shape}, since $\forall m \in M_{shape}$, $\Phi(\xi, m) = m \Longleftrightarrow \xi = 1$, which is the identity element in G. Also, given any $m, \bar{m} \in M_{shape}$, with $m =$

$(\kappa_1, \theta_1, \rho_1, \ldots, \kappa_n, \theta_n, \rho_n)$ and $\bar{m} = (\bar{\kappa}_1, \bar{\theta}_1, \bar{\rho}_1, \ldots, \bar{\kappa}_n, \bar{\theta}_n, \bar{\rho}_n)$, we have

$$\begin{aligned}\Psi(m) = \Psi(\bar{m}) &\Longleftrightarrow \kappa_i = \bar{\kappa}_i,\ \theta_i = \bar{\theta}_i,\ \frac{\rho_i}{\rho_1} = \frac{\bar{\rho}_i}{\bar{\rho}_1},\ i = 1, 2, \ldots, n \\ &\Longleftrightarrow \Phi\left(\frac{\bar{\rho}_1}{\rho_1}, m\right) = \bar{m}. \end{aligned} \tag{2.50}$$

In fact, we can show that the bundle $(M_{shape}, \Psi, \tilde{M}_{shape}, G)$ is a trivial principle bundle[2] with structure group $G = \mathbb{R}^+$, since the mapping $\gamma : \tilde{M}_{shape} \longrightarrow M_{shape}$ defined by

$$\gamma(\tilde{\rho}_1, \tilde{\kappa}_1, \tilde{\theta}_1, \ldots, \tilde{\rho}_n, \tilde{\kappa}_n, \tilde{\theta}_n) = (1, \tilde{\kappa}_1, \tilde{\theta}_1, \ldots, \tilde{\rho}_n, \tilde{\kappa}_n, \tilde{\theta}_n) \tag{2.51}$$

is a cross-section of the bundle (i.e. $\Psi \circ \gamma$ is the identity diffeomorphism on $\tilde{M}_{shape}$). Thus

$$M_{shape} \cong G \times \tilde{M}_{shape}, \tag{2.52}$$

with the explicit isomorphism

$$(\kappa_1, \theta_1, \rho_1, \ldots, \kappa_n, \theta_n, \rho_n) \longmapsto \Big(\rho_1, (\kappa_1, \theta_1, \tilde{\rho}_1, \ldots, \kappa_n, \theta_n, \tilde{\rho}_n)\Big), \tag{2.53}$$

where $\tilde{\rho}_i = \rho_i / \rho_1$.

One can demonstrate that G is not a symmetry group for our shape dynamics (2.45), but in section 2.4.2 we describe an important role for the group action in a related context.

[2] See, for instance, [21] for a discussion of principal bundles and cross sections.

2.2.6 Concepts of "shape"

Throughout our analysis, we encounter several different concepts of "shape". In section 2.2.2, we defined $M_{shape} = M_{state}/SE(2)$ as the "shape space", the space on which concepts of global rotation and translation of the collective have been quotiented out. In section 2.2.5 we go a step further by quotienting out differences which are due to dilations of the particle formation, so that points in $\tilde{M}_{shape} = M_{shape}/G$ correspond to particular shapes apart from any concept of scale. Following the convention in [59], we will refer to this concept of "shape without size" as "pure shape". This concept of shape corresponds to our intuitive geometric sense of shape and is often associated with Kendall[28].

2.3 Constant bearing pursuit

We wish to consider the particular context of n-agent *cyclic pursuit* systems (i.e. agent i pursues agent $i+1$ modulo n) in which each agent employs a *constant bearing (CB)* pursuit strategy. The CB pursuit strategy extends the concept of classical pursuit (i.e. "always move directly towards the current location of the target") by prescribing a fixed, possibly non-zero angle α_i between the pursuer's heading and the current location of the target, as depicted in figure 2.3. Note that for purposes of our analysis in this work, *we do not constrain α_i to be acute* but permit the full range of values $\alpha_i \in [0, 2\pi)$.

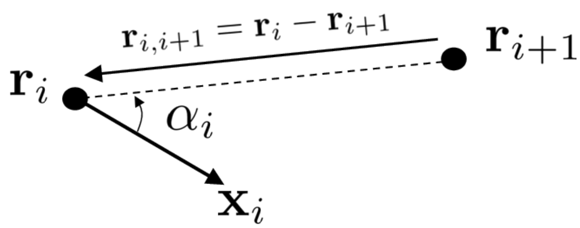

Figure 2.3: Illustration of the constant bearing (CB) pursuit strategy (agent i pursuing agent $i+1$), which prescribes a fixed, possibly non-zero angle α_i between the pursuer's heading and the current location of the target.

In terms of our original state variables, if we define the cost function

$$\Lambda_i \triangleq R(\alpha_i)\mathbf{x}_i \cdot \frac{\mathbf{r}_{i,i+1}}{|\mathbf{r}_{i,i+1}|}, \tag{2.54}$$

then we say agent i has attained CB pursuit of agent $i+1$ if $\Lambda_i = -1$. (Here $R(\alpha_i)$ is the rotation matrix defined in (1.2).) Noting that

$$\begin{aligned} R(\alpha_i)\mathbf{x}_i &= (R(\alpha_i)\mathbf{x}_i \cdot \mathbf{x}_i)\,\mathbf{x}_i + (R(\alpha_i)\mathbf{x}_i \cdot \mathbf{y}_i)\,\mathbf{y}_i \\ &= \cos(\alpha_i)\mathbf{x}_i + \sin(\alpha_i)\mathbf{y}_i, \end{aligned} \tag{2.55}$$

we can describe Λ_i in terms of our shape variables by

$$\begin{aligned} \Lambda_i &= \cos(\alpha_i)\mathbf{x}_i \cdot \frac{\mathbf{r}_{i,i+1}}{|\mathbf{r}_{i,i+1}|} + \sin(\alpha_i)\mathbf{y}_i \cdot \frac{\mathbf{r}_{i,i+1}}{|\mathbf{r}_{i,i+1}|} \\ &= -\cos(\alpha_i)\cos(\kappa_i) - \sin(\alpha_i)\sin(\kappa_i) \\ &= -\cos(\kappa_i - \alpha_i), \end{aligned} \tag{2.56}$$

from which it is clear that

$$\Lambda_i = -1 \iff \kappa_i = \alpha_i. \tag{2.57}$$

For an n-agent cyclic pursuit system in which each agent i employs the CB pursuit strategy with regard to agent $i+1$ (modulo n), we define the $(2n-3)$-dimensional *CB pursuit manifold* $M_{CB(\boldsymbol{\alpha})} \subset M_{shape}$ by

$$M_{CB(\boldsymbol{\alpha})} = \Big\{(\kappa_1, \theta_1, \rho_1, \ldots, \kappa_n, \theta_n, \rho_n) \in M_{shape} \mid \Lambda_i = -1, i = 1, 2, \ldots, n\Big\}, \quad (2.58)$$

where $\boldsymbol{\alpha} = (\alpha_1, \alpha_2, \ldots, \alpha_n)$.

A feedback law designed to attain the CB pursuit strategy was developed in [57], taking the form

$$u_{CB(\alpha_i)} = -\mu_i \left(R(\alpha_i)\mathbf{y}_i \cdot \frac{\mathbf{r}_{i,i+1}}{|\mathbf{r}_{i,i+1}|} \right) - \frac{1}{|\mathbf{r}_{i,i+1}|} \left(\frac{\mathbf{r}_{i,i+1}}{|\mathbf{r}_{i,i+1}|} \cdot \dot{\mathbf{r}}_{i,i+1}^{\perp} \right), \quad (2.59)$$

where $\mu_i > 0$ is a control gain. The corresponding shape variable formulation is given by

$$\begin{aligned} u_{CB(\alpha_i)} &= -\mu_i \left(R(\alpha_i)\mathbf{y}_i \cdot \frac{\mathbf{r}_{i,i+1}}{|\mathbf{r}_{i,i+1}|} \right) - \frac{1}{|\mathbf{r}_{i,i+1}|} \left(\frac{\mathbf{r}_{i,i+1}}{|\mathbf{r}_{i,i+1}|} \cdot \dot{\mathbf{r}}_{i,i+1}^{\perp} \right) \\ &= -\mu_i \left[(-\sin(\alpha_i)\mathbf{x}_i + \cos(\alpha_i)\mathbf{y}_i) \cdot \frac{\mathbf{r}_{i,i+1}}{|\mathbf{r}_{i,i+1}|} \right] - \frac{1}{|\mathbf{r}_{i,i+1}|} \left(\frac{\mathbf{r}_{i,i+1}}{|\mathbf{r}_{i,i+1}|} \cdot (\mathbf{y}_i - \mathbf{y}_{i+1}) \right) \\ &= -\mu_i \left[\sin(\alpha_i)\cos(\kappa_i) - \cos(\alpha_i)\sin(\kappa_i)\right] + \frac{1}{\rho_i}\left[\sin(\kappa_i) + \sin(\theta_{i+1})\right] \\ &= \mu_i \sin(\kappa_i - \alpha_i) + \frac{1}{\rho_i}\left[\sin(\kappa_i) + \sin(\theta_{i+1})\right]. \end{aligned} \quad (2.60)$$

Remark 2.3.1 By (2.57), we observe that the first term of the pursuit law (2.60) is identically zero once CB pursuit has been attained (i.e. $\Lambda_i = -1$), so that only the second term (in which the CB parameter α_i does not explicitly appear) remains. However, one should note that attainment of CB pursuit implies $\kappa_i \equiv \alpha_i$, and therefore the remaining second term will take the form $\frac{1}{\rho_i}\left[\sin(\alpha_i) + \sin(\theta_{i+1})\right]$.

If every agent uses a pursuit law of the form (2.60), then by substitution into (2.45) we have the closed-loop cyclic CB pursuit dynamics

$$\boxed{\begin{aligned}\dot{\kappa}_i &= -\mu_i \sin(\kappa_i - \alpha_i),\\ \dot{\theta}_i &= -\mu_i \sin(\kappa_i - \alpha_i) + \frac{1}{\rho_{i-1}}\left[\sin(\kappa_{i-1}) + \sin(\theta_i)\right] - \frac{1}{\rho_i}\left[\sin(\kappa_i) + \sin(\theta_{i+1})\right],\\ \dot{\rho}_i &= -\cos(\kappa_i) - \cos(\theta_{i+1}),\ i = 1, 2, \ldots, n,\end{aligned}} \tag{2.61}$$

with initial conditions subject to the constraint equations given by (2.19) and (2.20). One should note that the prohibition on sequential colocation (i.e. $\rho_i > 0$) is not necessarily enforced by these dynamics, thus (2.61) define incomplete vector fields on M_{shape}.

The following proposition describes certain properties of the submanifold $M_{CB(\boldsymbol{\alpha})}$ under the shape dynamics (2.61).

Proposition 2.3.2. *The CB pursuit manifold $M_{CB(\boldsymbol{\alpha})} \subset M_{shape}$ is invariant under the dynamics (2.61), in the sense of **Definition 1.3.2**. Furthermore, if $\gamma(t) = \big(\kappa_1(t), \theta_1(t), \rho_1(t), \ldots, \kappa_n(t), \theta_n(t), \rho_n(t)\big) \in M_{shape}$ is a trajectory of (2.61) which does not have finite escape time (i.e. $\rho_i(t) > 0$ for every finite $t \geq 0$), and $\Lambda_i(0) \neq 1,\ i = 1, 2, \ldots, n,$ then*

$$\Lambda_i(t) \longrightarrow -1 \ as\, t \longrightarrow \infty,\ i = 1, 2, \ldots, n, \tag{2.62}$$

i.e. $\gamma(t)$ converges asymptotically to $M_{CB(\boldsymbol{\alpha})}$.

Proof. By (2.56) and (2.61) we have

$$\dot{\Lambda}_i = \dot{\kappa}_i \sin(\kappa_i - \alpha_i) = -\mu_i \sin^2(\kappa_i - \alpha_i) = -\mu_i \left(1 - \Lambda_i^2\right),\ i = 1, 2, \ldots, n, \tag{2.63}$$

and thus $M_{CB(\boldsymbol{\alpha})}$ is invariant under (2.61). In fact, (2.63) implies that $\Lambda_i(0) = \pm 1 \implies \Lambda_i(t) = \pm 1,\ \forall t \geq 0$. We then assume $\Lambda_i(0) \neq \pm 1$ and, as in [57], write (2.63) as

$$\frac{\mathrm{d}\Lambda_i}{1-\Lambda_i^2} = -\mu_i \mathrm{d}t. \tag{2.64}$$

Integrating both sides of (2.64) yields

$$\int_{\Lambda_i(0)}^{\Lambda_i} \frac{\mathrm{d}\tilde{\Lambda}_i}{1-\tilde{\Lambda}_i^2} = -\mu_i \int_0^t \mathrm{d}\tilde{t} = -\mu_i t, \tag{2.65}$$

and since

$$\int_{\Lambda_i(0)}^{\Lambda_i} \frac{\mathrm{d}\tilde{\Lambda}_i}{1-\tilde{\Lambda}_i^2} = \int_{\Lambda_i(0)}^{\Lambda_i} \mathrm{d}\big(\tanh^{-1}(\tilde{\Lambda}_i)\big) = \tanh^{-1}(\Lambda_i) - \tanh^{-1}\big(\Lambda_i(0)\big), \tag{2.66}$$

we have

$$\Lambda_i(t) = \tanh\Big(\tanh^{-1}\big(\Lambda_i(0)\big) - \mu_i t\Big),\ i = 1, 2, \ldots, n. \tag{2.67}$$

Thus, since $\tanh(\cdot)$ is a monotone increasing function, we have $\Lambda_i(t) \longrightarrow -1$ as $t \longrightarrow \infty$. □

We can formulate reduced dynamics on $M_{CB(\boldsymbol{\alpha})}$ by substituting $\kappa_i \equiv \alpha_i$ into (2.61) to arrive at

$$\boxed{\begin{aligned} \dot{\theta}_i &= \frac{1}{\rho_{i-1}}\left[\sin(\alpha_{i-1}) + \sin(\theta_i)\right] - \frac{1}{\rho_i}\left[\sin(\alpha_i) + \sin(\theta_{i+1})\right], \\ \dot{\rho}_i &= -\left[\cos(\alpha_i) + \cos(\theta_{i+1})\right],\ i = 1, 2, \ldots, n, \end{aligned}} \tag{2.68}$$

with the initial conditions subject to the constraints

$$R\left(\sum_{i=1}^{n} (\pi + \alpha_i - \theta_i)\right) = \mathbb{1}, \tag{2.69}$$

$$\sum_{i=1}^{n} \rho_i R\left(\sum_{j=1}^{i} (\pi + \alpha_j - \theta_j)\right) = 0. \tag{2.70}$$

2.3.1 Comparison to previous work on cyclic pursuit

Having developed our cyclic CB pursuit framework, we pause to compare this formulation with previous work on cyclic pursuit. In [36], Marshall, Broucke and Francis use the kinematic unicycle model (which is mathematically equivalent to our model under unit speed assumption) and then propose an analogous shape variable parametrization. (The shape variables in [36] can be related to our variables by $(\alpha_i, \beta_i, r_i) = (\kappa_i, \theta_{i+1} - \kappa_i, \rho_i)$.) Their control law, which attempts to execute the *classical pursuit* strategy, can be expressed in terms of our shape variables by $u_i = \mu_i \kappa_i$, where $\mu_i > 0$ is a control gain. Though ideal cyclic classical pursuit results in eventual rendezvous of all agents, the non-ideal nature of this control law results in closed-loop cyclic pursuit dynamics for which there exist locally stable circling equilibria. These equilibrium formations are equilateral, with inter-agent separations governed (inversely) by the control gain k.

In [46], Pavone and Frazzoli use the Hilare-type mobile robot model, which can be viewed as a dynamical extension of the kinematic unicycle. They do not use shape variables, but in order to deal with the nonholonomic constraint, they define a "hand position" on the robot which is located on the robot centerline (but not on the wheel axis). Since the hand position (denoted by the vector $\mathbf{h}_i$) does not lie on the wheel axis, it is not subject to the nonholonomic constraint, and output feedback linearization yields the dynamics $\ddot{\mathbf{h}}_i = \boldsymbol{\nu}_i$, where $\boldsymbol{\nu}_i$ is viewed as the control input. In order to drive the hand velocity $\dot{\mathbf{h}}_i$ to a desired CB state (i.e. $\dot{\mathbf{h}}_i = R(\alpha)(\mathbf{h}_{i+1} - \mathbf{h}_i)$, where α is a common CB pursuit angle), the authors propose a CB pursuit law given by $\boldsymbol{\nu}_i = \mu_i\Big(R(\alpha)(\mathbf{h}_{i+1} - \mathbf{h}_i) - \dot{\mathbf{h}}_i\Big) + R(\alpha)(\dot{\mathbf{h}}_{i+1} - \dot{\mathbf{h}}_i)$, where $\mu_i > 0$ is a control gain. Implementing this control in a cyclic pursuit framework results in either rendezvous to a point, evenly spaced circling formations, or evenly spaced logarithmic spirals, depending on the value of α.

While the model we have presented in section 2.2.1 is mathematically equivalent to the kinematic unicycle model, there are significant distinctions between our work and that presented in [36, 46]. In constrast to [36], our control law (2.60) executes CB pursuit as well as CP, and results in closed-loop cyclic pursuit dynamics which render the CB pursuit manifold invariant and attractive (**Proposition 2.3.2**). In [36], circling equilibria exist (off of the CP pursuit manifold) because the agents never quite attain the CP strategy; in our work, we will demonstrate in section 2.4.1 that relative equilibria exist *on* the CB pursuit manifold, precisely because each agent does attain the CB strategy. The work in [46] introduces cyclic CB pursuit but only deals with the symmetric case, i.e. $\alpha_i = \alpha,\ i = 1, 2, \ldots, n$. Also, the nonholonomic constraints are circumvented by linearizing about a "hand" position to obtain more tractable double-integrator dynamics, while our work deals directly with the nonholonomic constraints which are inherent to the model.

2.4 Existence conditions for special solutions

2.4.1 Analysis of relative equilibria

Equilibria of the reduced dynamics (2.68) correspond to relative equilibria of the full system dynamics (2.2). As is demonstrated in [25], system dynamics of the form (2.2) permit only two types of relative equilibria: rectilinear and circling. For a rectilinear relative equilibrium, all the particle velocities are aligned (i.e. $\mathbf{x}_i \cdot \mathbf{x}_{i+1} = 1,\ i = 1, 2, \dots, n$) and $u_1 = u_2 = \cdots = u_n = 0$. For a circling relative equilibrium, the particles travel on a common closed circular trajectory separated by fixed chordal distances, with $u_1 = u_2 = \cdots = u_n = \frac{1}{r_c} \neq 0$, where r_c is the radius of the circular orbit.

The following proposition states necessary and sufficient conditions (in terms of the α_i CB parameters) for existence of relative equilibria on $M_{CB(\boldsymbol{\alpha})}$.

Proposition 2.4.1. *Consider an n-particle cyclic CB pursuit system evolving on $M_{CB(\boldsymbol{\alpha})}$ according to the shape dynamics (2.68) parametrized by $\{\alpha_1, \alpha_2, \dots, \alpha_n\}$.*

1. *A rectilinear relative equilibrium exists if and only if there exists a set of constants $\{\sigma_1, \sigma_2, \dots, \sigma_n\}$ such that $\sigma_i > 0,\ i = 1, 2, \dots, n$, and*

$$\sum_{i=1}^{n} \sigma_i e^{j(\alpha_i)} = 0, \tag{2.71}$$

(where $j = \sqrt{-1}$), in which case the corresponding equilibrium angles $\hat{\theta}_i$ and equilibrium side lengths $\hat{\rho}_i$ are given by

$$\hat{\theta}_i = \pi + \alpha_{i-1},\ \hat{\rho}_i = \sigma_i,\ i = 1, 2, \dots, n. \tag{2.72}$$

2. A circling relative equilibrium exists if and only if

$$i \ \sin(\alpha_{i-1})\sin(\alpha_i) > 0,\ i = 1, 2, \ldots, n, \tag{2.73}$$

$$ii \ \sin\left(\sum_{i=1}^{n} \alpha_i\right) = 0, \tag{2.74}$$

in which case the corresponding equilibrium angles $\hat{\theta}_i$ *and equilibrium side ratios* $\frac{\hat{\rho}_i}{\hat{\rho}_{i-1}}$ *are given by*

$$\hat{\theta}_i = \pi - \alpha_{i-1},\ \frac{\hat{\rho}_i}{\hat{\rho}_{i-1}} = \frac{\sin(\alpha_i)}{\sin(\alpha_{i-1})},\ i = 1, 2, \ldots, n. \tag{2.75}$$

Proof: A relative equilibrium exists if and only if there exists a choice of $\{\theta_1, \rho_1, \theta_2, \rho_2, \ldots, \theta_n, \rho_n\}$ which satisfies the closure constraint equations (2.69) and (2.70), and for which $\dot{\theta}_i = 0,\ \dot{\rho}_i = 0,\ i = 1, 2, \ldots, n$. From (2.68) we have[3]

$$\begin{aligned} &\dot{\rho}_i = 0 \Longleftrightarrow \cos(\alpha_i) + \cos(\theta_{i+1}) = 0,\ i = 1, 2, \ldots, n \\ &\dot{\theta}_i = 0 \Longleftrightarrow \begin{cases} \sin(\alpha_i) + \sin(\theta_{i+1}) = 0,\ i = 1, 2, \ldots, n, & \text{or} \\ \sin(\alpha_i) + \sin(\theta_{i+1}) \neq 0,\ \frac{\rho_i}{\rho_{i-1}} = \frac{\sin(\alpha_i)+\sin(\theta_{i+1})}{\sin(\alpha_{i-1})+\sin(\theta_i)} > 0,\ i = 1, 2, \ldots, n, \end{cases} \end{aligned} \tag{2.76}$$

[3]To see that these are the only possibilities, let $\gamma_i \triangleq \frac{1}{\rho_i}\left[\sin(\alpha_i) + \sin(\theta_{i+1})\right]$ so that $\dot{\theta}_i = \gamma_{i-1} - \gamma_i$. Then $\dot{\theta}_i = 0,\ i = 1, 2, \ldots, n$ if and only if $\gamma_{i-1} = \gamma_i,\ i = 1, 2, \ldots, n$. Therefore, if there exists $k \in \{1, 2, \ldots, n\}$ such that $\gamma_k = 0$ *and* it holds that $\dot{\theta}_i = 0,\ i = 1, 2, \ldots, n$, then we must have $\gamma_i = 0,\ i = 1, 2, \ldots, n$.

which, taken together, yields

$$\dot{\rho}_i = \dot{\theta}_i = 0 \Longleftrightarrow \begin{cases} \theta_{i+1} = \pi + \alpha_i,\ i = 1, 2, \ldots, n, & \text{or} \\ \theta_{i+1} = \pi - \alpha_i,\ \sin(\alpha_i) \neq 0,\ \frac{\rho_i}{\rho_{i-1}} = \frac{\sin(\alpha_i)}{\sin(\alpha_{i-1})} > 0,\ i = 1, 2, \ldots, n, \end{cases} \tag{2.77}$$

where the condition $\frac{\sin(\alpha_i)}{\sin(\alpha_{i-1})} > 0,\ i = 1, 2, \ldots, n$ (or, equivalently, $\sin(\alpha_{i-1})\sin(\alpha_i) > 0,\ i = 1, 2, \ldots, n$) is necessary to enforce our prohibition on sequential colocation (i.e. $\rho_i > 0,\ i = 1, 2, \ldots, n$).

We can associate the two cases in (2.77) to our two types of relative equilibria as follows. First, substituting the $M_{CB(\boldsymbol{\alpha})}$ constraint (i.e. $\kappa_i \equiv \alpha_i$) and $\theta_{i+1} = \pi + \alpha_i$ into (2.25), we have

$$\mathbf{x}_i \cdot \mathbf{x}_{i+1} = \cos(\pi + \alpha_i - (\pi + \alpha_i)) = 1,\ i = 1, 2, \ldots, n, \tag{2.78}$$

from which we conclude that the first case in (2.77) corresponds to a rectilinear equilibrium. We claim that the second case in (2.77) corresponds to a circling equilibrium, i.e. we claim the conditions in the second case imply that there exists a point $\mathbf{r}_{cc} \in \mathbb{R}^2$ (the circumcenter) such that

1. $|\mathbf{r}_{cc} - \mathbf{r}_i| = |\mathbf{r}_{cc} - \mathbf{r}_{i-1}|,\ i = 1, 2, \ldots, n$ (i.e., all particles are equidistant from the circumcenter),

2. $\mathbf{x}_i \cdot (\mathbf{r}_{cc} - \mathbf{r}_i) = 0,\ i = 1, 2, \ldots, n$ (i.e., each particle's velocity vector is perpendicular to the associated radial vector), and

3. $\left(\mathbf{x}_i^\perp \cdot (\mathbf{r}_{cc} - \mathbf{r}_{i-1})\right)\left(\mathbf{x}_{i-1}^\perp \cdot (\mathbf{r}_{cc} - \mathbf{r}_i)\right) > 0,\ i = 1, 2, \ldots, n$ (i.e. all particles are moving in the same direction, CCW or CW, around the circle).

As is demonstrated in appendix B, if the second case in (2.77) holds, then

$$\mathbf{r}_i + \frac{\rho_i}{2\sin(\alpha_i)}\mathbf{x}_i^{\perp} = \mathbf{r}_{i-1} + \frac{\rho_{i-1}}{2\sin(\alpha_{i-1})}\mathbf{x}_{i-1}^{\perp}, \ i = 1, 2, \ldots, n, \tag{2.79}$$

and therefore the assignment

$$\mathbf{r}_{cc} \triangleq \mathbf{r}_i + \frac{\rho_i}{2\sin(\alpha_i)}\mathbf{x}_i^{\perp}, \ i = 1, 2, \ldots, n \tag{2.80}$$

is consistent for all $i \in \{1, 2, \ldots, n\}$. By (2.77) we also have

$$\frac{\rho_i}{\sin(\alpha_i)} = \frac{\rho_{i-1}}{\sin(\alpha_{i-1})}, \ i = 1, 2, \ldots, n, \tag{2.81}$$

and therefore (2.80) implies

$$|\mathbf{r}_{cc} - \mathbf{r}_i| = \frac{1}{2}\left|\frac{\rho_i}{\sin(\alpha_i)}\right| = \frac{1}{2}\left|\frac{\rho_{i-1}}{\sin(\alpha_{i-1})}\right| = |\mathbf{r}_{cc} - \mathbf{r}_{i-1}|, \ i = 1, 2, \ldots, n, \tag{2.82}$$

establishing that all particles are equidistant from $\mathbf{r}_{cc}$. It follows from (2.80) that $\mathbf{x}_i \cdot (\mathbf{r}_{cc} - \mathbf{r}_i) = 0, \ i = 1, 2, \ldots, n$, and

$$\left(\mathbf{x}_i^{\perp} \cdot (\mathbf{r}_{cc} - \mathbf{r}_{i-1})\right)\left(\mathbf{x}_{i-1}^{\perp} \cdot (\mathbf{r}_{cc} - \mathbf{r}_i)\right) = \left(\frac{\rho_i}{2\sin(\alpha_i)}\right)\left(\frac{\rho_{i-1}}{2\sin(\alpha_{i-1})}\right) = \frac{\rho_i^2}{4\sin^2(\alpha_i)} > 0, \tag{2.83}$$

where we have made use of (2.81). Therefore we have established that the second case in (2.77) corresponds to a circling equilibrium.

Recall that θ_i and ρ_i must satisfy the constraint equations (2.69) and (2.70), and therefore we must check the assignments in (2.77) against the constraint equations to determine whether additional conditions must be imposed on the α_i parameters to guarantee existence of each type of relative equilibria. Beginning with the rectilinear equilibrium, we substitute $\theta_{i+1} = \pi + \alpha_i$ into the left-hand side of

(2.69) and observe that the constraint holds without additional conditions on the α_i parameters. Substituting $\theta_{i+1} = \pi + \alpha_i$ into the left-hand side of (2.70), we have

$$\begin{aligned}\sum_{i=1}^{n} \rho_i R\left(\sum_{j=1}^{i}(\pi + \alpha_j - \theta_j)\right) &= \sum_{i=1}^{n} \rho_i R\left(\sum_{j=1}^{i}(\alpha_j - \alpha_{j-1})\right) \\ &= \sum_{i=1}^{n} \rho_i R\left(\alpha_i - \alpha_n\right) \\ &= R\left(-\alpha_n\right)\sum_{i=1}^{n} \rho_i R\left(\alpha_i\right), \end{aligned} \tag{2.84}$$

and therefore (2.70) holds if and only if

$$\sum_{i=1}^{n} \rho_i R\left(\alpha_i\right) = 0. \tag{2.85}$$

Our rectilinear existence condition (2.71) then follows from (2.85).

In the case of the circling equilibrium, we first substitute the expressions from the second case from (2.77) into the left-hand side of (2.69) and arrive at

$$\begin{aligned}R\left(\sum_{i=1}^{n}(\pi + \alpha_i - \theta_i)\right) &= R\left(\sum_{i=1}^{n}(\alpha_i + \alpha_{i-1})\right) \\ &= R\left(2\sum_{i=1}^{n}\alpha_i\right). \end{aligned} \tag{2.86}$$

By (1.8) we have

$$R\left(2\sum_{i=1}^{n}\alpha_i\right) = \mathbb{1} \Longleftrightarrow \sin\left(\sum_{i=1}^{n}\alpha_i\right) = 0, \tag{2.87}$$

which establishes (2.74). We then test our θ_i, ρ_i assignments from (2.77) against the remaining closure constraint equation by substituting $\theta_{i+1} = \pi - \alpha_i$ and $\frac{\rho_i}{\rho_{i-1}} =$

$\frac{\sin(\alpha_i)}{\sin(\alpha_{i-1})}$ into the left-hand side of (2.70), which yields

$$\begin{aligned}
\sum_{i=1}^{n} \rho_i R\left(\sum_{j=1}^{i}(\pi+\alpha_j-\theta_j)\right) &= \rho_n \sum_{i=1}^{n} \frac{\rho_i}{\rho_n} R\left(\sum_{j=1}^{i}(\pi+\alpha_j-\theta_j)\right) \\
&= \rho_n \sum_{i=1}^{n} \frac{\sin(\alpha_i)}{\sin(\alpha_n)} R\left(\sum_{j=1}^{i}(\pi+\alpha_j-(\pi-\alpha_{j-1}))\right) \\
&= \frac{\rho_n}{\sin(\alpha_n)} \sum_{i=1}^{n} \sin(\alpha_i) R\left(\sum_{j=1}^{i}(\alpha_j+\alpha_{j-1})\right). \qquad (2.88)
\end{aligned}$$

In appendix B we show that

$$\sin(\alpha_n)\mathbb{1} + \sum_{i=1}^{n-1} \sin(\alpha_i) R\left(\sum_{j=1}^{i}(\alpha_j+\alpha_{j-1})\right) = \sin\left(\sum_{i=1}^{n}\alpha_i\right) R\left(\sum_{i=1}^{n-1}\alpha_i\right), \qquad (2.89)$$

and therefore (making use of (2.69)) we can express (2.88) as

$$\frac{\rho_n}{\sin(\alpha_n)}\left[\sin\left(\sum_{i=1}^{n}\alpha_i\right) R\left(\sum_{i=1}^{n-1}\alpha_i\right)\right]. \qquad (2.90)$$

Since this quantity is equal to zero (by application of (2.87)), our second closure constraint equation holds without requiring any additional conditions on the α_i parameters. □

2.4.2 Pure shape dynamics

In section 2.2.5 we demonstrated that $M_{shape} \cong G \times \tilde{M}_{shape}$, where $G = (\mathbb{R}^+, \times)$, with the explicit isomorphism

$$(\kappa_1, \theta_1, \rho_1, \ldots, \kappa_n, \theta_n, \rho_n) \longmapsto \Big(\rho_1, (\kappa_1, \theta_1, \tilde{\rho}_1, \ldots, \kappa_n, \theta_n, \tilde{\rho}_n)\Big), \qquad (2.91)$$

for

$$\tilde{\rho}_i = \rho_i/\rho_1. \qquad (2.92)$$

Recalling that $M_{CB(\boldsymbol{\alpha})}$ is a submanifold of M_{shape}, we define

$$\tilde{M}_{CB(\boldsymbol{\alpha})} = \left\{ (\theta_1, \tilde{\rho}_1, \ldots, \theta_n, \tilde{\rho}_n) \in M_{CB(\boldsymbol{\alpha})} \middle| \tilde{\rho}_1 \equiv 1;\ \tilde{\rho}_2, \ldots, \tilde{\rho}_n \in \mathbb{R}^+ \right\}, \tag{2.93}$$

and by an analogous process we have $M_{CB(\boldsymbol{\alpha})} \cong G \times \tilde{M}_{CB(\boldsymbol{\alpha})}$, with

$$(\theta_1, \rho_1, \ldots, \theta_n, \rho_n) \longmapsto \Big(\rho_1, (\theta_1, \tilde{\rho}_1, \ldots, \theta_n, \tilde{\rho}_n) \Big) \tag{2.94}$$

and $\tilde{\rho}_i$ defined by (2.92). The corresponding closure constraints for this alternative parametrization of $M_{CB(\boldsymbol{\alpha})}$ are given by (2.69) and

$$\sum_{i=1}^{n} \tilde{\rho}_i R \left(\sum_{j=1}^{i} (\pi + \alpha_j - \theta_j) \right) = 0. \tag{2.95}$$

Our dynamics (2.68) can also be formulated in terms of this alternative parametrization as follows. First, observe that

$$\begin{aligned}
\dot{\tilde{\rho}}_i &= \frac{\dot{\rho}_i}{\rho_1} - \frac{\rho_i \dot{\rho}_1}{\rho_1^2} \\
&= \frac{1}{\rho_1} \left(\dot{\rho}_i - \tilde{\rho}_i \dot{\rho}_1 \right) \\
&= \frac{1}{\rho_1} \Big(- \left[\cos(\alpha_i) + \cos(\theta_{i+1}) \right] + \tilde{\rho}_i \left[\cos(\alpha_1) + \cos(\theta_2) \right] \Big),\ i = 1, 2, \ldots, n,
\end{aligned} \tag{2.96}$$

and therefore (2.68) can be expressed as

$$\begin{aligned}
\dot{\rho}_1 &= - \left[\cos(\alpha_1) + \cos(\theta_2) \right], \\
\dot{\theta}_i &= \frac{1}{\rho_1} \left(\frac{1}{\tilde{\rho}_{i-1}} \left[\sin(\alpha_{i-1}) + \sin(\theta_i) \right] - \frac{1}{\tilde{\rho}_i} \left[\sin(\alpha_i) + \sin(\theta_{i+1}) \right] \right), \\
\dot{\tilde{\rho}}_i &= \frac{1}{\rho_1} \Big(- \left[\cos(\alpha_i) + \cos(\theta_{i+1}) \right] + \tilde{\rho}_i \left[\cos(\alpha_1) + \cos(\theta_2) \right] \Big),\ i = 1, 2, \ldots, n.
\end{aligned} \tag{2.97}$$

(Note that this includes the trivial equation $\dot{\tilde{\rho}}_1 \equiv 0$.)

Observe that the dynamics (2.97) can not be decomposed into self-contained sub-systems. However, by the change of variables

$$\lambda = \ln(\rho_1), \tag{2.98}$$

we have

$$\begin{aligned}
\dot{\lambda} &= -e^{-\lambda}\left[\cos(\alpha_1) + \cos(\theta_2)\right], \\
\dot{\theta}_i &= e^{-\lambda}\left(\frac{1}{\tilde{\rho}_{i-1}}\left[\sin(\alpha_{i-1}) + \sin(\theta_i)\right] - \frac{1}{\tilde{\rho}_i}\left[\sin(\alpha_i) + \sin(\theta_{i+1})\right]\right), \\
\dot{\tilde{\rho}}_i &= e^{-\lambda}\Big(-\left[\cos(\alpha_i) + \cos(\theta_{i+1})\right] + \tilde{\rho}_i\left[\cos(\alpha_1) + \cos(\theta_2)\right]\Big), \ i = 1, 2, \ldots, n. \qquad (2.99)
\end{aligned}$$

We then introduce the time-scaling

$$\tau = \int_0^t e^{-\lambda(\sigma)} d\sigma, \tag{2.100}$$

noting that $d\tau = e^{-\lambda(t)}dt$ and therefore

$$\frac{d\lambda}{d\tau} = \frac{d\lambda}{e^{-\lambda(t)}dt} = e^{\lambda(t)}\dot{\lambda}; \quad \frac{d\theta_i}{d\tau} = \frac{d\theta_i}{e^{-\lambda(t)}dt} = e^{\lambda(t)}\dot{\theta}_i; \quad \frac{d\tilde{\rho}_i}{d\tau} = \frac{d\tilde{\rho}_i}{e^{-\lambda(t)}dt} = e^{\lambda(t)}\dot{\tilde{\rho}}_i. \tag{2.101}$$

Then using the prime notation to denote differentiation with respect to τ, we have

$$\lambda^{'} = -\left[\cos(\alpha_1) + \cos(\theta_2)\right], \tag{2.102}$$

$$\theta_i^{'} = \frac{1}{\tilde{\rho}_{i-1}}\left[\sin(\alpha_{i-1}) + \sin(\theta_i)\right] - \frac{1}{\tilde{\rho}_i}\left[\sin(\alpha_i) + \sin(\theta_{i+1})\right], \tag{2.103}$$

$$\tilde{\rho}_i^{'} = -\left[\cos(\alpha_i) + \cos(\theta_{i+1})\right] + \tilde{\rho}_i\left[\cos(\alpha_2) + \cos(\theta_2)\right], \ i = 1, 2, \ldots, n, \tag{2.104}$$

and (2.103)-(2.104) form a self-contained sub-system which we refer to as the *pure shape dynamics*.

2.4.3 Pure shape equilibria

In section 2.4.1 we analyzed the possible equilibria for the reduced dynamics (2.68), which correspond to relative equilibria for the full system dynamics (2.2). In this section we consider the possible equilibria for the pure shape dynamics (2.103)-(2.104), which correspond to system trajectories which preserve pure shape, as depicted in figure 2.4. We refer to these types of system trajectories as *pure shape equilibria*, and note that circling and rectilinear equilibria are actually special cases of pure shape equilibria.

The following proposition states necessary and sufficient conditions for existence of pure shape equilibria, in terms of the α_i parameters and an angular quantity τ_k. (Note that the physical significance of the angle τ_k defined in the statement of the proposition will be discussed in **Remark 2.4.5**.)

Proposition 2.4.2. *Pure shape equilibria exist if and only if the conditions of* ***Proposition 2.4.1*** *are met or there exists an integer $k \in \{0, 1, 2, \ldots, n-1\}$ such that*

$$\sin(\alpha_i - \tau_k)\sin(\alpha_{i-1} - \tau_k) > 0, \; i = 1, 2, \ldots, n, \tag{2.105}$$

for $\tau_k \triangleq \left(\sum_{i=1}^{n} \frac{\alpha_i}{n}\right) - \frac{k}{n}\pi$. If (2.105) holds for a particular value of k, then the corresponding equilibrium values for θ_i and $\tilde{\rho}_i$ are given by

$$\begin{aligned} \hat{\theta}_i^{(k)} &= \pi - \alpha_{i-1} + 2\tau_k, \\ \hat{\tilde{\rho}}_i^{(k)} &= \frac{\sin(\alpha_i - \tau_k)}{\sin(\alpha_1 - \tau_k)}. \end{aligned} \tag{2.106}$$

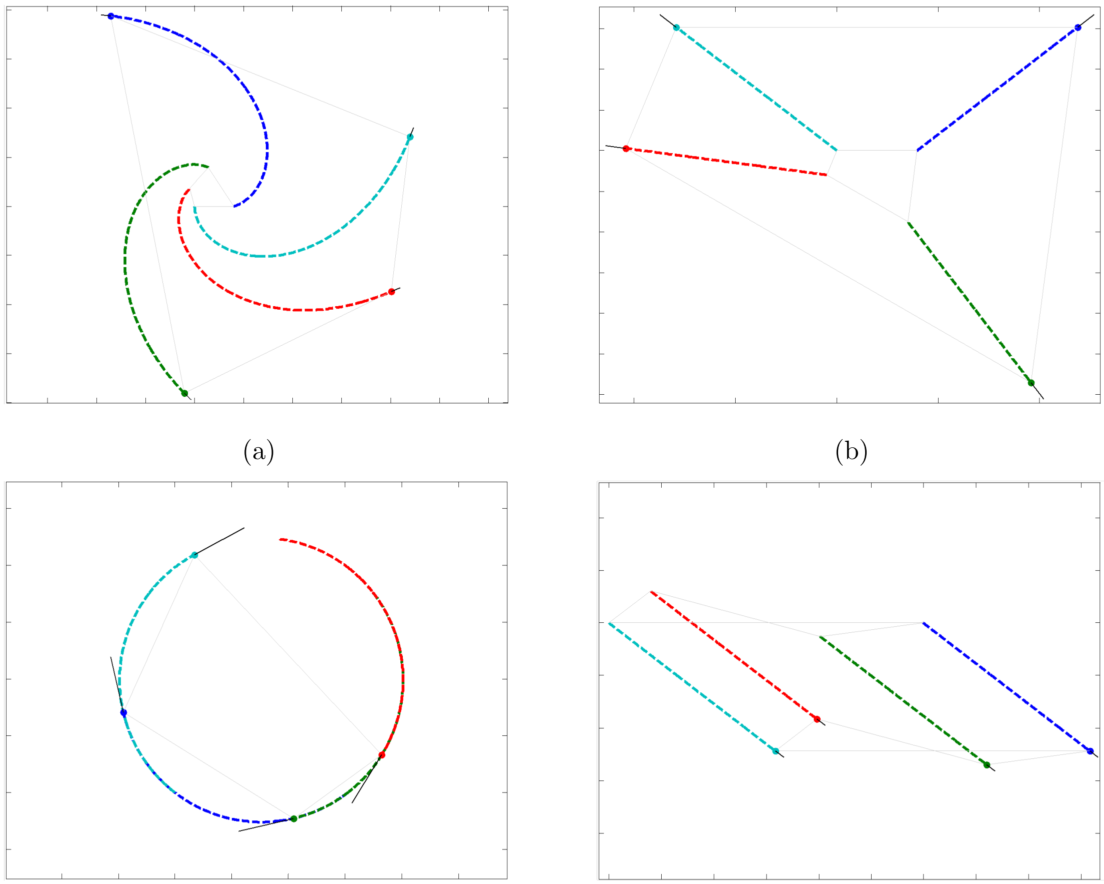

(a) (b) (c) (d)

Figure 2.4: These figures illustrate the planar trajectories which correspond to the four types of pure shape equilibria, including spirals (figure 2.4a), expansion/contraction without rotation (figure 2.4b), circling equilibria (figure 2.4c), and rectilinear equilibria (figure 2.4d).

Proof: Observe that equilibria for (2.103)-(2.104) exist if and only if there exists a choice of $\{\theta_1, \tilde{\rho}_1, \theta_2, \tilde{\rho}_2, \ldots, \theta_n, \tilde{\rho}_n\}$, with $\tilde{\rho}_1 \equiv 1$, which satisfies the closure constraint equations (2.69) and (2.95), and for which $\theta_i^{'} = 0,\ \tilde{\rho}_i^{'} = 0,\ i = 1, 2, \ldots, n$. From (2.103)-(2.104), we observe that[4]

$$\theta_i^{'} = 0 \Longleftrightarrow \begin{cases} \text{(Aa)}\ \ \sin(\alpha_i) + \sin(\theta_{i+1}) = 0,\ i = 1, 2, \ldots, n, & \text{or} \\ \text{(Ab)}\ \ \sin(\alpha_i) + \sin(\theta_{i+1}) \neq 0,\ \frac{\tilde{\rho}_i}{\tilde{\rho}_{i-1}} = \frac{\sin(\alpha_i)+\sin(\theta_{i+1})}{\sin(\alpha_{i-1})+\sin(\theta_i)} > 0,\ i = 1, 2, \ldots, n \end{cases}$$

$$\tilde{\rho}_i^{'} = 0 \Longleftrightarrow \begin{cases} \text{(Ba)}\ \ \cos(\alpha_i) + \cos(\theta_{i+1}) = 0,\ i = 1, 2, \ldots, n, & \text{or} \\ \text{(Bb)}\ \ \cos(\alpha_i) + \cos(\theta_{i+1}) \neq 0,\ \tilde{\rho}_i = \frac{\cos(\alpha_i)+\cos(\theta_{i+1})}{\cos(\alpha_1)+\cos(\theta_2)} > 0,\ i = 1, 2, \ldots, n, \end{cases} \tag{2.107}$$

and therefore the four possible cases corresponding to $\theta_i^{'} = 0,\ \tilde{\rho}_i^{'} = 0,\ i = 1, 2, \ldots, n$ are described by the four possible combinations of an element from the first pair of constraints (Aa and Ab) with an element from the second pair of constraints (Ba and Bb). From section 2.4.1 it is relatively straightforward to show that (Aa,Ba) corresponds to rectilinear relative equilibria and (Ab,Ba) corresponds to circling relative equilibria. We are left to investigate the (Aa,Bb) and (Ab,Bb) cases. We'll begin with the latter.

[4]Note that if $\cos(\alpha_j) + \cos(\theta_{j+1}) = 0$ for some $j = 2, \ldots, n$, then $\tilde{\rho}_j^{'} = 0 \Longrightarrow \cos(\alpha_1) + \cos(\theta_2) = 0$. This in turn implies $\tilde{\rho}_i^{'} = -\left[\cos(\alpha_i) + \cos(\theta_{i+1})\right],\ i = 1, 2, \ldots, n$, and equilibria conditions then require $\cos(\alpha_i) + \cos(\theta_{i+1}) = 0,\ i = 1, 2, \ldots, n$. The same type of reasoning can be applied to the $\theta_i^{'}$ dynamics as well.

First, observe from (2.92) that $\frac{\tilde{\rho}_i}{\tilde{\rho}_{i-1}} = \frac{\rho_i}{\rho_{i-1}}$ and

$$\tilde{\rho}_i = \frac{\cos(\alpha_i) + \cos(\theta_{i+1})}{\cos(\alpha_1) + \cos(\theta_2)},\ i = 1, 2, \ldots, n$$
$$\Longleftrightarrow \frac{\rho_i}{\rho_{i-1}} = \frac{\cos(\alpha_i) + \cos(\theta_{i+1})}{\cos(\alpha_{i-1}) + \cos(\theta_i)},\ i = 1, 2, \ldots, n, \tag{2.108}$$

and therefore if constraint (Ab) and (Bb) both hold, we have

$$\frac{\sin(\alpha_i) + \sin(\theta_{i+1})}{\sin(\alpha_{i-1}) + \sin(\theta_i)} = \frac{\cos(\alpha_i) + \cos(\theta_{i+1})}{\cos(\alpha_{i-1}) + \cos(\theta_i)},\ i = 1, 2, \ldots, n. \tag{2.109}$$

Employing appropriate sum-to-product trigonometric identities, the condition given by (2.109) can be expressed as

$$\frac{\sin\left(\frac{\alpha_i+\theta_{i+1}}{2}\right)\cos\left(\frac{\alpha_i-\theta_{i+1}}{2}\right)}{\sin\left(\frac{\alpha_{i-1}+\theta_i}{2}\right)\cos\left(\frac{\alpha_{i-1}-\theta_i}{2}\right)} = \frac{\cos\left(\frac{\alpha_i+\theta_{i+1}}{2}\right)\cos\left(\frac{\alpha_i-\theta_{i+1}}{2}\right)}{\cos\left(\frac{\alpha_{i-1}+\theta_i}{2}\right)\cos\left(\frac{\alpha_{i-1}-\theta_i}{2}\right)},\ i = 1, 2, \ldots, n, \tag{2.110}$$

which can be simplified to

$$\sin\left(\frac{\alpha_i + \theta_{i+1}}{2}\right)\cos\left(\frac{\alpha_{i-1} + \theta_i}{2}\right) - \cos\left(\frac{\alpha_i + \theta_{i+1}}{2}\right)\sin\left(\frac{\alpha_{i-1} + \theta_i}{2}\right) = 0 \tag{2.111}$$

(for $i = 1, 2, \ldots, n$) and subsequently

$$\sin\left(\frac{\alpha_i + \theta_{i+1} - \alpha_{i-1} - \theta_i}{2}\right) = 0,\ i = 1, 2, \ldots, n. \tag{2.112}$$

This holds if and only if

$$(\alpha_i + \theta_{i+1}) - (\alpha_{i-1} + \theta_i) = 0,\ i = 1, 2, \ldots, n, \tag{2.113}$$

i.e., if and only if the quantity $\alpha_{i-1} + \theta_i$ is the same for any value of i. Therefore we define

$$\psi = \alpha_{i-1} + \theta_i,\ i = 1, 2, \ldots, n \tag{2.114}$$

an angular quantity that has no dependence on i.

Our candidate equilibrium values must satisfy the closure constraints, and therefore we substitute (2.114) into the closure constraints (2.69) and (2.95) to check for constraints on the α_i parameters. We begin with the angular closure constraint (2.69), substituting (2.114) to obtain

$$\begin{aligned} \mathbb{1} &= R\left(\sum_{j=1}^{n}(\pi+\alpha_j-\theta_j)\right) \\ &= R\left(\sum_{j=1}^{n}(\pi+\alpha_j+\alpha_{j-1}-\psi)\right) \\ &= R\left(n(\pi-\psi)+2\sum_{j=1}^{n}\alpha_j\right). \end{aligned} \tag{2.115}$$

Before proceeding, we define the angle quantity $\bar{\alpha}\in[0,2\pi)$ by

$$\bar{\alpha} \triangleq \frac{1}{n}\sum_{i=1}^{n}\alpha_i, \tag{2.116}$$

with the convention that we *do not remove integer multiples of* 2π *from the summation prior to division by* n. Note that an equivalent (and less notationally ambiguous) expression for $\bar{\alpha}$ can be given by

$$\bar{\alpha} \triangleq \sum_{i=1}^{n}\frac{\alpha_i}{n}, \tag{2.117}$$

with no required convention concerning the handling of integer multiples of 2π since $\frac{\alpha_i}{n}\in\left[0,\frac{2\pi}{n}\right)$. Observe that

$$R(n\bar{\alpha}) = R\left(\sum_{j=1}^{n}\alpha_j\right), \tag{2.118}$$

and therefore (2.115) can be expressed as

$$\begin{aligned}\mathbb{1} &= R\Bigg(n\,(\pi-\psi)+2(n\bar{\alpha})\Bigg)\\ &= R\Bigg(n\Big(\pi-\psi+2\bar{\alpha}\Big)\Bigg)\end{aligned} \tag{2.119}$$

which holds if and only if the argument in the inner set of parentheses is equivalent to one of the n roots of unity. There are therefore n possible solutions for ψ, corresponding to

$$\pi-\psi+2\bar{\alpha}=\frac{2k\pi}{n},\ k=0,1,\ldots,n-1, \tag{2.120}$$

with addition understood to be carried out modulo 2π. Introducing the superscript k to explicitly denote the association with a particular root of unity , we have

$$\psi^{(k)}=\left(\frac{n-2k}{n}\right)\pi+2\bar{\alpha},\ k=0,1,\ldots,n-1, \tag{2.121}$$

and therefore by (2.114) the associated θ_i values for a particular value of k (denoted as $\theta_i^{(k)}$) are given by

$$\theta_i^{(k)}=\left(\frac{n-2k}{n}\right)\pi-\alpha_{i-1}+2\bar{\alpha},\ i=1,2,\ldots,n. \tag{2.122}$$

To summarize our efforts to this point, we can state that the angular closure constraint given by (2.69) and the equilibrium conditions given by the (Ab,Bb) pair from (2.107) can be simultaneously satisfied if and only if every θ_i takes the form $\theta_i=\theta_i^{(k)}$ for a particular $k\in\{0,1,2,\ldots,n-1\}$.

By applying the previously used sum-to-product trigonometric identities to constraint (Bb) from (2.107), we obtain

$$\begin{aligned}
\tilde{\rho}_i &= \frac{\cos(\alpha_i) + \cos(\theta_{i+1})}{\cos(\alpha_1) + \cos(\theta_2)} \\
&= \frac{\cos\left(\frac{\alpha_i+\theta_{i+1}}{2}\right)\cos\left(\frac{\alpha_i-\theta_{i+1}}{2}\right)}{\cos\left(\frac{\alpha_1+\theta_2}{2}\right)\cos\left(\frac{\alpha_1-\theta_2}{2}\right)} \\
&= \frac{\cos\left(\frac{\alpha_i+\theta_{i+1}}{2}\right)\cos\left(\frac{\alpha_i+\alpha_i-(\alpha_i+\theta_{i+1})}{2}\right)}{\cos\left(\frac{\alpha_1+\theta_2}{2}\right)\cos\left(\frac{\alpha_1+\alpha_1-(\alpha_1+\theta_2)}{2}\right)} \\
&= \frac{\cos\left(\frac{\psi}{2}\right)\cos\left(\alpha_i - \frac{\psi}{2}\right)}{\cos\left(\frac{\psi}{2}\right)\cos\left(\alpha_1 - \frac{\psi}{2}\right)} \\
&= \frac{\cos\left(\alpha_i - \frac{\psi}{2}\right)}{\cos\left(\alpha_1 - \frac{\psi}{2}\right)}.
\end{aligned} \tag{2.123}$$

Then substituting in $\psi = \psi^{(k)}$, we have

$$\begin{aligned}
\tilde{\rho}_i^{(k)} &= \frac{\cos\left(\alpha_i - \bar{\alpha} + \frac{k}{n}\pi - \frac{\pi}{2}\right)}{\cos\left(\alpha_1 - \bar{\alpha} + \frac{k}{n}\pi - \frac{\pi}{2}\right)} \\
&= \frac{\sin\left(\alpha_i - \bar{\alpha} + \frac{k}{n}\pi\right)}{\sin\left(\alpha_1 - \bar{\alpha} + \frac{k}{n}\pi\right)}.
\end{aligned} \tag{2.124}$$

As will be further explained in **Remark 2.4.5**, the quantity $-(\psi^{(k)} - \pi)/2$ has an appealing geometric property, and therefore we denote

$$\tau_k \triangleq -(\psi^{(k)} - \pi)/2 = \bar{\alpha} - \frac{k}{n}\pi, \tag{2.125}$$

as in the statement of the proposition. Then in terms of τ_k our expressions in (2.122) and (2.124) can be written as

$$\begin{aligned}
\theta_i^{(k)} &= \pi - \alpha_{i-1} + 2\tau_k,\ i = 1, 2, \ldots, n, \\
\tilde{\rho}_i^{(k)} &= \frac{\sin\left(\alpha_i - \tau_k\right)}{\sin\left(\alpha_1 - \tau_k\right)},\ i = 1, 2, \ldots, n.
\end{aligned} \tag{2.126}$$

Since $\tilde{\rho}_i^{(k)}$ must be strictly positive for every $i = 1, 2, \ldots, n$, we incur an additional condition which the α_i parameters must satisfy, namely $\sin\left(\alpha_i - \tau_k\right)\sin\left(\alpha_{i-1} - \tau_k\right) >$

$0,\ i = 1, 2, \ldots, n$, as stated in the proposition.

Lastly, we must also show that the expressions for $\theta_i^{(k)}$ and $\tilde{\rho}_i^{(k)}$ given by (2.126) satisfy the remaining closure constraint. Substituting (2.126) into the left-hand side of (2.95), we obtain

$$\sum_{i=1}^{n} \tilde{\rho}_i^{(k)} R\left(\sum_{j=1}^{i}(\pi + \alpha_j - \theta_i^{(k)})\right) = \sum_{i=1}^{n} \frac{\sin(\alpha_i - \tau_k)}{\sin(\alpha_1 - \tau_k)} R\left(\sum_{j=1}^{i}(\alpha_j + \alpha_{j-1} - 2\tau_k)\right)$$
$$= \frac{1}{\sin(\alpha_1 - \tau_k)} \sum_{i=1}^{n} \sin(\alpha_i - \tau_k)\, R\left(\sum_{j=1}^{i}(\alpha_j - \tau_k) + (\alpha_{j-1} - \tau_k)\right). \tag{2.127}$$

Since (2.127) is similar in form to (2.88) (with $\alpha_i - \tau_k$ taking the place of α_i), we can make use of analogous calculations to express (2.127) as

$$\frac{1}{\sin(\alpha_1 - \tau_k)} \left[\sin\left(\sum_{i=1}^{n}(\alpha_i - \tau_k)\right) R\left(\sum_{i=1}^{n-1}(\alpha_i - \tau_k)\right)\right]. \tag{2.128}$$

Observe that

$$\begin{aligned}
\sin\left(\sum_{i=1}^{n}(\alpha_i - \tau_k)\right) &= \sin\left(\sum_{i=1}^{n}\left(\alpha_i - \bar{\alpha} + \frac{k}{n}\pi\right)\right) \\
&= \sin\left(\left(\sum_{i=1}^{n}\alpha_i\right) - n\bar{\alpha} + k\pi\right) \\
&= \sin(k\pi), \qquad (2.129)
\end{aligned}$$

and therefore (2.128) is equal to the zero matrix, i.e. the remaining closure constraint is satisfied without requiring any additional conditions on the α_i parameters.

In summary, the closure constraints given by (2.69) and (2.95) and the equilibrium constraints given by the (Ab,Bb) pair from (2.107) can be simultaneously satisfied if and only if there exists an integer $k \in \{0, 1, 2, \ldots, n-1\}$ such that the condition $\sin(\alpha_i - \tau_k)\sin(\alpha_{i-1} - \tau_k) > 0,\ i = 1, 2, \ldots, n$ is satisfied. If a particular value of k satisfies this condition, then the corresponding equilibrium values of θ_i and $\tilde{\rho}_i$ are given by (2.126).

To complete the proof, we will demonstrate that solutions corresponding to the final constraint pair (Aa,Bb) from (2.107) are actually a subset of the solutions already described (i.e. those associated with the (Ab,Bb) constraint pair). We begin by observing that if constraint (Aa) holds, we must have $\cos(\alpha_i) + \cos(\theta_{i+1}) = 0$ or $\cos(\alpha_i) - \cos(\theta_{i+1}) = 0$. Since the former is ruled out by constraint (Bb), then we must have $\cos(\alpha_i) - \cos(\theta_{i+1}) = 0$, which along with constraint (Aa) gives us

$$\theta_i = -\alpha_{i-1}. \tag{2.130}$$

Substituting this definition into the side ratio definition given by constraint (Bb), we have

$$\begin{aligned}\tilde{\rho}_i &= \frac{\cos(\alpha_i) + \cos(\theta_{i+1})}{\cos(\alpha_1) + \cos(\theta_2)} \\ &= \frac{\cos(\alpha_i) + \cos(-\alpha_i)}{\cos(\alpha_1) + \cos(-\alpha_1)} \\ &= \frac{\cos(\alpha_i)}{\cos(\alpha_1)},\end{aligned} \tag{2.131}$$

and therefore we require

$$\cos(\alpha_i)\cos(\alpha_1) > 0,\ i = 1, 2, \ldots, n. \tag{2.132}$$

Substitution of (2.130) into our angular closure constraint (2.69) gives us

$$\begin{aligned}\mathbb{1} = R\left(\sum_{i=1}^{n}(\pi + \alpha_i - \theta_i)\right) &= R\left(\sum_{i=1}^{n}(\pi + \alpha_i + \alpha_{i-1})\right) \\ &= R\left(n\pi + 2\sum_{i=1}^{n}\alpha_i\right) \\ &= \begin{cases} R\left(\pi + 2\sum_{i=1}^{n}\alpha_i\right), & \text{for } n \text{ odd} \\ R\left(2\sum_{i=1}^{n}\alpha_i\right), & \text{for } n \text{ even} \end{cases}, \end{aligned} \tag{2.133}$$

which holds if and only if

$$\begin{cases} R\left(\sum_{i=1}^{n}\alpha_i\right) = R\left(\frac{\pi}{2}\right) \text{ or } R\left(\frac{3\pi}{2}\right), & \text{for } n \text{ odd} \\ R\left(\sum_{i=1}^{n}\alpha_i\right) = R(0) \text{ or } R(\pi), & \text{for } n \text{ even} \end{cases}, \tag{2.134}$$

or, equivalently,

$$\begin{cases} \cos\left(\sum_{i=1}^{n}\alpha_i\right) = 0, & \text{for } n \text{ odd} \\ \sin\left(\sum_{i=1}^{n}\alpha_i\right) = 0, & \text{for } n \text{ even} \end{cases}. \tag{2.135}$$

Then substituting (2.130) and (2.131) into the left side of our remaining closure constraint (2.95), we have

$$\begin{aligned}\sum_{i=1}^{n}\tilde{\rho}_i R\left(\sum_{j=1}^{i}(\pi + \alpha_j - \theta_j)\right) &= \sum_{i=1}^{n}\frac{\cos(\alpha_i)}{\cos(\alpha_1)}R\left(\sum_{j=1}^{i}(\pi + \alpha_j + \alpha_{j-1})\right) \\ &= \frac{1}{\cos(\alpha_1)}\sum_{i=1}^{n}\cos(\alpha_i)R\left(\sum_{j=1}^{i}(\pi + \alpha_j + \alpha_{j-1})\right),\end{aligned} \tag{2.136}$$

and a calculation detailed in appendix B demonstrates that this is equivalent to

$$\begin{cases} \frac{1}{\cos(\alpha_1)}\left[\cos\left(\sum_{i=1}^{n}\alpha_i\right)R\left(\sum_{i=1}^{n-1}\alpha_i\right)\right], & \text{for } n \text{ odd} \\ -\frac{1}{\cos(\alpha_1)}\left[\sin\left(\sum_{i=1}^{n}\alpha_i\right)R\left(\frac{\pi}{2} + \sum_{i=1}^{n-1}\alpha_i\right)\right], & \text{for } n \text{ even.} \end{cases} \tag{2.137}$$

By (2.135) these expressions are equal to zero in both cases (i.e. for n odd or even), and therefore the second closure constraint holds without additional conditions on the α_i parameters.

It would therefore appear that (2.132) and (2.135) describe additional equilibrium existence conditions which are not included in the previously described conditions associated with the (Ab,Bb) constraint pair. However, we claim that if $\{\alpha_1, \alpha_2, \ldots, \alpha_n\}$ satisfy (2.132) and (2.135), then there exists $k \in \{0, 1, 2, \ldots, n-1\}$ such that

$$\sin\left(\alpha_i - \tau_k\right) \sin\left(\alpha_{i-1} - \tau_k\right) > 0, \; i = 1, 2, \ldots, n, \tag{2.138}$$

and therefore proposition (2.4.2) is complete as stated. To show this, we first recall from (2.118) that $R(n\bar{\alpha}) = R\left(\sum_{j=1}^{n} \alpha_j\right)$ and therefore if (2.135) holds (equivalently, if (2.133) holds) we have

$$R\left(2n\bar{\alpha}\right) = \begin{cases} R\left(\pi\right), & \text{for } n \text{ odd} \\ \mathbb{1}, & \text{for } n \text{ even} \end{cases}. \tag{2.139}$$

Therefore, if (2.135) holds, then $\bar{\alpha}$ must take the form

$$\bar{\alpha} = \begin{cases} \frac{\pi}{2n} + \ell\left(\frac{\pi}{n}\right), & \text{for } n \text{ odd} \\ \ell\left(\frac{\pi}{n}\right), & \text{for } n \text{ even} \end{cases}, \tag{2.140}$$

with $\ell \in \{0, 1, 2, \ldots, 2n-1\}$ given by the actual value of the quantity $\sum_{j=1}^{n} \alpha_j$. Then choosing $k \in \{0, 1, 2, \ldots, n-1\}$ by

$$k = \begin{cases} \ell + \left(\frac{n+1}{2}\right) \pmod{n}, & \text{for } n \text{ odd} \\ \ell + \left(\frac{n}{2}\right) \pmod{n}, & \text{for } n \text{ even} \end{cases}, \tag{2.141}$$

we observe that substitution of (2.140) and (2.141) into (2.125) yields $\tau_k = \pm\pi/2$. For such a choice of k, we have

$$\sin(\alpha_i - \tau_k)\sin(\alpha_{i-1} - \tau_k) = \cos(\alpha_i)\cos(\alpha_{i-1}),\ i = 1, 2, \ldots, n, \tag{2.142}$$

and since $\cos(\alpha_i)\cos(\alpha_{i-1}) > 0,\ i = 1, 2, \ldots, n$ (by (2.132)), we see that (2.138) holds. □

Remark 2.4.3 The four constraint pairs (Aa,Ba), (Aa,Bb), (Ab,Ba), (Ab,Bb) from the proof of **Proposition 2.4.2** correspond to four types of pure shape equilibria, as depicted in figure 2.4. (Aa,Ba) corresponds to rectilinear equilibria, (Ab,Ba) corresponds to circling equilibria, (Ab,Bb) corresponds to spirals, and (Aa,Bb) corresponds to pure expansion (or contraction) without rotation.

The following corollary to **Proposition 2.4.2** establishes that the planar tracjetories corresponding to pure shape equilibria (with the exception of rectilinear equilibria) are cyclic (i.e. circumscribable).

Corollary 2.4.4. *If condition (2.105) holds, then the formations described by (2.106) are cyclic (i.e. circumscribable). The circumcenter of the associated circumcircle is located at*

$$\mathbf{r}_{cc} = \mathbf{r}_i + \frac{\rho_i}{2\sin(\alpha_i - \tau_k)} R\left(\tau_k + \frac{\pi}{2}\right)\mathbf{x}_i,\ i = 1, 2, \ldots, n, \tag{2.143}$$

and the radius is given by

$$r_c \triangleq |\mathbf{r}_{cc} - \mathbf{r}_i| = \frac{\rho_i}{2\,|\sin(\alpha_i - \tau_k)|},\ i = 1, 2, \ldots, n. \tag{2.144}$$

Proof: The proof is analogous to that presented in the second case in **Proposition 2.4.1** and hinges on demonstrating that the formulation of the circumcenter $\mathbf{r}_{cc}$ given by (2.143) is in fact consistent for all $i \in \{1, 2, \ldots, n\}$. In other words, we must show that

$$\left[\mathbf{r}_{i-1} + \frac{\rho_{i-1}}{2\sin(\alpha_{i-1} - \tau_k)} R\left(\tau_k + \frac{\pi}{2}\right)\mathbf{x}_{i-1}\right] - \left[\mathbf{r}_i + \frac{\rho_i}{2\sin(\alpha_i - \tau_k)} R\left(\tau_k + \frac{\pi}{2}\right)\mathbf{x}_i\right] = \mathbf{0} \tag{2.145}$$

for $i = 1, 2, \ldots, n$. First, by (2.35) (with $\kappa_i \equiv \alpha_i$) and (2.36), we have

$$\mathbf{x}_i = \frac{1}{\rho_{i-1}} R(-\theta_i)(\mathbf{r}_{i-1} - \mathbf{r}_i),\ i = 1, 2, \ldots, n, \tag{2.146}$$

and

$$\mathbf{x}_{i-1} = -\frac{1}{\rho_{i-1}} R(-\alpha_{i-1})(\mathbf{r}_{i-1} - \mathbf{r}_i),\ i = 1, 2, \ldots, n, \tag{2.147}$$

and substitution into the left-hand side of (2.145) yields

$$\begin{aligned}
&\left[\mathbf{r}_{i-1} + \frac{\rho_{i-1}}{2\sin(\alpha_{i-1} - \tau_k)} R\left(\tau_k + \frac{\pi}{2}\right)\left(-\frac{1}{\rho_{i-1}} R(-\alpha_{i-1})(\mathbf{r}_{i-1} - \mathbf{r}_i)\right)\right] \\
&\qquad - \left[\mathbf{r}_i + \frac{\rho_i}{2\sin(\alpha_i - \tau_k)} R\left(\tau_k + \frac{\pi}{2}\right)\left(\frac{1}{\rho_{i-1}} R(-\theta_i)(\mathbf{r}_{i-1} - \mathbf{r}_i)\right)\right] \\
&= (\mathbf{r}_{i-1} - \mathbf{r}_i) - \frac{1}{2\sin(\alpha_{i-1} - \tau_k)} R\left(\tau_k + \frac{\pi}{2} - \alpha_{i-1}\right)(\mathbf{r}_{i-1} - \mathbf{r}_i) \\
&\qquad - \left(\frac{\rho_i}{\rho_{i-1}}\right) \frac{1}{2\sin(\alpha_i - \tau_k)} R\left(\tau_k + \frac{\pi}{2} - \theta_i\right)(\mathbf{r}_{i-1} - \mathbf{r}_i).
\end{aligned} \tag{2.148}$$

Then by substituting the values for θ_i and $\frac{\rho_i}{\rho_{i-1}} = \frac{\tilde{\rho}_i}{\tilde{\rho}_{i-1}}$ given by (2.106), we can further simplify (2.148) to

$$\begin{aligned}
&\left\{\mathbb{1} - \frac{1}{2\sin(\alpha_{i-1} - \tau_k)} R\left(\tau_k + \frac{\pi}{2} - \alpha_{i-1}\right)\right. \\
&\qquad \left. - \left(\frac{\sin(\alpha_i - \tau_k)}{\sin(\alpha_{i-1} - \tau_k)}\right) \frac{1}{2\sin(\alpha_i - \tau_k)} R\left(\tau_k + \frac{\pi}{2} - (\pi - \alpha_{i-1} + 2\tau_k)\right)\right\}(\mathbf{r}_{i-1} - \mathbf{r}_i)
\end{aligned} \tag{2.149}$$

which yields

$$\left\{\mathbb{1} - \frac{1}{2\sin(\alpha_{i-1}-\tau_k)}\left[R\left(\tau_k + \frac{\pi}{2} - \alpha_{i-1}\right) + R\left(-\tau_k - \frac{\pi}{2} + \alpha_{i-1}\right)\right]\right\}(\mathbf{r}_{i-1} - \mathbf{r}_i). \tag{2.150}$$

Application of (1.7) to (2.150) yields

$$\left\{\mathbb{1} - \frac{1}{2\sin(\alpha_{i-1}-\tau_k)} 2\cos\left(\tau_k + \frac{\pi}{2} - \alpha_{i-1}\right)\mathbb{1}\right\}(\mathbf{r}_{i-1} - \mathbf{r}_i), \tag{2.151}$$

and we then employ the trigonometric identity $\cos\left(\frac{\pi}{2} - \phi\right) = \sin(\phi)$ to establish (2.145).

Therefore (2.143) is in fact consistent for all $i \in \{1, 2, \ldots, n\}$, and consequently

$$|\mathbf{r}_{cc} - \mathbf{r}_i| = \frac{1}{2}\left|\frac{\rho_i}{\sin(\alpha_i - \tau_k)}\right|, \; i = 1, 2, \ldots, n. \tag{2.152}$$

By (2.106) we have $\frac{\rho_i}{\rho_{i-1}} = \frac{\sin(\alpha_i - \tau_k)}{\sin(\alpha_{i-1}-\tau_k)}, \; i = 1, 2, \ldots, n$, and therefore

$$\frac{\rho_i}{\sin(\alpha_i - \tau_k)} = \frac{\rho_{i-1}}{\sin(\alpha_{i-1} - \tau_k)}, \; i = 1, 2, \ldots, n. \tag{2.153}$$

It follows from (2.152) and (2.153) that

$$|\mathbf{r}_{cc} - \mathbf{r}_1| = |\mathbf{r}_{cc} - \mathbf{r}_2| = \cdots = |\mathbf{r}_{cc} - \mathbf{r}_n|, \tag{2.154}$$

from which (2.144) follows directly. □

Remark 2.4.5 By (2.143) and (2.144) we have

$$\frac{\mathbf{r}_{cc} - \mathbf{r}_i}{|\mathbf{r}_{cc} - \mathbf{r}_i|} = \operatorname{sgn}\left(\sin(\alpha_i - \tau_k)\right) R\left(\tau_k + \frac{\pi}{2}\right)\mathbf{x}_i, \tag{2.155}$$

from which we obtain

$$R\left(\tau_k\right)\mathbf{x}_i = \begin{cases} R\left(-\frac{\pi}{2}\right)\frac{\mathbf{r}_{cc} - \mathbf{r}_i}{|\mathbf{r}_{cc} - \mathbf{r}_i|}, & \text{for } \sin(\alpha_i - \tau_k) > 0 \\ R\left(\frac{\pi}{2}\right)\frac{\mathbf{r}_{cc} - \mathbf{r}_i}{|\mathbf{r}_{cc} - \mathbf{r}_i|}, & \text{for } \sin(\alpha_i - \tau_k) < 0 \end{cases}. \tag{2.156}$$

Since $\frac{\mathbf{r}_{cc}-\mathbf{r}_i}{|\mathbf{r}_{cc}-\mathbf{r}_i|}$ is the unit vector pointing in the direction from particle $\mathbf{r}_i$ towards the circumcenter, we see that the angle τ_k represents a common angular deviation between $\mathbf{x}_i$ and a unit vector tangent to the circumcircle at $\mathbf{r}_i$. (Whether the unit tangent vector points in a CW or CCW direction depends on the sign of $\sin(\alpha_i - \tau_k)$.) This is illustrated in figure 2.5a and 2.5b for the case when $\sin(\alpha_i - \tau_k) > 0$.

From (2.155) we can characterize the spiraling motions in terms of growth (expansion vs. contraction) and direction of rotation (clockwise vs. counterclockwise). As is clear from figures 2.5a and 2.5b, we will have expansion if $\frac{\mathbf{r}_{cc}-\mathbf{r}_i}{|\mathbf{r}_{cc}-\mathbf{r}_i|} \cdot \mathbf{x}_i < 0$ and contraction if $\frac{\mathbf{r}_{cc}-\mathbf{r}_i}{|\mathbf{r}_{cc}-\mathbf{r}_i|} \cdot \mathbf{x}_i > 0$. Observe from (2.155) that

$$\begin{aligned}
\frac{\mathbf{r}_{cc}-\mathbf{r}_i}{|\mathbf{r}_{cc}-\mathbf{r}_i|} \cdot \mathbf{x}_i &= \operatorname{sgn}\left(\sin(\alpha_i - \tau_k)\right) \left(R\left(\tau_k + \frac{\pi}{2}\right) \mathbf{x}_i \right) \cdot \mathbf{x}_i \\
&= \operatorname{sgn}\left(\sin(\alpha_i - \tau_k)\right) \cos\left(\tau_k + \frac{\pi}{2}\right) \\
&= -\operatorname{sgn}\left(\sin(\alpha_i - \tau_k)\right) \sin\left(\tau_k\right), \; i = 1, 2, \ldots, n, \qquad (2.157)
\end{aligned}$$

which yields the same value for every i. Therefore, defining the *expansion coefficient*

$$\gamma_{\boldsymbol{\alpha},k} \triangleq \operatorname{sgn}\big(\sin(\alpha_1 - \tau_k)\big) \sin\left(\tau_k\right), \qquad (2.158)$$

we have

$$\text{Expansion} \iff \gamma_{\boldsymbol{\alpha},k} > 0, \quad \text{Contraction} \iff \gamma_{\boldsymbol{\alpha},k} < 0. \qquad (2.159)$$

For $\gamma_{\boldsymbol{\alpha},k} = 0$ we have a circling equilibrium (i.e. neither expanding nor contracting).

Also, note that $\left(\frac{\mathbf{r}_{cc}-\mathbf{r}_i}{|\mathbf{r}_{cc}-\mathbf{r}_i|}\right)^{\perp}$ always points in a CW direction (regardless of

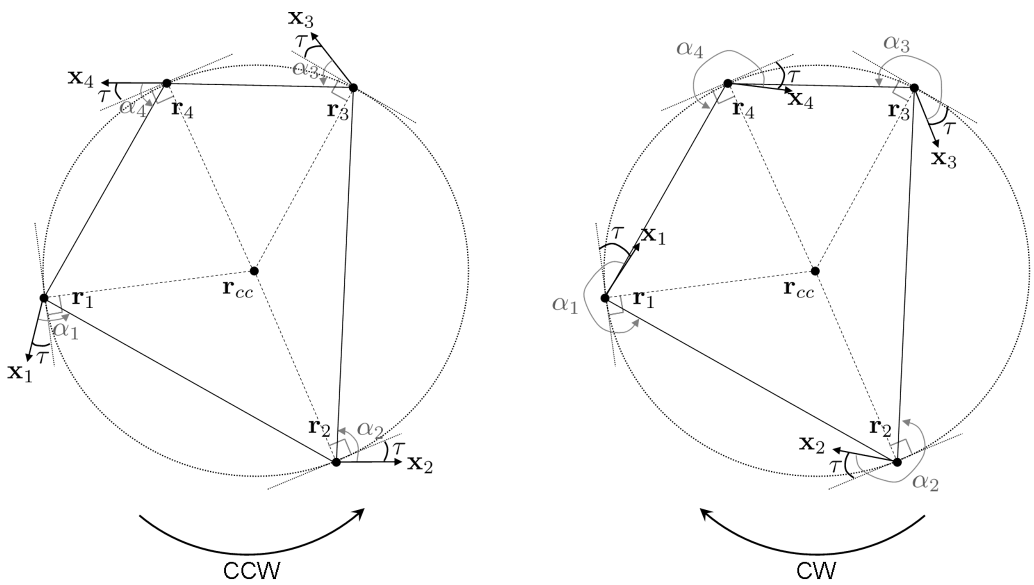

(a) (b)

Figure 2.5: These figures depict representative counter-clockwise (figure 2.5a) and clockwise (figure 2.5b) spirals and demonstrate the significance of the angle τ.

whether the direction of rotational motion is CW or CCW), and

$$
\begin{aligned}
\left(\frac{\mathbf{r}_{cc}-\mathbf{r}_i}{|\mathbf{r}_{cc}-\mathbf{r}_i|}\right)^{\perp}\cdot\mathbf{x}_i &= \left(R\left(\frac{\pi}{2}\right)\left(\frac{\mathbf{r}_{cc}-\mathbf{r}_i}{|\mathbf{r}_{cc}-\mathbf{r}_i|}\right)\right)\cdot\mathbf{x}_i \\
&= \operatorname{sgn}\left(\sin(\alpha_i-\tau_k)\right)\left(R\left(\frac{\pi}{2}\right)R\left(\tau_k+\frac{\pi}{2}\right)\mathbf{x}_i\right)\cdot\mathbf{x}_i \\
&= \operatorname{sgn}\left(\sin(\alpha_i-\tau_k)\right)\cos\left(\tau_k+\pi\right) \\
&= -\operatorname{sgn}\left(\sin(\alpha_i-\tau_k)\right)\cos\left(\tau_k\right),\ i=1,2,\ldots,n.
\end{aligned}
\tag{2.160}
$$

Since (2.160) yields the same value for every i, we define the *rotation coefficient*

$$
\beta_{\boldsymbol{\alpha},k} \triangleq \operatorname{sgn}\big(\sin(\alpha_1-\tau_k)\big)\cos\left(\tau_k\right), \tag{2.161}
$$

for which we have

$$
\text{CCW rotation} \iff \beta_{\boldsymbol{\alpha},k} > 0, \quad \text{CW rotation} \iff \beta_{\boldsymbol{\alpha},k} < 0. \tag{2.162}
$$

For $\beta_{\boldsymbol{\alpha},k} = 0$, the formation experiences pure expansion (or contraction) without rotation, as in figure 2.4b.

Remark 2.4.6 It is important to note from **Proposition 2.4.2** that **multiple pure shape equilibria can exist for a particular choice of** $\boldsymbol{\alpha} = (\alpha_1, \alpha_2, \ldots, \alpha_n)$. This is best understood by considering the symmetric case, presented in section 2.4.4, where $\alpha_1 = \alpha_2 = \ldots = \alpha_n$. For this case, we show that there always exists exactly $n-1$ unique pure shape equilibria, as illustrated in figure 2.6 for the particular case $\alpha_1 = \alpha_2 = \alpha_3 = \alpha_4 = \alpha_5 = \pi/2$.

2.4.4 Analysis of the symmetric case $\alpha_1 = \alpha_2 = \cdots = \alpha_n$

For the symmetric case $\alpha_1 = \alpha_2 = \cdots = \alpha_n = \alpha \in [0, 2\pi)$, we can apply the results of the previous sections to fully characterize existence of relative equilibria and pure shape equilibria in terms of the single parameter α. First, substitution of $\alpha_1 = \alpha_2 = \cdots = \alpha_n = \alpha$ into the rectilinear equilibrium existence condition (2.71) from **Proposition 2.4.1** implies that rectilinear equilibria exist if and only if there exists $\{\sigma_1, \sigma_2, \ldots, \sigma_n\}$ such that $\sigma_i > 0,\ i = 1, 2, \ldots, n$ and $e^{j\alpha}\left(\sum_{i=1}^{n} \sigma_i\right) = 0$. Since this latter condition requires at least one of the σ_i to be nonpositive, we conclude that the symmetric case admits no rectilinear equilibria.

As for circling equilibria, we note that the first existence condition (2.73) of

Proposition 2.4.1 requires

$$\sin(\alpha_{i-1})\sin(\alpha_i) = \sin^2(\alpha) > 0, \tag{2.163}$$

which holds as long as $\alpha \neq 0, \pi$. Then since the second existence condition (2.74) requires

$$0 = \sin\left(\sum_{i=1}^{n} \alpha_i\right) = \sin(n\alpha), \tag{2.164}$$

we conclude that circling equilibria exist if and only if $\alpha = \ell\pi/n$, for $\ell = 1, 2, \ldots, n-1, n+1, \ldots, 2n-1$. If such circling equilibria exist, then by (2.75) we have the equilibrium values $\hat{\theta}_i = \pi - \alpha = (n-\ell)\pi/n$ and $\hat{\rho}_i/\hat{\rho}_{i-1} = 1$, i.e. the equilibrium shape is equilateral.

To address the existence of pure shape equilibria for the symmetric case, we apply **Proposition 2.4.2**, first noting that

$$\tau_k = \left(\sum_{i=1}^{n} \frac{\alpha_i}{n}\right) - \frac{k}{n}\pi = \alpha - \frac{k}{n}\pi. \tag{2.165}$$

Thus $\sin(\alpha_i - \tau_k) = \sin(\alpha - (\alpha - k\pi/n)) = \sin(k\pi/n)$ for every $i = 1, 2, \ldots, n$, and pure shape equilibria exist if and only if there exists $k \in \{0, 1, 2, \ldots, n-1\}$ such that

$$\sin(\alpha_i - \tau_k)\sin(\alpha_{i-1} - \tau_k) = \sin^2(k\pi/n) > 0. \tag{2.166}$$

Since (2.166) holds for $k = 1, 2, \ldots, n-1$, we have established that the symmetric case always admits exactly $n-1$ pure shape equilibria (identified by their corresponding k-value). Furthermore, since $\sin(\alpha - \tau_k) = \sin(k\pi/n) > 0$ for every $k = 1, 2, \ldots, n-1$, substitution of (2.165) into (2.158) and (2.161) yields

$$\gamma_{\boldsymbol{\alpha},k} = \sin(\alpha - k\pi/n), \quad \beta_{\boldsymbol{\alpha},k} = \cos(\alpha - k\pi/n). \tag{2.167}$$

At equilibrium, we have $\hat{\theta}_i^{(k)} = \pi - \alpha + 2\tau_k = \alpha + (n-2k)\pi/n$ and $\hat{\rho}_i^{(k)}/\hat{\rho}_{i-1}^{(k)} = 1$, i.e. the equilibrium shapes are equilateral in this case as well.

We summarize these results with the following proposition.

Proposition 2.4.7. *Consider an n-particle cyclic CB pursuit system evolving on $M_{CB(\boldsymbol{\alpha})}$ according to the shape dynamics (2.68) parametrized by $\{\alpha_1, \alpha_2, \dots, \alpha_n\}$, where $\alpha_1 = \alpha_2 = \cdots = \alpha_n = \alpha \in [0, 2\pi)$. The following statements hold:*

1. *No rectilinear equilibria exist;*

2. *Circling equilibria exist if and only if $\alpha = \ell\pi/n$, for $\ell = 1, 2, \dots, n-1, n+1, \dots, 2n-1$, in which case the equilibrium values satisfy*

$$\hat{\theta}_i = (n-\ell)\pi/n, \quad \hat{\rho}_i/\hat{\rho}_{i-1} = 1,\ i = 1, 2, \dots, n; \tag{2.168}$$

3. *There exist exactly $n-1$ unique pure shape equilibria, each identified with a unique value of $k \in \{1, 2, \dots, n-1\}$. The equilibrium values satisfy*

$$\hat{\theta}_i^{(k)} = \alpha + (n-2k)\pi/n, \quad \hat{\rho}_i^{(k)}/\hat{\rho}_{i-1}^{(k)} = 1,\ i = 1, 2, \dots, n, \tag{2.169}$$

and the expansion and rotation coefficients describing the evolution of the corresponding trajectories in the physical space are given by

$$\gamma_{\boldsymbol{\alpha},k} = \sin\left(\alpha - k\pi/n\right), \quad \beta_{\boldsymbol{\alpha},k} = \cos\left(\alpha - k\pi/n\right). \tag{2.170}$$

Proof. Follows from the preceding discussion. □

Remark 2.4.8 The behavior of these $n-1$ symmetric pure shape equilibria is best understood by considering low-dimensional cases, such as the three-particle case which we present in section 3.7.1.

Remark 2.4.9 If a circling equilibrium exists for the symmetric case (i.e. $\alpha = \ell\pi/n$, for $\ell = 1, 2, \ldots, n-1, n+1, \ldots, 2n-1$), then we can show that it corresponds to one of the $n-1$ pure shape equilibria. First, if $\ell \in \{1, 2, \ldots, n-1\}$, then letting $k = \ell$ in (2.169), we have

$$\hat{\theta}_i^{(\ell)} = \ell\pi/n + (n-2\ell)\pi/n = (n-\ell)\pi/n, \ i = 1, 2, \ldots, n, \tag{2.171}$$

which corresponds with the equilibrium circling values given by (2.168). If $\ell \in \{n+1, n+2, \ldots, 2n-1\}$, then letting $k = \ell - n$ yields

$$\hat{\theta}_i^{(\ell-n)} = \ell\pi/n + \big(n - 2(\ell-n)\big)\pi/n = (n-\ell)\pi/n + 2n(\pi/n) = (n-\ell)\pi/n, \tag{2.172}$$

for $i = 1, 2, \ldots, n$, which again corresponds with (2.168).

In figure 2.6, we display trajectories corresponding to the four unique pure shape equilibria which exist for the particular case $n = 5$, $\alpha_i = \pi/2$. Observe that both outward spirals (top figures) and inward spirals (bottom figures) are possible, with initial conditions dictating system behavior.

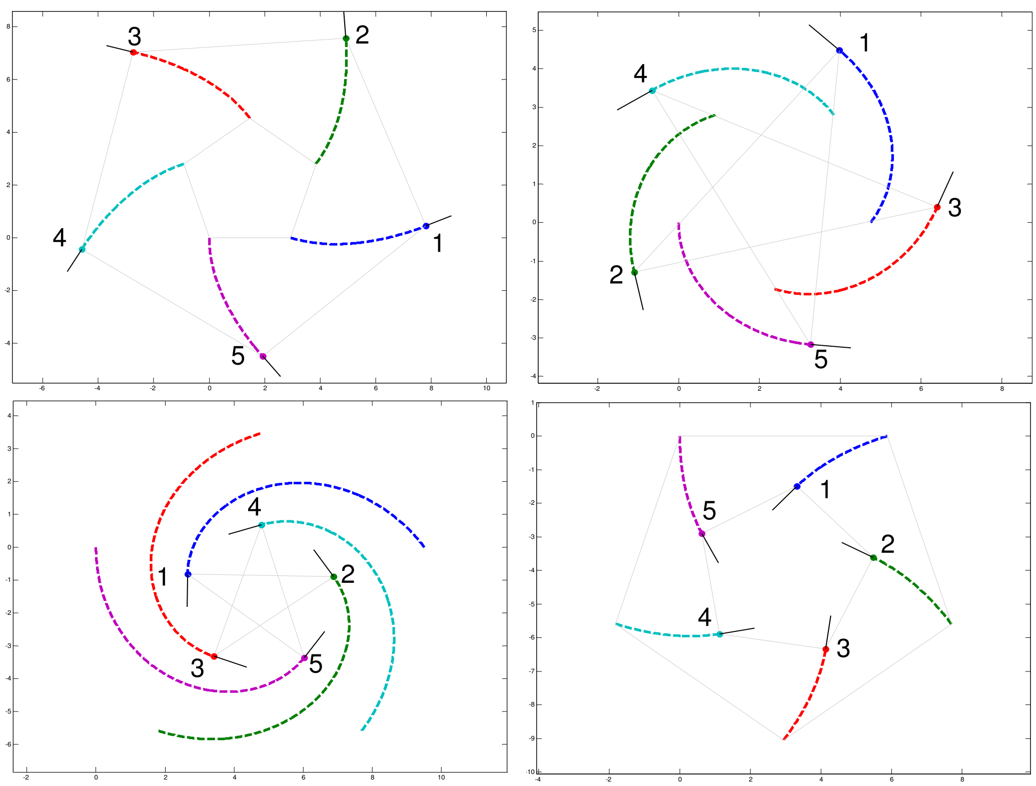

Figure 2.6: This figure illustrates the four unique pure shape equilibria which exist for the particular case $\alpha_1 = \alpha_2 = \alpha_3 = \alpha_4 = \alpha_5 = \pi/2$. In each figure, initial conditions were chosen such that the particle formation started in one of the pure shape equilibrium configurations.

Chapter 3

Low-dimensional planar cases: mutual CB pursuit and three-particle cyclic CB pursuit

3.1 Introduction

In chapter 2, we developed a framework for analyzing n-agent cyclic CB pursuit systems and presented some general results which apply for any value of n, most notably the convergence to the invariant submanifold $M_{CB(\boldsymbol{\alpha})}$ (presented in **Proposition 2.3.2**) and the characterization of existence conditions for special solutions such as relative equilibria and pure shape equilibria (**Propositions 2.4.1** and **2.4.2**). While stability analysis for these special solutions proves very difficult for arbitrary n, in this chapter we demonstrate that the low-dimensional cases ($n = 2$ and $n = 3$) yield a body of rich (and sometimes surprising) results.

For the $n = 2$ "mutual pursuit" case, we demonstrate in section 3.2 that the shape dynamics are integrable, and we derive closed-form solutions for the system evolution on the full shape space M_{shape}. (See **Proposition 3.2.1**.) We then consider the reduced dynamics restricted to the CB pursuit manifold $M_{CB(\alpha_1,\alpha_2)}$ and derive closed-form solutions for reconstruction of the corresponding trajectories in the physical space. Of interest is the comparison of the current work on mutual CB pursuit with the analysis of mutual motion camouflage pursuit in [39]. In particular, we note that the mutual motion camouflage dynamics in [39] are conservative and give rise to periodic trajectories, while the mutual CB pursuit system is dissipative and results in convergence to the invariant manifold $M_{CB(\alpha_1,\alpha_2)}$, on which the reduced dynamics are one-dimensional and linear in the time variable.

In sections 3.3 through 3.7 we consider the $n = 3$ case, first deriving two-dimensional pure shape dynamics (by means of a rescaling of the time variable) which enables phase portrait analysis and stability characterization for the rectilinear equilibria (section 3.5), circling equilibria (section 3.6), and shape-preserving pure shape equilibria (section 3.7). In the course of analyzing three-particle rectilinear equilibria, we demonstrate that a particular choice of parameters results in periodic orbits in the two-dimensional space of pure shape, corresponding to remarkable precessing motions of the three-body system in the full physical space. (See section 3.5.3.) The techniques of reduction and symmetry which we employ here have parallels in recent work on periodic orbits in the Newtonian three-body problem. (See, for instance, [10], [42], and [6].) However, the present context of unit-mass particles interacting through unidirectional pursuit laws is significantly different from the context of celestial mechanics governed by gravitational forces, which provides the foundation of the analysis in the referenced work.

3.2 Mutual CB pursuit ($n = 2$)

3.2.1 Integrable shape dynamics

For the $n = 2$ case, M_{shape} is three-dimensional and our closure constraint equations (2.19) and (2.20) can be easily solved to yield an explicit three variable parametrization. First, substitution of (2.19) into (2.20) results in

$$\rho_1 R(\pi + \kappa_1 - \theta_1) + \rho_2 \mathbb{1} = 0, \tag{3.1}$$

which can be expanded into

$$\begin{aligned} &\rho_1 \cos(\pi + \kappa_1 - \theta_1) + \rho_2 = 0, \\ &\rho_1 \sin(\pi + \kappa_1 - \theta_1) = 0. \end{aligned} \tag{3.2}$$

Since ρ_1 and ρ_2 must be positive, the second equation in (3.2) requires $\sin(\pi + \kappa_1 - \theta_1) = 0$, and it follows that the only valid solution for the pair of equations in (3.2) is given by $\theta_1 = \kappa_1$ with $\rho_1 = \rho_2$. Then by substitution back into (2.19), we have

$$\theta_1 = \kappa_1, \quad \theta_2 = \kappa_2, \quad \rho_1 = \rho_2 = \rho, \tag{3.3}$$

and by (2.61), our mutual CB pursuit dynamics are given by

$$\begin{aligned} \dot{\kappa}_1 &= -\mu_1 \sin(\kappa_1 - \alpha_1), \\ \dot{\kappa}_2 &= -\mu_2 \sin(\kappa_2 - \alpha_2), \\ \dot{\rho} &= -\cos(\kappa_1) - \cos(\kappa_2), \end{aligned} \tag{3.4}$$

with no constraints aside from $\rho > 0$. In fact, we will demonstrate in the following analysis that these shape dynamics can be integrated to obtain closed-form solutions.

Noting that the $\dot{\kappa}_i$ dynamics can be reformulated as

$$\dot{\kappa}_i = -\mu_i \sin\left(\frac{\kappa_i - \alpha_i}{2} + \frac{\kappa_i - \alpha_i}{2}\right) = -2\mu_i \sin\left(\frac{\kappa_i - \alpha_i}{2}\right)\cos\left(\frac{\kappa_i - \alpha_i}{2}\right),\ i = 1, 2, \tag{3.5}$$

we define the change of variables

$$\chi_i \triangleq \tan\left(\frac{\kappa_i - \alpha_i}{2}\right),\ i = 1, 2, \tag{3.6}$$

which is valid for $\kappa_i \neq \alpha_i + \pi$. (In fact, $\kappa_i = \alpha_i + \pi$ is an equilibrium point for the $\dot{\kappa}_i$ dynamics, and therefore it is sufficient to require $\kappa_i(0) \neq \alpha_i + \pi$ to ensure that (3.6) is well-defined.) Then differentiating (3.6), we have

$$\begin{aligned}
\dot{\chi}_i &= \sec^2\left(\frac{\kappa_i - \alpha_i}{2}\right)\left(\frac{\dot{\kappa}_i}{2}\right) \\
&= -\mu_i \sec^2\left(\frac{\kappa_i - \alpha_i}{2}\right)\sin\left(\frac{\kappa_i - \alpha_i}{2}\right)\cos\left(\frac{\kappa_i - \alpha_i}{2}\right) \\
&= -\mu_i \tan\left(\frac{\kappa_i - \alpha_i}{2}\right) \\
&= -\mu_i \chi_i,\ i = 1, 2,
\end{aligned} \tag{3.7}$$

and therefore

$$\chi_i(t) = \chi_i(0)e^{-\mu_i t},\ i = 1, 2, \tag{3.8}$$

where $\chi_i(0) = \tan\left(\frac{1}{2}(\kappa_i(0) - \alpha_i)\right)$. Then expressing our results in terms of the original variables, we have (for $i = 1, 2$)

$$\kappa_i(t) = \begin{cases} \alpha_i + 2\arctan\left(C_i e^{-\mu_i t}\right) & \text{for } C_i = \tan\left(\frac{1}{2}(\kappa_i^0 - \alpha_i)\right),\ \kappa_i(0) = \kappa_i^0 \neq \alpha_i + \pi, \\ \alpha_i + \pi & \text{for } \kappa_i(0) = \alpha_i + \pi. \end{cases} \tag{3.9}$$

Substituting (3.9) into the $\dot{\rho}$ dynamics from (3.4), we have

$$\begin{aligned}\dot{\rho}(t) &= -\sum_{i=1}^{2} \cos\Big(\alpha_i + 2\arctan\left(C_i e^{-\mu_i t}\right)\Big) \\ &= -\sum_{i=1}^{2} \Big[\cos(\alpha_i)\cos\Big(2\arctan\left(C_i e^{-\mu_i t}\right)\Big) - \sin(\alpha_i)\sin\Big(2\arctan\left(C_i e^{-\mu_i t}\right)\Big)\Big],\end{aligned} \tag{3.10}$$

and by applying standard double-angle trigonometric identities, we note that

$$\begin{aligned}\cos\Big(2\arctan\left(C_i e^{-\mu_i t}\right)\Big) &= \frac{1-\tan^2\big(\arctan\left(C_i e^{-\mu_i t}\right)\big)}{1+\tan^2\big(\arctan\left(C_i e^{-\mu_i t}\right)\big)} = \frac{1-\left(C_i e^{-\mu_i t}\right)^2}{1+\left(C_i e^{-\mu_i t}\right)^2}, \\ \sin\Big(2\arctan\left(C_i e^{-\mu_i t}\right)\Big) &= \frac{2\tan\big(\arctan\left(C_i e^{-\mu_i t}\right)\big)}{1+\tan^2\big(\arctan\left(C_i e^{-\mu_i t}\right)\big)} = \frac{2C_i e^{-\mu_i t}}{1+\left(C_i e^{-\mu_i t}\right)^2}.\end{aligned} \tag{3.11}$$

Substituting (3.11) into (3.10) and integrating both sides yields

$$\rho(t) = \rho(0) - \sum_{i=1}^{2}\left[\cos(\alpha_i)\int_0^t \frac{1-\left(C_i e^{-\mu_i\sigma}\right)^2}{1+\left(C_i e^{-\mu_i\sigma}\right)^2} d\sigma - \sin(\alpha_i)\int_0^t \frac{2C_i e^{-\mu_i\sigma}}{1+\left(C_i e^{-\mu_i\sigma}\right)^2} d\sigma\right], \tag{3.12}$$

and integrating by substitution (with $u = C_i e^{-\mu_i\sigma}$, $du = -\mu_i C_i e^{-\mu_i\sigma} d\sigma = -\mu_i u d\sigma$) results in

$$\begin{aligned}\rho(t) = \rho(0) - \sum_{i=1}^{2}\Bigg[&\cos(\alpha_i)\int_{C_i}^{C_i e^{-\mu_i t}} \frac{1-u^2}{1+u^2}\left(-\frac{du}{\mu_i u}\right) \\ &- \sin(\alpha_i)\int_{C_i}^{C_i e^{-\mu_i t}} \frac{2u}{1+u^2}\left(-\frac{du}{\mu_i u}\right)\Bigg] \\ = \rho(0) + \sum_{i=1}^{2}\frac{1}{\mu_i}&\left[\cos(\alpha_i)\int_{C_i}^{C_i e^{-\mu_i t}} \frac{1-u^2}{u(1+u^2)} du - \sin(\alpha_i)\int_{C_i}^{C_i e^{-\mu_i t}} \frac{2}{1+u^2} du\right] \\ = \rho(0) + \sum_{i=1}^{2}\frac{1}{\mu_i}&\left[\cos(\alpha_i)\ln\left(\frac{u}{1+u^2}\right)\Bigg|_{C_i}^{C_i e^{-\mu_i t}} - 2\sin(\alpha_i)\arctan(u)\Bigg|_{C_i}^{C_i e^{-\mu_i t}}\right].\end{aligned} \tag{3.13}$$

Then noting that

$$\begin{aligned}
\ln\left(\frac{u}{1+u^2}\right)\Bigg|_{C_i}^{C_i e^{-\mu_i t}} &= \ln\left(\frac{C_i e^{-\mu_i t}}{1+(C_i e^{-\mu_i t})^2}\right) - \ln\left(\frac{C_i}{1+C_i^2}\right) \\
&= \ln\left(e^{-\mu_i t}\frac{C_i\left(1+C_i^2\right)}{C_i\left(1+(C_i e^{-\mu_i t})^2\right)}\right) \\
&= -\mu_i t + \ln\left(\frac{1+C_i^2}{1+C_i^2 e^{-2\mu_i t}}\right),
\end{aligned}$$

and

$$\arctan(u)\Bigg|_{C_i}^{C_i e^{-\mu_i t}} = \arctan\left(C_i e^{-\mu_i t}\right) - \arctan\left(C_i\right) = \arctan\left(\frac{C_i\left(e^{-\mu_i t}-1\right)}{1+C_i^2 e^{-\mu_i t}}\right),$$

we can state the closed-form solution in terms of the following proposition.

Proposition 3.2.1. *The mutual CB pursuit shape dynamics (3.4) are integrable and yield the closed-form solutions*

$$\kappa_i(t) = \alpha_i + 2\arctan\left(C_i e^{-\mu_i t}\right),\ i = 1, 2, \tag{3.14}$$

$$\begin{aligned}
\rho(t) = \rho(0) &- \left[\cos(\alpha_1) + \cos(\alpha_2)\right] t \\
&+ \sum_{i=1}^{2} \frac{1}{\mu_i}\left[\cos(\alpha_i)\ln\left(\frac{1+C_i^2}{1+C_i^2 e^{-2\mu_i t}}\right) - 2\sin(\alpha_i)\arctan\left(\frac{C_i\left(e^{-\mu_i t}-1\right)}{1+C_i^2 e^{-\mu_i t}}\right)\right],
\end{aligned} \tag{3.15}$$

for $\kappa_i(0) = \kappa_i^0 \neq \alpha_i + \pi$, $C_i = \tan\left(\frac{1}{2}(\kappa_i^0 - \alpha_i)\right)$, $\rho(0) = \rho_0 > 0$, *and* $t < t_c$, *where* t_c *is the minimum time such that* $\rho(t_c) = 0$, *with* $t_c = \infty$ *if* $\rho(t) > 0$ *for all finite* t.

For $\kappa_i(0) = \alpha_i + \pi$, *it holds that* $\kappa_i(t) \equiv \alpha_i + \pi$, $i = 1, 2$, *and* $\rho(t) = \rho_0 + [\cos(\alpha_1) + \cos(\alpha_2)]\,t$ *for* $t < t_c$, *where* $t_c = \rho_0/[\cos(\alpha_1) + \cos(\alpha_2)]$ *for* $\cos(\alpha_1) + \cos(\alpha_2) < 0$ *and* $t_c = \infty$ *else.*

Proof. The proof follows from the previous discussion, with the additional assumption $t < t_c$ required to enforce our non-collision hypothesis. □

Remark 3.2.2 For $\kappa_i(0) \neq \alpha_i + \pi$, **Proposition 3.2.1** implies that $\kappa_i(t) \longrightarrow \alpha_i$ as $t \longrightarrow \infty$, i.e. the system asymptotically approaches the CB Pursuit Manifold $M_{CB(\alpha_1,\alpha_2)}$. This also follows from the general result stated in **Proposition 2.3.2**.

Remark 3.2.3 For the general n-particle case, the same process detailed here can be used to integrate the $\dot{\kappa}_i$ dynamics from (2.61), yielding analagous closed-form solutions for κ_i. However, unlike the two-particle case, the $\dot{\rho}_i$ dynamics can not be subsequently integrated due to their dependence on the θ_i variables.

3.2.2 Center of mass trajectory

While the previous section considered the system evolution on the entire shape space, we now restrict our attention to the submanifold $M_{CB(\alpha_1,\alpha_2)}$. This approach enables a straightforward reconstruction of the corresponding particle trajectories in the plane, by deriving closed-form solutions for both the baseline vector

$$\mathbf{r} \triangleq \mathbf{r}_1 - \mathbf{r}_2 \tag{3.16}$$

and the center of mass $\mathbf{z} \triangleq \frac{1}{2}(\mathbf{r}_1 + \mathbf{r}_2)$.

Since $|\mathbf{r}| = \rho$, and on $M_{CB(\alpha_1,\alpha_2)}$ we have $\kappa_1 \equiv \alpha_1$ and $\kappa_2 \equiv \alpha_2$, substitution into (3.15) yields

$$|\mathbf{r}(t)| = \rho(t) = \rho_0 - \eta_+ t, \tag{3.17}$$

where we have defined

$$\eta_+ \triangleq \cos(\alpha_1) + \cos(\alpha_2). \tag{3.18}$$

Note that if $\eta_+ > 0$, then (3.17) implies that there will be collision in finite time, and therefore we restrict our analysis to $t < t_c$, where

$$t_c = \begin{cases} \rho_0/\eta_+ & \text{for } \eta_+ > 0 \\ \infty & \text{for } \eta_+ \leq 0. \end{cases} \tag{3.19}$$

Observe that (2.24) provides the $M_{CB(\alpha_1,\alpha_2)}$ relations

$$\begin{aligned} \mathbf{x}_1 \cdot \frac{\mathbf{r}}{|\mathbf{r}|} &= -\cos(\alpha_1), \quad \mathbf{y}_1 \cdot \frac{\mathbf{r}}{|\mathbf{r}|} = -\sin(\alpha_1), \\ \mathbf{x}_2 \cdot \frac{\mathbf{r}}{|\mathbf{r}|} &= \cos(\alpha_2), \quad \mathbf{y}_2 \cdot \frac{\mathbf{r}}{|\mathbf{r}|} = \sin(\alpha_2). \end{aligned} \tag{3.20}$$

We proceed by deriving a closed-form solution for the evolution of the baseline vector $\mathbf{r}$. First, we observe that

$$\begin{aligned} \frac{d}{dt}\left(\frac{\mathbf{r}}{|\mathbf{r}|}\right) &= \frac{1}{|\mathbf{r}|^2}\left[\dot{\mathbf{r}}\,|\mathbf{r}| - \mathbf{r}\frac{d\,(|\mathbf{r}|)}{dt}\right] \\ &= \frac{1}{|\mathbf{r}|}\left[\dot{\mathbf{r}} - \left(\dot{\mathbf{r}} \cdot \frac{\mathbf{r}}{|\mathbf{r}|}\right)\frac{\mathbf{r}}{|\mathbf{r}|}\right] \\ &= \frac{1}{|\mathbf{r}|}\left(\dot{\mathbf{r}} \cdot \frac{\mathbf{r}^\perp}{|\mathbf{r}|}\right)\frac{\mathbf{r}^\perp}{|\mathbf{r}|}, \end{aligned} \tag{3.21}$$

where the last step follows from the decomposition of $\dot{\mathbf{r}}$ in the basis vectors $\frac{\mathbf{r}}{|\mathbf{r}|}$ and $\frac{\mathbf{r}^\perp}{|\mathbf{r}|}$. By (2.2) we have $\dot{\mathbf{r}} = \mathbf{x}_1 - \mathbf{x}_2$ and $\dot{\mathbf{r}}^\perp = \mathbf{y}_1 - \mathbf{y}_2$, and therefore application of

(1.11) and (3.20) to (3.21) yields

$$
\begin{aligned}
\frac{d}{dt}\left(\frac{\mathbf{r}}{|\mathbf{r}|}\right) &= \frac{1}{|\mathbf{r}|}\left((\mathbf{x}_1-\mathbf{x}_2)\cdot\frac{\mathbf{r}^\perp}{|\mathbf{r}|}\right)\frac{\mathbf{r}^\perp}{|\mathbf{r}|} \\
&= \frac{1}{\rho}\left(-(\mathbf{y}_1-\mathbf{y}_2)\cdot\frac{\mathbf{r}}{|\mathbf{r}|}\right)R\left(\frac{\pi}{2}\right)\frac{\mathbf{r}}{|\mathbf{r}|} \\
&= \frac{1}{\rho_0-\eta_+ t}\Big(\sin(\alpha_1)+\sin(\alpha_2)\Big)\begin{pmatrix} 0 & -1 \\ 1 & 0 \end{pmatrix}\frac{\mathbf{r}}{|\mathbf{r}|} \\
&= \begin{pmatrix} 0 & -\frac{\omega_+}{\rho_0-\eta_+ t} \\ \frac{\omega_+}{\rho_0-\eta_+ t} & 0 \end{pmatrix}\frac{\mathbf{r}}{|\mathbf{r}|},
\end{aligned} \tag{3.22}
$$

where we have defined

$$
\omega_+ \triangleq \sin(\alpha_1)+\sin(\alpha_2). \tag{3.23}
$$

If $\eta_+ = 0$, then (3.22) is a linear time-invariant system with transition matrix

$$
\exp\begin{pmatrix} 0 & -\frac{\omega_+}{\rho_0}t \\ \frac{\omega_+}{\rho_0}t & 0 \end{pmatrix} = \begin{pmatrix} \cos\left(\frac{\omega_+}{\rho_0}t\right) & -\sin\left(\frac{\omega_+}{\rho_0}t\right) \\ \sin\left(\frac{\omega_+}{\rho_0}t\right) & \cos\left(\frac{\omega_+}{\rho_0}t\right) \end{pmatrix} = R\left(\frac{\omega_+}{\rho_0}t\right). \tag{3.24}
$$

For $\eta_+ \neq 0$, similar calculations yield the transition matrix for the linear time-varying system which is given by

$$
R\left(\int_0^t \frac{\omega_+}{\rho_0-\eta_+\sigma}d\sigma\right) = R\left(\frac{-\omega_+}{\eta_+}\ln\left(\rho_0-\eta_+\sigma\right)\Big|_0^t\right) = R\left(\frac{-\omega_+}{\eta_+}\ln\left(\frac{\rho_0-\eta_+ t}{\rho_0}\right)\right). \tag{3.25}
$$

Therefore by (3.17), (3.22), (3.24) and (3.25), we have an explicit solution for the evolution of the baseline vector $\mathbf{r}$ given by

$$
\mathbf{r}(t) = \begin{cases} \frac{\rho_0-\eta_+ t}{\rho_0}R\left(\frac{-\omega_+}{\eta_+}\ln\left(\frac{\rho_0-\eta_+ t}{\rho_0}\right)\right)\mathbf{r}_0 & \text{for } \eta_+ \neq 0 \\ R\left(\frac{\omega_+}{\rho_0}t\right)\mathbf{r}_0 & \text{for } \eta_+ = 0, \end{cases}
$$

$$
\text{for } \mathbf{r}(0)=\mathbf{r}_0,\ \rho_0 = |\mathbf{r}_0|\,,\ t<t_c, \tag{3.26}
$$

where t_c is defined by (3.19).

In the following proposition we complete the reconstruction problem by characterizing the trajectory of the center of mass in terms of the parameters

$$\begin{aligned} \omega_+ &\triangleq \sin(\alpha_1) + \sin(\alpha_2), \quad \omega_- \triangleq \sin(\alpha_1) - \sin(\alpha_2), \\ \eta_+ &\triangleq \cos(\alpha_1) + \cos(\alpha_2), \quad \eta_- \triangleq \cos(\alpha_1) - \cos(\alpha_2), \end{aligned} \tag{3.27}$$

which satisfy the identity

$$\omega_+\omega_- = \sin^2(\alpha_1) - \sin^2(\alpha_2) = -\cos^2(\alpha_1) + \cos^2(\alpha_2) = -\eta_+\eta_-. \tag{3.28}$$

Proposition 3.2.4. *Consider a two-particle mutual CB pursuit system operating on $M_{CB(\alpha_1,\alpha_2)}$ according to the dynamics (2.2) with $\nu_i = 1$ and u_i given by (2.59). Let the initial conditions be given by $\mathbf{r}_i(0) = \mathbf{r}_i^0$ and $\mathbf{x}_i(0) = \mathbf{x}_i^0$, $i = 1, 2$. Define the change of coordinates $\tilde{\mathbf{r}}_i \triangleq \mathbf{r}_i - \mathbf{r}_c$, where $\mathbf{r}_c$ is given by*

$$\mathbf{r}_c \triangleq \begin{cases} \mathbf{z}_0 - \sigma_0 \left(\frac{\mathbf{r}(0)}{|\mathbf{r}(0)|} \right)^{\perp} & \text{for } \omega_+ \neq 0, \\ 0 & \text{for } \omega_+ = 0, \end{cases} \tag{3.29}$$

with $\mathbf{z}_0 = \frac{1}{2}\left(\mathbf{r}_1^0 + \mathbf{r}_2^0\right)$ and $\sigma_0 = \frac{\rho_0}{2}\left(\frac{\eta_-}{\omega_+}\right)$. Then the trajectory of the center of mass $\mathbf{z} \triangleq \frac{1}{2}(\mathbf{r}_1 + \mathbf{r}_2)$ can be given in the new coordinates $\tilde{\mathbf{z}} = \mathbf{z} - \mathbf{r}_c$ by the following:

(i) if $\omega_+ = 0$, then $\tilde{\mathbf{z}}(t) = \tilde{\mathbf{z}}_0 + \dfrac{1}{2}\left(\mathbf{x}_1^0 + \mathbf{x}_2^0\right) t$,

(ii) if $\omega_+ \neq 0$ but $\eta_+ = 0$, then $\tilde{\mathbf{z}}(t) = R\left(\dfrac{\omega_+}{\rho_0} t\right) \tilde{\mathbf{z}}_0$,

(iii) if ω_+ and η_+ are both nonzero, then

$$\tilde{\mathbf{z}}(t) = \left(\frac{\rho_0 - \eta_+ t}{\rho_0}\right) R\left(\frac{-\omega_+}{\eta_+} \ln\left(\frac{\rho_0 - \eta_+ t}{\rho_0}\right)\right) \tilde{\mathbf{z}}_0, \tag{3.30}$$

for $t < t_c$, where t_c is defined by (3.19).

Proof. Figure 3.1 depicts representative trajectories for each of the cases described in **Proposition 3.2.4** and proves helpful in illustrating the proof. On $M_{CB(\alpha_1,\alpha_2)}$, it follows from (3.20) that $\mathbf{x}_1(t) = -R(-\alpha_1)\frac{\mathbf{r(t)}}{|\mathbf{r(t)}|}$ and $\mathbf{x}_2(t) = R(-\alpha_2)\frac{\mathbf{r}(t)}{|\mathbf{r}(t)|}$. Therefore if $\omega_+ = 0$, then by (3.26) we have $\frac{\mathbf{r}(t)}{|\mathbf{r}(t)|} \equiv \frac{\mathbf{r}_0}{|\mathbf{r}_0|}$ and hence $\mathbf{x}_i(t) \equiv \mathbf{x}_i^0$. Thus $\dot{\mathbf{z}}(t) = \frac{1}{2}\left(\mathbf{x}_1^0 + \mathbf{x}_2^0\right)$, from which the first claim of the proposition follows.

For $\omega_+ \neq 0$, we will demonstrate that the center of mass follows either a circling or spiraling trajectory[1] centered on the point $\mathbf{r}_c$. We can resolve $\tilde{\mathbf{z}}$ into component vectors as

$$\tilde{\mathbf{z}} = \left(\tilde{\mathbf{z}} \cdot \frac{\mathbf{r}}{|\mathbf{r}|}\right)\frac{\mathbf{r}}{|\mathbf{r}|} + \left(\tilde{\mathbf{z}} \cdot \frac{\mathbf{r}^\perp}{|\mathbf{r}|}\right)\frac{\mathbf{r}^\perp}{|\mathbf{r}|}, \tag{3.31}$$

and the main thrust of the proof is to demonstrate that the first term is identically zero, (i.e. we have chosen the shifted coordinates such that $\tilde{\mathbf{z}}$ is always orthogonal to $\frac{\mathbf{r}}{|\mathbf{r}|}$), and to derive a suitable form for the second term. We proceed by defining

$$\gamma \triangleq \tilde{\mathbf{z}} \cdot \frac{\mathbf{r}}{|\mathbf{r}|}, \quad \sigma \triangleq \tilde{\mathbf{z}} \cdot \frac{\mathbf{r}^\perp}{|\mathbf{r}|}, \tag{3.32}$$

noting that

$$\begin{aligned}
\sigma(0) &= \tilde{\mathbf{z}}(0) \cdot \left(\frac{\mathbf{r}(0)}{|\mathbf{r}(0)|}\right)^\perp = (\mathbf{z}(0) - \mathbf{r}_c) \cdot \left(\frac{\mathbf{r}(0)}{|\mathbf{r}(0)|}\right)^\perp = \sigma_0, \\
\gamma(0) &= \tilde{\mathbf{z}}(0) \cdot \frac{\mathbf{r}(0)}{|\mathbf{r}(0)|} = (\mathbf{z}(0) - \mathbf{r}_c) \cdot \frac{\mathbf{r}(0)}{|\mathbf{r}(0)|} = \sigma_0 \left(\frac{\mathbf{r}_0}{|\mathbf{r}_0|}\right)^\perp \cdot \frac{\mathbf{r}_0}{|\mathbf{r}_0|} = 0,
\end{aligned} \tag{3.33}$$

where σ_0 is defined in the statement of the proposition. Then making use of (3.20)

[1]For the special case where $\eta_- \triangleq \cos(\alpha_1) - \cos(\alpha_2) = 0$, we have $\sigma(t) \equiv 0$, and in this case the radius of rotation is zero (i.e., the center of mass is fixed).

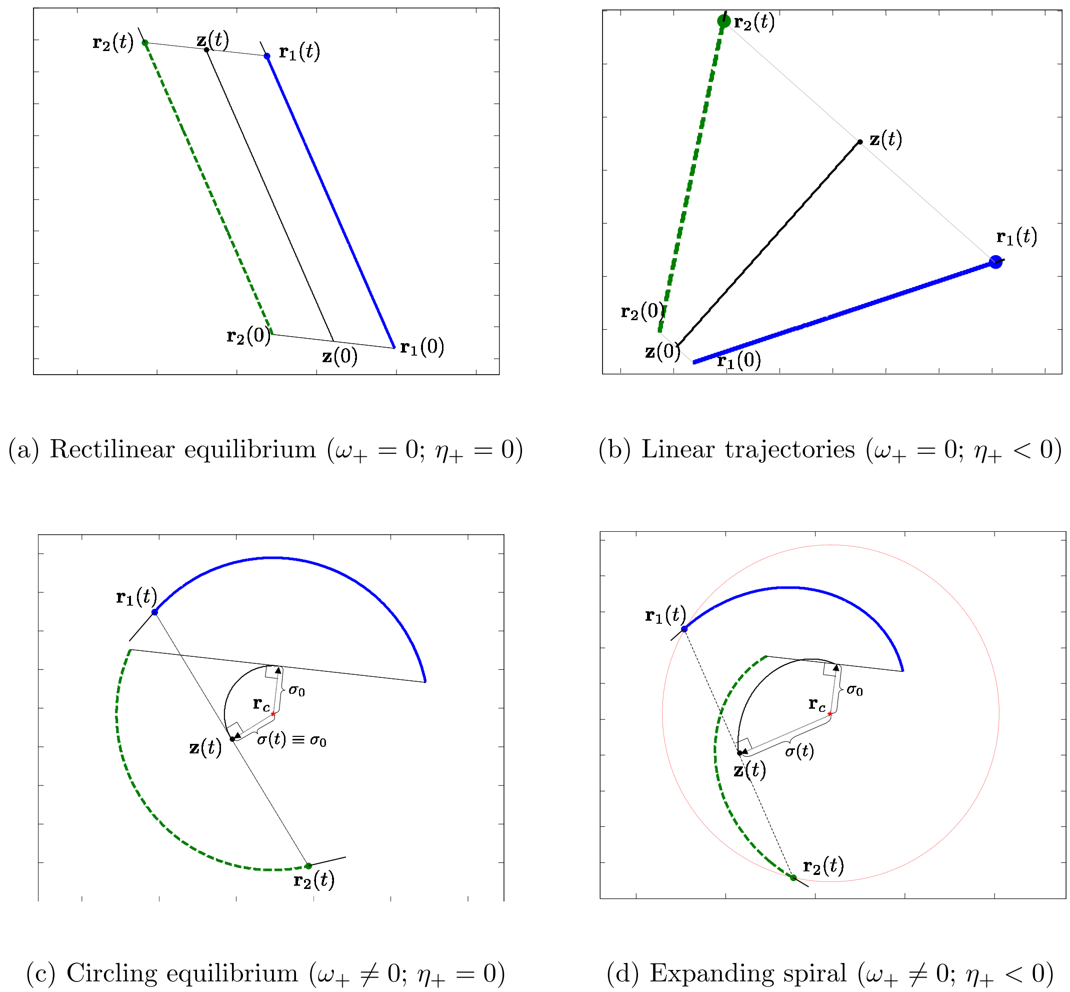

(a) Rectilinear equilibrium ($\omega_+ = 0$; $\eta_+ = 0$)

(b) Linear trajectories ($\omega_+ = 0$; $\eta_+ < 0$)

(c) Circling equilibrium ($\omega_+ \neq 0$; $\eta_+ = 0$)

(d) Expanding spiral ($\omega_+ \neq 0$; $\eta_+ < 0$)

Figure 3.1: These figures illustrate representative trajectories for each of the cases discussed in **Proposition 3.2.4**. The thicker trajectories denote the movement of $\mathbf{r}_1(t)$ (solid) and $\mathbf{r}_2(t)$ (dashed), and the thinner solid trajectory denotes the center of mass $\mathbf{z}(t)$. Note that the point $\mathbf{r}_c$ has been chosen such that $\tilde{\mathbf{z}}(t) = \mathbf{z}(t) - \mathbf{r}_c$ is always orthogonal to $\mathbf{r}(t) = \mathbf{r}_1(t) - \mathbf{r}_2(t)$.

and (3.22), we take the derivatives of σ and γ to obtain

$$
\begin{aligned}
\dot{\sigma} &= \left(\dot{\tilde{\mathbf{z}}} \cdot \frac{\mathbf{r}^{\perp}}{|\mathbf{r}|}\right) + \tilde{\mathbf{z}} \cdot \left(\frac{d}{dt}\left(\frac{\mathbf{r}}{|\mathbf{r}|}\right)\right)^{\perp} \\
&= \frac{1}{2}\left((\mathbf{x}_1 + \mathbf{x}_2) \cdot \frac{\mathbf{r}^{\perp}}{|\mathbf{r}|}\right) + \tilde{\mathbf{z}} \cdot \left(\left(\frac{\omega_+}{\rho_0 - \eta_+ t}\right)\frac{\mathbf{r}^{\perp}}{|\mathbf{r}|}\right)^{\perp} \\
&= -\frac{1}{2}\left((\mathbf{y}_1 + \mathbf{y}_2) \cdot \frac{\mathbf{r}}{|\mathbf{r}|}\right) - \left(\frac{\omega_+}{\rho_0 - \eta_+ t}\right)\left(\tilde{\mathbf{z}} \cdot \frac{\mathbf{r}}{|\mathbf{r}|}\right) \\
&= \frac{\omega_-}{2} - \left(\frac{\omega_+}{\rho_0 - \eta_+ t}\right)\gamma
\end{aligned} \tag{3.34}
$$

and

$$
\begin{aligned}
\dot{\gamma} &= \left(\dot{\tilde{\mathbf{z}}} \cdot \frac{\mathbf{r}}{|\mathbf{r}|}\right) + \tilde{\mathbf{z}} \cdot \left(\frac{d}{dt}\left(\frac{\mathbf{r}}{|\mathbf{r}|}\right)\right) \\
&= \frac{1}{2}\left((\mathbf{x}_1 + \mathbf{x}_2) \cdot \frac{\mathbf{r}}{|\mathbf{r}|}\right) + \tilde{\mathbf{z}} \cdot \left(\left(\frac{\omega_+}{\rho_0 - \eta_+ t}\right)\frac{\mathbf{r}^{\perp}}{|\mathbf{r}|}\right) \\
&= -\frac{\eta_-}{2} + \left(\frac{\omega_+}{\rho_0 - \eta_+ t}\right)\sigma.
\end{aligned} \tag{3.35}
$$

Then differentiating (3.35), we have

$$
\begin{aligned}
\ddot{\gamma} &= \left(\frac{\omega_+ \eta_+}{(\rho_0 - \eta_+ t)^2}\right)\sigma + \left(\frac{\omega_+}{\rho_0 - \eta_+ t}\right)\dot{\sigma} \\
&= \left(\frac{\eta_+}{\rho_0 - \eta_+ t}\right)\left(\frac{\omega_+}{\rho_0 - \eta_+ t}\right)\sigma + \left(\frac{\omega_+}{\rho_0 - \eta_+ t}\right)\left(\frac{\omega_-}{2}\right) - \left(\frac{\omega_+}{\rho_0 - \eta_+ t}\right)^2\gamma \\
&= \left(\frac{\eta_+}{\rho_0 - \eta_+ t}\right)\left(\dot{\gamma} + \frac{\eta_-}{2}\right) + \left(\frac{\omega_+}{\rho_0 - \eta_+ t}\right)\left(\frac{\omega_-}{2}\right) - \left(\frac{\omega_+}{\rho_0 - \eta_+ t}\right)^2\gamma \\
&= \left(\frac{\eta_+}{\rho_0 - \eta_+ t}\right)\dot{\gamma} - \left(\frac{\omega_+}{\rho_0 - \eta_+ t}\right)^2\gamma,
\end{aligned} \tag{3.36}
$$

where the last step follows by application of (3.28). By (3.33) and (3.35) we have $\gamma(0) = 0$ and $\dot{\gamma}(0) = -\frac{\eta_-}{2} + \left(\frac{\omega_+}{\rho_0}\right)\sigma_0 = 0$, and thus (3.36) implies $\gamma \equiv 0$. Hence (3.31) simplifies to

$$\tilde{\mathbf{z}} = \sigma\frac{\mathbf{r}^{\perp}}{|\mathbf{r}|}, \tag{3.37}$$

and (3.34) becomes

$$\dot{\sigma} = \frac{\omega_-}{2}. \tag{3.38}$$

By (3.33) we have $\sigma(0) = \sigma_0$, and therefore integrating (3.38) yields

$$\begin{aligned}
\sigma(t) &= \sigma_0 + \left(\frac{\omega_-}{2}\right) t \\
&= \frac{1}{2}\left(\rho_0\left(\frac{\eta_-}{\omega_+}\right) + (\omega_-)t\right) \\
&= \frac{1}{2\omega_+}\left(\rho_0\eta_- + (\omega_+\omega_-)t\right) \\
&= \frac{1}{2\omega_+}\left(\rho_0\eta_- - (\eta_+\eta_-)t\right) \\
&= \frac{\eta_-}{2\omega_+}\left(\rho_0 - \eta_+ t\right) \\
&= \frac{\sigma_0}{\rho_0}\rho(t), \qquad (3.39)
\end{aligned}$$

where we have made use of (3.17) and (3.28). To complete the proof, we substitute (3.26) and (3.39) into (3.37) to obtain

$$\begin{aligned}
\tilde{\mathbf{z}} &= \frac{\sigma_0}{\rho_0}\mathbf{r}^{\perp} \\
&= \begin{cases} \frac{\rho_0-\eta_+ t}{\rho_0} R\left(\frac{-\omega_+}{\eta_+}\ln\left(\frac{\rho_0-\eta_+ t}{\rho_0}\right)\right)\frac{\sigma_0}{\rho_0}\mathbf{r}_0^{\perp} & \text{for } \eta_+ \neq 0 \\ R\left(\frac{\omega_+}{\rho_0}t\right)\frac{\sigma_0}{\rho_0}\mathbf{r}_0^{\perp} & \text{for } \eta_+ = 0, \end{cases} \\
&= \begin{cases} \frac{\rho_0-\eta_+ t}{\rho_0} R\left(\frac{-\omega_+}{\eta_+}\ln\left(\frac{\rho_0-\eta_+ t}{\rho_0}\right)\right)\tilde{\mathbf{z}}_0 & \text{for } \eta_+ \neq 0 \\ R\left(\frac{\omega_+}{\rho_0}t\right)\tilde{\mathbf{z}}_0 & \text{for } \eta_+ = 0. \end{cases} \qquad (3.40)
\end{aligned}$$

□

Remark 3.2.5 Observe that the trajectories of the individual agents can be reconstructured from (3.26) and (3.30) by

$$\tilde{\mathbf{r}}_1 = \tilde{\mathbf{z}} + \frac{1}{2}\mathbf{r} \quad \text{and} \quad \tilde{\mathbf{r}}_2 = \tilde{\mathbf{z}} - \frac{1}{2}\mathbf{r}. \tag{3.41}$$

We can provide physical interpretations of the three cases in **Proposition 3.2.4** as follows. In the first case (i.e. $\omega_+ = 0$), the baseline vector $\mathbf{r}$ does not rotate, and the agents (and the center of mass) follow linear trajectories[2]. The case where both $\omega_+ = 0$ and $\eta_+ = 0$ corresponds to a rectilinear equilibrium. The second case in **Proposition 3.2.4** ($\omega_+ \neq 0$, $\eta_+ = 0$) corresponds to a circling equilibrium, and the last case ($\omega_+ \neq 0$, $\eta_+ \neq 0$) corresponds to a pure shape equilibrium with spiraling out (for $\eta_+ < 0$) or spiraling in (for $\eta_+ > 0$). For the circling equilibria and pure shape equilibria, we note that $\eta_- = 0 \implies \sigma_0 = 0 \implies \tilde{\mathbf{z}}_0 = 0 \implies \tilde{\mathbf{z}} \equiv 0$, i.e. if $\eta_- = 0$ then the center of mass is fixed at its initial position.

3.3 Three-particle pure shape dynamics

In section 2.4.2 we described the $(2n-4)$-dimensional manifold $\tilde{M}_{CB(\boldsymbol{\alpha})}$ and the associated (time-scaled) pure shape dynamics given by (2.103)-(2.104). In this section we focus on the $n = 3$ case, making use of constraint equations to explicitly demonstrate the reduction to two-dimensional pure shape dynamics on $\tilde{M}_{CB(\alpha_1,\alpha_2,\alpha_3)}$, a process which is illustrated in figure 3.2. Rather than beginning with the dynamics in (2.103)-(2.104), we choose to start directly from the original $M_{CB(\alpha_1,\alpha_2,\alpha_3)}$ dynamics (2.68) and use an approach analogous to that in section 2.4.2. For convenience,

[2]In the special cases $\alpha_1 = \alpha_2 = 0$ and $\alpha_1 = \alpha_2 = \pi$, the agents follow linear trajectories but the center of mass is fixed.

we restate the $M_{CB(\alpha_1,\alpha_2,\alpha_3)}$ dynamics here,

$$\dot{\theta}_i = \frac{\sin(\alpha_{i-1}) + \sin(\theta_i)}{\rho_{i-1}} - \frac{\sin(\alpha_i) + \sin(\theta_{i+1})}{\rho_i},$$
$$\dot{\rho}_i = -\left[\cos(\alpha_i) + \cos(\theta_{i+1})\right],\ i = 1, 2, 3, \tag{3.42}$$

recalling the governing constraint equations

$$R\left(\sum_{i=1}^{3}(\pi + \alpha_i - \theta_i)\right) = \mathbb{1}, \tag{3.43}$$
$$\sum_{i=1}^{3}\rho_i R\left(\sum_{j=1}^{i}(\pi + \alpha_j - \theta_j)\right) = 0. \tag{3.44}$$

As a first step, we eliminate θ_1, θ_3, and ρ_3 by means of (3.43) and (3.44), so that we can explicitly describe our shape dynamics in terms of only θ_2, ρ_1, and ρ_2. We first note that (3.43) implies

$$\sum_{i=1}^{3}(\pi + \alpha_i - \theta_i) = 0, \tag{3.45}$$

and therefore $\theta_1 = \pi + \alpha_1 + \alpha_2 + \alpha_3 - \theta_2 - \theta_3$. Then substitution into (3.44) yields

$$\begin{aligned} 0 &= \rho_1 R(\pi + \alpha_1 - \theta_1) + \rho_2 R(\alpha_1 + \alpha_2 - \theta_1 - \theta_2) + \rho_3 \mathbb{1} \\ &= \rho_1 R(-\alpha_2 - \alpha_3 + \theta_2 + \theta_3) + \rho_2 R(\pi - \alpha_3 + \theta_3) + \rho_3 \mathbb{1} \\ &= R(\theta_3)\Big[\rho_1 R(\theta_2 - \alpha_2 - \alpha_3) + \rho_2 R(\pi - \alpha_3) + \rho_3 R(-\theta_3)\Big], \end{aligned} \tag{3.46}$$

and since elements of $SO(2)$ are nonsingular (i.e. $R(\theta_3)$ is nonsingular), the term in brackets must be the zero matrix. Writing this component-wise gives us

$$\rho_3 \sin(\theta_3) = \rho_1 \sin(\theta_2 - \alpha_2 - \alpha_3) + \rho_2 \sin(\alpha_3),$$
$$\rho_3 \cos(\theta_3) = -\rho_1 \cos(\theta_2 - \alpha_2 - \alpha_3) + \rho_2 \cos(\alpha_3). \tag{3.47}$$

By summing the square of each equation in (3.47), we have

$$\rho_3^2 = \rho_1^2 + 2\rho_1\rho_2\Big(\sin(\theta_2 - \alpha_2 - \alpha_3)\sin(\alpha_3) - \cos(\theta_2 - \alpha_2 - \alpha_3)\cos(\alpha_3)\Big) + \rho_2^2$$
$$= \rho_1^2 - 2\rho_1\rho_2\cos(\theta_2 - \alpha_2) + \rho_2^2$$
$$= \rho_1^2\left[1 - 2\left(\frac{\rho_2}{\rho_1}\right)\cos(\theta_2 - \alpha_2) + \left(\frac{\rho_2}{\rho_1}\right)^2\right], \tag{3.48}$$

which, by the strict positivity of ρ_3, yields

$$\rho_3 = \rho_1 P(\rho_1, \rho_2, \theta_2), \tag{3.49}$$

where $P(\rho_1, \rho_2, \theta_2) \triangleq \sqrt{\left(\frac{\rho_2}{\rho_1}\right)^2 - 2\left(\frac{\rho_2}{\rho_1}\right)\cos(\theta_2 - \alpha_2) + 1}$. We restrict our analysis to M_{shape} (i.e. no sequential colocation), and thus we forbid $\rho_1 = \rho_2$ with $\theta_2 = \alpha_2$, which is the only condition under which $P(\rho_1, \rho_2, \theta_2) = 0$. Then substituting (3.47) and (3.49) into (3.42), we have an equivalent representation of our three-particle shape dynamics on $M_{CB(\alpha_1,\alpha_2,\alpha_3)}$, given by

$$\dot{\theta}_2 = \frac{1}{\rho_1}\left[\sin(\alpha_1) + \sin(\theta_2)\right] - \frac{1}{\rho_2}\left[\sin(\alpha_2) + \frac{\sin(\theta_2 - \alpha_2 - \alpha_3) + \frac{\rho_2}{\rho_1}\sin(\alpha_3)}{P(\rho_1, \rho_2, \theta_2)}\right],$$
$$\dot{\rho}_1 = -\cos(\alpha_1) - \cos(\theta_2),$$
$$\dot{\rho}_2 = -\cos(\alpha_2) - \frac{-\cos(\theta_2 - \alpha_2 - \alpha_3) + \frac{\rho_2}{\rho_1}\cos(\alpha_3)}{P(\rho_1, \rho_2, \theta_2)}. \tag{3.50}$$

These dynamics are subject only to the strict positivity constraints on ρ_1, ρ_2, and $P(\rho_1, \rho_2, \theta_2)$.

Letting

$$\tilde{\lambda} \triangleq \ln(\rho_2/\rho_1) \tag{3.51}$$

and denoting

$$P \triangleq \sqrt{e^{2\tilde{\lambda}} - 2e^{\tilde{\lambda}}\cos(\theta_2 - \alpha_2) + 1}, \tag{3.52}$$

we have

$$
\begin{aligned}
\dot{\tilde{\lambda}} &= \frac{1}{\left(\frac{\rho_2}{\rho 1}\right)} \left\{ \left(\frac{1}{\rho_1}\right) \left[\left(\frac{-\rho_2}{\rho_1}\right) \dot{\rho}_1 + \dot{\rho}_2 \right] \right\} \\
&= \frac{1}{e^{\tilde{\lambda}}\rho_1} \left\{ e^{\tilde{\lambda}} \Big(\cos(\alpha_1) + \cos(\theta_2) \Big) - \cos(\alpha_2) + \frac{1}{P} \Big(\cos(\theta_2 - \alpha_2 - \alpha_3) - e^{\tilde{\lambda}} \cos(\alpha_3) \Big) \right\} \\
&= \frac{1}{e^{\tilde{\lambda}}\rho_1 P} \left\{ P \left[e^{\tilde{\lambda}} \Big(\cos(\alpha_1) + \cos(\theta_2) \Big) - \cos(\alpha_2) \right] + \cos(\theta_2 - \alpha_2 - \alpha_3) - e^{\tilde{\lambda}} \cos(\alpha_3) \right\},
\end{aligned}
\tag{3.53}
$$

and

$$
\dot{\theta}_2 = \frac{1}{e^{\tilde{\lambda}}\rho_1 P} \left\{ P \left[e^{\tilde{\lambda}} \Big(\sin(\alpha_1) + \sin(\theta_2) \Big) - \sin(\alpha_2) \right] - \sin(\theta_2 - \alpha_2 - \alpha_3) - e^{\tilde{\lambda}} \sin(\alpha_3) \right\},
\tag{3.54}
$$

with $\dot{\rho}_1$ defined as in (3.50). We then introduce a scaling of the time variable[3]

$$
\tau \triangleq \int_0^t \frac{1}{e^{\tilde{\lambda}(\sigma)}\rho_1(\sigma)P(\sigma)} d\sigma,
\tag{3.55}
$$

so that

$$
\frac{d\theta_2}{d\tau} = \frac{d\theta_2}{dt}\frac{dt}{d\tau} = \dot{\theta}_2 e^{\tilde{\lambda}(t)} \rho_1(t) P(t).
\tag{3.56}
$$

(Note that an analogous statement holds for $\frac{d\tilde{\lambda}}{d\tau}$ and $\frac{d\rho_1}{d\tau}$.) Letting the prime superscript denote differentiation with respect to the scaled time variable τ, we then

[3]This time scaling is analogous to that in (2.100) but takes a slightly different form. The re-use of τ and the prime superscript (in (3.57)-(3.59)) is a slight abuse of notation but should be clear from the context.

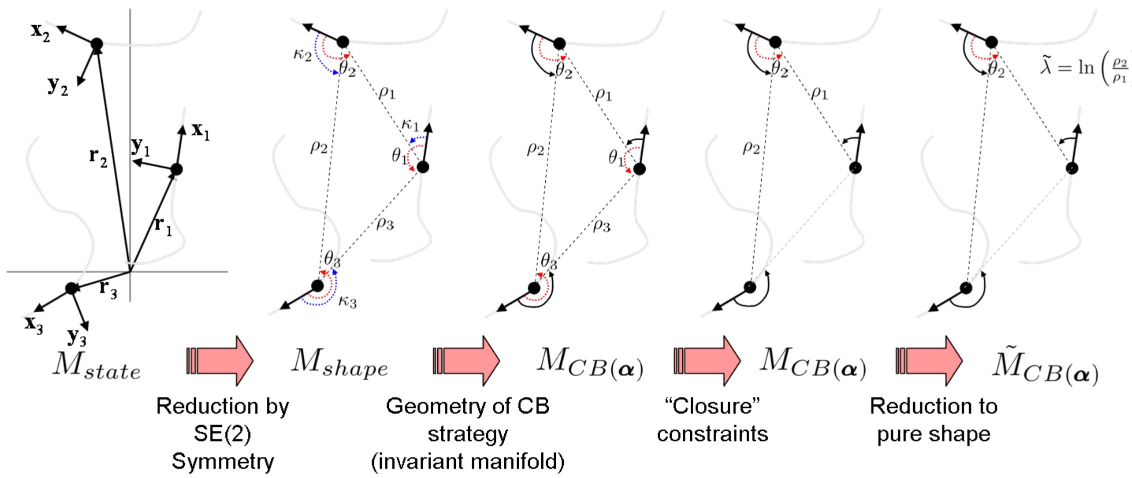

Figure 3.2: This figure illustrates the process by which we reduce a $3n$-dimensional system to a $(2n-4)$-dimensional system by means of symmetry, geometry, and algebraic constraints. In each figure, the labeled variables are the quantities which are free to vary. Note that in the step from M_{shape} to $M_{CB(\boldsymbol{\alpha})}$ the dotted κ_i angles are replaced by solid black curves, indicating that $\kappa_i \equiv \alpha_i$ on $M_{CB(\boldsymbol{\alpha})}$ while θ_i angles remain free to vary.

have

$$\theta_2' = P\left[e^{\tilde{\lambda}}\Big(\sin(\alpha_1) + \sin(\theta_2)\Big) - \sin(\alpha_2)\right] - \sin(\theta_2 - \alpha_2 - \alpha_3) - e^{\tilde{\lambda}}\sin(\alpha_3), \quad (3.57)$$

$$\tilde{\lambda}' = P\left[e^{\tilde{\lambda}}\Big(\cos(\alpha_1) + \cos(\theta_2)\Big) - \cos(\alpha_2)\right] + \cos(\theta_2 - \alpha_2 - \alpha_3) - e^{\tilde{\lambda}}\cos(\alpha_3), \quad (3.58)$$

$$\rho_1' = -e^{\tilde{\lambda}}\rho_1 P\left[\cos(\alpha_1) + \cos(\theta_2)\right]. \quad (3.59)$$

As was discussed in section 2.4.2, the time-scaling renders (3.57) and (3.58) as a self-contained system in $\left\{\theta_2, \tilde{\lambda}\right\}$, describing the pure shape evolution on the punctured cylinder

$$\tilde{M}_{CB(\alpha_1,\alpha_2,\alpha_3)} \cong S^1 \times \mathbb{R} - \{(\alpha_2, 0)\}. \quad (3.60)$$

(As discussed previously, the deletion of the point $\{(\alpha_2, 0)\}$ is necessary to maintain our prohibition on sequential colocation, but it is not enforced by the dynamics (3.57) and (3.58).)

Figure 3.2 provides a summary of the reduction process in the specific context of the three-particle case. In the three-particle case, this final reduction to a two-dimensional system greatly facilitates an analysis of system stability properties, since it permits techniques of phase plane analysis. In what follows, we use the two-dimensional dynamics (3.57)-(3.58) to analyze the stability properties of rectilinear, circling, and spiraling equilibria.

3.4 Linearization of the $\left\{\theta_2, \tilde{\lambda}\right\}$ three-particle pure shape dynamics

A portion of our stability analysis for the three-particle case depends on the linearization of the $\left\{\theta_2, \tilde{\lambda}\right\}$ dynamics (3.57)-(3.58), and therefore we present the general form of the Jacobian matrix here.

First, we note from (3.52) that

$$\begin{aligned}
\frac{\partial P}{\partial \theta_2} &= \frac{1}{2P}\left(2e^{\tilde{\lambda}}\sin(\theta_2 - \alpha_2)\right) = \frac{e^{\tilde{\lambda}}}{P}\sin(\theta_2 - \alpha_2), \\
\frac{\partial P}{\partial \tilde{\lambda}} &= \frac{1}{2P}\left(2e^{2\tilde{\lambda}} - 2e^{\tilde{\lambda}}\cos(\theta_2 - \alpha_2)\right) = \frac{e^{\tilde{\lambda}}}{P}\left(e^{\tilde{\lambda}} - \cos(\theta_2 - \alpha_2)\right).
\end{aligned} \tag{3.61}$$

Then denoting $x \triangleq \left(\theta_2, \tilde{\lambda}\right)^T$ and

$$\begin{aligned}
g_1(\theta_2, \tilde{\lambda}) &\triangleq \theta_2', \\
g_2(\theta_2, \tilde{\lambda}) &\triangleq \tilde{\lambda}',
\end{aligned} \tag{3.62}$$

our Jacobian matrix is given by

$$\left(\frac{\partial g}{\partial x}\right) = \begin{pmatrix} \frac{\partial g_1}{\partial \theta_2} & \frac{\partial g_1}{\partial \tilde{\lambda}} \\ \\ \frac{\partial g_2}{\partial \theta_2} & \frac{\partial g_2}{\partial \tilde{\lambda}} \end{pmatrix}, \tag{3.63}$$

with the elements given by (see appendix C for details):

$$\begin{aligned}
\frac{\partial g_1}{\partial \theta_2} &= \frac{1}{P}\Big\{e^{3\tilde{\lambda}}\cos(\theta_2) + e^{2\tilde{\lambda}}\Big(\sin(\theta_2-\alpha_2)\left[\sin(\alpha_1)+\sin(\theta_2)\right] - 2\cos(\theta_2-\alpha_2)\cos(\theta_2)\Big) \\
&\qquad + e^{\tilde{\lambda}}\Big(\cos(\theta_2) - \sin(\theta_2-\alpha_2)\sin(\alpha_2)\Big) - P\cos(\theta_2-\alpha_2-\alpha_3)\Big\}, \qquad (3.64) \\
\frac{\partial g_1}{\partial \tilde{\lambda}} &= \frac{e^{\tilde{\lambda}}}{P}\Big\{2e^{2\tilde{\lambda}}\left[\sin(\alpha_1)+\sin(\theta_2)\right] - e^{\tilde{\lambda}}\Big(\sin(\alpha_2) + 3\cos(\theta_2-\alpha_2)\left[\sin(\alpha_1)+\sin(\theta_2)\right]\Big) \\
&\qquad + \cos(\theta_2-\alpha_2)\sin(\alpha_2) + \left[\sin(\alpha_1)+\sin(\theta_2)\right] - P\sin(\alpha_3)\Big\}, \qquad (3.65) \\
\frac{\partial g_2}{\partial \theta_2} &= \frac{1}{P}\Big\{-e^{3\tilde{\lambda}}\sin(\theta_2) + e^{2\tilde{\lambda}}\Big(\sin(\theta_2-\alpha_2)\left[\cos(\alpha_1)+\cos(\theta_2)\right] + 2\cos(\theta_2-\alpha_2)\sin(\theta_2)\Big) \\
&\qquad - e^{\tilde{\lambda}}\Big(\sin(\theta_2) + \sin(\theta_2-\alpha_2)\cos(\alpha_2)\Big) - P\sin(\theta_2-\alpha_2-\alpha_3)\Big\}, \qquad (3.66) \\
\frac{\partial g_2}{\partial \tilde{\lambda}} &= \frac{e^{\tilde{\lambda}}}{P}\Big\{2e^{2\tilde{\lambda}}\left[\cos(\alpha_1)+\cos(\theta_2)\right] - e^{\tilde{\lambda}}\Big(\cos(\alpha_2) + 3\cos(\theta_2-\alpha_2)\left[\cos(\alpha_1)+\cos(\theta_2)\right]\Big) \\
&\qquad + \cos(\theta_2-\alpha_2)\cos(\alpha_2) + \left[\cos(\alpha_1)+\cos(\theta_2)\right] - P\cos(\alpha_3)\Big\}. \qquad (3.67)
\end{aligned}$$

3.5 Stability analysis for three-particle rectilinear equilibria

In section 2.4.1 we derived existence conditions for rectilinear equilibria on $M_{CB(\boldsymbol{\alpha})}$, as well as descriptions of the equilibrium values for θ_i and ρ_i. In the three-particle case, we can fully classify the possible types of rectilinear equilibria and state an explicit form for the equilibrium side lengths. (We state the proposition in terms of the equilibrium values for the original ρ_i variables, but the result can be readily expressed in terms of the pure shape variables as well.)

Proposition 3.5.1. *The three-particle $M_{CB(\alpha_1,\alpha_2,\alpha_3)}$ dynamics (3.42) permit two types of rectilinear equilibria, characterized by*

- *Type 1:* $\alpha_k = \alpha_{k+1} = \alpha_{k+2} + \pi,$ *for some* $k \in \{1, 2, 3\}$,
- *Type 2:* $\sin(\alpha_{i-1} - \alpha_i)\sin(\alpha_i - \alpha_{i+1}) > 0,\ i = 1, 2, 3.$

The equilibrium side lengths ($\hat{\rho}_i$) for each type of rectilinear equilibria are characterized by

- *Type 1:* $\hat{\rho}_k + \hat{\rho}_{k+1} = \hat{\rho}_{k+2}$*, where the indices correspond to those in the Type 1 definition,*
- *Type 2:* $\frac{\hat{\rho}_2}{\hat{\rho}_1} = \frac{\sin(\alpha_3-\alpha_1)}{\sin(\alpha_2-\alpha_3)},\ \frac{\hat{\rho}_3}{\hat{\rho}_1} = \frac{\sin(\alpha_1-\alpha_2)}{\sin(\alpha_2-\alpha_3)}.$

Proof. Suppose that $\sin(\alpha_k - \alpha_{k+1}) = 0$ for some $k \in \{1, 2, 3\}$. Then it holds that either $\alpha_k = \alpha_{k+1}$ or $\alpha_k = \pi + \alpha_{k+1}$. If $\alpha_k = \alpha_{k+1}$, then substituting into (2.71) (with $\sigma_i = \hat{\rho}_i$) we have

$$\hat{\rho}_{k+2} e^{j\alpha_{k+2}} = -(\hat{\rho}_k + \hat{\rho}_{k+1}) e^{j\alpha_{k+1}}, \tag{3.68}$$

and since $\hat{\rho}_i > 0$, a rectilinear equilibrium exists only if

$$\alpha_{k+2} = \pi + \alpha_{k+1}, \quad \hat{\rho}_{k+2} = \hat{\rho}_k + \hat{\rho}_{k+1}. \tag{3.69}$$

Alternatively, if $\alpha_k = \pi + \alpha_{k+1}$, then the constraint (2.71) yields

$$\hat{\rho}_{k+2} e^{j\alpha_{k+2}} = (\hat{\rho}_k - \hat{\rho}_{k+1}) e^{j\alpha_{k+1}}, \tag{3.70}$$

in which case a rectilinear equilibrium exists if either

$$\alpha_{k+2} = \alpha_{k+1},\ \hat{\rho}_{k+2} = \hat{\rho}_k - \hat{\rho}_{k+1}, \tag{3.71}$$

or

$$\alpha_{k+2} = \pi + \alpha_{k+1},\ \hat{\rho}_{k+2} = \hat{\rho}_{k+1} - \hat{\rho}_k, \tag{3.72}$$

with $\hat{\rho}_k$ and $\hat{\rho}_{k+1}$ chosen such that $\hat{\rho}_{k+2} > 0$. Hence, we have demonstrated that

$$\sin(\alpha_1 - \alpha_2) = 0 \Longleftrightarrow \sin(\alpha_2 - \alpha_3) = 0 \Longleftrightarrow \sin(\alpha_3 - \alpha_1) = 0 \tag{3.73}$$

and that the Type 1 definition satisfies rectilinear equilibrium existence conditions with the $\hat{\rho}_i$ assignments described in the statement of the proposition.

Now suppose $\sin(\alpha_i - \alpha_{i+1}) \neq 0,\ i = 1, 2, 3$. Then rectilinear equilibrium existence conditions (i.e. (2.71)) require

$$\frac{\hat{\rho}_2}{\hat{\rho}_1} e^{j\alpha_2} + \frac{\hat{\rho}_3}{\hat{\rho}_1} e^{j\alpha_3} = -e^{j\alpha_1}, \tag{3.74}$$

which can be expanded and represented in matrix form as

$$\begin{pmatrix} \sin(\alpha_2) & \sin(\alpha_3) \\ \cos(\alpha_2) & \cos(\alpha_3) \end{pmatrix} \begin{pmatrix} \frac{\hat{\rho}_2}{\hat{\rho}_1} \\ \frac{\hat{\rho}_3}{\hat{\rho}_1} \end{pmatrix} = - \begin{pmatrix} \sin(\alpha_1) \\ \cos(\alpha_1) \end{pmatrix}. \tag{3.75}$$

Noting that

$$\det \begin{pmatrix} \sin(\alpha_2) & \sin(\alpha_3) \\ \cos(\alpha_2) & \cos(\alpha_3) \end{pmatrix} = \sin(\alpha_2)\cos(\alpha_3) - \sin(\alpha_3)\cos(\alpha_2) = \sin(\alpha_2 - \alpha_3) \neq 0, \tag{3.76}$$

we can solve (3.75) to obtain

$$\begin{pmatrix} \frac{\hat{\rho}_2}{\hat{\rho}_1} \\ \\ \frac{\hat{\rho}_3}{\hat{\rho}_1} \end{pmatrix} = -\left(\frac{1}{\sin(\alpha_2-\alpha_3)}\right) \begin{pmatrix} \cos(\alpha_3) & -\sin(\alpha_3) \\ \\ -\cos(\alpha_2) & \sin(\alpha_2) \end{pmatrix} \begin{pmatrix} \sin(\alpha_1) \\ \\ \cos(\alpha_1) \end{pmatrix}$$
$$= -\left(\frac{1}{\sin(\alpha_2-\alpha_3)}\right) \begin{pmatrix} \sin(\alpha_1-\alpha_3) \\ \\ \sin(\alpha_2-\alpha_1) \end{pmatrix}$$
$$= \begin{pmatrix} \frac{\sin(\alpha_3-\alpha_1)}{\sin(\alpha_2-\alpha_3)} \\ \\ \frac{\sin(\alpha_1-\alpha_2)}{\sin(\alpha_2-\alpha_3)} \end{pmatrix}. \tag{3.77}$$

Since $\frac{\hat{\rho}_i}{\hat{\rho}_{i-1}}$ must be positive (and the denominators must be non-zero), rectilinear equilibria exist only if the Type 2 condition is satisfied. □

Proposition 3.5.2. *All Type 2 rectilinear equilibria are unstable.*

Proof. We establish the claim by demonstrating that the Jacobian associated with the linearization of the pure shape dynamics (3.57)-(3.58) about any Type 2 rectilinear equilibrium must have an eigenvalue with positive real part. By (3.49), (3.51), **Proposition 2.4.1**, and **Proposition 3.5.1**, the equilibrium values for $\theta_2, e^{\tilde{\lambda}}$, and P (at a Type 2 rectilinear equilibrium) are given by

$$\theta_2 = \pi + \alpha_1, \quad e^{\tilde{\lambda}} = \frac{\sin(\alpha_3-\alpha_1)}{\sin(\alpha_2-\alpha_3)}, \quad P = \frac{\sin(\alpha_1-\alpha_2)}{\sin(\alpha_2-\alpha_3)}. \tag{3.78}$$

By substitution of these values into (3.63)-(3.67) and subsequent simplifications detailed in appendix C, we have the Jacobian for Type 2 rectilinear equilibria

$$\left(\frac{\partial g}{\partial x}\right)_{rect} = \begin{pmatrix} \frac{\partial g_1}{\partial \theta_2} & \frac{\partial g_1}{\partial \tilde{\lambda}} \\ \\ \frac{\partial g_2}{\partial \theta_2} & \frac{\partial g_2}{\partial \tilde{\lambda}} \end{pmatrix}, \tag{3.79}$$

where

$$
\begin{aligned}
\frac{\partial g_1}{\partial \theta_2} &= \frac{-\cos(\alpha_1)\sin(\alpha_3-\alpha_1)\sin(\alpha_1-\alpha_2)+\cos(\alpha_2)\sin^2(\alpha_2-\alpha_3)\cos(\alpha_3-\alpha_1)}{\sin^2(\alpha_2-\alpha_3)}, \\
\frac{\partial g_1}{\partial \tilde{\lambda}} &= \cos(\alpha_2)\sin(\alpha_3-\alpha_1), \\
\frac{\partial g_2}{\partial \theta_2} &= \frac{\sin(\alpha_1)\sin(\alpha_3-\alpha_1)\sin(\alpha_1-\alpha_2)-\sin(\alpha_2)\sin^2(\alpha_2-\alpha_3)\cos(\alpha_3-\alpha_1)}{\sin^2(\alpha_2-\alpha_3)}, \\
\frac{\partial g_2}{\partial \tilde{\lambda}} &= -\sin(\alpha_2)\sin(\alpha_3-\alpha_1). \qquad (3.80)
\end{aligned}
$$

The determinant of (3.79) is given by

$$
\begin{aligned}
\det\left(\frac{\partial g}{\partial x}\right)_{rect} &= \frac{\sin(\alpha_3-\alpha_1)}{\sin^2(\alpha_2-\alpha_3)}\Big(\sin(\alpha_2)\cos(\alpha_1)\sin(\alpha_3-\alpha_1)\sin(\alpha_1-\alpha_2) \\
&\quad -\sin(\alpha_2)\cos(\alpha_2)\sin^2(\alpha_2-\alpha_3)\cos(\alpha_3-\alpha_1) \\
&\quad -\sin(\alpha_1)\cos(\alpha_2)\sin(\alpha_3-\alpha_1)\sin(\alpha_1-\alpha_2) \\
&\quad +\sin(\alpha_2)\cos(\alpha_2)\sin^2(\alpha_2-\alpha_3)\cos(\alpha_3-\alpha_1)\Big) \\
&= \frac{\sin(\alpha_3-\alpha_1)}{\sin^2(\alpha_2-\alpha_3)}\Big(-\sin(\alpha_3-\alpha_1)\sin(\alpha_1-\alpha_2)\Big[\sin(\alpha_1)\cos(\alpha_2) \\
&\quad -\sin(\alpha_2)\cos(\alpha_1)\Big]\Big) \\
&= \frac{-\sin^2(\alpha_1-\alpha_2)\sin^2(\alpha_3-\alpha_1)}{\sin^2(\alpha_2-\alpha_3)}, \qquad (3.81)
\end{aligned}
$$

which is strictly negative. Since the eigenvalues of a two-by-two matrix A are given by

$$
\lambda = \frac{1}{2}\left(\mathrm{tr}(A) \pm \sqrt{\mathrm{tr}^2(A) - 4\det(A)}\right), \qquad (3.82)
$$

and the determinant of (3.79) is strictly negative, it must hold that the eigenvalues of (3.79) are real, and that one is positive and one is negative. Therefore all Type 2 rectilinear equilibria are unstable. □

The rest of this section is devoted to analyzing Type 1 rectilinear equilibria. In working with Type 1 rectilinear equilibria, we assume without loss of generality that $\alpha_1 = \alpha_2 = \alpha = \pi + \alpha_3$ for some $\alpha \in [0, 2\pi)$. We investigate stability properties of such rectilinear equlibria on $M_{CB(\alpha,\alpha,\pi+\alpha)}$ by considering their projections onto the submanifold $\tilde{M}_{CB(\alpha,\alpha,\pi+\alpha)}$ defined in (3.60).

By substitution of $\alpha_1 = \alpha_2 = \alpha = \pi + \alpha_3$ into (3.57)-(3.58), we arrive at

$$\begin{aligned}
\theta_2' &= P\left[e^{\tilde{\lambda}}\Big(\sin(\alpha) + \sin(\theta_2)\Big) - \sin(\alpha)\right] - \sin(\theta_2 - 2\alpha + \pi) + e^{\tilde{\lambda}}\sin(\alpha), \\
\tilde{\lambda}' &= P\left[e^{\tilde{\lambda}}\Big(\cos(\alpha) + \cos(\theta_2)\Big) - \cos(\alpha)\right] + \cos(\theta_2 - 2\alpha + \pi) + e^{\tilde{\lambda}}\cos(\alpha),
\end{aligned} \tag{3.83}$$

where $P = \sqrt{e^{2\tilde{\lambda}} - 2e^{\tilde{\lambda}}\cos(\theta_2 - \alpha) + 1}$. From (2.72) we have the equilibrium value for θ_2, given by $\hat{\theta}_2 = \pi + \alpha_1 = \pi + \alpha$, and we therefore define an angular error variable

$$\phi \triangleq \theta_2 - \hat{\theta}_2 = \theta_2 - \pi - \alpha, \tag{3.84}$$

so that $\phi = 0 \Longleftrightarrow \theta_2 = \hat{\theta}_2$. (See figure 3.3.) Denoting

$$P \triangleq \sqrt{e^{2\tilde{\lambda}} + 2e^{\tilde{\lambda}}\cos(\phi) + 1}, \tag{3.85}$$

we can formulate $\left\{\phi, \tilde{\lambda}\right\}$ dynamics as

$$\boxed{\begin{aligned}
\phi' &= P\left[e^{\tilde{\lambda}}\Big(\sin(\alpha) - \sin(\phi + \alpha)\Big) - \sin(\alpha)\right] - \sin(\phi - \alpha) + e^{\tilde{\lambda}}\sin(\alpha), \\
\tilde{\lambda}' &= P\left[e^{\tilde{\lambda}}\Big(\cos(\alpha) - \cos(\phi + \alpha)\Big) - \cos(\alpha)\right] + \cos(\phi - \alpha) + e^{\tilde{\lambda}}\cos(\alpha).
\end{aligned}} \tag{3.86}$$

These dynamics evolve on a manifold (punctured cylinder) which is diffeomorphic to $\tilde{M}_{CB(\alpha,\alpha,\pi+\alpha)}$ as defined in (3.60), and therefore we will consider the $\left\{\phi, \tilde{\lambda}\right\}$ dynamics

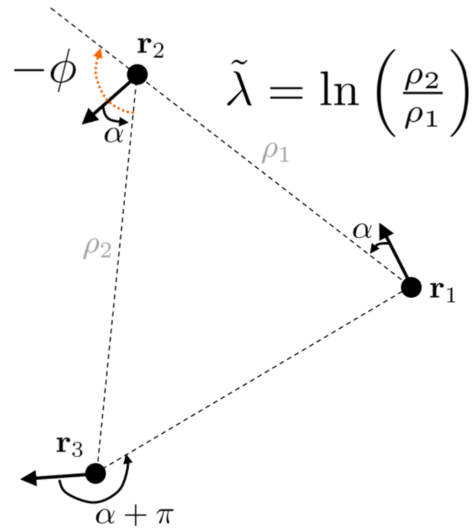

Figure 3.3: Depiction of the $\left\{\phi, \tilde{\lambda}\right\}$ variables. Note that $\phi = 0$ at a Type 1 rectilinear equilibrium.

as evolving on $\tilde{M}_{CB(\alpha,\alpha,\pi+\alpha)}$. (The excluded point in terms of the $\left\{\phi, \tilde{\lambda}\right\}$ variables is given by $\phi = \pi, \tilde{\lambda} = 0$.)

It should be noted that the only equilibria which exist for these pure shape dynamics (3.86) correspond to Type 1 rectilinear equilibria (for the full dynamics). This is explicitly demonstrated by the following proposition.

Proposition 3.5.3. *The equilibria for the dynamics (3.86) are given by the set*

$$\tilde{M}_\alpha = \left\{(\phi, \tilde{\lambda}) \in \tilde{M}_{CB(\alpha,\alpha,\pi+\alpha)} \;\middle|\; \phi = 0\right\} \tag{3.87}$$

Proof. First note that

$$P(0, \tilde{\lambda}) = \sqrt{e^{2\tilde{\lambda}} + 2e^{\tilde{\lambda}} + 1} = e^{\tilde{\lambda}} + 1, \tag{3.88}$$

from which it follows by straightforward calculation that $\phi'(0, \tilde{\lambda}) = 0 = \tilde{\lambda}'(0, \tilde{\lambda})$. To prove necessity, we suppose that a relative equilibrium exists, i.e. $\phi^{'} = 0 = \tilde{\lambda}'$. Then

$$\begin{aligned}
0 &= -\cos(\alpha)\phi^{'} + \sin(\alpha)\tilde{\lambda}^{'} \\
&= Pe^{\tilde{\lambda}}\left[\cos(\alpha)\sin(\phi+\alpha) - \sin(\alpha)\cos(\phi+\alpha)\right] \\
&\qquad + \left[\cos(\alpha)\sin(\phi-\alpha) + \sin(\alpha)\cos(\phi-\alpha)\right] \\
&= \left(Pe^{\tilde{\lambda}} + 1\right)\sin(\phi).
\end{aligned} \tag{3.89}$$

Since P and $e^{\tilde{\lambda}}$ are strictly positive, we must have $\sin(\phi) = 0$, i.e. $\phi = 0$ or π. Having already verified that $\phi = 0$ corresponds to a relative equilibrium, we check $\phi = \pi$ by observing that

$$P(\pi, \tilde{\lambda}) = \sqrt{e^{2\tilde{\lambda}} - 2e^{\tilde{\lambda}} + 1} = e^{\tilde{\lambda}} - 1 \tag{3.90}$$

and substituting into (3.86) to get

$$\begin{aligned}
\phi^{'}(\pi, \tilde{\lambda}) &= 2\sin(\alpha)e^{\tilde{\lambda}}(e^{\tilde{\lambda}} - 1) \\
\tilde{\lambda}^{'}(\pi, \tilde{\lambda}) &= 2\cos(\alpha)e^{\tilde{\lambda}}(e^{\tilde{\lambda}} - 1).
\end{aligned} \tag{3.91}$$

Since the point $(\phi, \tilde{\lambda}) = (\pi, 0)$ is excluded from $\tilde{M}_{CB(\alpha,\alpha,\pi+\alpha)}$, we have demonstrated that it is not possible for both equations in (3.91) to be zero, and therefore $\phi = \pi$ can not correspond to a relative equilibrium. □

Remark 3.5.4 Observe that $\tilde{M}_\alpha$ denotes *a continuum of equilibria* for the dynamics given by (3.86), corresponding to a continuum of Type 1 rectilinear equilibria for the full system.

Although we typically have considered α as a fixed parameter, in the ensuing discussion it will sometimes prove helpful to view $\phi^{'}$ and $\tilde{\lambda}^{'}$ as functions of three variables α, ϕ, and $\tilde{\lambda}$, defining

$$\begin{aligned}
\phi' &= g_1(\alpha,\phi,\tilde{\lambda}) \triangleq P\left[e^{\tilde{\lambda}}\Big(\sin(\alpha)-\sin(\phi+\alpha)\Big)-\sin(\alpha)\right]-\sin(\phi-\alpha)+e^{\tilde{\lambda}}\sin(\alpha),\\
\tilde{\lambda}' &= g_2(\alpha,\phi,\tilde{\lambda}) \triangleq P\left[e^{\tilde{\lambda}}\Big(\cos(\alpha)-\cos(\phi+\alpha)\Big)-\cos(\alpha)\right]+\cos(\phi-\alpha)+e^{\tilde{\lambda}}\cos(\alpha).
\end{aligned} \tag{3.92}$$

Before proceeding with our stability analysis, we state the following proposition regarding a particular property of the vector field (3.86) in the vicinity of the set $\tilde{M}_\alpha$.

Proposition 3.5.5. *Let $\phi \in (0,\pi)\cup(\pi,2\pi)$ so that*

$$F(\alpha,\phi,\tilde{\lambda}) \triangleq \frac{\partial\phi}{\partial\tilde{\lambda}} = \frac{g_1(\alpha,\phi,\tilde{\lambda})}{g_2(\alpha,\phi,\tilde{\lambda})} \tag{3.93}$$

is well-defined. Then for any fixed $\alpha \in [0,2\pi)$ and $\tilde{\lambda}_0 \in \mathbb{R}$,

$$\lim_{\phi\to 0} F(\alpha,\phi,\tilde{\lambda}_0) = -\frac{\cos(\alpha)}{\sin(\alpha)}. \tag{3.94}$$

Proof. In **Proposition 3.5.3** we proved that $g_1(\alpha,0,\tilde{\lambda}_0) = g_2(\alpha,0,\tilde{\lambda}_0) = 0$ for any $\alpha \in [0,2\pi)$ and any $\tilde{\lambda}_0 \in \mathbb{R}$, and therefore we can apply L'Hôpital's rule to the limit calculation in (3.94). From (3.85) we have

$$\frac{\partial P}{\partial\phi} = \frac{1}{2P}(-2\sin(\phi)e^{\tilde{\lambda}_0}) = -\frac{e^{\tilde{\lambda}_0}}{P}\sin(\phi), \tag{3.95}$$

and therefore

$$\begin{aligned}
\frac{\partial g_1(\alpha,\phi,\tilde{\lambda}_0)}{\partial\phi} &= \left(-\frac{e^{\tilde{\lambda}_0}}{P}\sin(\phi)\right)\left[e^{\tilde{\lambda}_0}\Big(\sin(\alpha)-\sin(\phi+\alpha)\Big)-\sin(\alpha)\right]\\
&\quad + P\Big(-e^{\tilde{\lambda}_0}\cos(\phi+\alpha)\Big)-\cos(\phi-\alpha)
\end{aligned} \tag{3.96}$$

and

$$\frac{\partial g_2(\alpha,\phi,\tilde{\lambda}_0)}{\partial \phi} = \left(-\frac{e^{\tilde{\lambda}_0}}{P}\sin(\phi)\right)\left[e^{\tilde{\lambda}_0}\Big(\cos(\alpha)-\cos(\phi+\alpha)\Big)-\cos(\alpha)\right]$$

$$+ P\Big(e^{\tilde{\lambda}_0}\sin(\phi+\alpha)\Big)-\sin(\phi-\alpha) \tag{3.97}$$

Then, making use of (3.88), our limit calculation becomes

$$\begin{aligned}
\lim_{\phi\to 0}\frac{g_1(\alpha,\phi,\tilde{\lambda}_0)}{g_2(\alpha,\phi,\tilde{\lambda}_0)} = \lim_{\phi\to 0}\frac{\frac{\partial g_1(\alpha,\phi,\tilde{\lambda}_0)}{\partial\phi}}{\frac{\partial g_2(\alpha,\phi,\tilde{\lambda}_0)}{\partial\phi}} &= \frac{-\Big(e^{\tilde{\lambda}_0}+1\Big)\,e^{\tilde{\lambda}_0}\cos(\alpha)-\cos(\alpha)}{\big(e^{\tilde{\lambda}_0}+1\big)\,e^{\tilde{\lambda}_0}\sin(\alpha)+\sin(\alpha)} \\
&= \frac{-\cos(\alpha)\Big(\Big(e^{\tilde{\lambda}_0}+1\Big)\,e^{\tilde{\lambda}_0}+1\Big)}{\sin(\alpha)\Big(\big(e^{\tilde{\lambda}_0}+1\big)\,e^{\tilde{\lambda}_0}+1\Big)} \\
&= -\frac{\cos(\alpha)}{\sin(\alpha)}.
\end{aligned} \tag{3.98}$$

□

3.5.1 Analysis of the $\alpha = 0$ case for Type 1 rectilinear equilibria

For the $\alpha = 0$ case, our dynamics (3.86) simplify to

$$\begin{aligned}
\phi' &= -\sin(\phi)\big(Pe^{\tilde{\lambda}}+1\big), \\
\tilde{\lambda}' &= P\left[e^{\tilde{\lambda}}\Big(1-\cos(\phi)\Big)-1\right]+\cos(\phi)+e^{\tilde{\lambda}}.
\end{aligned} \tag{3.99}$$

Defining

$$H_0(\phi,\tilde{\lambda}) \triangleq -1-\cos(\phi), \tag{3.100}$$

we have

$$H_0' = -\sin^2(\phi)\big(Pe^{\tilde{\lambda}}+1\big) = H_0(H_0+2)\big(Pe^{\tilde{\lambda}}+1\big), \tag{3.101}$$

from which it is apparent that the submanifolds defined respectively by $H_0 = 0$ and $H_0 = -2$ are both invariant under the dynamics (3.99), in the sense of **Definition 1.3.2**. Noting that $H_0 = -2 \Longleftrightarrow \phi = 0$, we see that the latter invariant submanifold corresponds to our set of rectilinear equilibria $\tilde{M}_0$ from (3.87). We define the other invariant submanifold as

$$\Delta = \left\{ (\phi, \tilde{\lambda}) \in \tilde{M}_{CB(0,0,\pi)} \;\middle|\; H_0 = 0 \right\}$$
$$= \left\{ (\phi, \tilde{\lambda}) \in \tilde{M}_{CB(0,0,\pi)} \;\middle|\; \phi = \pi \right\}, \tag{3.102}$$

noting that the one-dimensional reduced dynamics on Δ are characterized by $\tilde{\lambda}' = 2e^{\tilde{\lambda}}\left(e^{\tilde{\lambda}} - 1\right)$, i.e. all trajectories on Δ move away from the point $\tilde{\lambda} = 0$. These two invariant manifolds (and representative particle formations on M_{state}) are depicted in the phase portrait[4] for the $\alpha = 0$ case, in figure 3.4. Since $\phi \in S^1$ and therefore $\phi = 0$ is identified with $\phi = 2\pi$, the phase portrait should be viewed as a punctured cylinder which has been cut along the set $\tilde{M}_0$ and unwrapped.

The following proposition summarizes the stability analysis for the $\alpha = 0$ case, demonstrating that Δ is unstable and $\tilde{M}_0$ is attractive on all but a thin subset of $\tilde{M}_{CB(0,0,\pi)}$.

Proposition 3.5.6. *Let $\tilde{M}_{CB(0,0,\pi)}$, $\tilde{M}_0$ and Δ be defined as in (3.60), (3.87) and (3.102) respectively. Any trajectory of (3.99) starting in the set*

$$\tilde{M}_{CB(0,0,\pi)} - \Delta \tag{3.103}$$

[4] All phase portraits were created with the *pplane* tool for MATLAB, available at http://www.math.rice.edu/~dfield/.

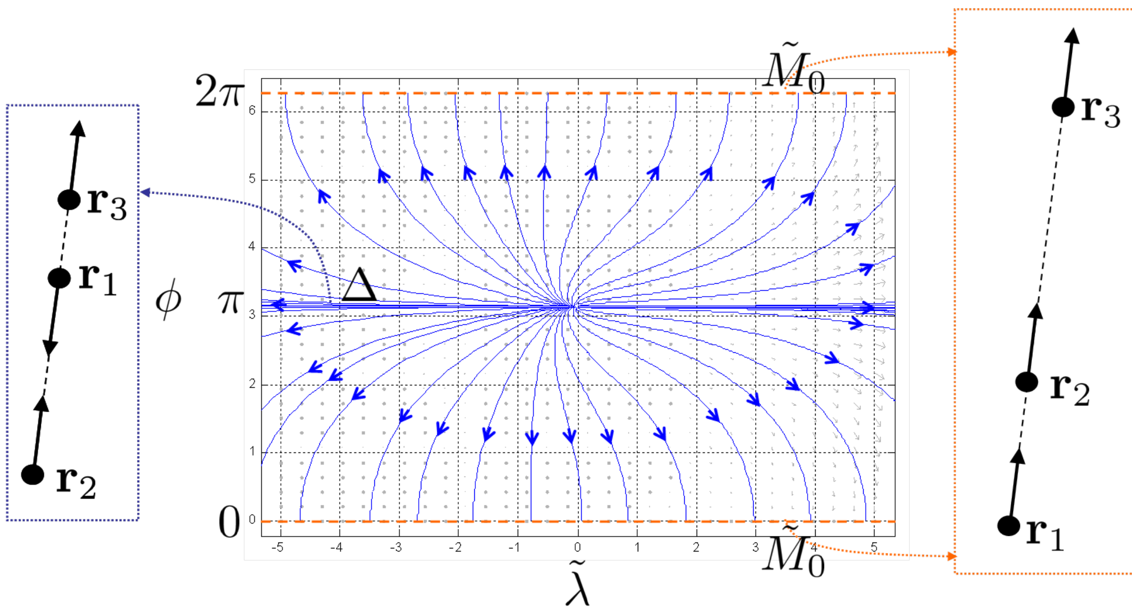

Figure 3.4: Depiction of the $\left\{\phi, \tilde{\lambda}\right\}$ phase portrait for the $\alpha = 0$ case, which should be viewed as a (punctured) cylinder which has been cut along the set $\tilde{M}_0$ and unwrapped. Also depicted are representative particle formations (from the full physical space) which correspond to each of the invariant submanifolds $\tilde{M}_0$ and Δ.

converges asymptotically to $\tilde{M}_0$.

Proof. Let H_0 be defined as in (3.100), and define

$$\Omega_0^\epsilon = \left\{(\phi, \tilde{\lambda}) \in \tilde{M}_{CB(0,0,\pi)} \;\middle|\; H_0 \leq -\epsilon\right\}, \tag{3.104}$$

where ϵ satisfies $0 < \epsilon \leq 2$. Note that Ω_0^ϵ is closed and positively invariant under the dynamics (3.99). From (3.101), it is clear that $H_0^{'} \leq 0$ on Ω_0^ϵ with $H_0^{'} = 0$ on Ω_0^ϵ if and only if $H_0 = -2$, which corresponds to the invariant set $\tilde{M}_0$. Though Ω_0^ϵ is not bounded as a set, we claim that every trajectory of (3.99) which starts in Ω_0^ϵ is bounded. To prove this claim, we argue by contradiction. If such a trajectory were unbounded, then it must become unbounded in $\tilde{\lambda}$ (since it cannot cross $\tilde{M}_0$ or Δ). Since there are no equilibrium points contained in Ω_0^ϵ except for the set $\tilde{M}_0$, and $H_0^{'} < 0$ on $\Omega_0^\epsilon - \tilde{M}_0$, it must be that the trajectory asymptotically approaches the set $\tilde{M}_0$ while becoming unbounded in the direction $\tilde{\lambda} = +\infty$ or $\tilde{\lambda} = -\infty$. However, by **Proposition 3.5.5** it holds that $\lim_{\phi \to 0} \frac{\partial \phi}{\partial \tilde{\lambda}} = -\infty$, and therefore $\tilde{M}_0$ can not serve as an asymptote for the trajectory. Hence, the trajectory must be bounded, and therefore by Birkhoff's theorem the ω-limit set is nonempty, compact and invariant. Asymptotic convergence to $\tilde{M}_0$ follows as in the steps in the proof of LaSalle's Invariance Principle [29]. Finally, since ϵ can be arbitrarily small, it follows that the region of convergence is given by $\tilde{M}_{CB(0,0,\pi)} - \Delta$. $\square$

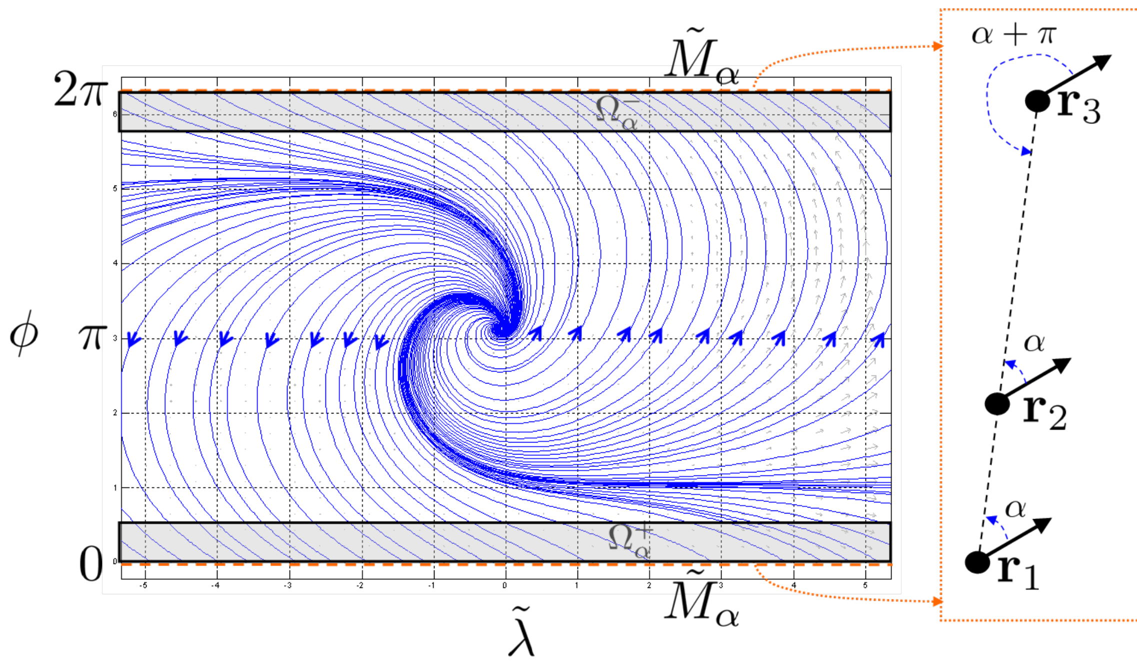

Figure 3.5: This figure displays the $(\tilde{\lambda}, \phi)$ phase portrait for $\alpha = \pi/3$, representing the $\alpha \in (0, \pi/2) \cup (3\pi/2, 2\pi)$ case. The phase portrait should be viewed as an unwrapped punctured cylinder, so that $\phi = 0$ is identified with $\phi = 2\pi$. The set of rectilinear equilibria is denoted as $\tilde{M}_\alpha$, and the set $\Omega_\alpha = \Omega_\alpha^+ \cup \tilde{M}_\alpha \cup \Omega_\alpha^-$ is the set on which we demonstrate boundedness of trajectories and convergence to $\tilde{M}_\alpha$.

3.5.2 Analysis of the $\alpha \in (0, \pi/2) \cup (3\pi/2, 2\pi)$ case for Type 1 rectilinear equilibria

For $\alpha \in (0, \pi/2) \cup (3\pi/2, 2\pi)$, our dynamics are as stated in (3.86). The phase portrait (as displayed in figure 3.5 for $\alpha = \pi/3$) suggests that most trajectories converge asymptotically to the equilibrium set $\tilde{M}_\alpha$, a result which we prove analytically for trajectories starting in a particular set. We begin by characterizing the sign of ϕ' and $\tilde{\lambda}'$ on various regions.

Proposition 3.5.7. *Let*

$$\phi' = g_1(\alpha,\phi,\tilde{\lambda}) \triangleq P\left[e^{\tilde{\lambda}}\Big(\sin(\alpha)-\sin(\phi+\alpha)\Big)-\sin(\alpha)\right]-\sin(\phi-\alpha)+e^{\tilde{\lambda}}\sin(\alpha),$$
$$\tilde{\lambda}' = g_2(\alpha,\phi,\tilde{\lambda}) \triangleq P\left[e^{\tilde{\lambda}}\Big(\cos(\alpha)-\cos(\phi+\alpha)\Big)-\cos(\alpha)\right]+\cos(\phi-\alpha)+e^{\tilde{\lambda}}\cos(\alpha),$$
$$(3.105)$$

and define the sets

$$\Omega^+_{\alpha^+} = \Big\{(\alpha,\phi,\tilde{\lambda}) \in (0,\pi/2)\times \tilde{M}_{CB(\alpha,\alpha,\pi+\alpha)} \;\Big|\; \sin(\phi)>0,\ \cos(\phi)\geq \max\left[\cos(\alpha),\sin(\alpha)\right]\Big\},$$
$$\Omega^-_{\alpha^+} = \Big\{(\alpha,\phi,\tilde{\lambda}) \in (0,\pi/2)\times \tilde{M}_{CB(\alpha,\alpha,\pi+\alpha)} \;\Big|\; \sin(\phi)<0,\ \cos(\phi)\geq \max\left[\cos(\alpha),\sin(\alpha)\right]\Big\}. \qquad (3.106)$$

Then on $\Omega^+_{\alpha^+}$ it holds that $g_1(\alpha,\phi,\tilde{\lambda})<0$ and $g_2(\alpha,\phi,\tilde{\lambda})>0$, and on $\Omega^-_{\alpha^+}$ it holds that $g_1(\alpha,\phi,\tilde{\lambda})>0$ and $g_2(\alpha,\phi,\tilde{\lambda})<0$.

Proof. The proof of **Proposition 3.5.7** is provided in appendix C. □

The following corollary extends our results to the case $\alpha \in (3\pi/2, 2\pi)$.

Corollary 3.5.8. *Define g_1 and g_2 as in (3.105) and define the sets*

$$\Omega^+_{\alpha^-} = \Big\{(\alpha,\phi,\tilde{\lambda}) \in (3\pi/2,2\pi)\times \tilde{M}_{CB(\alpha,\alpha,\pi+\alpha)} \;\Big|\; \sin(\phi)>0,\ \cos(\phi)\geq \max\left[\cos(\alpha),-\sin(\alpha)\right]\Big\},$$
$$\Omega^-_{\alpha^-} = \Big\{(\alpha,\phi,\tilde{\lambda}) \in (3\pi/2,2\pi)\times \tilde{M}_{CB(\alpha,\alpha,\pi+\alpha)} \;\Big|\; \sin(\phi)<0,\ \cos(\phi)\geq \max\left[\cos(\alpha),-\sin(\alpha)\right]\Big\}. \qquad (3.107)$$

Then on $\Omega^+_{\alpha^-}$ it holds that $g_1(\alpha,\phi,\tilde{\lambda})<0$ and $g_2(\alpha,\phi,\tilde{\lambda})<0$, and on $\Omega^-_{\alpha^-}$ it holds that $g_1(\alpha,\phi,\tilde{\lambda})>0$ and $g_2(\alpha,\phi,\tilde{\lambda})>0$.

Proof. First, recalling that $P(-\phi, \tilde{\lambda}) = P(\phi, \tilde{\lambda})$, we note that for any $(\alpha, \phi, \tilde{\lambda}) \in [0, 2\pi) \times \tilde{M}_{CB(\alpha,\alpha,\pi+\alpha)}$ it holds that

$$\begin{aligned} g_1(-\alpha, -\phi, \tilde{\lambda}) &= P\left[e^{\tilde{\lambda}}\Big(\sin(-\alpha) - \sin(-\phi - \alpha)\Big) - \sin(-\alpha)\right] \\ &\qquad - \sin(-\phi + \alpha) + e^{\tilde{\lambda}} \sin(-\alpha) \\ &= -\left\{P\left[e^{\tilde{\lambda}}\Big(\sin(\alpha) - \sin(\phi + \alpha)\Big) - \sin(\alpha)\right] - \sin(\phi - \alpha) + e^{\tilde{\lambda}} \sin(\alpha)\right\} \\ &= -g_1(\alpha, \phi, \tilde{\lambda}), \end{aligned} \tag{3.108}$$

and

$$\begin{aligned} g_2(-\alpha, -\phi, \tilde{\lambda}) &= P\left[e^{\tilde{\lambda}}\Big(\cos(-\alpha) - \cos(-\phi - \alpha)\Big) - \cos(-\alpha)\right] \\ &\qquad + \cos(-\phi + \alpha) + e^{\tilde{\lambda}} \cos(-\alpha) \\ &= P\left[e^{\tilde{\lambda}}\Big(\cos(\alpha) - \cos(\phi + \alpha)\Big) - \cos(\alpha)\right] + \cos(\phi - \alpha) + e^{\tilde{\lambda}} \cos(\alpha) \\ &= g_2(\alpha, \phi, \tilde{\lambda}). \end{aligned} \tag{3.109}$$

Then defining $\tilde{\alpha} = -\alpha$ and $\tilde{\phi} = -\phi$, and making use of **Proposition 3.5.7** as well as our definitions of $\Omega^+_{\alpha^+}$ and $\Omega^-_{\alpha^+}$ from (3.106), we have

$$
\begin{aligned}
&(\alpha,\phi,\tilde{\lambda}) \in \Omega^+_{\alpha^-} \implies \sin(\alpha) < 0,\ \cos(\alpha) > 0,\ \sin(\phi) > 0, \\
&\qquad\qquad\qquad\qquad \cos(\phi) \geq \max\left[\cos(\alpha), -\sin(\alpha)\right] \\
&\implies \sin(-\tilde{\alpha}) < 0,\ \cos(-\tilde{\alpha}) > 0,\ \sin(-\tilde{\phi}) > 0,\ \cos(-\tilde{\phi}) \geq \max\left[\cos(-\tilde{\alpha}), -\sin(-\tilde{\alpha})\right] \\
&\implies \sin(\tilde{\alpha}) > 0,\ \cos(\tilde{\alpha}) > 0,\ \sin(\tilde{\phi}) < 0,\ \cos(\tilde{\phi}) \geq \max\left[\cos(\tilde{\alpha}), \sin(\tilde{\alpha})\right] \\
&\implies (\tilde{\alpha},\tilde{\phi},\tilde{\lambda}) \in \Omega^-_{\tilde{\alpha}^+} \\
&\implies g_1(\tilde{\alpha},\tilde{\phi},\tilde{\lambda}) > 0,\ g_2(\tilde{\alpha},\tilde{\phi},\tilde{\lambda}) < 0 \\
&\implies g_1(-\alpha,-\phi,\tilde{\lambda}) > 0,\ g_2(-\alpha,-\phi,\tilde{\lambda}) < 0 \\
&\implies -g_1(\alpha,\phi,\tilde{\lambda}) > 0,\ g_2(\alpha,\phi,\tilde{\lambda}) < 0 \\
&\implies g_1(\alpha,\phi,\tilde{\lambda}) < 0,\ g_2(\alpha,\phi,\tilde{\lambda}) < 0. \qquad (3.110)
\end{aligned}
$$

(Note that we have also used (3.108) and (3.109).) Similarly, we have

$$
\begin{aligned}
&(\alpha,\phi,\tilde{\lambda}) \in \Omega^-_{\alpha^-} \implies \sin(\alpha) < 0,\ \cos(\alpha) > 0,\ \sin(\phi) < 0, \\
&\qquad\qquad\qquad\qquad \cos(\phi) \geq \max\left[\cos(\alpha), -\sin(\alpha)\right] \\
&\implies \sin(-\tilde{\alpha}) < 0,\ \cos(-\tilde{\alpha}) > 0,\ \sin(-\tilde{\phi}) < 0,\ \cos(-\tilde{\phi}) \geq \max\left[\cos(-\tilde{\alpha}), -\sin(-\tilde{\alpha})\right] \\
&\implies \sin(\tilde{\alpha}) > 0,\ \cos(\tilde{\alpha}) > 0,\ \sin(\tilde{\phi}) > 0,\ \cos(\tilde{\phi}) \geq \max\left[\cos(\tilde{\alpha}), \sin(\tilde{\alpha})\right] \\
&\implies (\tilde{\alpha},\tilde{\phi},\tilde{\lambda}) \in \Omega^+_{\tilde{\alpha}^+} \\
&\implies g_1(\tilde{\alpha},\tilde{\phi},\tilde{\lambda}) < 0,\ g_2(\tilde{\alpha},\tilde{\phi},\tilde{\lambda}) > 0 \\
&\implies -g_1(\alpha,\phi,\tilde{\lambda}) < 0,\ g_2(\alpha,\phi,\tilde{\lambda}) > 0 \\
&\implies g_1(\alpha,\phi,\tilde{\lambda}) > 0,\ g_2(\alpha,\phi,\tilde{\lambda}) > 0. \qquad (3.111)
\end{aligned}
$$

□

Based on the previous results, we state and prove the following proposition concerning boundedness of trajectories.

Proposition 3.5.9. *For any fixed* $\alpha \in (0, \pi/2) \cup (3\pi/2, 2\pi)$*, we define*

$$\Omega_\alpha = \left\{ (\phi, \tilde{\lambda}) \in \tilde{M}_{CB(\alpha,\alpha,\pi+\alpha)} \;\middle|\; \cos(\phi) \geq \max\Big[\cos(\alpha), |\sin(\alpha)|\Big] \right\}. \tag{3.112}$$

Every trajectory of the system (3.105) which starts in Ω_α *is bounded.*

Proof. First, observe that if we make use (3.106) and (3.107) to define

$$\begin{aligned} \Omega_\alpha^+ &\triangleq \Omega_{\alpha^-}^+ \cup \Omega_{\alpha^+}^+, \\ \Omega_\alpha^- &\triangleq \Omega_{\alpha^-}^- \cup \Omega_{\alpha^+}^-, \end{aligned} \tag{3.113}$$

then $\Omega_\alpha = \Omega_\alpha^+ \cup \tilde{M}_\alpha \cup \Omega_\alpha^-$ (with $\tilde{M}_\alpha$ as defined in (3.87)), as depicted in figure 3.5. Per **Proposition 3.5.3**, $\tilde{M}_\alpha$ is the set which contains all of the equilibrium points for the dynamics (3.105), and hence there are no equilibria contained in the sets Ω_α^+ and Ω_α^-. Clearly Ω_α is a closed set, and by applying the results of **Proposition 3.5.7** and **Corollary 3.5.8** on the boundary of Ω_α, one can show that Ω_α is also positively invariant under the dynamics (3.105).

We proceed by contradiction. Suppose a trajectory starting in Ω_α is unbounded. Since $\tilde{M}_\alpha$ is a set of equilibria (and hence all trajectories in $\tilde{M}_\alpha$ are by definition bounded), the trajectory must start in $\Omega_\alpha^+ \cup \Omega_\alpha^-$. Without loss of generality, we assume the trajectory starts in Ω_α^+. By **Proposition 3.5.7** and **Corollary 3.5.8**, we have $\phi' < 0$ on Ω_α^+ with $\tilde{\lambda}'$ monotonic, and therefore it must be that the trajectory asymptotically approaches the set $\tilde{M}_\alpha$ while becoming unbounded in the direction $\tilde{\lambda} = +\infty$ or $\tilde{\lambda} = -\infty$. However, by **Proposition 3.5.5** we have

$$\lim_{\phi \to 0} \frac{\partial \phi}{\partial \tilde{\lambda}} = -\frac{\cos(\alpha)}{\sin(\alpha)} \neq 0, \tag{3.114}$$

and therefore $\tilde{M}_\alpha$ can not serve as an asymptote for the trajectory. Hence, the trajectory must be bounded. $\square$

Theorem 3.5.10. *Let* $\alpha \in (0, \pi/2) \cup (3\pi/2, 2\pi)$ *and define* Ω_α *as in (3.112) and* $\tilde{M}_\alpha$ *as in (3.87). Every trajectory of (3.105) starting in* Ω_α *converges asymptotically to* $\tilde{M}_\alpha$*.*

Proof. Letting $V = -\cos(\phi)$, we have $V' = \phi' \sin(\phi)$. Then by the results of **Proposition 3.5.3**, **Proposition 3.5.7**, and **Corollary 3.5.8** we have $V' \leq 0$ on Ω_α with $V' = 0$ if and only if $(\phi, \tilde{\lambda}) \in \tilde{M}_\alpha$. By **Proposition 3.5.9** it holds that Ω_α is closed and positively invariant under the dynamics (3.105), and every trajectory starting in Ω_α is bounded. Therefore by Birkhoff's theorem the ω-limit set is nonempty, compact and invariant, and asymptotic convergence to $\tilde{M}_\alpha$ follows as in the steps in the proof of LaSalle's Invariance Principle [29]. $\square$

3.5.3 Analysis of the $\alpha = \frac{\pi}{2}$ case for Type 1 rectilinear equilibria

Substitution of $\alpha = \pi/2$ into the dynamics (3.86) yields

$$\begin{aligned} \phi' &= P\left[e^{\tilde{\lambda}}\Big(1 - \cos(\phi)\Big) - 1\right] + \cos(\phi) + e^{\tilde{\lambda}}, \\ \tilde{\lambda}' &= \sin(\phi)\big(Pe^{\tilde{\lambda}} + 1\big). \end{aligned} \tag{3.115}$$

The phase portrait (displayed in figure 3.6) reveals some remarkable properties of the trajectories of these dynamics. Analogous to previous cases, the set $\tilde{M}_{\pi/2}$ consists of a continuum of equilibria which correspond to Type 1 rectilinear equilibria for the full dynamics, but unlike the previous cases, there is no set on which trajectories converge asymptotically to $\tilde{M}_{\pi/2}$. Rather, all trajectories that do not start on $\tilde{M}_{\pi/2}$ exhibit periodic behavior in the $\left\{\phi, \tilde{\lambda}\right\}$ space, depicted in the phase portrait as counter-clockwise closed orbits. (Analogous clockwise orbits appear in the $\alpha = 3\pi/2$ case.) The corresponding particle trajectories in the plane display precession, as illustrated in figure 3.7. The analysis proceeds as follows.

In the following discussion, we will often employ the change of variables

$$\delta \triangleq \cos(\phi) \tag{3.116}$$

where $\left\{\delta, \tilde{\lambda}\right\}$ evolve on the space

$$D_{\delta,\tilde{\lambda}} = [-1, 1] \times \mathbb{R} - \{(-1, 0)\}\,. \tag{3.117}$$

Associated dynamics are given by

$$\begin{aligned}
\delta' &= -\sin(\phi)\phi' \\
&= -\operatorname{sgn}(\sin(\phi))(\sqrt{1-\delta^2})\Big(P\big(e^{\tilde{\lambda}} - \delta e^{\tilde{\lambda}} - 1\big) + \big(e^{\tilde{\lambda}} + \delta\big)\Big), \\
\tilde{\lambda}' &= \operatorname{sgn}(\sin(\phi))(\sqrt{1-\delta^2})\big(Pe^{\tilde{\lambda}} + 1\big),
\end{aligned} \tag{3.118}$$

where $\operatorname{sgn}(\cdot)$ is the signum function and we denote $P \triangleq \sqrt{e^{2\tilde{\lambda}} + 2\delta e^{\tilde{\lambda}} + 1}$. As written, these dynamics are not self-contained because of the sign ambiguity, but by dividing

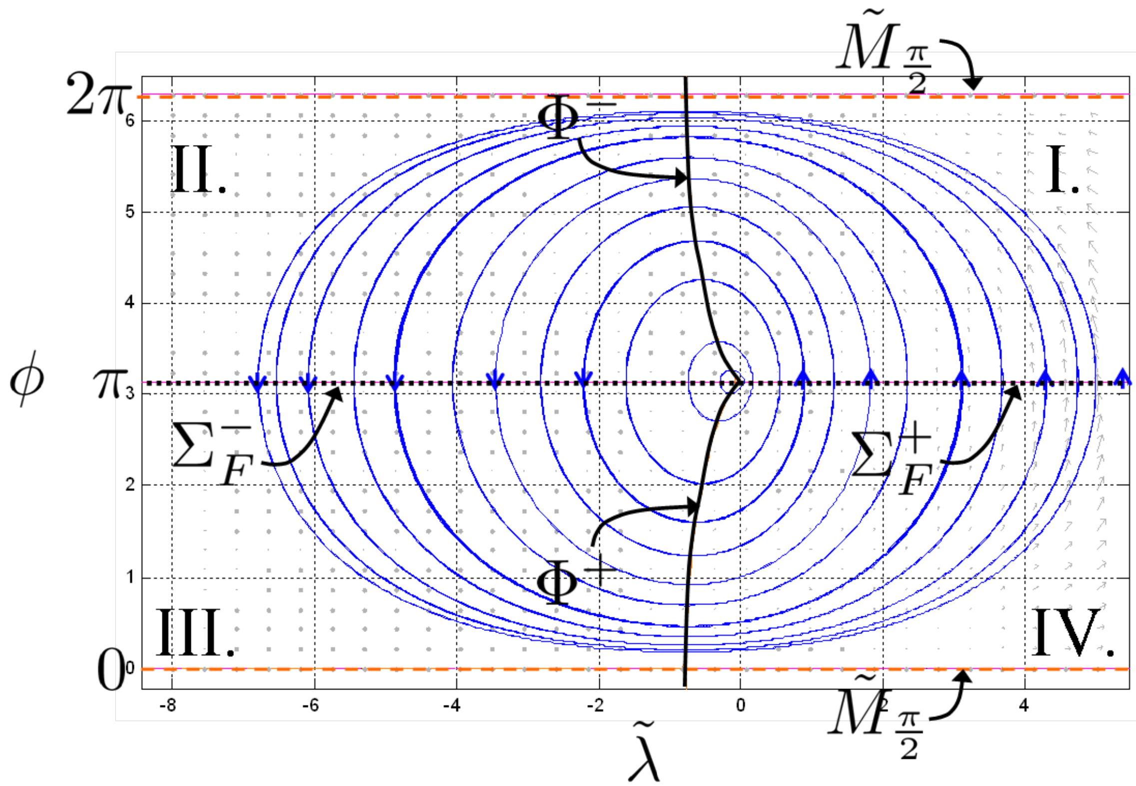

Figure 3.6: Depiction of the $\left\{\phi, \tilde{\lambda}\right\}$ phase portrait for the $\alpha = \pi/2$ case. Analogous to previous cases, the set $\tilde{M}_{\pi/2}$ consists of a continuum of rectilinear equilibria. However, in this case the phase portrait shows that all trajectories not starting on $\tilde{M}_{\pi/2}$ are in fact periodic in the $\left\{\phi, \tilde{\lambda}\right\}$ phase space. Note that the set $\Phi = \Phi^{+} \cup \Phi^{-}$ corresponds to the nullcline ($\phi' = 0$), and the set $\Sigma_F = \Sigma_F^{+} \cup \Sigma_F^{-}$ corresponds to the nullcline ($\tilde{\lambda}' = 0$), which is also the fixed-point set for the reverser F defined in **Proposition 3.5.14**.

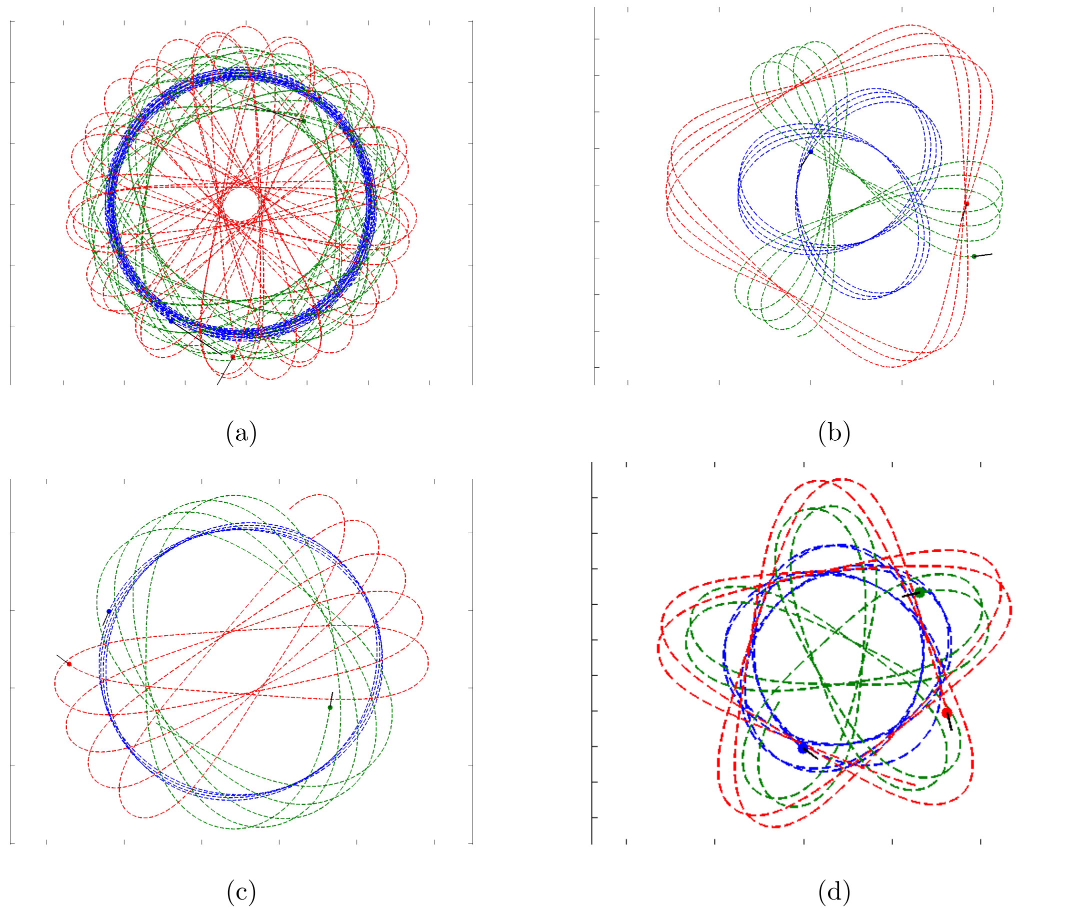

(a) (b) (c) (d)

Figure 3.7: These MATLAB plots illustrate 3-particle motions in the plane for different initial conditions arising in the $\alpha = \pi/2$ case. The associated phase space i.e. $(\phi, \tilde{\lambda})$ trajectories are periodic, and result in the precessing behavior in physical space depicted here.

the two equations we have

$$\frac{d\delta}{d\tilde{\lambda}} = \frac{-\Big(P\big(e^{\tilde{\lambda}} - \delta e^{\tilde{\lambda}} - 1\big) + \big(e^{\tilde{\lambda}} + \delta\big)\Big)}{Pe^{\tilde{\lambda}} + 1}, \tag{3.119}$$

with the second derivative (see appendix C for derivation) given by

$$\begin{aligned}\frac{d^2\delta}{d\tilde{\lambda}^2} = \frac{-e^{\tilde{\lambda}}}{P\left(Pe^{\tilde{\lambda}}+1\right)^2}\Bigg\{&P\left(e^{2\tilde{\lambda}} + 2\delta e^{\tilde{\lambda}} + 2\right) - e^{3\tilde{\lambda}} + e^{2\tilde{\lambda}}(2 - 5\delta)\\ &+ e^{\tilde{\lambda}}(-6\delta^2 + 3\delta - 1) + (1 - 3\delta)\Bigg\}.\end{aligned} \tag{3.120}$$

The following proposition establishes sign definiteness of $\frac{d^2\delta}{d\tilde{\lambda}^2}$ on a particular region, which will prove helpful in the subsequent analysis.

Proposition 3.5.11. $\frac{d^2\delta}{d\tilde{\lambda}^2} < 0$ *on the set* $\left\{(\delta, \tilde{\lambda}) \in D_{\delta,\tilde{\lambda}} \;\middle|\; \delta \in [1/25, 1)\right\}$.

Proof. The proof is provided in appendix C. □

We proceed with our analysis of the $\alpha = \pi/2$ case, using the notion of reversible dynamics as in [39].

Definition 3.5.12 (Involution). A diffeomorphism $F : M \longrightarrow M$ from a manifold M to itself is said to be an *involution* if $F \neq id_M$, the identity diffeomorphism, and $F^2 = id_M$, i.e. $F(F(m)) = m, \forall m \in M$.

Definition 3.5.13 (F-reversibility). A vector field X defined over a manifold M is said to be *F-reversible* if there exists an involution F such that $F_*(X) = -X$, i.e. F maps orbits of X to orbits of X, reversing the time parametrization. Here $(F_*(X))(m) = (DF)_{F^{-1}(m)}X(F^{-1}(m))\ \forall m \in M$ is the push-forward of F. We call F the *reverser* of X.

Proposition 3.5.14. *The vector field defined by (3.115) is F-reversible, with reverser* $F(\phi, \tilde{\lambda}) = (-\phi, \tilde{\lambda})$.

Proof. Identifying the vector field from (3.115) as $X(\phi, \tilde{\lambda})$, we have $X_1(\phi, \tilde{\lambda}) = \phi'$ and $X_2(\phi, \tilde{\lambda}) = \tilde{\lambda}'$. Observe from (3.85) that $P(-\phi, \tilde{\lambda}) = P(\phi, \tilde{\lambda})$, and hence direct calculation from (3.115) establishes that $X_1(-\phi, \tilde{\lambda}) = X_1(\phi, \tilde{\lambda})$ and $X_2(-\phi, \tilde{\lambda}) = -X_2(\phi, \tilde{\lambda})$. Therefore,

$$\begin{aligned}(F_*(X))(\phi, \tilde{\lambda}) &= (DF)_{(-\phi,\tilde{\lambda})} X(-\phi, \tilde{\lambda}) \\ &= \begin{bmatrix} -1 & 0 \\ 0 & 1 \end{bmatrix} \begin{bmatrix} X_1(\phi, \tilde{\lambda}) \\ -X_2(\phi, \tilde{\lambda}) \end{bmatrix} \\ &= -X(\phi, \tilde{\lambda}), \end{aligned} \tag{3.121}$$

which establishes the claim. □

Proposition 3.5.14 leads us to the following theorem of Birkhoff [4].

Theorem 3.5.15. ***(G.D. Birkhoff)***. *Let X be an F-reversible vector field on M and Σ_F the fixed-point set of the reverser F. If an orbit of X through a point of Σ_F intersects Σ_F in another point, then it is periodic.*

For the fixed point set $\Sigma_F = \left\{(\phi, \tilde{\lambda}) : \phi = \pi\right\}$ of our reverser F (defined in **Proposition 3.5.14**), in order to employ Birkhoff's theorem to show all trajectories (not starting on $\tilde{M}_{\pi/2}$) are periodic, we must show that all trajectories intersect Σ_F twice. (Note that here Σ_F is also the nullcline ($\tilde{\lambda}' = 0$).) First we demonstrate that our nullclines partition the phase space into four regions. We start by defining

$$\Phi^{+} \triangleq \left\{ \left(\phi, \tilde{\lambda}\right) \in \tilde{M}_{CB(\alpha,\alpha,\pi+\alpha)} \left| \phi^{'} = 0;\ \sin(\phi) > 0 \right. \right\},$$
$$\Phi^{-} \triangleq \left\{ \left(\phi, \tilde{\lambda}\right) \in \tilde{M}_{CB(\alpha,\alpha,\pi+\alpha)} \left| \phi^{'} = 0;\ \sin(\phi) < 0 \right. \right\}, \tag{3.122}$$

so that $\Phi \triangleq \Phi^{+} \cup \Phi^{-}$ represents the nullcline $(\phi^{'} = 0)$. Similarly, we define

$$\Sigma_F^{+} \triangleq \left\{ \left(\phi, \tilde{\lambda}\right) \in \tilde{M}_{CB(\alpha,\alpha,\pi+\alpha)} \left| \tilde{\lambda}^{'} = 0;\ \tilde{\lambda} > 0 \right. \right\},$$
$$\Sigma_F^{-} \triangleq \left\{ \left(\phi, \tilde{\lambda}\right) \in \tilde{M}_{CB(\alpha,\alpha,\pi+\alpha)} \left| \tilde{\lambda}^{'} = 0;\ \tilde{\lambda} < 0 \right. \right\}, \tag{3.123}$$

so that $\Sigma_F = \Sigma_F^{+} \cup \Sigma_F^{-}$.

Proposition 3.5.16. *The nullclines $\Phi = \Phi^{+} \cup \Phi^{-}$ and $\Sigma_F = \Sigma_F^{+} \cup \Sigma_F^{-}$ partition the phase portrait for the dynamics (3.115) into four regions (as depicted in figure 3.6) defined by*

- *region I, with borders Φ^{-}, Σ_F^{+}, and $\tilde{M}_{\pi/2}$;*
- *region II, with borders Φ^{-}, Σ_F^{-}, and $\tilde{M}_{\pi/2}$;*
- *region III, with borders Φ^{+}, Σ_F^{-}, and $\tilde{M}_{\pi/2}$;*
- *region IV, with borders Φ^{+}, Σ_F^{+}, and $\tilde{M}_{\pi/2}$.*

Furthermore, the sign of the dynamics (3.115) is characterized by

- *region I: $\phi^{'} > 0$, $\tilde{\lambda}^{'} < 0$;*
- *region II: $\phi^{'} < 0$, $\tilde{\lambda}^{'} < 0$;*
- *region III: $\phi^{'} < 0$, $\tilde{\lambda}^{'} > 0$;*

- *region IV:* $\phi' > 0$, $\tilde{\lambda}' > 0$.

Proof. Analytical computation of the nullcline Φ proves difficult, but we establish **Proposition 3.5.16** by a combination of analytical methods and phase plane computation tools.

We denote

$$\phi' = g_1(\delta, \tilde{\rho}) \triangleq \left(\sqrt{\tilde{\rho}^2 + 2\delta\tilde{\rho} + 1}\right)(\tilde{\rho} - 1 - \delta\tilde{\rho}) + (\tilde{\rho} + \delta), \tag{3.124}$$

employing the notation $\delta \triangleq \cos(\phi)$ and $\tilde{\rho} \triangleq e^{\tilde{\lambda}}$, and characterize Φ by considering the quantity

$$\begin{aligned}
G_1(\delta, \tilde{\rho}) &= g_1(\delta, \tilde{\rho}) \left[\left(\sqrt{\tilde{\rho}^2 + 2\delta\tilde{\rho} + 1}\right)(\tilde{\rho} - 1 - \delta\tilde{\rho}) - (\tilde{\rho} + \delta)\right] \\
&= \left[\left(\sqrt{\tilde{\rho}^2 + 2\delta\tilde{\rho} + 1}\right)(\tilde{\rho} - 1 - \delta\tilde{\rho}) + (\tilde{\rho} + \delta)\right] \times \\
&\qquad \left[\left(\sqrt{\tilde{\rho}^2 + 2\delta\tilde{\rho} + 1}\right)(\tilde{\rho} - 1 - \delta\tilde{\rho}) - (\tilde{\rho} + \delta)\right] \\
&= (\tilde{\rho}^2 + 2\delta\tilde{\rho} + 1)\Big(\tilde{\rho}(1 - \delta) - 1\Big)^2 - (\tilde{\rho} + \delta)^2 \\
&= (\tilde{\rho}^2 + 2\delta\tilde{\rho} + 1)\Big(\tilde{\rho}^2(1 - \delta)^2 - 2\tilde{\rho}(1 - \delta) + 1\Big) - \tilde{\rho}^2 - 2\delta\tilde{\rho} - \delta^2 \\
&= (\tilde{\rho}^2 + 2\delta\tilde{\rho} + 1)\Big(\tilde{\rho}^2(1 - \delta)^2 - 2\tilde{\rho}(1 - \delta)\Big) + (1 - \delta^2) \\
&= (1 - \delta)\Big[(\tilde{\rho}^2 + 2\delta\tilde{\rho} + 1)\Big(\tilde{\rho}^2(1 - \delta) - 2\tilde{\rho}\Big) + (1 + \delta)\Big] \\
&= (1 - \delta)\Big[(1 - \delta)\tilde{\rho}^4 - 2(\delta^2 - \delta + 1)\tilde{\rho}^3 + (1 - 5\delta)\tilde{\rho}^2 - 2\tilde{\rho} + (1 + \delta)\Big].
\end{aligned} \tag{3.125}$$

Since $g_1(\delta, \tilde{\rho})$ is a factor of $G_1(\delta, \tilde{\rho})$, we note that *the set of all roots of $g_1(\delta, \tilde{\rho})$ is contained in the set of all roots of $G_1(\delta, \tilde{\rho})$*. Therefore we can determine candidate roots for $g_1(\delta, \tilde{\rho})$ by considering the roots of $G_1(\delta, \tilde{\rho})$, which is more amenable to analysis.

In order to characterize Φ, we state and prove the following facts.

1. *For any* $\delta \in (-1, 1)$, *it holds that* $g_1(\delta, 1) > 0$. We establish this claim by analyzing the roots of the related expression $G_1(\delta, 1)$. Fixing $\tilde{\rho} = 1$ we have

$$\begin{aligned} G_1(\delta, 1) &= (1-\delta)(-2\delta^2 - 3\delta - 1) \\ &= 2(\delta - 1)(\delta + 1)\left(\delta + \frac{1}{2}\right), \end{aligned} \tag{3.126}$$

and hence the roots of $G_1(\delta, 1)$ are $\delta = 1, -1, -\frac{1}{2}$. Therefore in the interval $\delta \in (-1, 1)$, $\delta = -\frac{1}{2}$ is the only candidate root for $g_1(\delta, 1)$. However, direct substitution yields

$$g_1\left(-\frac{1}{2}, 1\right) = \left(\sqrt{2 + 2\left(-\frac{1}{2}\right)}\right)\left(\frac{1}{2}\right) + (1 - \frac{1}{2}) = 1 \neq 0, \tag{3.127}$$

and therefore we can conclude that there does not exist $\delta \in (-1, 1)$ satisfying $g_1(\delta, 1) = 0$. Since $g_1(\delta, 1)$ is continuous in δ, the Intermediate Value Theorem states that the image of $g_1(\delta, 1)$ must be an interval. Since zero is not included in that interval, $g_1(\delta, 1)$ must be either strictly positive or strictly negative for all values of $\delta \in (-1, 1)$, and since, for example, $g_1(0, 1) > 0$, our claim is established.

2. *Let* $\tilde{\rho}_0$ *be the one real root satisfying* $\tilde{\rho}_0^3 + 2\tilde{\rho}_0^2 + \tilde{\rho}_0 - 1 = 0$, *i.e.* $\tilde{\rho}_0 \approx .4656$.

Then for any $\delta \in (-1,1)$, it holds that $g_1(\delta, \tilde{\rho}_0) < 0$. First, observe that

$$\begin{aligned} G_1(\delta, \tilde{\rho}_0) &= (1-\delta)\Big[(-2\tilde{\rho}_0^3)\delta^2 + (-\tilde{\rho}_0^4 + 2\tilde{\rho}_0^3 - 5\tilde{\rho}_0^2 + 1)\delta \\ &\qquad\qquad + (\tilde{\rho}_0^4 - 2\tilde{\rho}_0^3 + \tilde{\rho}_0^2 - 2\tilde{\rho}_0 + 1)\Big] \\ &= (1-\delta)\Big\{(-2\tilde{\rho}_0^3)\delta^2 + \delta\Big[(-\tilde{\rho}_0^4 + 4\tilde{\rho}_0^3 - \tilde{\rho}_0^2 + 2\tilde{\rho}_0 - 1) \\ &\qquad - 2(\tilde{\rho}_0^3 + 2\tilde{\rho}_0^2 + \tilde{\rho}_0 - 1)\Big] + (\tilde{\rho}_0^4 - 2\tilde{\rho}_0^3 + \tilde{\rho}_0^2 - 2\tilde{\rho}_0 + 1)\Big\} \\ &= (1-\delta)\Big\{(-2\tilde{\rho}_0^3)\delta^2 + (-\tilde{\rho}_0^4 + 4\tilde{\rho}_0^3 - \tilde{\rho}_0^2 + 2\tilde{\rho}_0 - 1)\delta \\ &\qquad + (\tilde{\rho}_0^4 - 2\tilde{\rho}_0^3 + \tilde{\rho}_0^2 - 2\tilde{\rho}_0 + 1)\Big\} \\ &= (1-\delta)(\delta-1)\Big((-2\tilde{\rho}_0^3)\delta - (\tilde{\rho}_0^4 - 2\tilde{\rho}_0^3 + \tilde{\rho}_0^2 - 2\tilde{\rho}_0 + 1)\Big) \\ &= (1-\delta)^2\Big(2\tilde{\rho}_0^3\delta + (\tilde{\rho}_0^4 - 2\tilde{\rho}_0^3 + \tilde{\rho}_0^2 - 2\tilde{\rho}_0 + 1)\Big), \end{aligned} \tag{3.128}$$

i.e. the roots of $G_1(\delta, \tilde{\rho}_0)$ are $\delta = 1, \frac{1}{2\tilde{\rho}_0^3}(\tilde{\rho}_0^4 - 2\tilde{\rho}_0^3 + \tilde{\rho}_0^2 - 2\tilde{\rho}_0 + 1)$. Denoting the second root as δ_0, one can verify that $g_1(\delta_0, \tilde{\rho}_0) \neq 0$, and therefore $g_1(\delta_0, \tilde{\rho}_0)$ has no roots in the interval $\delta \in (-1,1)$. Again, by application of the Intermediate Value Theorem we conclude that $g_1(\delta, \tilde{\rho}_0)$ must be either strictly positive or strictly negative, and by direct calculation one can readily verify that in fact $g_1(\delta, \tilde{\rho}_0) < 0$ for any $\delta \in (-1,1)$.

3. *For any $\delta \in (-1,1)$ there exists $\tilde{\rho} \in (\tilde{\rho}_0, 1)$ such that $g_1(\delta, \tilde{\rho}) = 0$.* This claim follows from the previous two claims by invoking the continuity of $g_1(\delta, \tilde{\rho})$ and the Intermediate Value Theorem.

4. *For any $\delta \in (-1,1)$, there must be an odd number of distinct values of $\tilde{\rho}$ satisfying $g_1(\delta, \tilde{\rho}) = 0$.* Observe that for any fixed value of $\delta \in (-1,1)$, we

have

$$\lim_{\tilde{\rho}\to 0} g_1(\delta,\tilde{\rho}) = -1+\delta < 0 \tag{3.129}$$

and

$$\lim_{\tilde{\rho}\to +\infty} g_1(\delta,\tilde{\rho}) = \lim_{\tilde{\rho}\to +\infty} \left(\sqrt{\tilde{\rho}^2+2\delta\tilde{\rho}+1}\right)(\tilde{\rho}(1-\delta)-1)+(\tilde{\rho}+\delta) = +\infty \tag{3.130}$$

since $\tilde{\rho}(1-\delta)-1>0$ for $\tilde{\rho}>1/(1-\delta)$. Therefore as $\tilde{\rho}$ goes from 0 to positive infinity, $g_1(\delta,\tilde{\rho})$ experiences a sign change from negative to positive, hence there must be an odd number of distinct values of $\tilde{\rho}$ satisfying $g_1(\delta,\tilde{\rho})=0$.

5. *For any $\delta\in(-1,1)$, there must be either 0, 2, or 4 values of $\tilde{\rho}$ satisfying $G_1(\delta,\tilde{\rho})=0$.* Since $G_1(\delta,\tilde{\rho})$ is a fourth-order polynomial in $\tilde{\rho}$ with real coefficients, any complex roots must appear in complex conjugate pairs. Therefore there must be an even number of real roots.

Claim (3) establishes that for any $\delta\in(-1,1)$ there *exists* $\tilde{\rho}\in(\tilde{\rho}_0,1)$ such that $g_1(\delta,\tilde{\rho})=0$. High-precision numerical computation of the nullcline Φ demonstrates that for any $\delta\in(-1,1)$ there is in fact a *unique* $\tilde{\rho}$ such that $g_1(\delta,\tilde{\rho})=0$, i.e. Φ consists of a single (continuous) branch of roots and partitions the phase space into two parts, as depicted in figure 3.6. Thus ϕ' changes sign exactly one time as $\tilde{\lambda}$ is varied from $-\infty$ to ∞, and by claims (1) and (2) we conclude that $\phi'<0$ to the left of the nullcline Φ and $\phi'>0$ to the right of the nullcline. The rest of the proposition follows readily from the definition of Σ.

□

We now state the following theorem.

Theorem 3.5.17. *Every trajectory of the system (3.115) which starts on the set* $\tilde{M}_{CB(\frac{\pi}{2},\frac{\pi}{2},\frac{3\pi}{2})} - \tilde{M}_{\pi/2}$ *is periodic.*

Proof. Based on the characterization of the phase space provided by **Proposition 3.5.16**, we proceed with the application of the Birkhoff theorem by (a) first showing that trajectories starting on Σ_F^+ must reach Φ^-, and (b) showing that a trajectory starting on Φ^- must reach Σ_F^-. (Refer to figure 3.6.) First, observe that any trajectory starting on Σ_F^+ must enter into region I, since $\phi' > 0$ and $\tilde{\lambda}' = 0$ on Σ_F^+. In region I we have $\phi' > 0$ and $\tilde{\lambda}' < 0$, and therefore the trajectory must either reach Φ^- or asymptotically approach one of the equilibrium points in the set $\tilde{M}_{\pi/2}$. We will prove that the latter case is not possible, i.e. that no point in the portion of $\tilde{M}_{\pi/2}$ which borders region I can be a limit point for a trajectory of (3.115) which starts from Σ_F^+.

The foregoing analysis is simplified by working in terms of $\delta \triangleq \cos(\phi)$ rather than ϕ itself. Suppose there is a point $(\delta, \tilde{\lambda}) = (1, \tilde{\lambda}^*) \in \tilde{M}_{\pi/2}$ which is a limit point for a trajectory which starts from Σ_F^+. If we define $\tilde{\lambda}_0$ as the value of $\tilde{\lambda}$ at the point where Φ^- meets the set $\tilde{M}_{\pi/2}$ (i.e. $\tilde{\lambda}_0 = \ln(\tilde{\rho}_0)$, where $\tilde{\rho}_0$ is as defined in the statement above (3.128)), then our candidate limit point should satisfy $\tilde{\lambda}^* \geq \tilde{\lambda}_0$.

Then, as is illustrated in figures 3.8a and 3.8b, the trajectory must enter the set[5]

$$\Psi = \left\{ (\delta, \tilde{\lambda}) \in D_{\delta,\tilde{\lambda}} \;\middle|\; \tilde{\lambda}^* < \tilde{\lambda} \leq \tilde{\lambda}^* + 1,\ 1/25 \leq \delta < 1 \right\}, \tag{3.131}$$

either entering Ψ by way of the boundary on the right-hand side, which we denote as

$$\partial\Psi_R = \left\{ (\delta, \tilde{\lambda}) \in \Psi \;\middle|\; \tilde{\lambda} = \tilde{\lambda}^* + 1 \right\} \tag{3.132}$$

or through the lower boundary, which we denote as

$$\partial\Psi_L = \left\{ (\delta, \tilde{\lambda}) \in \Psi \;\middle|\; \delta = 1/25 \right\}. \tag{3.133}$$

(The first case is depicted in figure 3.8a, and the second case is depicted in figure 3.8b.) It follows directly from **Proposition 3.5.11** and **Proposition 3.5.16** that $\frac{\partial\delta}{\partial\tilde{\lambda}}(\delta, \tilde{\lambda}) < 0$ and $\frac{\partial^2\delta}{\partial\tilde{\lambda}^2}(\delta, \tilde{\lambda}) < 0$ for any $(\delta, \tilde{\lambda}) \in \Psi$, with $\frac{\partial\delta}{\partial\tilde{\lambda}}(\delta, \tilde{\lambda})$ and $\frac{\partial^2\delta}{\partial\tilde{\lambda}^2}(\delta, \tilde{\lambda})$ defined by (3.119) and (3.120) respectively. We'll deal separately with the two families of trajectories, those which pass through $\partial\Psi_R$ and those which pass through $\partial\Psi_L$.

We first address the trajectories which pass through $\partial\Psi_R$. We start by defining the function $f_\delta : [1/25, 1) \longrightarrow \mathbb{R}$ by

$$\begin{aligned} f_\delta(\delta) &= \delta + \left(\tilde{\lambda}^* - (\tilde{\lambda}^* + 1)\right) \frac{\partial\delta}{\partial\tilde{\lambda}}(\delta, \tilde{\lambda}^* + 1) \\ &= \delta + \frac{P\left(e^{(\tilde{\lambda}^*+1)} - \delta e^{(\tilde{\lambda}^*+1)} - 1\right) + e^{(\tilde{\lambda}^*+1)} + \delta}{Pe^{(\tilde{\lambda}^*+1)} + 1}, \end{aligned} \tag{3.134}$$

where $P = P(\delta, \tilde{\lambda}^* + 1) = \sqrt{e^{2(\tilde{\lambda}^*+1)} + 2\delta e^{(\tilde{\lambda}^*+1)} + 1}$. Clearly f_δ takes the form of some type of first-order approximation, a statement which we will make more precise

[5] As will become clear later in the proof, we define Ψ in this fashion (in particular, setting $\delta \geq 1/25$) so that we can employ **Proposition 3.5.11**.

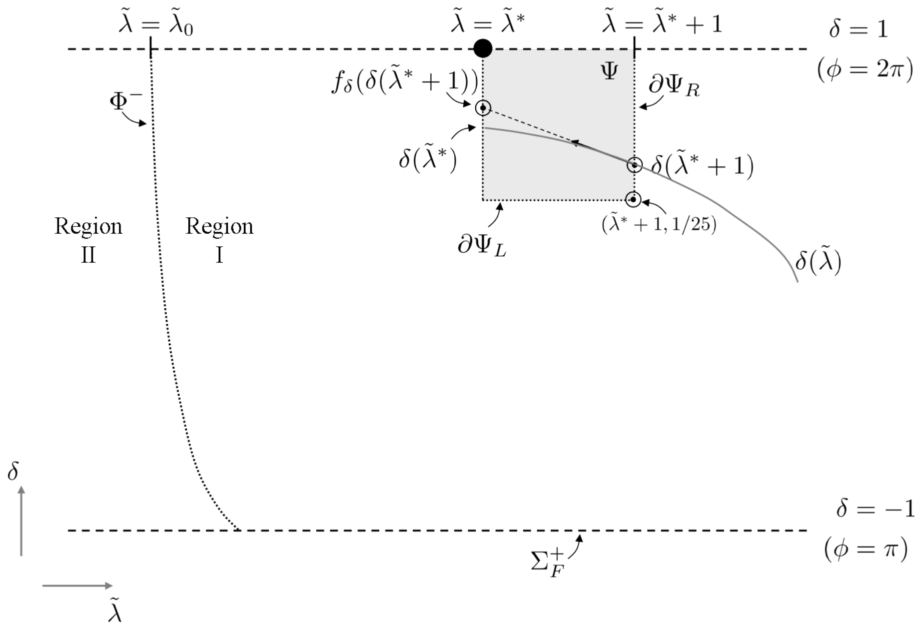

(a)

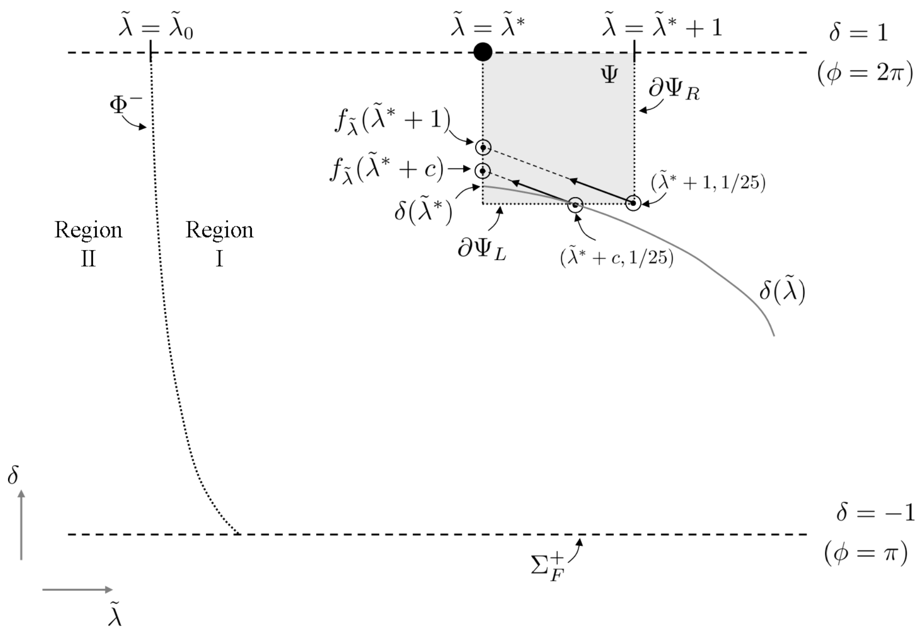

(b)

Figure 3.8: These figures illustrate generic trajectories in region I near a candidate limit point ($\phi = 2\pi, \tilde{\lambda} = \tilde{\lambda}^*$), passing through either $\partial\Psi_R$ (figure 3.8a) or $\partial\Psi_L$ (figure 3.8b). As is depicted, every trajectory which enters the set Ψ is bounded away from the candidate limit point ($\phi = 2\pi, \tilde{\lambda} = \tilde{\lambda}^*$).

later. First we prove that $f_\delta(\delta) < 1$ for every $\delta \in [1/25, 1)$. Observe that

$$\begin{aligned}
1 - f_\delta(\delta) &= 1 - \delta - \frac{P\big(e^{(\tilde{\lambda}^*+1)} - \delta e^{(\tilde{\lambda}^*+1)} - 1\big) + e^{(\tilde{\lambda}^*+1)} + \delta}{Pe^{(\tilde{\lambda}^*+1)} + 1} \\
&= \frac{1}{Pe^{(\tilde{\lambda}^*+1)} + 1}\Big\{(1-\delta)\left(Pe^{(\tilde{\lambda}^*+1)} + 1\right) \\
&\qquad - \left(Pe^{(\tilde{\lambda}^*+1)}(1-\delta) - P + e^{(\tilde{\lambda}^*+1)} + \delta\right)\Big\} \\
&= \frac{1}{Pe^{(\tilde{\lambda}^*+1)} + 1}\left\{P + \left(-e^{(\tilde{\lambda}^*+1)} + 1 - 2\delta\right)\right\}, \qquad (3.135)
\end{aligned}$$

and therefore we can establish our claim by demonstrating that the term in braces is positive. Since we want to prove this for arbitrary values of $\tilde{\lambda}^* \in [\tilde{\lambda}_0, \infty)$, we will temporarily view $\tilde{\lambda}^*$ as a variable, defining $g : [1/25, 1) \times [\tilde{\lambda}_0, \infty) \longrightarrow \mathbb{R}$ by

$$g(\delta, \tilde{\lambda}^*) \triangleq P + \left(-e^{(\tilde{\lambda}^*+1)} + 1 - 2\delta\right). \qquad (3.136)$$

We then proceed by considering the related quantity

$$\begin{aligned}
G(\delta, \tilde{\lambda}^*) &= g(\delta, \tilde{\lambda}^*)\left[P - \left(-e^{(\tilde{\lambda}^*+1)} + 1 - 2\delta\right)\right] \\
&= \left[P + \left(-e^{(\tilde{\lambda}^*+1)} + 1 - 2\delta\right)\right]\left[P - \left(-e^{(\tilde{\lambda}^*+1)} + 1 - 2\delta\right)\right] \\
&= P^2 - \left(-e^{(\tilde{\lambda}^*+1)} + 1 - 2\delta\right)^2 \\
&= \left(e^{2(\tilde{\lambda}^*+1)} + 2\delta e^{(\tilde{\lambda}^*+1)} + 1\right) - \left(e^{2(\tilde{\lambda}^*+1)} - 2e^{(\tilde{\lambda}^*+1)}(1-2\delta) + (1-2\delta)^2\right) \\
&= e^{(\tilde{\lambda}^*+1)}(2 - 2\delta) + 1 - \left(1 - 4\delta + 4\delta^2\right) \\
&= 2(1-\delta)\left(e^{(\tilde{\lambda}^*+1)} + 2\delta\right). \qquad (3.137)
\end{aligned}$$

Clearly $G(\delta, \tilde{\lambda}^*) \neq 0$ on $[1/25, 1) \times [\tilde{\lambda}_0, \infty)$, and therefore $g(\delta, \tilde{\lambda}^*) \neq 0$ on $[1/25, 1) \times [\tilde{\lambda}_0, \infty)$. Then since g is a continuous function on a connected subset of $\mathbb{R}^2$, by the Intermediate Value Theorem it must hold that the image of g is an interval which does not contain zero, i.e. it is either strictly positive or strictly negative. We can verify that it is in fact positive by checking, for example, the sign of $g(1/2, 0)$. Therefore $f_\delta(\delta) < 1$ for every $\delta \in [1/25, 1)$ and for every $\tilde{\lambda}^* \in [\tilde{\lambda}_0, \infty)$.

Since $\frac{\partial \delta}{\partial \tilde{\lambda}}(\delta, \tilde{\lambda}) < 0$ and $\frac{\partial^2 \delta}{\partial \tilde{\lambda}^2}(\delta, \tilde{\lambda}) < 0$ for any $(\delta, \tilde{\lambda}) \in \Psi$, we can view the portion of a trajectory that lies in Ψ as a concave function $\delta(\tilde{\lambda})$ defined on the interval $(\tilde{\lambda}^*, \tilde{\lambda}^* + c]$ for some $0 < c \leq 1$. (Note that $c = 1$ for trajectories which pass through $\partial\Psi_R$ and $c \leq 1$ for trajectories which pass through $\partial\Psi_L$.) Then f_δ, as defined in (3.134), maps every trajectory $\delta(\tilde{\lambda})$ passing through $\partial\Psi_R$ to the corresponding first-order approximation of $\delta(\tilde{\lambda}^*)$. Since these trajectory functions are each concave, each function $\delta(\tilde{\lambda})$ must lie below all of its tangents, i.e.

$$\delta(\tilde{\lambda}^*) < f_\delta(\delta(\tilde{\lambda}^* + 1)) < 1, \tag{3.138}$$

where the latter inequality was established above. Therefore all trajectories which pass through $\partial\Psi_R$ are bounded away from the proposed limit point.

We address the trajectories which pass through $\partial\Psi_L$ by comparing them to the trajectory which passes through the point at the intersection of $\partial\Psi_L$ and $\partial\Psi_R$, i.e. the bottom right-hand corner of Ψ where $\delta = 1/25$ and $\tilde{\lambda} = \tilde{\lambda}^* + 1$. We define the function $f_{\tilde{\lambda}} : (\tilde{\lambda}^*, \tilde{\lambda}^* + 1] \longrightarrow \mathbb{R}$ by

$$f_{\tilde{\lambda}}(\tilde{\lambda}) = 1/25 + (\tilde{\lambda}^* - \tilde{\lambda}) \frac{\partial \delta}{\partial \tilde{\lambda}}(1/25, \tilde{\lambda}), \tag{3.139}$$

which maps every trajectory $\delta(\tilde{\lambda})$ passing through $\partial\Psi_L$ to the corresponding first order approximation of $\delta(\tilde{\lambda}^*)$. In this case, we claim that $f_{\tilde{\lambda}}(\tilde{\lambda}) \leq f_{\tilde{\lambda}}(\tilde{\lambda}^* + 1)$ for every $\tilde{\lambda} \in (\tilde{\lambda}^*, \tilde{\lambda}^* + 1]$. We establish the claim as follows. First, for any $(\delta, \tilde{\lambda}) \in \partial\Psi_L$

we have $\frac{\partial\delta}{\partial\tilde{\lambda}}(\delta, \tilde{\lambda}) < 0$ and $\frac{\partial}{\partial\tilde{\lambda}}\left(\frac{\partial\delta}{\partial\tilde{\lambda}}(\delta, \tilde{\lambda})\right) < 0$, and therefore

$$\frac{\partial\delta}{\partial\tilde{\lambda}}(1/25, \tilde{\lambda}^* + 1) \leq \frac{\partial\delta}{\partial\tilde{\lambda}}(1/25, \tilde{\lambda}) < 0, \ \forall\tilde{\lambda} \in (\tilde{\lambda}^*, \tilde{\lambda}^* + 1]. \tag{3.140}$$

Hence

$$\begin{aligned}
f_{\tilde{\lambda}}(\tilde{\lambda}) - f_{\tilde{\lambda}}(\tilde{\lambda}^* + 1) &= (\tilde{\lambda}^* - \tilde{\lambda})\frac{\partial\delta}{\partial\tilde{\lambda}}(1/25, \tilde{\lambda}) - \left(\tilde{\lambda}^* - (\tilde{\lambda}^* + 1)\right)\frac{\partial\delta}{\partial\tilde{\lambda}}(1/25, \tilde{\lambda}^* + 1) \\
&= (\tilde{\lambda}^* - \tilde{\lambda})\frac{\partial\delta}{\partial\tilde{\lambda}}(1/25, \tilde{\lambda}) + \frac{\partial\delta}{\partial\tilde{\lambda}}(1/25, \tilde{\lambda}^* + 1) \\
&\leq (\tilde{\lambda}^* - \tilde{\lambda} + 1)\frac{\partial\delta}{\partial\tilde{\lambda}}(1/25, \tilde{\lambda}) \\
&\leq 0, \qquad (3.141)
\end{aligned}$$

which establishes the claim. Observe that $f_{\tilde{\lambda}}(\tilde{\lambda}^* + 1) = f_\delta(1/25)$, and we have already established that $f_\delta(1/25) < 1$. Therefore, for every trajectory $\delta(\tilde{\lambda})$ which passes through $\partial\Psi_L$, we have

$$\delta(\tilde{\lambda}^*) < f_{\tilde{\lambda}}(\tilde{\lambda}) \leq f_{\tilde{\lambda}}(\tilde{\lambda}^* + 1) < 1, \tag{3.142}$$

where the first inequality follows from the concavity of the $\delta(\tilde{\lambda})$ trajectories. (See figure 3.8b.) Hence, these trajectories are also bounded away from the proposed limit point, and since all steps of our proof hold for arbitrary values of $\tilde{\lambda}^* \in \mathbb{R}$, we have demonstrated that no point in the portion of $\tilde{M}_{\pi/2}$ which borders region I can serve as a limit point for a trajectory which starts from Σ_F^+.

We have established that every trajectory which starts on Σ_F^+ must reach Φ^-. Since $\tilde{\lambda}' < 0$ on Φ^-, the trajectory must continue into region II. As previously noted, there are no equilibria in the interior of region II, and on region II we have $\phi' < 0$ and $\tilde{\lambda}' < 0$. In the proof of **Proposition 3.5.16** we demonstrated that if $(\phi, \tilde{\lambda}) \in \Phi$

then $\tilde{\lambda} < 0$, and therefore trajectories in region II may not asymptotically approach the excluded point at $(\phi = \pi, \tilde{\lambda} = 0)$ as a limit point. Therefore, all trajectories must either reach Σ_F^- or move towards $\tilde{\lambda} = -\infty$ along a horizontal asymptote. If such an asymptote existed, then $\phi^{'} = 0$ on the asymptote itself. However, we have already established that $\phi^{'} < 0$ on all of region II and can also readily show that $\phi^{'} < 0$ on Σ_F^-, and therefore there cannot exist such a horizontal asymptote which would prevent trajectories from reaching Σ_F^-. It follows by **Theorem 3.5.15** that every trajectory is periodic. $\square$

3.5.4 Analysis of the $\alpha \in (\pi/2, 3\pi/2)$ case for Type 1 rectilinear equilibria

For $\alpha \in (\pi/2, 3\pi/2)$, our dynamics are as stated in (3.86). The phase portrait, displayed in figure 3.9, reveals that the equilibria of $\tilde{M}_\alpha$ are unstable in this case. We can formally prove instability of the equilibria in $\tilde{M}_\alpha$ by observing that linearization of the dynamics (3.86) about an equilibrium point $(0, \tilde{\lambda}^0) \in \tilde{M}_\alpha$ yields the Jacobian matrix

$$\left(e^{2\tilde{\lambda}_0} + e^{\tilde{\lambda}_0} + 1\right) \begin{bmatrix} -\cos(\alpha) & 0 \\ \sin(\alpha) & 0 \end{bmatrix}, \tag{3.143}$$

which has an eigenvalue at $-\left(e^{2\tilde{\lambda}_0} + e^{\tilde{\lambda}_0} + 1\right)\cos(\alpha) > 0$ (for $\alpha \in (\pi/2, 3\pi/2)$). Generic trajectories on $\tilde{M}_{CB(\alpha,\alpha,\pi+\alpha)}$ tend to spiral in towards the excluded point $\phi = \pi, \tilde{\lambda} = 0$, which implies that $\rho_3/\rho_1 \longrightarrow 0$.

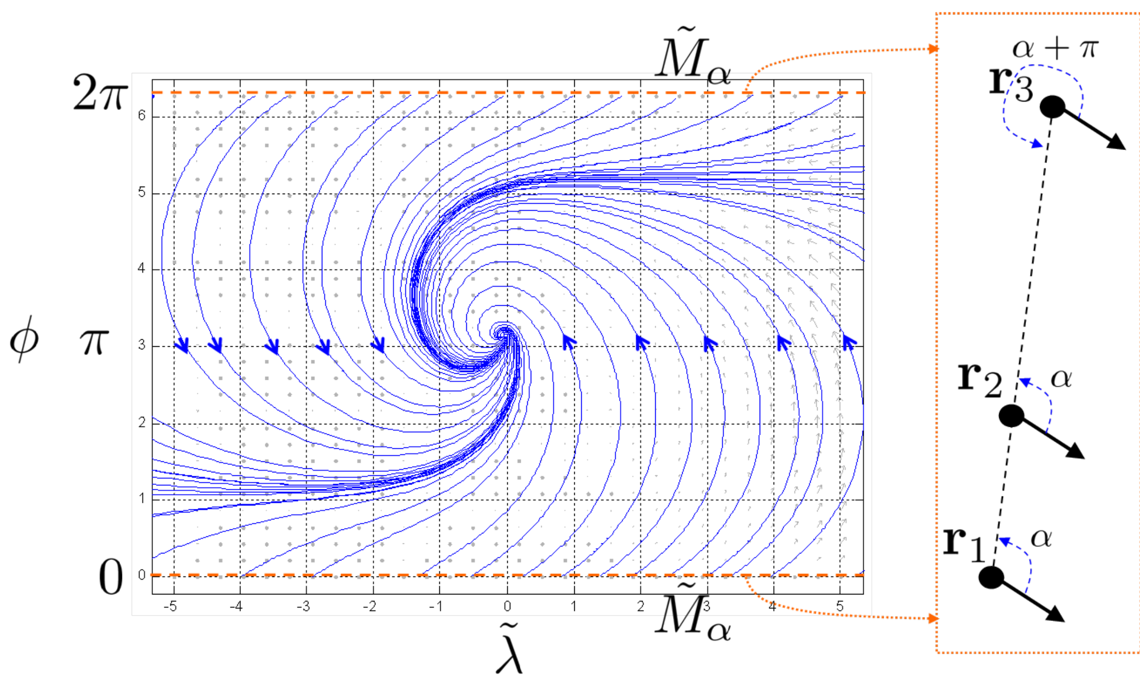

Figure 3.9: Depiction of the $\left\{\phi, \tilde{\lambda}\right\}$ phase portrait for $\alpha = 2\pi/3$, representing the $\alpha \in (\pi/2, 3\pi/2)$ case. Here the equilibria of $\tilde{M}_\alpha$ are unstable, and trajectories asymptotically approach $\phi = \pi, \tilde{\lambda} = 0$, i.e. $\rho_3/\rho_1 \longrightarrow 0$.

3.6 Stability analysis for three-particle circling equilibria

In section 2.4.1 we derived existence conditions for circling equilibria on $M_{CB(\boldsymbol{\alpha})}$ and provided descriptions of the equilibrium values for θ_i and ρ_i (see **Proposition 2.4.1**). It should be noted from (2.75) that the equilibrium values for the side lengths $\hat{\rho}_i$ are expressed in terms of their ratios as opposed to their absolute values, describing a continuum of circling equilibria rather than an isolated equilibrium point. Recall from section 2.4.2 that $M_{CB(\boldsymbol{\alpha})} \cong \mathbb{R}^+ \times \tilde{M}_{CB(\boldsymbol{\alpha})}$, with the projection function $\Psi : M_{CB(\boldsymbol{\alpha})} \longrightarrow \tilde{M}_{CB(\boldsymbol{\alpha})}$ defined by

$$\Psi(\theta_1, \rho_1, \theta_2, \rho_2 \ldots, \theta_n, \rho_n) = \left(\theta_1, \frac{\rho_1}{\rho_1}, \theta_2, \frac{\rho_2}{\rho_1} \ldots, \theta_n, \frac{\rho_n}{\rho_1}\right), \tag{3.144}$$

and therefore the continuum of circling equilibria is actually a fiber $\Psi^{-1}(m)$ over a particular $m \in \tilde{M}_{CB(\boldsymbol{\alpha})}$.

For the three-particle case, we developed an alternative parametrization for $M_{CB(\alpha_1,\alpha_2,\alpha_3)}$ and $\tilde{M}_{CB(\alpha_1,\alpha_2,\alpha_3)}$ in section 3.3 in terms of $(\theta_2, \tilde{\lambda}, \rho_1)$, for which the corresponding projection function is given by

$$\Psi(\theta_2, \tilde{\lambda}, \rho_1) = (\theta_2, \tilde{\lambda}). \tag{3.145}$$

We let X denote the vector field defined by (3.57)-(3.58)-(3.59) and $\tilde{X}$ denote the projected vector field (3.57)-(3.58). If a point $(\theta_2, \tilde{\lambda}) \in \tilde{M}_{CB(\alpha_1,\alpha_2,\alpha_3)}$ is an equilibrium point for the projected vector field $\tilde{X}$, then the manifold $\Psi^{-1}(\theta_2, \tilde{\lambda}) \in M_{CB(\alpha_1,\alpha_2,\alpha_3)}$ is invariant under the vector field X. If $\alpha_1, \alpha_2, \alpha_3$ satisfy the circling equilibrium existence conditions of **Proposition 2.4.1**, then making use of (2.75), we define

$$M_{circ} \triangleq \Psi^{-1}\left(\pi - \alpha_1, \ln\left(\frac{\sin(\alpha_2)}{\sin(\alpha_1)}\right)\right). \tag{3.146}$$

We can discuss stability properties of these types of invariant manifolds in terms of the stability of the projected point. Analogous to Definition 5.1.1 in [56], we make the following definition:

Definition 3.6.1 Let $(\theta_2, \tilde{\lambda}) \in \tilde{M}_{CB(\alpha_1,\alpha_2,\alpha_3)}$ be an equilibrium point for the projected vector field $\tilde{X}$. Then $\Psi^{-1}(\theta_2, \tilde{\lambda}) \in M_{CB(\alpha_1,\alpha_2,\alpha_3)}$ is a *(asymptotically) stable invariant submanifold* with respect to the vector field X if $(\theta_2, \tilde{\lambda})$ is a (asymptotically) stable equilibrium point for the projected vector field $\tilde{X}$.

Stability of three-particle circling equilibria is characterized by the following theorem. (We also restate the existence conditions for the sake of completeness and clarity.)

Theorem 3.6.2. *Given a three-particle cyclic CB pursuit system evolving on the manifold $M_{CB(\alpha_1,\alpha_2,\alpha_3)}$ according to the shape dynamics (2.68), a circling relative equilibrium exists if and only if*

$$\begin{aligned} &i.\ \ \sin(\alpha_{i-1})\sin(\alpha_i) > 0,\ i = 1,2,3,\\ &ii.\ \ \sin\left(\sum_{i=1}^{3}\alpha_i\right) = 0. \end{aligned} \tag{3.147}$$

Moreover, the stability of such three-particle circling equilibria can be characterized as follows:

1. *if* $\cos\left(\sum_{i=1}^{3}\alpha_i\right) = 1$, *then any associated circling equilibrium is unstable;*

2. *if* $\cos\left(\sum_{i=1}^{3}\alpha_i\right) = -1$, *then* M_{circ} *is an asymptotically stable invariant submanifold, in the sense of* ***Definition 3.6.1***.

Proof. The existence conditions are simply re-stated from **Proposition 2.4.1**. We prove the stability claims by analysis of the linearization of the $\left\{\theta_2, \tilde{\lambda}\right\}$ dynamics (3.57)-(3.58). Substituting the equilibrium values from (2.75) into (3.64), (3.65), (3.66) and (3.67), we have the following form for the Jacobian[6]:

$$\left(\frac{\partial g}{\partial x}\right)_{circ} = \begin{bmatrix} \frac{\sin^2(\alpha_1+\alpha_2)-\sin(\alpha_1)\sin(\alpha_2)\cos(\alpha_1)\cos(\alpha_2)}{\cos\left(\sum_{i=1}^{3}\alpha_i\right)\sin^2(\alpha_1)} & \frac{-\sin(\alpha_2)\Big(\sin(\alpha_1+\alpha_2)+\sin(\alpha_2)\cos(\alpha_1)\Big)}{\cos\left(\sum_{i=1}^{3}\alpha_i\right)\sin(\alpha_1)} \\ \frac{\sin(\alpha_2)\Big(\sin(\alpha_1+\alpha_2)+\sin(\alpha_1)\cos(\alpha_2)\Big)}{\cos\left(\sum_{i=1}^{3}\alpha_i\right)\sin(\alpha_1)} & \cos\left(\sum_{i=1}^{3}\alpha_i\right)\sin^2(\alpha_2) \end{bmatrix}. \tag{3.148}$$

Since $\cos^2\left(\sum_{i=1}^{3}\alpha_i\right) = 1$, we can express the determinant as

$$\begin{aligned} \det\left(\frac{\partial g}{\partial x}\right)_{circ} &= \frac{\sin^2(\alpha_2)}{\sin^2(\alpha_1)}\Big(\sin^2(\alpha_1+\alpha_2) - \sin(\alpha_1)\sin(\alpha_2)\cos(\alpha_1)\cos(\alpha_2)\Big) \\ &\quad + \frac{\sin^2(\alpha_2)}{\sin^2(\alpha_1)}\Big(\sin^2(\alpha_1+\alpha_2) + \sin(\alpha_1)\sin(\alpha_2)\cos(\alpha_1)\cos(\alpha_2) \\ &\qquad + \sin(\alpha_1+\alpha_2)\Big(\sin(\alpha_1)\cos(\alpha_2) + \cos(\alpha_1)\sin(\alpha_2)\Big)\Big) \\ &= \frac{3\sin^2(\alpha_2)\sin^2(\alpha_1+\alpha_2)}{\sin^2(\alpha_1)}, \end{aligned} \tag{3.149}$$

and the eigenvalues of $\left(\frac{\partial g}{\partial x}\right)_{circ}$ take the form

$$\lambda = \frac{1}{2}\left[\left(\frac{\partial g}{\partial x}\right)_{11} + \left(\frac{\partial g}{\partial x}\right)_{22}\right] \pm \frac{1}{2}\sqrt{\left[\left(\frac{\partial g}{\partial x}\right)_{11} + \left(\frac{\partial g}{\partial x}\right)_{22}\right]^2 - 4\det\left(\frac{\partial g}{\partial x}\right)_{circ}}, \tag{3.150}$$

[6]See appendix C.

where the two-digit subscripts indicate indices of matrix elements. Observe from (3.149) that $\det\left(\frac{\partial g}{\partial x}\right)_{circ} > 0$ (since $\sin(\alpha_i) \neq 0$ and $\sin(\alpha_1+\alpha_2) \neq 0$), and therefore if the eigenvalues are real, they must have the same sign. It follows that

$$
\begin{aligned}
\operatorname{sgn}\Big(Re(\lambda)\Big) &= \operatorname{sgn}\left(\left(\frac{\partial g}{\partial x}\right)_{11} + \left(\frac{\partial g}{\partial x}\right)_{22}\right) \\
&= \operatorname{sgn}\left(\frac{1}{\cos\left(\sum_{i=1}^{3}\alpha_i\right)\sin^2(\alpha_1)}\Big(\sin^2(\alpha_1+\alpha_2)\right. \\
&\qquad \left.- \sin(\alpha_1)\sin(\alpha_2)\cos(\alpha_1)\cos(\alpha_2) + \sin^2(\alpha_1)\sin^2(\alpha_2)\Big)\right) \\
&= \operatorname{sgn}\left(\frac{1}{\cos\left(\sum_{i=1}^{3}\alpha_i\right)\sin^2(\alpha_1)}\Big(\sin^2(\alpha_1+\alpha_2)\right. \\
&\qquad \left.- \sin(\alpha_1)\sin(\alpha_2)\Big(\cos(\alpha_1)\cos(\alpha_2) - \sin(\alpha_1)\sin(\alpha_2)\Big)\Big)\right) \\
&= \operatorname{sgn}\left(\frac{1-\cos^2(\alpha_1+\alpha_2) - \sin(\alpha_1)\sin(\alpha_2)\cos(\alpha_1+\alpha_2)}{\cos\left(\sum_{i=1}^{3}\alpha_i\right)\sin^2(\alpha_1)}\right) \\
&= \operatorname{sgn}\left(\frac{1-\cos(\alpha_1+\alpha_2)\Big(\cos(\alpha_1+\alpha_2) + \sin(\alpha_1)\sin(\alpha_2)\Big)}{\cos\left(\sum_{i=1}^{3}\alpha_i\right)\sin^2(\alpha_1)}\right) \\
&= \operatorname{sgn}\left(\frac{1-\cos(\alpha_1+\alpha_2)\cos(\alpha_1)\cos(\alpha_2)}{\cos\left(\sum_{i=1}^{3}\alpha_i\right)\sin^2(\alpha_1)}\right) \\
&= \operatorname{sgn}\left(\cos\left(\sum_{i=1}^{3}\alpha_i\right)\right).
\end{aligned}
\tag{3.151}
$$

(The last equality follows from the fact that $\sin(\alpha_i) \neq 0$ and therefore $\cos(\alpha_1 + \alpha_2)\cos(\alpha_1)\cos(\alpha_2) < 1$.) The claims of the proof then follow from (3.151). □

3.7 Stability analysis for three-particle pure shape equilibria

In section **Proposition 2.4.2** we determined existence conditions for a type of system trajectory which we called "pure shape equilibria". These system trajectories correspond to equilibria for the dynamics (2.103)-(2.104) and include circling equilibria as a special case. Analogous to the approach in section 3.6, we define

$$M_k \triangleq \Psi^{-1}\left(\hat{\theta}_2, \hat{\tilde{\lambda}}\right) = \Psi^{-1}\left(\pi - \alpha_1 + 2\tau_k, \ln\left(\frac{\sin(\alpha_2 - \tau_k)}{\sin(\alpha_1 - \tau_k)}\right)\right), \tag{3.152}$$

where Ψ is the projection function defined by (3.145). Stability properties for three-particle pure shape equilibria are characterized by the following theorem[7]. As with the circling case, we include the (restated) existence conditions for the sake of completeness and clarity.

Theorem 3.7.1. *Given a three-particle cyclic CB pursuit system evolving on the manifold $M_{CB(\alpha_1,\alpha_2,\alpha_3)}$ according to the shape dynamics (2.68), a pure shape equilibrium exists if and only if there exists an integer $k \in \{0, 1, 2\}$ such that*

$$\sin(\alpha_i - \tau_k)\sin(\alpha_{i-1} - \tau_k) > 0,\ i = 1, 2, 3, \tag{3.153}$$

for

$$\tau_k \triangleq \left(\sum_{i=1}^{3} \frac{\alpha_i}{3}\right) - \frac{k\pi}{3}. \tag{3.154}$$

[7] Rectilinear relative equilibria are also included in **Proposition 2.4.2** but are not considered here, since we have already analyzed the stability properties of rectilinear equilibria in section 3.5.

Moreover, the stability of such pure shape equilibria can be characterized in terms of the stability coefficient

$$\Phi_{\boldsymbol{\alpha},k} \triangleq \sum_{i=1}^{3} \sin(\alpha_i - \tau_k)\sin(\alpha_{i+1} - \tau_k)\cos(\alpha_{i+2} - 2\tau_k) \tag{3.155}$$

as follows:

1. *if* $\Phi_{\boldsymbol{\alpha},k} < 0$*, then any associated pure shape equilibrium is unstable;*

2. *if* $\Phi_{\boldsymbol{\alpha},k} > 0$*, then* M_k *is an asymptotically stable invariant submanifold.*

Proof. Substituting the equilibrium values for θ_i and $\tilde{\rho}_i = \frac{\rho_i}{\rho_1}$ (from (2.106)) into (3.64), (3.65), (3.66) and (3.67), we demonstrate in appendix C that the evaluated Jacobian takes the form

$$\left(\frac{\partial g}{\partial x}\right)_{PS} = \begin{bmatrix} \frac{\cos(\tau_k)D+\sin(\tau_k)CS_1}{\cos(k\pi)\sin^2(\alpha_1-\tau_k)} & \frac{\sin(\alpha_2-\tau_k)\left(-\cos(\tau_k)S_2+\sin(\tau_k)C\right)}{\cos(k\pi)\sin(\alpha_1-\tau_k)} \\ \frac{\cos(\tau_k)CS_1-\sin(\tau_k)D}{\cos(k\pi)\sin^2(\alpha_1-\tau_k)} & \frac{\sin(\alpha_2-\tau_k)\left(\cos(\tau_k)C+\sin(\tau_k)S_2\right)}{\cos(k\pi)\sin(\alpha_1-\tau_k)} \end{bmatrix}, \tag{3.156}$$

where

$$\begin{aligned} S_1 &= \sin(\alpha_1 + \alpha_2 - 2\tau_k) + \sin(\alpha_1 - \tau_k)\cos(\alpha_2 - \tau_k), \\ S_2 &= \sin(\alpha_1 + \alpha_2 - 2\tau_k) + \sin(\alpha_2 - \tau_k)\cos(\alpha_1 - \tau_k), \\ C &= \sin(\alpha_1 - \tau_k)\sin(\alpha_2 - \tau_k), \\ D &= \sin^2(\alpha_1 + \alpha_2 - 2\tau_k) - \sin(\alpha_1 - \tau_k)\sin(\alpha_2 - \tau_k)\cos(\alpha_1 - \tau_k)\cos(\alpha_2 - \tau_k). \end{aligned} \tag{3.157}$$

Note that $\cos^2(k\pi) = 1$, and therefore the determinant is given by

$$
\begin{aligned}
\det\left(\frac{\partial g}{\partial x}\right)_{PS} &= \left(\frac{\sin(\alpha_2-\tau_k)}{\sin^3(\alpha_1-\tau_k)}\right)\Big[\cos^2(\tau_k)CD + \cos(\tau_k)\sin(\tau_k)(S_2D + C^2S_1) \\
&\qquad + \sin^2(\tau_k)CS_1S_2\Big] \\
&\quad - \left(\frac{\sin(\alpha_2-\tau_k)}{\sin^3(\alpha_1-\tau_k)}\right)\Big[-\cos^2(\tau_k)CS_1S_2 + \cos(\tau_k)\sin(\tau_k)(S_2D + C^2S_1) \\
&\qquad - \sin^2(\tau_k)CD\Big] \\
&= \frac{\sin(\alpha_2-\tau_k)}{\sin^3(\alpha_1-\tau_k)}\Big[\cos^2(\tau_k)C(D+S_1S_2) + \sin^2(\tau_k)C(D+S_1S_2)\Big] \\
&= \frac{\sin(\alpha_2-\tau_k)}{\sin^3(\alpha_1-\tau_k)}\Big(\sin(\alpha_1-\tau_k)\sin(\alpha_2-\tau_k)\Big)(D+S_1S_2) \\
&= \frac{\sin^2(\alpha_2-\tau_k)}{\sin^2(\alpha_1-\tau_k)}(D+S_1S_2). \qquad (3.158)
\end{aligned}
$$

We can further simplify by observing that

$$
\begin{aligned}
D + S_1S_2 &= \sin^2(\alpha_1+\alpha_2-2\tau_k) - \sin(\alpha_1-\tau_k)\sin(\alpha_2-\tau_k)\cos(\alpha_1-\tau_k)\cos(\alpha_2-\tau_k) \\
&\quad + \sin^2(\alpha_1+\alpha_2-2\tau_k) + \sin(\alpha_1+\alpha_2-2\tau_k)\Big[\sin(\alpha_1-\tau_k)\cos(\alpha_2-\tau_k) \\
&\qquad + \sin(\alpha_2-\tau_k)\cos(\alpha_1-\tau_k)\Big] \\
&\qquad\quad + \sin(\alpha_1-\tau_k)\sin(\alpha_2-\tau_k)\cos(\alpha_1-\tau_k)\cos(\alpha_2-\tau_k) \\
&= 3\sin^2(\alpha_1+\alpha_2-2\tau_k), \qquad (3.159)
\end{aligned}
$$

and therefore

$$
\det\left(\frac{\partial g}{\partial x}\right)_{PS} = \frac{3\sin^2(\alpha_2-\tau_k)\sin^2(\alpha_1+\alpha_2-2\tau_k)}{\sin^2(\alpha_1-\tau_k)}. \qquad (3.160)
$$

The eigenvalues of $\left(\frac{\partial g}{\partial x}\right)_{PS}$ take the form

$$
\lambda = \frac{1}{2}\left[\left(\frac{\partial g}{\partial x}\right)_{11} + \left(\frac{\partial g}{\partial x}\right)_{22}\right] \pm \frac{1}{2}\sqrt{\left[\left(\frac{\partial g}{\partial x}\right)_{11} + \left(\frac{\partial g}{\partial x}\right)_{22}\right]^2 - 4\det\left(\frac{\partial g}{\partial x}\right)_{PS}}, \qquad (3.161)
$$

(where the two-digit subscripts indicate indices of matrix elements), and since $\det\left(\frac{\partial g}{\partial x}\right)_{PS} \geq 0$, it follows that the real parts of the eigenvalues both have the same sign, given by

$$\operatorname{sgn}\Big(Re(\lambda)\Big) = \operatorname{sgn}\left(\left(\frac{\partial g}{\partial x}\right)_{11} + \left(\frac{\partial g}{\partial x}\right)_{22}\right). \tag{3.162}$$

Defining

$$\tilde{\Phi}_{\boldsymbol{\alpha},k} \triangleq \left(\frac{\partial g}{\partial x}\right)_{11} + \left(\frac{\partial g}{\partial x}\right)_{22}, \tag{3.163}$$

we observe that

$$\begin{aligned}
\tilde{\Phi}_{\boldsymbol{\alpha},k} &= \frac{\cos(\tau_k)D + \sin(\tau_k)CS_1}{\cos(k\pi)\sin^2(\alpha_1 - \tau_k)} + \frac{\sin(\alpha_2 - \tau_k)\Big(\cos(\tau_k)C + \sin(\tau_k)S_2\Big)}{\cos(k\pi)\sin(\alpha_1 - \tau_k)} \\
&= \frac{1}{\cos(k\pi)\sin^2(\alpha_1 - \tau_k)}\Big[\cos(\tau_k)D + \sin(\tau_k)CS_1 \\
&\qquad + \sin(\alpha_1 - \tau_k)\sin(\alpha_2 - \tau_k)\Big(\cos(\tau_k)C + \sin(\tau_k)S_2\Big)\Big] \\
&= \frac{1}{\cos(k\pi)\sin^2(\alpha_1 - \tau_k)}\Big[\cos(\tau_k)D + \sin(\tau_k)CS_1 + C\Big(\cos(\tau_k)C + \sin(\tau_k)S_2\Big)\Big] \\
&= \frac{1}{\cos(k\pi)\sin^2(\alpha_1 - \tau_k)}\Big[\cos(\tau_k)\Big(D + C^2\Big) + \sin(\tau_k)C\Big(S_1 + S_2\Big)\Big].
\end{aligned} \tag{3.164}$$

To further simplify, we note that

$$\begin{aligned}
\cos^2(\alpha_1 + \alpha_2 - 2\tau_k) &= \Big(\cos(\alpha_1 - \tau_k)\cos(\alpha_2 - \tau_k) - \sin(\alpha_1 - \tau_k)\sin(\alpha_2 - \tau_k)\Big)^2 \\
&= \cos^2(\alpha_1 - \tau_k)\cos^2(\alpha_2 - \tau_k) + \sin^2(\alpha_1 - \tau_k)\sin^2(\alpha_2 - \tau_k) \\
&\quad - 2\cos(\alpha_1 - \tau_k)\cos(\alpha_2 - \tau_k)\sin(\alpha_1 - \tau_k)\sin(\alpha_2 - \tau_k),
\end{aligned} \tag{3.165}$$

and therefore

$$
\begin{aligned}
D + C^2 &= \sin^2(\alpha_1 + \alpha_2 - 2\tau_k) - \sin(\alpha_1 - \tau_k)\sin(\alpha_2 - \tau_k)\cos(\alpha_1 - \tau_k)\cos(\alpha_2 - \tau_k) \\
&\quad + \sin^2(\alpha_1 - \tau_k)\sin^2(\alpha_2 - \tau_k) \\
&= \sin^2(\alpha_1 + \alpha_2 - 2\tau_k) - \sin(\alpha_1 - \tau_k)\sin(\alpha_2 - \tau_k)\cos(\alpha_1 - \tau_k)\cos(\alpha_2 - \tau_k) \\
&\quad + \cos^2(\alpha_1 + \alpha_2 - 2\tau_k) - \Big[\cos^2(\alpha_1 - \tau_k)\cos^2(\alpha_2 - \tau_k) \\
&\qquad - 2\cos(\alpha_1 - \tau_k)\cos(\alpha_2 - \tau_k)\sin(\alpha_1 - \tau_k)\sin(\alpha_2 - \tau_k)\Big] \\
&= 1 - \cos^2(\alpha_1 - \tau_k)\cos^2(\alpha_2 - \tau_k) \\
&\quad + \cos(\alpha_1 - \tau_k)\cos(\alpha_2 - \tau_k)\sin(\alpha_1 - \tau_k)\sin(\alpha_2 - \tau_k) \\
&= 1 - \cos(\alpha_1 - \tau_k)\cos(\alpha_2 - \tau_k)\Big[\cos(\alpha_1 - \tau_k)\cos(\alpha_2 - \tau_k) \\
&\qquad - \sin(\alpha_1 - \tau_k)\sin(\alpha_2 - \tau_k)\Big] \\
&= 1 - \cos(\alpha_1 - \tau_k)\cos(\alpha_2 - \tau_k)\cos(\alpha_1 + \alpha_2 - 2\tau_k). \qquad (3.166)
\end{aligned}
$$

We also have

$$
\begin{aligned}
S_1 + S_2 &= 2\sin(\alpha_1 + \alpha_2 - 2\tau_k) + \sin(\alpha_1 - \tau_k)\cos(\alpha_2 - \tau_k) + \sin(\alpha_2 - \tau_k)\cos(\alpha_1 - \tau_k) \\
&= 3\sin(\alpha_1 + \alpha_2 - 2\tau_k), \qquad (3.167)
\end{aligned}
$$

and observing from (3.154) that

$$
\begin{aligned}
\alpha_1 + \alpha_2 - 2\tau_k &= \left(\sum_{i=1}^{3}\alpha_i\right) - 3\tau_k - (\alpha_3 - \tau_k) \\
&= \left(\sum_{i=1}^{3}\alpha_i\right) - \left[\left(\sum_{i=1}^{3}\alpha_i\right) - k\pi\right] - (\alpha_3 - \tau_k) \\
&= k\pi - (\alpha_3 - \tau_k), \qquad (3.168)
\end{aligned}
$$

we see that (3.164) can be expressed as

$$\begin{aligned}
\tilde{\Phi}_{\boldsymbol{\alpha},k} = &\bigg[\cos(\tau_k)\Big(1 - \cos(\alpha_1 - \tau_k)\cos(\alpha_2 - \tau_k)\cos(\alpha_1 + \alpha_2 - 2\tau_k)\Big) \\
&+ 3\sin(\tau_k)\sin(\alpha_1 - \tau_k)\sin(\alpha_2 - \tau_k)\sin(\alpha_1 + \alpha_2 - 2\tau_k)\bigg]\frac{1}{\cos(k\pi)\sin^2(\alpha_1 - \tau_k)} \\
= &\bigg[\cos(\tau_k)\Big(1 - \cos(\alpha_1 - \tau_k)\cos(\alpha_2 - \tau_k)\cos\big(k\pi - (\alpha_3 - \tau_k)\big)\Big) \\
&+ 3\sin(\tau_k)\sin(\alpha_1 - \tau_k)\sin(\alpha_2 - \tau_k)\sin\big(k\pi - (\alpha_3 - \tau_k)\big)\bigg]\frac{1}{\cos(k\pi)\sin^2(\alpha_1 - \tau_k)} \\
= &\bigg[\cos(\tau_k)\Big(1 - \cos(k\pi)\cos(\alpha_1 - \tau_k)\cos(\alpha_2 - \tau_k)\cos(\alpha_3 - \tau_k)\Big) \\
&- 3\cos(k\pi)\sin(\tau_k)\sin(\alpha_1 - \tau_k)\sin(\alpha_2 - \tau_k)\sin(\alpha_3 - \tau_k)\bigg]\frac{1}{\cos(k\pi)\sin^2(\alpha_1 - \tau_k)} \\
= &\frac{1}{\sin^2(\alpha_1 - \tau_k)}\bigg[\cos(\tau_k)\Big(\cos(k\pi) - \cos(\alpha_1 - \tau_k)\cos(\alpha_2 - \tau_k)\cos(\alpha_3 - \tau_k)\Big) \\
&\qquad - 3\sin(\tau_k)\sin(\alpha_1 - \tau_k)\sin(\alpha_2 - \tau_k)\sin(\alpha_3 - \tau_k)\bigg].
\end{aligned} \tag{3.169}$$

We can further simplify by noting from (3.154) that

$$\begin{aligned}
\cos(k\pi) &= \cos\left(\left(\sum_{i=1}^{3}\alpha_i\right) - 3\tau_k\right) \\
&= \cos\left(\sum_{i=1}^{3}(\alpha_i - \tau_k)\right) \\
&= \cos(\alpha_1 - \tau_k)\cos(\alpha_2 - \tau_k + \alpha_3 - \tau_k) - \sin(\alpha_1 - \tau_k)\sin(\alpha_2 - \tau_k + \alpha_3 - \tau_k) \\
&= \cos(\alpha_1 - \tau_k)\left[\cos(\alpha_2 - \tau_k)\cos(\alpha_3 - \tau_k) - \sin(\alpha_2 - \tau_k)\sin(\alpha_3 - \tau_k)\right] \\
&\qquad - \sin(\alpha_1 - \tau_k)\left[\sin(\alpha_2 - \tau_k)\cos(\alpha_3 - \tau_k) + \cos(\alpha_2 - \tau_k)\sin(\alpha_3 - \tau_k)\right],
\end{aligned} \tag{3.170}$$

and hence (3.169) becomes

$$
\begin{aligned}
\tilde{\Phi}_{\boldsymbol{\alpha},k} = \frac{1}{\sin^2(\alpha_1-\tau_k)}\Big\{ & \cos(\tau_k)\Big[-\cos(\alpha_1-\tau_k)\sin(\alpha_2-\tau_k)\sin(\alpha_3-\tau_k) \\
& - \sin(\alpha_1-\tau_k)\sin(\alpha_2-\tau_k)\cos(\alpha_3-\tau_k) \\
& - \sin(\alpha_1-\tau_k)\cos(\alpha_2-\tau_k)\sin(\alpha_3-\tau_k)\Big] \\
& - 3\sin(\tau_k)\sin(\alpha_1-\tau_k)\sin(\alpha_2-\tau_k)\sin(\alpha_3-\tau_k)\Big\} \\
= \frac{-1}{\sin^2(\alpha_1-\tau_k)}\Big\{ & \sin(\alpha_2-\tau_k)\sin(\alpha_3-\tau_k)\Big[\cos(\tau_k)\cos(\alpha_1-\tau_k) \\
& + \sin(\tau_k)\sin(\alpha_1-\tau_k)\Big] \\
& + \sin(\alpha_1-\tau_k)\sin(\alpha_2-\tau_k)\Big[\cos(\tau_k)\cos(\alpha_3-\tau_k)+\sin(\tau_k)\sin(\alpha_3-\tau_k)\Big] \\
& + \sin(\alpha_1-\tau_k)\sin(\alpha_3-\tau_k)\Big[\cos(\tau_k)\cos(\alpha_2-\tau_k)+\sin(\tau_k)\sin(\alpha_2-\tau_k)\Big]\Big\} \\
= \frac{-1}{\sin^2(\alpha_1-\tau_k)}\Big\{ & \sin(\alpha_2-\tau_k)\sin(\alpha_3-\tau_k)\cos(\alpha_1-2\tau_k) \\
& + \sin(\alpha_1-\tau_k)\sin(\alpha_2-\tau_k)\cos(\alpha_3-2\tau_k) \\
& + \sin(\alpha_1-\tau_k)\sin(\alpha_3-\tau_k)\cos(\alpha_2-2\tau_k)\Big\} \\
= \frac{-1}{\sin^2(\alpha_1-\tau_k)} & \left\{\sum_{i=1}^{3}\sin\left(\alpha_i-\tau_k\right)\sin\left(\alpha_{i+1}-\tau_k\right)\cos\left(\alpha_{i+2}-2\tau_k\right)\right\}. \qquad (3.171)
\end{aligned}
$$

Thus the eigenvalues of the linearization matrix satisfy

$$
\begin{aligned}
\operatorname{sgn}\Big(Re(\lambda)\Big) &= \operatorname{sgn}\left(\tilde{\Phi}_{\boldsymbol{\alpha},k}\right) \\
&= \operatorname{sgn}\left(\frac{-1}{\sin^2(\alpha_1-\tau_k)}\left\{\sum_{i=1}^{3}\sin\left(\alpha_i-\tau_k\right)\sin\left(\alpha_{i+1}-\tau_k\right)\cos\left(\alpha_{i+2}-2\tau_k\right)\right\}\right) \\
&= -\operatorname{sgn}\left(\sum_{i=1}^{3}\sin\left(\alpha_i-\tau_k\right)\sin\left(\alpha_{i+1}-\tau_k\right)\cos\left(\alpha_{i+2}-2\tau_k\right)\right) \\
&= -\operatorname{sgn}(\Phi_{\boldsymbol{\alpha},k}), \qquad (3.172)
\end{aligned}
$$

where $\Phi_{\boldsymbol{\alpha},k}$ is as defined in (3.155). For $\Phi_{\boldsymbol{\alpha},k} < 0$, both eigenvalues are in the righthalf plane and the equilibrium shape is unstable. For $\Phi_{\boldsymbol{\alpha},k} > 0$, both eigenvalues are in the left-half plane, and the invariant submanifold M_k is asymptotically stable in the sense defined in section 3.6. $\square$

Remark 3.7.2 The stability criterion for pure shape equilibria can be related to the associated equilibrium shape as follows. Observe from (3.171) that

$$\begin{aligned}\tilde{\Phi}_{\boldsymbol{\alpha},k} = & -\cos(\alpha_1 - 2\tau_k)\left(\frac{\sin(\alpha_2-\tau_k)}{\sin(\alpha_1-\tau_k)}\right)\left(\frac{\sin(\alpha_3-\tau_k)}{\sin(\alpha_1-\tau_k)}\right)\\ & -\cos(\alpha_2-2\tau_k)\left(\frac{\sin(\alpha_3-\tau_k)}{\sin(\alpha_1-\tau_k)}\right) - \cos(\alpha_3-2\tau_k)\left(\frac{\sin(\alpha_2-\tau_k)}{\sin(\alpha_1-\tau_k)}\right)\\ = & \cos(\pi-\alpha_1+2\tau_k)\left(\frac{\sin(\alpha_2-\tau_k)}{\sin(\alpha_1-\tau_k)}\right)\left(\frac{\sin(\alpha_3-\tau_k)}{\sin(\alpha_1-\tau_k)}\right)\\ & +\cos(\pi-\alpha_2+2\tau_k)\left(\frac{\sin(\alpha_3-\tau_k)}{\sin(\alpha_1-\tau_k)}\right) + \cos(\pi-\alpha_3+2\tau_k)\left(\frac{\sin(\alpha_2-\tau_k)}{\sin(\alpha_1-\tau_k)}\right),\end{aligned} \tag{3.173}$$

and substituting the equilibrium values given in (2.106), we have

$$\tilde{\Phi}_{\boldsymbol{\alpha},k} = \cos\left(\hat{\theta}_2^{(k)}\right)\left(\frac{\hat{\rho}_2^{(k)}}{\hat{\rho}_1^{(k)}}\right)\left(\frac{\hat{\rho}_3^{(k)}}{\hat{\rho}_1^{(k)}}\right) + \cos\left(\hat{\theta}_3^{(k)}\right)\left(\frac{\hat{\rho}_3^{(k)}}{\hat{\rho}_1^{(k)}}\right) + \cos\left(\hat{\theta}_1^{(k)}\right)\left(\frac{\hat{\rho}_2^{(k)}}{\hat{\rho}_1^{(k)}}\right). \tag{3.174}$$

3.7.1 Symmetric case: $\alpha_1 = \alpha_2 = \alpha_3$

For the three-particle symmetric case $\alpha_1 = \alpha_2 = \alpha_3 = \alpha \in [0, 2\pi)$, **Proposition 2.4.7** implies that circling equilibria exist if and only if $\alpha = \frac{\pi}{3}, \frac{2\pi}{3}, \frac{4\pi}{3}$, or $\frac{5\pi}{3}$, and by **Theorem 3.6.2**, the $\alpha = \frac{2\pi}{3}, \frac{4\pi}{3}$ equilibria are unstable and the $\alpha = \frac{\pi}{3}, \frac{5\pi}{3}$ equilibria are asymptotically stable.

Proposition 2.4.7 implies that for any value of α, there always exist exactly two pure shape equilibria, which we identify with $k = 1$ and $k = 2$. In figure 3.10,

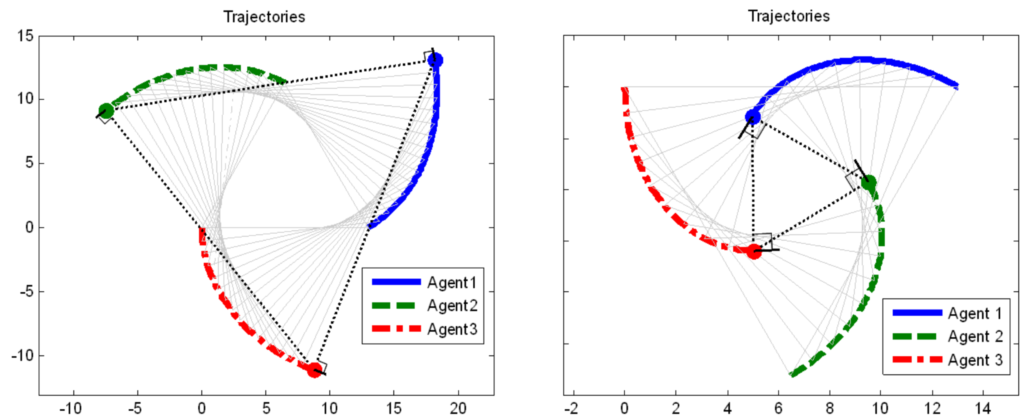

Figure 3.10: Depiction of the two pure shape equilibria which exist for the case $\alpha_1 = \alpha_2 = \alpha_3 = \frac{\pi}{2}$.

we depict the two pure shape equilibria which exist for the case $\alpha_1 = \alpha_2 = \alpha_3 = \frac{\pi}{2}$. Note that the pure shape equilibria correspond to equilateral triangle formations in the physical space, with equilibrium values for the $k = 1$ and $k = 2$ pure shape equilibria given (respectively) by

$$\hat{\theta}_i^{(1)} = \alpha + \pi/3, \; i = 1, 2, \ldots, n,$$
$$\hat{\theta}_i^{(2)} = \alpha - \pi/3, \; i = 1, 2, \ldots, n. \tag{3.175}$$

(These equilibrium values follow directly from **Proposition 2.4.7**, which applies specifically to the symmetric case.)

Stability properties of the pure shape equilibria can be characterized by application of **Theorem 3.7.1**. Substituting $\alpha_1 = \alpha_2 = \alpha_3 = \alpha$ into (3.154) yields $\tau_k = \alpha - k\pi/3$, and therefore our stability coefficient (3.155) simplifies to

$$\Phi_{\boldsymbol{\alpha},k} = 3\sin^2(\alpha - \tau_k)\cos(\alpha - 2\tau_k) = 3\sin^2(k\pi/3)\cos(-\alpha + 2k\pi/3). \tag{3.176}$$

Since we are interested only in the sign of $\Phi_{\boldsymbol{\alpha},k}$, we can characterize stability in terms of the normalized stability coefficient

$$\Phi_{\alpha,k} = \frac{\Phi_{\boldsymbol{\alpha},k}}{3\sin^2(k\pi/3)} = \cos(\alpha - 2k\pi/3). \tag{3.177}$$

We observe that $\Phi_{\alpha,1} = 0$ for $\alpha = \pi/6, 7\pi/6$ and $\Phi_{\alpha,2} = 0$ for $\alpha = 5\pi/6, 11\pi/6$, and substitution into (3.160) and (3.161) demonstrates that the eigenvalues of the linearization about the corresponding pure shape equilibrium in each of these critical cases are given by $\lambda = \pm(3/2)j$. Phase portrait analysis suggests that the critical cases associated with $\alpha = \pi/6$ and $\alpha = 11\pi/6$ are in fact asymptotically stable and that those associated with $\alpha = 5\pi/6$ and $\alpha = 7\pi/6$ are unstable.

In figure 3.11 we display the normalized stability coefficients ($\Phi_{\alpha,1}$, $\Phi_{\alpha,2}$), as well as the expansion coefficients ($\gamma_{\boldsymbol{\alpha},1}$, $\gamma_{\boldsymbol{\alpha},2}$) and rotation coefficients ($\beta_{\boldsymbol{\alpha},1}$, $\beta_{\boldsymbol{\alpha},2}$) from **Proposition 2.4.7**. These figures provide a graphical characterization of the stability, expansion, and rotation properties of the planar formations corresponding to the two unique pure shape equilibria which exist for every value of α, and they are best understood by choosing a particular value of α and considering the corresponding "slice" across the three graphs. From the top graph, we note that for $\alpha \in (5\pi/6, 7\pi/6)$ (region III), both pure shape equilibria are asymptotically stable, while $\alpha \in [0, \pi/6) \cup (11\pi/6, 2\pi]$ (regions I and V) implies that both are unstable. We also note that the zero crossings in the middle graph correspond to circling equilibria, and the zero crossings in the bottom graph correspond to pure expansion/contraction without rotation. Lastly, by comparing the top graph with the middle graph, one observes that stability properties do not seem to directly correlate with expansion characteristics, since we observe unstable/expanding, unstable/contracting, asymptotically stable/expanding, and asymptotically stable/contracting combinations. However, we find it interesting that in the cases where an expanding pure shape equilibrium coexists with a contracting pure shape equilibrium (i.e. for $\alpha \in (\pi/3, 2\pi/3) \cup (4\pi/3, 5\pi/3)$) (regions II and IV), the expanding solution is always asymptotically stable and the contracting solution is unstable.

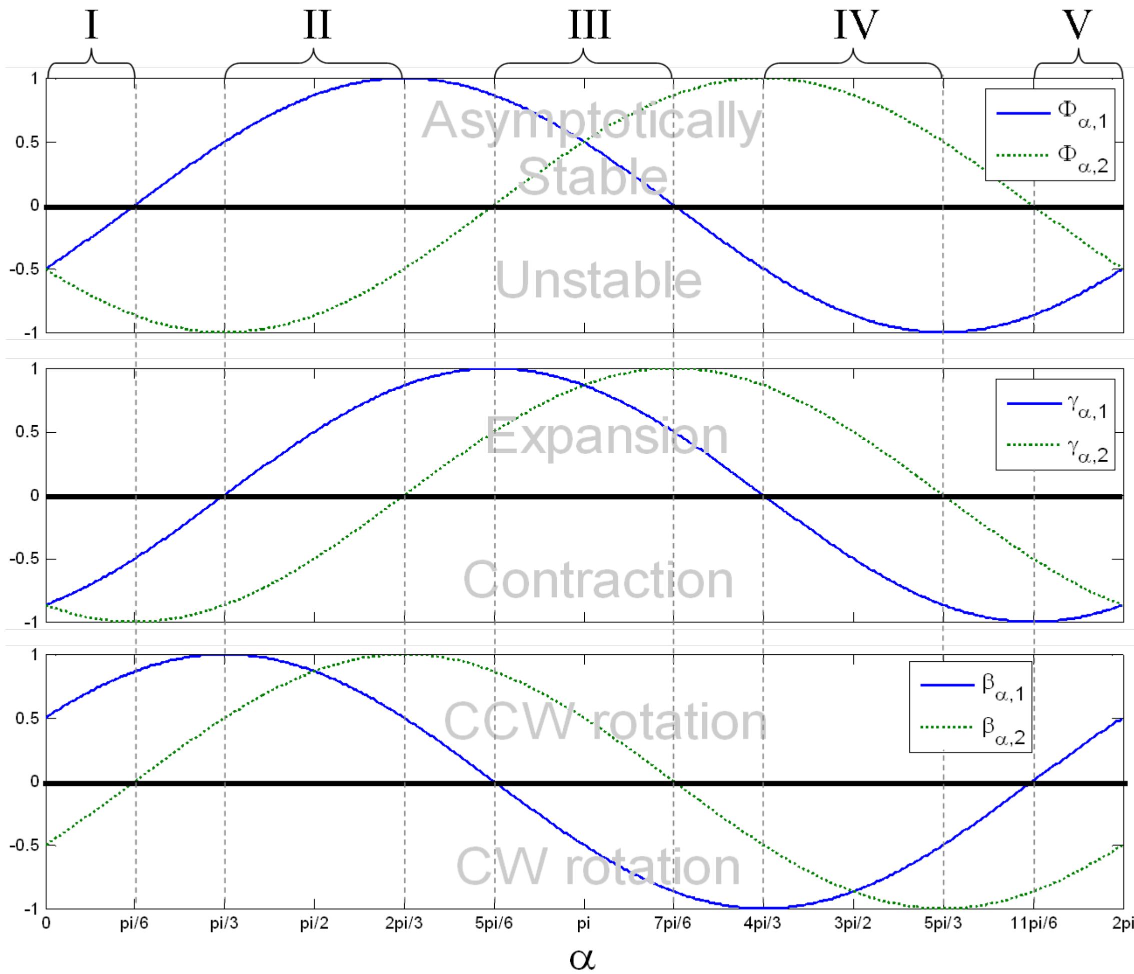

Figure 3.11: As discussed in section 3.7.1, for a three-particle cyclic CB pursuit system with $\alpha_1 = \alpha_2 = \alpha_3 = \alpha$, there always exists two unique pure shape equilibria. For every value of α, these figures characterize the stability, expansion, and rotation properties of the planar formations corresponding to those two pure shape equilibria. For example, if $\alpha = \pi/2$ as in figure 3.10, both of the particle formations rotate in a CCW direction, one expanding and the other contracting, and the expanding formation is asymptotically stable while the contracting formation is unstable.

Chapter 4

Constant Bearing pursuit in three dimensions

4.1 Introduction

In this chapter we extend our analysis of cyclic CB pursuit to three-dimensional space[1], for which we envision possible technological applications such as collective control of "flocks" of UAV's. The CB pursuit strategy is particularly interesting because it is observed in nature, specifically in the high speed stoop behavior of the peregrine falcon diving from great heights to hunt prey ([55],[34]). Using natural Frenet frames to develop a model for describing particles tracing out curves in $\mathbb{R}^3$, we propose a definition for the three-dimensional CB pursuit strategy and derive a novel control law (4.15) to execute the strategy. Note that the 3-D case does not readily yield a useful parametrization of the shape space, so we carry out our analysis with the state space (vector) variables defined in section 4.2.

Similar to the planar CB pursuit law, the three-dimensional pursuit law involves both a relative bearing error and a term related to the motion camouflage law in [48]. In **Proposition 4.3.7** we prove that the 3-D analogue of the CB pur-

[1]This work was originally developed with Justh and Krishnaprasad and presented in [16].

suit manifold is invariant and attractive under the closed-loop cyclic CB pursuit dynamics, with reduced dynamics on the manifold given by (4.21). Section 4.4 is devoted to the special case of $n = 2$ (i.e. mutual CB pursuit), in analogy with 3-D mutual motion camouflage (MMC) investigated in [40]. This case reveals the presence of conservation laws leading to explicit integrability of the dynamics, a key contribution of this chapter. The chapter ends with conditions for existence of rectilinear and planar circling relative equilibrium motions for n-agent cyclic CB pursuit dynamics.

The most relevant previous work on three-dimensional cyclic CB pursuit is found in [47], in which Ramirez-Riberos, et al., use a double-integrator model of the form $\ddot{\mathbf{r}}_i = \mathbf{u}_i$, where $\mathbf{r}_i \in \mathbb{R}^3$ is the position of the i^{th} agent and $\mathbf{u}_i$ is an acceleration control. The authors consider control laws of the form

$$\mathbf{u}_i = k_d R_z(\alpha)(\mathbf{r}_{i+1} - \mathbf{r}_i) + R_z(\alpha)(\dot{\mathbf{r}}_{i+1} - \dot{\mathbf{r}}_i) - k_c k_d \mathbf{r}_i - (k_c + k_d)\dot{\mathbf{r}}_i, \quad k_d \in \mathbb{R}^+,\ k_c \in \mathbb{R}, \tag{4.1}$$

where $R_z(\alpha) \in SO(3)$ is the rotation[2] by α about the z axis $(0,0,1)^T$, given by

$$R_z(\alpha) = \begin{pmatrix} \cos(\alpha) & \sin(\alpha) & 0 \\ -\sin(\alpha) & \cos(\alpha) & 0 \\ 0 & 0 & 1 \end{pmatrix}, \tag{4.2}$$

[2] In [47] the authors use the form given by (4.2), which represents *clockwise* rotation by α radians in the plane. By a small abuse of notation, we use $R_z(\alpha)$ in appendix D (see (D.5)) to represent the corresponding *counterclockwise* in the plane.

as well as the "generalized cyclic-pursuit control law"

$$\mathbf{u}_i = k_1 R_z^2(\alpha)\big((\mathbf{r}_{i+2} - \mathbf{r}_{i+1}) - (\mathbf{r}_{i+1} - \mathbf{r}_i)\big) + k_2 R_z(\alpha)(\dot{\mathbf{r}}_{i+1} - \dot{\mathbf{r}}_i), \quad k_1, k_2 \in \mathbb{R}. \tag{4.3}$$

In contrast, our model (4.4) constrains the control forces to be gyroscopic so that the speed of each particle remains constant, i.e. $\ddot{\mathbf{r}}_i = \mathbf{u}_i = u_i \mathbf{y}_i + v_i \mathbf{z}_i$, where $\mathbf{y}_i$ and $\mathbf{z}_i$ lie in the plane normal to the velocity $\dot{\mathbf{r}}_i$, and u_i, v_i are scalar curvature controls. (Constant speed assumptions are appropriate for certain vehicles and birds which require a minimum forward speed in order to stay aloft.) Also, we define a fundamentally different notion of three-dimensional CB pursuit (**Definition 4.3.2**), which is more natural and does not require a notion of a common reference axis (i.e., the z-axis $(0, 0, 1)^T$), and we permit diversity of CB pursuit angle parameters.

4.2 Modeling pursuit interactions in three dimensions

Analogous to the discussion in section 2.2.1, we model a system of agents moving in three-dimensional space as unit-mass particles tracing out twice continuously-differentiable curves, with system dynamics derived from the natural Frenet frame equations. (See, for example, [26] for details.) As in figure 4.1, the state of the i^{th} particle (i.e. agent) with respect to a fixed inertial frame is denoted by the position vector $\mathbf{r}_i$ and the respective natural Frenet frames $(\mathbf{x}_i, \mathbf{y}_i, \mathbf{z}_i)$. If we constrain the agents to move at unit speed, then the dynamics of a system of n agents can be described by

$$
\begin{aligned}
\dot{\mathbf{r}}_i &= \mathbf{x}_i, \\
\dot{\mathbf{x}}_i &= u_i \mathbf{y}_i + v_i \mathbf{z}_i, \\
\dot{\mathbf{y}}_i &= -u_i \mathbf{x}_i, \\
\dot{\mathbf{z}}_i &= -v_i \mathbf{x}_i, \ i = 1, 2, \ldots, n,
\end{aligned} \tag{4.4}
$$

where u_i and v_i are the natural curvatures viewed as controls, and are required to be $SE(3)$-invariant (in the sense of **Definition 1.3.1**). As in the planar case, we define the baseline vector $\mathbf{r}_{i,i+1} = \mathbf{r}_i - \mathbf{r}_{i+1}$, with addition in the indices interpreted as modulo n, and prohibit "sequential colocation" (i.e. we assume $|\mathbf{r}_{i,i+1}| > 0$ for all t). Explicitly, we let the state space

$$
M_{state} = \Big\{ (\mathbf{r}_1, \mathbf{x}_1, \mathbf{y}_1, \mathbf{z}_1, \ldots, \mathbf{r}_n, \mathbf{x}_n, \mathbf{y}_n, \mathbf{z}_n) \mid \mathbf{r}_i \neq \mathbf{r}_{i+1}, \ i = 1, 2, \ldots, n \Big\}, \tag{4.5}
$$

where it is understood that $\mathbf{r}_i \in \mathbb{R}^3$ and that $\{\mathbf{x}_i, \mathbf{y}_i, \mathbf{z}_i\}$ are orthonormal vectors in $\mathbb{R}^3$ for each i.

In contrast to the planar case, in this chapter we will deal exclusively with the system dynamics on the full state manifold M_{state} (and on an analogous version of the CB pursuit manifold, viewed as a submanifold of M_{state}) in terms of the vector variables $\mathbf{r}_i, \mathbf{x}_i, \mathbf{y}_i$, and $\mathbf{z}_i$. We take this approach because the shape space $M_{state}/SE(3)$ does not readily yield an advantageous scalar parametrization analogous to the $\kappa_i, \theta_i, \rho_i$ variables (see section 2.2.3) for the planar case.

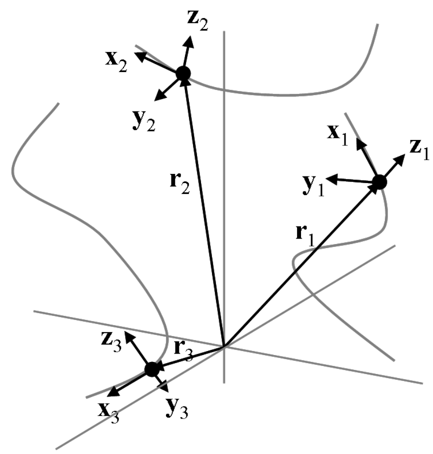

Figure 4.1: Illustration of particle positions and corresponding natural Frenet frames for three particles interacting in three-dimensional space.

4.3 Pursuit strategies and steering laws in three dimensions

As described in chapters 1 and 2, steering laws for the execution of planar pursuit strategies have been developed for classical pursuit and constant bearing pursuit [57] as well as motion camouflage pursuit [27]. A three-dimensional version of the motion camouflage pursuit law was also developed in [48]. Here we derive pursuit laws for the execution of classical pursuit and constant bearing pursuit strategies in $\mathbb{R}^3$.

4.3.1 Classical Pursuit

The classical pursuit strategy specifies that the pursuer should always move directly towards the current location of the pursuee. As in the planar case (see section 2.3), we define our cost function by

$$\Lambda_i^{CP} = \mathbf{x}_i \cdot \frac{\mathbf{r}_{i,i+1}}{|\mathbf{r}_{i,i+1}|}, \tag{4.6}$$

noting that $\Lambda_i^{CP} \in [-1, 1]$ and $\Lambda_i^{CP} = -1$ corresponds to attainment of the CP strategy. With the following notation

$$\bar{x}_i \triangleq \mathbf{x}_i \cdot \frac{\mathbf{r}_{i,i+1}}{|\mathbf{r}_{i,i+1}|}, \quad \bar{y}_i \triangleq \mathbf{y}_i \cdot \frac{\mathbf{r}_{i,i+1}}{|\mathbf{r}_{i,i+1}|}, \quad \bar{z}_i \triangleq \mathbf{z}_i \cdot \frac{\mathbf{r}_{i,i+1}}{|\mathbf{r}_{i,i+1}|}, \tag{4.7}$$

we have,

Proposition 4.3.1. *Consider a two-particle system in which* (u_2, v_2) *are arbitrary (but continuous and bounded) and* (u_1, v_1) *are prescribed by*

$$\begin{aligned} u_1 &= -\mu_1 \bar{y}_1 - \frac{1}{|\mathbf{r}|}\left[\mathbf{z}_1 \cdot \left(\dot{\mathbf{r}} \times \frac{\mathbf{r}}{|\mathbf{r}|}\right)\right] \\ v_1 &= -\mu_1 \bar{z}_1 + \frac{1}{|\mathbf{r}|}\left[\mathbf{y}_1 \cdot \left(\dot{\mathbf{r}} \times \frac{\mathbf{r}}{|\mathbf{r}|}\right)\right], \end{aligned} \tag{4.8}$$

where $\mu_1 > 0$ *is a control gain and* $\mathbf{r} \triangleq \mathbf{r}_1 - \mathbf{r}_2$*. Then under the closed-loop dynamics (4.4),* $\dot{\Lambda}_1^{CP} \leq 0$ *with* $\dot{\Lambda}_1^{CP} = 0$ *if and only if* $\Lambda_1^{CP} = \pm 1$*.*

Proof. We proceed by differentiating Λ_1^{CP} along trajectories of the closed loop dynamics. First, note that

$$\frac{d}{dt}\left(\frac{\mathbf{r}}{|\mathbf{r}|}\right) = \frac{\mathbf{w}}{|\mathbf{r}|}, \tag{4.9}$$

where $\mathbf{w}$, the transverse component of the relative velocity, is defined by

$$\mathbf{w} = \dot{\mathbf{r}} - \left(\dot{\mathbf{r}} \cdot \frac{\mathbf{r}}{|\mathbf{r}|}\right)\frac{\mathbf{r}}{|\mathbf{r}|} = \frac{\mathbf{r}}{|\mathbf{r}|} \times \left(\dot{\mathbf{r}} \times \frac{\mathbf{r}}{|\mathbf{r}|}\right). \tag{4.10}$$

(See [48] and [57].) Then differentiating Λ_1^{CP}, we have

$$\begin{aligned}
\dot{\Lambda}_1^{CP} &= \dot{\mathbf{x}}_1 \cdot \frac{\mathbf{r}}{|\mathbf{r}|} + \mathbf{x}_1 \cdot \frac{d}{dt}\left(\frac{\mathbf{r}}{|\mathbf{r}|}\right) \\
&= u_1\bar{y}_1 + v_1\bar{z}_1 + \frac{1}{|\mathbf{r}|}\left(\mathbf{x}_1 \cdot \mathbf{w}\right) \\
&= \left\{-\mu_1\bar{y}_1 - \frac{1}{|\mathbf{r}|}\left[\mathbf{z}_1 \cdot \left(\dot{\mathbf{r}} \times \frac{\mathbf{r}}{|\mathbf{r}|}\right)\right]\right\}\bar{y}_1 \\
&\quad + \left\{-\mu_1\bar{z}_1 + \frac{1}{|\mathbf{r}|}\left[\mathbf{y}_1 \cdot \left(\dot{\mathbf{r}} \times \frac{\mathbf{r}}{|\mathbf{r}|}\right)\right]\right\}\bar{z}_1 + \frac{1}{|\mathbf{r}|}\left(\mathbf{x}_1 \cdot \mathbf{w}\right) \\
&= -\mu_1\bar{y}_1^2 - \mu_1\bar{z}_1^2 + \frac{1}{|\mathbf{r}|}\left(\mathbf{x}_1 \cdot \mathbf{w}\right) - \frac{1}{|\mathbf{r}|}\left\{\left[\mathbf{z}_1 \cdot \left(\dot{\mathbf{r}} \times \frac{\mathbf{r}}{|\mathbf{r}|}\right)\right]\bar{y}_1 - \bar{z}_1\left[\mathbf{y}_1 \cdot \left(\dot{\mathbf{r}} \times \frac{\mathbf{r}}{|\mathbf{r}|}\right)\right]\right\}.
\end{aligned} \tag{4.11}$$

By writing out the full expressions for $\bar{y}_1$ and $\bar{z}_1$ and applying the identity $(\mathbf{a} \times \mathbf{b}) \cdot (\mathbf{c} \times \mathbf{d}) = (\mathbf{a} \cdot \mathbf{c})(\mathbf{b} \cdot \mathbf{d}) - (\mathbf{a} \cdot \mathbf{d})(\mathbf{b} \cdot \mathbf{c})$ for arbitrary vectors $\mathbf{a}, \mathbf{b}, \mathbf{c}, \mathbf{d}$, we then have

$$\begin{aligned}
\dot{\Lambda}_1^{CP} &= -\mu_1\left(1 - \bar{x}_1^2\right) + \frac{1}{|\mathbf{r}|}\left(\mathbf{x}_1 \cdot \mathbf{w}\right) - \frac{1}{|\mathbf{r}|}\left\{\left(\mathbf{z}_1 \times \mathbf{y}_1\right) \cdot \left[\left(\dot{\mathbf{r}} \times \frac{\mathbf{r}}{|\mathbf{r}|}\right) \times \frac{\mathbf{r}}{|\mathbf{r}|}\right]\right\} \\
&= -\mu_1\left(1 - \left(\Lambda_1^{CP}\right)^2\right) + \frac{1}{|\mathbf{r}|}\left(\mathbf{x}_1 \cdot \mathbf{w}\right) - \frac{1}{|\mathbf{r}|}\left\{-\mathbf{x}_1 \cdot \left[-\frac{\mathbf{r}}{|\mathbf{r}|} \times \left(\dot{\mathbf{r}} \times \frac{\mathbf{r}}{|\mathbf{r}|}\right)\right]\right\} \\
&= -\mu_1\left(1 - \left(\Lambda_1^{CP}\right)^2\right),
\end{aligned} \tag{4.12}$$

The claims of **Proposition 4.3.1** readily follow from (4.12). □

4.3.2 Definition of the Constant Bearing Pursuit strategy

In the planar case, the notion of constant bearing strategy simply extends CP by specifying a fixed, possibly nonzero angle between pursuer heading and the relative location of the target. The following specifies an extension of this idea to three dimensions.

Definition 4.3.2 (CB pursuit strategy) Given a two-particle system with dynamics (4.4) and a parameter $a_1 \in [-1, 1]$, we say particle 1 has attained the CB(a_1) pursuit strategy if $\mathbf{x}_1 \cdot \frac{\mathbf{r}}{|\mathbf{r}|} = a_1$.

Remark 4.3.3 Given a scalar parameter $a \in [-1, 1]$ and an arbitrary unit vector $\mathbf{q}$ regarded as a point on the unit sphere S^2, the set $\left\{ \mathbf{y} \in S^2 \;\middle|\; \mathbf{q} \cdot \mathbf{y} = a \right\}$ defines a *small circle* (i.e. the intersection of a sphere with a plane that does not pass through the center of the sphere)[3]. Since $\mathbf{x}_1$ and $\frac{\mathbf{r}}{|\mathbf{r}|}$ are both unit vectors, we can think of the CB(a_1) pursuit strategy as prescribing a small circle centered around the point $\frac{\mathbf{r}}{|\mathbf{r}|} \in S^2$. CB($a_1$) pursuit holds when $\mathbf{x}_1$ lies on that small circle.

Remark 4.3.4 Observe that this definition of the three-dimensional CB pursuit strategy is fundamentally different from the planar version presented in section 2.3 (i.e. $R(\alpha)\mathbf{x}_1 \cdot \frac{\mathbf{r}}{|\mathbf{r}|} = -1$, where $R(\alpha)\mathbf{x}_1$ is the vector $\mathbf{x}_1$ rotated counterclockwise in the plane by the angle α) in that the planar version prescribed not only a constant bearing angular offset but also a particular direction (i.e. counterclockwise) for the offset. We can relate the CB strategy presented here to the planar strategy as follows. Given unit vectors $\mathbf{x}_1$ and $\frac{\mathbf{r}}{|\mathbf{r}|}$ in the plane and the two statements $R(\alpha)\mathbf{x}_1 \cdot \frac{\mathbf{r}}{|\mathbf{r}|} = -1$ and $\mathbf{x}_1 \cdot \frac{\mathbf{r}}{|\mathbf{r}|} = a$, we seek to define the relationship between α and a. If we define θ as the signed angle (CCW rotation positive) from $\mathbf{x}_1$ to $\frac{\mathbf{r}}{|\mathbf{r}|}$, then $\cos\theta = a$ and

[3] More precisely, the set $\left\{ \mathbf{y} \in S^2 \;\middle|\; \mathbf{q} \cdot \mathbf{y} = a \right\}$ describes a small circle only if $a \neq 0$. For $a = 0$, it defines a great circle.

$|\theta - \alpha| = \pi$, i.e.

$$\cos(\theta - \alpha) = \cos\theta \cos\alpha + \sin\theta \sin\alpha = -1. \tag{4.13}$$

This relationship holds only if $(\cos\alpha, \sin\alpha) = -(\cos\theta, \sin\theta)$, and since $\cos\theta = a$ and $\sin\theta = \pm\sqrt{1-a^2}$, the two discrete possibilities are given by $(\cos\alpha, \sin\alpha) = (-a, \mp\sqrt{1-a^2})$. Therefore the CB strategy of **Definition 4.3.2** differs from the planar strategy (presented in section 2.3) in that it allows for two discrete possibilities for pursuit geometries as opposed to the single geometry prescribed by the planar strategy.

We define a CB cost function[4] for agent i by

$$\Lambda_i = \frac{1}{2}\left[\left(\mathbf{x}_i \cdot \frac{\mathbf{r}_{i,i+1}}{|\mathbf{r}_{i,i+1}|}\right) - a_i\right]^2 = \frac{1}{2}\left(\bar{x}_i - a_i\right)^2, \tag{4.14}$$

with $0 \leq \Lambda_i \leq \max\left[\frac{1}{2}(-1-a_i)^2, \frac{1}{2}(1-a_i)^2\right]$. Then the CB pursuit strategy defined above is equivalent to $\Lambda_i = 0$.

Remark 4.3.5 At first glance, it may appear that a viable alternative definition for the three-dimensional CB pursuit strategy is obtained by letting $\tilde{\Lambda} \triangleq B\mathbf{x}_1 \cdot \frac{\mathbf{r}}{|\mathbf{r}|}$, where $B \in SO(3)$ (the rotation group in three dimensions), and then defining the CB pursuit strategy by $\tilde{\Lambda} = -1$. This definition is appealing since it is the obvious extension of the previously mentioned planar CB pursuit strategy. However,

[4]This constitutes a small abuse of notation since we have already used Λ_i to refer to the planar CB cost function in (2.54), but the context will make it readily apparent as to which quantity we refer to.

a few straightforward calculations reveal that $\tilde{\Lambda}$ is not invariant to rotations of the coordinate frame (i.e. not $SO(3)$-invariant) and therefore all associated pursuit laws will be inadmissible under our framework (unless B is the identity matrix).

4.3.3 A feedback law for CB Pursuit

Proposition 4.3.6. *Consider a two-particle system in which (u_2, v_2) are arbitrary (but continuous and bounded) and (u_1, v_1) are prescribed by*

$$\begin{aligned} u_1 &= -\mu_1\Big(\bar{x}_1 - a_1\Big)\bar{y}_1 - \frac{1}{|\mathbf{r}|}\left[\mathbf{z}_1 \cdot \left(\dot{\mathbf{r}} \times \frac{\mathbf{r}}{|\mathbf{r}|}\right)\right] \\ v_1 &= -\mu_1\Big(\bar{x}_1 - a_1\Big)\bar{z}_1 + \frac{1}{|\mathbf{r}|}\left[\mathbf{y}_1 \cdot \left(\dot{\mathbf{r}} \times \frac{\mathbf{r}}{|\mathbf{r}|}\right)\right], \end{aligned} \tag{4.15}$$

where $\mu_1 > 0$ is a control gain. Then under the closed-loop dynamics (4.4), $\dot{\Lambda}_1 \leq 0$ with $\dot{\Lambda}_1 = 0$ if and only if $\Lambda_1 = 0$ or $\mathbf{x}_1 \cdot \frac{\mathbf{r}}{|\mathbf{r}|} = \pm 1$.

Proof. By a series of calculations analogous to the derivation of (4.12), it is possible to show that

$$\dot{\Lambda}_1 = -\mu_1 \left(\bar{x}_1 - a_1\right)^2 \left(1 - \bar{x}_1^2\right) = -2\mu_1 \Lambda_1 \left(1 - \bar{x}_1^2\right), \tag{4.16}$$

from which the result follows. □

4.3.4 An invariant submanifold for cyclic CB pursuit

As in the planar case, we define the submanifold of system states for which each agent i pursues agent $(i+1)$ modulo n with a pursuit law of the form (4.15), and all agents have attained CB pursuit. Since $\Lambda_i = 0$ if and only if agent i has attained CB pursuit of agent $(i+1)$, we define the submanifold $M_{CB(\mathbf{a})} \subset M_{state}$ by

$$M_{CB(\mathbf{a})} = \Big\{ (\mathbf{r}_1, \mathbf{x}_1, \mathbf{y}_1, \mathbf{z}_1, \ldots, \mathbf{r}_n, \mathbf{x}_n, \mathbf{y}_n, \mathbf{z}_n) \in M_{state} \mid \Lambda_i = 0,\ i = 1, 2, \ldots, n \Big\}, \tag{4.17}$$

where $\mathbf{a} = \{a_1, a_2, \ldots, a_n\}$. It follows from an argument analogous to that in **Proposition 4.3.6** that $M_{CB(\mathbf{a})}$ is an invariant manifold under cyclic pursuit dynamics (in the sense that the closed-loop vector field is tangent to the manifold). In the following proposition we prove asymptotic convergence to $M_{CB(\mathbf{a})}$ under suitable conditions.

Proposition 4.3.7. *Consider the n-particle cyclic CB pursuit system governed by the closed-loop dynamics (4.4) with curvature controls for the i^{th} agent prescribed by*

$$\begin{aligned} u_i &= -\mu_i \left(\bar{x}_i - a_i\right) \bar{y}_i - \frac{1}{|\mathbf{r}_{i,i+1}|} \left[\mathbf{z}_i \cdot \left(\dot{\mathbf{r}}_{i,i+1} \times \frac{\mathbf{r}_{i,i+1}}{|\mathbf{r}_{i,i+1}|} \right) \right] \\ v_i &= -\mu_i \left(\bar{x}_i - a_i\right) \bar{z}_i + \frac{1}{|\mathbf{r}_{i,i+1}|} \left[\mathbf{y}_i \cdot \left(\dot{\mathbf{r}}_{i,i+1} \times \frac{\mathbf{r}_{i,i+1}}{|\mathbf{r}_{i,i+1}|} \right) \right], \end{aligned} \tag{4.18}$$

where $\mu_i > 0$ and we assume $a_i \neq \pm 1$. Define the set

$$\begin{aligned} \Omega_\epsilon = \Big\{ \big(\mathbf{r}_1, \mathbf{x}_1, \mathbf{y}_1, \mathbf{z}_1, \ldots, \mathbf{r}_n, \mathbf{x}_n, \mathbf{y}_n, \mathbf{z}_n \big) \in M_{state} \mid \\ \Lambda_i \leq -\epsilon + \min \left[\frac{1}{2}(-1 - a_i)^2, \frac{1}{2}(1 - a_i)^2 \right],\ i = 1, 2, \ldots, n \Big\} \end{aligned} \tag{4.19}$$

for $0 < \epsilon \ll \min_{i \in \{1,2,\ldots,n\}} \frac{1}{2}(\pm 1 - a_i)^2$. Then any bounded trajectory starting in Ω_ϵ which does not have finite escape time (i.e. $\rho_i(t) > 0$ for every finite $t \geq 0$) converges to $M_{CB(\mathbf{a})}$.

Proof. Note that Ω_ϵ is closed (but not necessarily bounded) and excludes states for which $\bar{x}_i = \pm 1$ for any i. Also, it follows from application of (4.16) (for each $i = 1, 2, \ldots, n$) that Ω_ϵ is positively invariant under (4.4). Making use of (4.14) we define $\Lambda = \sum_{i=1}^{n} \Lambda_i$, observing from (4.16) that

$$\dot{\Lambda} = -2 \sum_{i=1}^{n} \mu_i \Lambda_i \left(1 - \bar{x}_i^2\right) \tag{4.20}$$

and therefore $\dot{\Lambda} \leq 0$ on Ω_ϵ with $\dot{\Lambda} = 0$ on Ω_ϵ if and only if $\Lambda_i = 0,\ i = 1, 2, \ldots, n$. The hypothesis of boundedness of the trajectory ensures by Birkhoff's theorem the ω-limit set is nonempty, compact and invariant. Asymptotic convergence to $M_{CB(\mathbf{a})}$ follows as in the steps in the proof of LaSalle's Invariance Principle [29]. $\square$

Note that on $M_{CB(\mathbf{a})}$ the terms of the controls (4.18) which involve the gains μ_i are identically zero, and therefore we can formulate reduced (closed-loop) dynamics on $M_{CB(\mathbf{a})}$ for $i = 1, 2, \ldots, n$ as

$$\begin{aligned}
\dot{\mathbf{r}}_i &= \mathbf{x}_i, \\
\dot{\mathbf{x}}_i &= \frac{-1}{|\mathbf{r}_{i,i+1}|} \Bigg[\left(\mathbf{z}_i \cdot \left(\dot{\mathbf{r}}_{i,i+1} \times \frac{\mathbf{r}_{i,i+1}}{|\mathbf{r}_{i,i+1}|} \right) \right) \mathbf{y}_i \\
&\qquad\qquad - \left(\mathbf{y}_i \cdot \left(\dot{\mathbf{r}}_{i,i+1} \times \frac{\mathbf{r}_{i,i+1}}{|\mathbf{r}_{i,i+1}|} \right) \right) \mathbf{z}_i \Bigg] \\
\dot{\mathbf{y}}_i &= \frac{1}{|\mathbf{r}_{i,i+1}|} \left[\mathbf{z}_i \cdot \left(\dot{\mathbf{r}}_{i,i+1} \times \frac{\mathbf{r}_{i,i+1}}{|\mathbf{r}_{i,i+1}|} \right) \right] \mathbf{x}_i, \\
\dot{\mathbf{z}}_i &= \frac{-1}{|\mathbf{r}_{i,i+1}|} \left[\mathbf{y}_i \cdot \left(\dot{\mathbf{r}}_{i,i+1} \times \frac{\mathbf{r}_{i,i+1}}{|\mathbf{r}_{i,i+1}|} \right) \right] \mathbf{x}_i.
\end{aligned} \tag{4.21}$$

4.4 Mutual CB pursuit in three dimensions

As a first step towards understanding the behavior of our system under cyclic CB pursuit, we analyze the two-particle "mutual CB pursuit" case. (This can be compared with the planar analysis of mutual CB pursuit presented in chapter 3 as well as the analysis of three-dimensional "mutual motion camouflage" in [40].)

For analysis of two-particle systems in three dimensions, [26] demonstrates the utility of considering the reduced system $(\mathbf{r}, \mathbf{x}_1, \mathbf{x}_2)$ evolving on $\mathbb{R}^3 \times S^2 \times S^2$, where $\mathbf{r} \triangleq \mathbf{r}_1 - \mathbf{r}_2$. Starting from (4.21), we derive the $(\mathbf{r}, \mathbf{x}_1, \mathbf{x}_2)$ dynamics on $M_{CB(\mathbf{a})}$ by first computing

$$\begin{aligned}
\dot{\mathbf{x}}_1 &= \frac{1}{|\mathbf{r}|}\left[\mathbf{z}_1\Big(\Big(\dot{\mathbf{r}} \times \frac{\mathbf{r}}{|\mathbf{r}|}\Big) \cdot \mathbf{y}_1\Big) - \mathbf{y}_1\Big(\Big(\dot{\mathbf{r}} \times \frac{\mathbf{r}}{|\mathbf{r}|}\Big) \cdot \mathbf{z}_1\Big)\right] \\
&= \frac{1}{|\mathbf{r}|}\left[\Big(\dot{\mathbf{r}} \times \frac{\mathbf{r}}{|\mathbf{r}|}\Big) \times \Big(\mathbf{z}_1 \times \mathbf{y}_1\Big)\right] \\
&= \frac{1}{|\mathbf{r}|}\left[\mathbf{x}_1 \times \Big(\dot{\mathbf{r}} \times \frac{\mathbf{r}}{|\mathbf{r}|}\Big)\right].
\end{aligned} \tag{4.22}$$

Here we have made use of the so-called BAC-CAB identity.

Doing similar computations for particle 2, we arrive at

$$\begin{aligned}
\dot{\mathbf{r}} &= \mathbf{x}_1 - \mathbf{x}_2, \\
\dot{\mathbf{x}}_1 &= \frac{1}{|\mathbf{r}|}\left[\mathbf{x}_1 \times \Big(\dot{\mathbf{r}} \times \frac{\mathbf{r}}{|\mathbf{r}|}\Big)\right] = \frac{1}{|\mathbf{r}|}\left(\mathbf{x}_1 \times \boldsymbol{\ell}\right), \\
\dot{\mathbf{x}}_2 &= \frac{1}{|\mathbf{r}|}\left[\mathbf{x}_2 \times \Big(\dot{\mathbf{r}} \times \frac{\mathbf{r}}{|\mathbf{r}|}\Big)\right] = \frac{1}{|\mathbf{r}|}\left(\mathbf{x}_2 \times \boldsymbol{\ell}\right),
\end{aligned} \tag{4.23}$$

with

$$\boldsymbol{\ell} \triangleq \dot{\mathbf{r}} \times \frac{\mathbf{r}}{|\mathbf{r}|} \tag{4.24}$$

and initial conditions governed by the $M_{CB(\mathbf{a})}$ constraints.

4.4.1 Explicit solutions for system behavior on $M_{CB(\mathbf{a})}$

As an aid to intuition, we note that the dynamics of the baseline vector $\mathbf{r}$ can be reformulated as

$$\begin{aligned}
\dot{\mathbf{r}} &= \left(\dot{\mathbf{r}} \cdot \frac{\mathbf{r}}{|\mathbf{r}|}\right) \frac{\mathbf{r}}{|\mathbf{r}|} + \left[\dot{\mathbf{r}} - \left(\dot{\mathbf{r}} \cdot \frac{\mathbf{r}}{|\mathbf{r}|}\right) \frac{\mathbf{r}}{|\mathbf{r}|}\right] \\
&= \left(\dot{\mathbf{r}} \cdot \frac{\mathbf{r}}{|\mathbf{r}|}\right) \frac{\mathbf{r}}{|\mathbf{r}|} + \left[\dot{\mathbf{r}}\left(\frac{\mathbf{r}}{|\mathbf{r}|} \cdot \frac{\mathbf{r}}{|\mathbf{r}|}\right) - \frac{\mathbf{r}}{|\mathbf{r}|}\left(\frac{\mathbf{r}}{|\mathbf{r}|} \cdot \dot{\mathbf{r}}\right)\right] \\
&= \left(\dot{\mathbf{r}} \cdot \frac{\mathbf{r}}{|\mathbf{r}|}\right) \frac{\mathbf{r}}{|\mathbf{r}|} + \frac{\mathbf{r}}{|\mathbf{r}|} \times \left(\dot{\mathbf{r}} \times \frac{\mathbf{r}}{|\mathbf{r}|}\right) \\
&= \frac{1}{|\mathbf{r}|}\left(\dot{\mathbf{r}} \cdot \frac{\mathbf{r}}{|\mathbf{r}|}\right) \mathbf{r} - \frac{1}{|\mathbf{r}|}\left(\dot{\mathbf{r}} \times \frac{\mathbf{r}}{|\mathbf{r}|}\right) \times \mathbf{r}.
\end{aligned} \tag{4.25}$$

(See [48] for background and a similar approach.) The first term captures the lengthening or shortening of the baseline vector $\mathbf{r}$, and the second term is related to the angular velocity of $\mathbf{r}$ (with $\mathbf{r}$ viewed as an extensible rod from the perspective of particle 1). Addressing the former term, we first note that $\dot{\mathbf{r}} \cdot \frac{\mathbf{r}}{|\mathbf{r}|} = \frac{d}{dt}(|\mathbf{r}|)$. Defining $\rho \triangleq |\mathbf{r}|$, we have

$$\dot{\rho} = (\mathbf{x}_1 - \mathbf{x}_2) \cdot \frac{\mathbf{r}}{|\mathbf{r}|} = a_1 + a_2, \tag{4.26}$$

and obtain

$$\rho(t) = (a_1 + a_2)\, t + \rho_0, \text{ for } \rho_0 = |\mathbf{r}(0)|\,. \tag{4.27}$$

Turning to the second term in (4.25), we begin our analysis by demonstrating that the vector cross product $\boldsymbol{\ell} = \dot{\mathbf{r}} \times \frac{\mathbf{r}}{|\mathbf{r}|}$ is in fact a fixed vector. Noting that $\frac{\mathbf{r}}{|\mathbf{r}|} \cdot \boldsymbol{\ell} = 0$

and $\dot{\mathbf{r}} \cdot \boldsymbol{\ell} = 0$, we take the derivative to get

$$
\begin{aligned}
\dot{\boldsymbol{\ell}} &= \left[(\dot{\mathbf{x}}_1 - \dot{\mathbf{x}}_2) \times \frac{\mathbf{r}}{|\mathbf{r}|} \right] + \left[\dot{\mathbf{r}} \times \frac{d}{dt}\Big(\frac{\mathbf{r}}{|\mathbf{r}|} \Big) \right] \\
&= \frac{1}{|\mathbf{r}|} \left[\big((\mathbf{x}_1 - \mathbf{x}_2) \times \boldsymbol{\ell} \big) \times \frac{\mathbf{r}}{|\mathbf{r}|} \right] + \left[\dot{\mathbf{r}} \times \frac{\mathbf{w}}{|\mathbf{r}|} \right] \\
&= -\frac{1}{|\mathbf{r}|} \left[\frac{\mathbf{r}}{|\mathbf{r}|} \times \Big(\dot{\mathbf{r}} \times \boldsymbol{\ell} \Big) \right] + \frac{1}{|\mathbf{r}|} \left[\dot{\mathbf{r}} \times \Big(\frac{\mathbf{r}}{|\mathbf{r}|} \times \boldsymbol{\ell} \Big) \right] \\
&= -\frac{1}{|\mathbf{r}|} \left[\dot{\mathbf{r}} \Big(\frac{\mathbf{r}}{|\mathbf{r}|} \cdot \boldsymbol{\ell} \Big) - \boldsymbol{\ell} \Big(\dot{\mathbf{r}} \cdot \frac{\mathbf{r}}{|\mathbf{r}|} \Big) \right] + \frac{1}{|\mathbf{r}|} \left[\frac{\mathbf{r}}{|\mathbf{r}|} \Big(\dot{\mathbf{r}} \cdot \boldsymbol{\ell} \Big) - \boldsymbol{\ell} \Big(\dot{\mathbf{r}} \cdot \frac{\mathbf{r}}{|\mathbf{r}|} \Big) \right] \\
&= 0,
\end{aligned} \tag{4.28}
$$

where we have made use of (4.9). Substituting this result as well as our results from (4.26) and (4.27) into (4.25), we can express our $\mathbf{r}$ dynamics as

$$
\dot{\mathbf{r}}(t) = \frac{1}{a_+ t + \rho_0} \left[a_+ \mathbb{1} - \hat{\boldsymbol{\ell}} \right] \mathbf{r}(t), \tag{4.29}
$$

where we denote $a_+ = a_1 + a_2$ and make use of the operator $\hat{}: \mathbb{R}^3 \longrightarrow \mathfrak{so}(3)$ which maps any 3-vector $\Gamma = (\Gamma_1, \Gamma_2, \Gamma_3)$ to a skew-symmetric matrix defined by

$$
\hat{\Gamma} = \begin{pmatrix} 0 & -\Gamma_3 & \Gamma_2 \\ \Gamma_3 & 0 & -\Gamma_1 \\ -\Gamma_2 & \Gamma_1 & 0 \end{pmatrix}. \tag{4.30}
$$

Since $a_+ \mathbb{1}$ and $\hat{\boldsymbol{\ell}}$ commute, for $a_+ \neq 0$ we can derive an explicit solution for $\mathbf{r}(t)$ by

$$
\begin{aligned}
\mathbf{r}(t) &= \exp\left(\int_0^t \frac{a_+}{a_+ \tau + \rho_0} d\tau \right) \exp\left(-\hat{\boldsymbol{\ell}} \int_0^t \frac{1}{a_+ \tau + \rho_0} d\tau \right) \mathbf{r}(0) \\
&= \exp\left(\ln(a_+ \tau + \rho_0) \Big|_0^t \right) \exp\left(-\frac{1}{a_+} \hat{\boldsymbol{\ell}} \ln(a_+ \tau + \rho_0) \Big|_0^t \right) \mathbf{r}(0) \\
&= \frac{a_+ t + \rho_0}{\rho_0} \exp\left(-\frac{1}{a_+} \hat{\boldsymbol{\ell}} \ln\left(\frac{a_+ t + \rho_0}{\rho_0} \right) \right) \mathbf{r}(0).
\end{aligned} \tag{4.31}
$$

A straightforward calculation based on (4.29) easily yields the result for the $a_+ = 0$ case, and we can therefore write our complete solution as

$$\mathbf{r}(t) = \begin{cases} \frac{a_+ t+\rho_0}{\rho_0} \exp\left(-\frac{1}{a_+}\hat{\boldsymbol{\ell}} \ln\left(\frac{a_+ t+\rho_0}{\rho_0}\right)\right)\mathbf{r}_0 & \text{for } a_+ \neq 0 \\ \exp\left(-\frac{1}{\rho_0}\hat{\boldsymbol{\ell}} t\right)\mathbf{r}_0 & \text{for } a_+ = 0, \end{cases}$$

$$\text{for } \mathbf{r}(0) = \mathbf{r}_0,\ \rho_0 = |\mathbf{r}_0|\,,\ \mathbf{x}_i(0) = \mathbf{x}_i^0,\ \boldsymbol{\ell} = \left(\mathbf{x}_1^0 - \mathbf{x}_2^0\right) \times \frac{\mathbf{r}_0}{|\mathbf{r}_0|}. \tag{4.32}$$

Similarly, by analogous calculations from (4.23) we have (for $i = 1, 2$)

$$\mathbf{x}_i(t) = \begin{cases} \exp\left(-\frac{1}{a_+}\hat{\boldsymbol{\ell}} \ln\left(\frac{a_+ t+\rho_0}{\rho_0}\right)\right)\mathbf{x}_i^0 & \text{for } a_+ \neq 0 \\ \exp\left(-\frac{1}{\rho_0}\hat{\boldsymbol{\ell}} t\right)\mathbf{x}_i^0 & \text{for } a_+ = 0. \end{cases} \tag{4.33}$$

4.4.2 Center of mass trajectory

Prior to stating and proving a proposition concerning the motion of the center of mass, we note the following calculation. Define $\Theta \in [-1, 1]$ as

$$\Theta \triangleq (\mathbf{x}_1 \times \mathbf{x}_2) \cdot \frac{\mathbf{r}}{|\mathbf{r}|}, \tag{4.34}$$

the signed volume of the parallelepiped with edges $\mathbf{x}_1, \mathbf{x}_2, \frac{\mathbf{r}}{|\mathbf{r}|}$. Then using the fact that $\mathbf{x}_1 \times \mathbf{x}_2 = (\mathbf{x}_1 - \mathbf{x}_2) \times \mathbf{x}_2 = \dot{\mathbf{r}} \times \mathbf{x}_2$ and $\mathbf{x}_1 \times \mathbf{x}_2 = \mathbf{x}_1 \times (\mathbf{x}_2 - \mathbf{x}_1) = \mathbf{x}_1 \times (-\dot{\mathbf{r}})$, one can show that

$$\Theta = -\mathbf{x}_1 \cdot \boldsymbol{\ell} \ = \ -\mathbf{x}_2 \cdot \boldsymbol{\ell}. \tag{4.35}$$

By differentiating (4.35) along trajectories of (4.23), it follows readily that Θ is a constant value on $M_{CB(\mathbf{a})}$.

Proposition 4.4.1. *Consider a two-particle system operating on $M_{CB(\mathbf{a})}$ according to the closed-loop mutual CB pursuit dynamics (4.23) with initial conditions $\mathbf{r}_i(0) = \mathbf{r}_i^0$ and $\mathbf{x}_i(0) = \mathbf{x}_i^0$, $i = 1, 2$. Define the change of coordinates $\tilde{\mathbf{r}}_i \triangleq \mathbf{r}_i - \mathbf{r}_c$, where $\mathbf{r}_c$ is defined by*

$$\mathbf{r}_c \triangleq \begin{cases} \mathbf{z}_0 - \sigma_0 \left(\frac{\mathbf{r}_0}{|\mathbf{r}_0|} \times \frac{\boldsymbol{\ell}}{|\boldsymbol{\ell}|} \right) & \text{for } \boldsymbol{\ell} \neq 0, \\ 0 & \text{for } \boldsymbol{\ell} = 0, \end{cases} \tag{4.36}$$

with $\mathbf{z}_0 = \frac{1}{2}\left(\mathbf{r}_1^0 + \mathbf{r}_2^0\right)$, $\sigma_0 = -\frac{a_-}{2|\boldsymbol{\ell}|}\rho_0$, $a_- \triangleq a_1 - a_2$, and $\mathbf{r}_0$, ρ_0, and $\boldsymbol{\ell}$ as in (4.32). Then the trajectory of the center of mass $\mathbf{z} \triangleq \frac{1}{2}(\mathbf{r}_1 + \mathbf{r}_2)$ can be given in the new coordinates $\tilde{\mathbf{z}} = \mathbf{z} - \mathbf{r}_c$ by the following:

(i.) if $\boldsymbol{\ell} = 0$, then $\tilde{\mathbf{z}}(t) = \tilde{\mathbf{z}}_0 + \dfrac{1}{2}\left(\mathbf{x}_1^0 + \mathbf{x}_2^0\right) t$

(ii.) if $\boldsymbol{\ell} \neq 0$, but $a_- = 0$, then $\tilde{\mathbf{z}}(t) = -\dfrac{\Theta}{|\boldsymbol{\ell}|^2}\boldsymbol{\ell} t$

(iii.) if $\boldsymbol{\ell} \neq 0$, $a_- \neq 0$, but $a_+ = 0$, then $\tilde{\mathbf{z}}(t) = \exp\left(-\dfrac{1}{\rho_0}\hat{\boldsymbol{\ell}} t\right)\tilde{\mathbf{z}}_0 - \dfrac{\Theta}{|\boldsymbol{\ell}|^2}\boldsymbol{\ell} t$

(iv.) if $\boldsymbol{\ell}, a_-$ and a_+ are all nonzero, then

$$\tilde{\mathbf{z}}(t) = c(t) \exp\left(-\frac{1}{a_+}\hat{\boldsymbol{\ell}} \ln\left(c(t)\right)\right) \tilde{\mathbf{z}}_0 - \frac{\Theta}{|\boldsymbol{\ell}|^2}\boldsymbol{\ell} t, \tag{4.37}$$

with $a_+ \triangleq a_1 + a_2$, $c(t) = \frac{a_+ t + \rho_0}{\rho_0}$, and $t < t_c$, where $t_c = \rho_0/(-a_+)$ for $a_+ < 0$, and $t_c = \infty$ otherwise.

Proof. We first note from (4.27) that if $a_+ < 0$, then $\rho(t_c) = 0$ for $t_c = \rho_0/(-a_+)$, and therefore we assume $t < t_c$, as stated in the proposition.

Assume $\boldsymbol{\ell} \neq 0$. We will demonstrate that the center of mass follows either a circling, helical, or spiral trajectory centered on the point $\mathbf{r}_c$. We can resolve $\tilde{\mathbf{z}}$ into component vectors as

$$\tilde{\mathbf{z}} = \left(\tilde{\mathbf{z}} \cdot \frac{\mathbf{r}}{|\mathbf{r}|}\right) \frac{\mathbf{r}}{|\mathbf{r}|} + \left(\tilde{\mathbf{z}} \cdot \frac{\boldsymbol{\ell}}{|\boldsymbol{\ell}|}\right) \frac{\boldsymbol{\ell}}{|\boldsymbol{\ell}|} + \left[\tilde{\mathbf{z}} \cdot \left(\frac{\mathbf{r}}{|\mathbf{r}|} \times \frac{\boldsymbol{\ell}}{|\boldsymbol{\ell}|}\right)\right] \left(\frac{\mathbf{r}}{|\mathbf{r}|} \times \frac{\boldsymbol{\ell}}{|\boldsymbol{\ell}|}\right). \tag{4.38}$$

The main thrust of the proof is to demonstrate that the first term is identically zero, the second term is linear in t, and that self-contained dynamics (and a resulting closed-form solution) can be derived for the third term. We address the first term by defining

$$\gamma \triangleq \left(\tilde{\mathbf{z}} \cdot \frac{\mathbf{r}}{|\mathbf{r}|}\right) \tag{4.39}$$

and making use of (4.9)-(4.10) to obtain the derivatives

$$\begin{aligned} \dot{\gamma} &= \left(\frac{1}{2}(\mathbf{x}_1 + \mathbf{x}_2) \cdot \frac{\mathbf{r}}{|\mathbf{r}|}\right) + \frac{\tilde{\mathbf{z}}}{|\mathbf{r}|} \cdot \left[\dot{\mathbf{r}} - \left(\dot{\mathbf{r}} \cdot \frac{\mathbf{r}}{|\mathbf{r}|}\right) \frac{\mathbf{r}}{|\mathbf{r}|}\right] \\ &= \frac{a_-}{2} + \frac{1}{\rho}\Big(\tilde{\mathbf{z}} \cdot (\mathbf{x}_1 - \mathbf{x}_2) - a_+\gamma\Big), \end{aligned} \tag{4.40}$$

and

$$\begin{aligned} \ddot{\gamma} &= \frac{-\dot{\rho}}{\rho^2}\Big(\tilde{\mathbf{z}} \cdot (\mathbf{x}_1 - \mathbf{x}_2) - a_+\gamma\Big) + \frac{1}{\rho}\Big(\dot{\tilde{\mathbf{z}}} \cdot (\mathbf{x}_1 - \mathbf{x}_2) + \tilde{\mathbf{z}} \cdot (\dot{\mathbf{x}}_1 - \dot{\mathbf{x}}_2) - a_+\dot{\gamma}\Big) \\ &= \frac{-a_+}{\rho^2}\Big(\tilde{\mathbf{z}} \cdot (\mathbf{x}_1 - \mathbf{x}_2) - a_+\gamma\Big) \\ &\quad + \frac{1}{\rho}\left[\frac{1}{2}(\mathbf{x}_1 + \mathbf{x}_2) \cdot (\mathbf{x}_1 - \mathbf{x}_2) + \tilde{\mathbf{z}} \cdot \left(\frac{1}{\rho}(\mathbf{x}_1 - \mathbf{x}_2) \times \left(\dot{\mathbf{r}} \times \frac{\mathbf{r}}{|\mathbf{r}|}\right)\right) - a_+\dot{\gamma}\right] \\ &= \frac{-a_+}{\rho^2}\Big(\tilde{\mathbf{z}} \cdot \dot{\mathbf{r}} - a_+\gamma\Big) + \frac{1}{\rho^2}\left[\tilde{\mathbf{z}} \cdot \left(\dot{\mathbf{r}} \times \left(\dot{\mathbf{r}} \times \frac{\mathbf{r}}{|\mathbf{r}|}\right)\right)\right] - \frac{a_+}{\rho}\dot{\gamma}. \end{aligned} \tag{4.41}$$

Then since

$$\tilde{\mathbf{z}} \cdot \left(\dot{\mathbf{r}} \times \left(\dot{\mathbf{r}} \times \frac{\mathbf{r}}{|\mathbf{r}|}\right)\right) = (\tilde{\mathbf{z}} \times \dot{\mathbf{r}}) \cdot \left(\dot{\mathbf{r}} \times \frac{\mathbf{r}}{|\mathbf{r}|}\right) = (\tilde{\mathbf{z}} \cdot \dot{\mathbf{r}}) \left(\dot{\mathbf{r}} \cdot \frac{\mathbf{r}}{|\mathbf{r}|}\right) - \left(\tilde{\mathbf{z}} \cdot \frac{\mathbf{r}}{|\mathbf{r}|}\right) (\dot{\mathbf{r}} \cdot \dot{\mathbf{r}}), \tag{4.42}$$

(4.41) simplifies to

$$\begin{aligned}\ddot{\gamma} &= \frac{-a_+}{\rho^2}\Big(\tilde{\mathbf{z}}\cdot\dot{\mathbf{r}} - a_+\gamma\Big) + \frac{1}{\rho^2}\Big[(\tilde{\mathbf{z}}\cdot\dot{\mathbf{r}})\,a_+ - \gamma\,(\dot{\mathbf{r}}\cdot\dot{\mathbf{r}})\Big] - \frac{a_+}{\rho}\dot{\gamma} \\ &= \frac{a_+^2 - |\dot{\mathbf{r}}|^2}{\rho^2}\gamma - \frac{a_+}{\rho}\dot{\gamma}. \end{aligned} \tag{4.43}$$

Initial values for γ and $\dot{\gamma}$ are given by

$$\begin{aligned}\gamma(0) &= (\mathbf{z}(0) - \mathbf{r}_c)\cdot\frac{\mathbf{r}(0)}{|\mathbf{r}(0)|} = \sigma_0\left(\frac{\mathbf{r}_0}{|\mathbf{r}_0|}\times\frac{\boldsymbol{\ell}}{|\boldsymbol{\ell}|}\right)\cdot\frac{\mathbf{r}_0}{|\mathbf{r}_0|} = 0, \\ \dot{\gamma}(0) &= \frac{a_-}{2} + \frac{1}{\rho_0}\Big[\tilde{\mathbf{z}}(0)\cdot\big(\mathbf{x}_1(0) - \mathbf{x}_2(0)\big) - a_+\gamma(0)\Big] \\ &= \frac{a_-}{2} + \frac{\sigma_0}{\rho_0}\left[\left(\frac{\mathbf{r}_0}{|\mathbf{r}_0|}\times\frac{\boldsymbol{\ell}}{|\boldsymbol{\ell}|}\right)\cdot\dot{\mathbf{r}}(0)\right] \\ &= \frac{a_-}{2} - \frac{a_-}{2\,|\boldsymbol{\ell}|}\left[\left(\dot{\mathbf{r}}(0)\times\frac{\mathbf{r}_0}{|\mathbf{r}_0|}\right)\cdot\frac{\boldsymbol{\ell}}{|\boldsymbol{\ell}|}\right] \\ &= \frac{a_-}{2} - \frac{a_-}{2\,|\boldsymbol{\ell}|}\left[\boldsymbol{\ell}\cdot\frac{\boldsymbol{\ell}}{|\boldsymbol{\ell}|}\right] = 0, \end{aligned} \tag{4.44}$$

and therefore (4.43) implies $\gamma = \left(\tilde{\mathbf{z}}\cdot\frac{\mathbf{r}}{|\mathbf{r}|}\right) \equiv 0$, i.e. (4.38) simplifies to

$$\tilde{\mathbf{z}} = \left(\tilde{\mathbf{z}}\cdot\frac{\boldsymbol{\ell}}{|\boldsymbol{\ell}|}\right)\frac{\boldsymbol{\ell}}{|\boldsymbol{\ell}|} + \left[\tilde{\mathbf{z}}\cdot\left(\frac{\mathbf{r}}{|\mathbf{r}|}\times\frac{\boldsymbol{\ell}}{|\boldsymbol{\ell}|}\right)\right]\left(\frac{\mathbf{r}}{|\mathbf{r}|}\times\frac{\boldsymbol{\ell}}{|\boldsymbol{\ell}|}\right). \tag{4.45}$$

Now note that

$$\frac{d}{dt}\left(\tilde{\mathbf{z}}\cdot\frac{\boldsymbol{\ell}}{|\boldsymbol{\ell}|}\right) = \frac{1}{2}\left(\mathbf{x}_1 + \mathbf{x}_2\right)\cdot\frac{\boldsymbol{\ell}}{|\boldsymbol{\ell}|} = -\frac{\Theta}{|\boldsymbol{\ell}|}, \tag{4.46}$$

and therefore integrating both sides yields

$$\tilde{\mathbf{z}}(t)\cdot\frac{\boldsymbol{\ell}}{|\boldsymbol{\ell}|} = -\frac{\Theta}{|\boldsymbol{\ell}|}t + \sigma_0\left(\frac{\mathbf{r}_0}{|\mathbf{r}_0|}\times\frac{\boldsymbol{\ell}}{|\boldsymbol{\ell}|}\right)\cdot\frac{\boldsymbol{\ell}}{|\boldsymbol{\ell}|} = -\frac{\Theta}{|\boldsymbol{\ell}|}t. \tag{4.47}$$

Therefore the first term in (4.45) is linear in t, and substitution of (4.47) into (4.45) supplies the simplified expression

$$\tilde{\mathbf{z}} = -\frac{\Theta}{|\boldsymbol{\ell}|}t + \left[\tilde{\mathbf{z}}\cdot\left(\frac{\mathbf{r}}{|\mathbf{r}|}\times\frac{\boldsymbol{\ell}}{|\boldsymbol{\ell}|}\right)\right]\left(\frac{\mathbf{r}}{|\mathbf{r}|}\times\frac{\boldsymbol{\ell}}{|\boldsymbol{\ell}|}\right). \tag{4.48}$$

In order to simplify the last term, we let

$$\sigma \triangleq \tilde{\mathbf{z}} \cdot \left(\frac{\mathbf{r}}{|\mathbf{r}|} \times \frac{\boldsymbol{\ell}}{|\boldsymbol{\ell}|} \right), \tag{4.49}$$

observing that

$$\sigma(0) = \sigma_0 \left(\frac{\mathbf{r}_0}{|\mathbf{r}_0|} \times \frac{\boldsymbol{\ell}}{|\boldsymbol{\ell}|} \right) \cdot \left(\frac{\mathbf{r}_0}{|\mathbf{r}_0|} \times \frac{\boldsymbol{\ell}}{|\boldsymbol{\ell}|} \right) = \sigma_0, \tag{4.50}$$

and define

$$\bar{\mathbf{z}} = \left[\tilde{\mathbf{z}} \cdot \left(\frac{\mathbf{r}}{|\mathbf{r}|} \times \frac{\boldsymbol{\ell}}{|\boldsymbol{\ell}|} \right) \right] \left(\frac{\mathbf{r}}{|\mathbf{r}|} \times \frac{\boldsymbol{\ell}}{|\boldsymbol{\ell}|} \right) = \sigma \left(\frac{\mathbf{r}}{|\mathbf{r}|} \times \frac{\boldsymbol{\ell}}{|\boldsymbol{\ell}|} \right). \tag{4.51}$$

By direct calculation (making use of (4.9)-(4.10) and (4.24)) we have

$$\begin{aligned}
\dot{\sigma} &= \dot{\tilde{\mathbf{z}}} \cdot \left(\frac{\mathbf{r}}{|\mathbf{r}|} \times \frac{\boldsymbol{\ell}}{|\boldsymbol{\ell}|} \right) + \tilde{\mathbf{z}} \cdot \frac{\mathbf{1}}{|\mathbf{r}|} \left[\left(\frac{\mathbf{r}}{|\mathbf{r}|} \times \boldsymbol{\ell} \right) \times \frac{\boldsymbol{\ell}}{|\boldsymbol{\ell}|} \right] \\
&= \frac{\mathbf{x}_1 + \mathbf{x}_2}{2\,|\boldsymbol{\ell}|} \cdot \left[\frac{\mathbf{r}}{|\mathbf{r}|} \times \left(\dot{\mathbf{r}} \times \frac{\mathbf{r}}{|\mathbf{r}|} \right) \right] - \frac{\tilde{\mathbf{z}}}{|\mathbf{r}|} \cdot \left[\frac{\mathbf{r}}{|\mathbf{r}|} \left(\boldsymbol{\ell} \cdot \frac{\boldsymbol{\ell}}{|\boldsymbol{\ell}|} \right) - \boldsymbol{\ell} \left(\frac{\mathbf{r}}{|\mathbf{r}|} \cdot \frac{\boldsymbol{\ell}}{|\boldsymbol{\ell}|} \right) \right] \\
&= \frac{1}{2\,|\boldsymbol{\ell}|} \left[\left(\mathbf{x}_1 \times \frac{\mathbf{r}}{|\mathbf{r}|} \right) \cdot \left(\dot{\mathbf{r}} \times \frac{\mathbf{r}}{|\mathbf{r}|} \right) + \left(\mathbf{x}_2 \times \frac{\mathbf{r}}{|\mathbf{r}|} \right) \cdot \left(\dot{\mathbf{r}} \times \frac{\mathbf{r}}{|\mathbf{r}|} \right) \right] - \frac{\tilde{\mathbf{z}}}{|\mathbf{r}|} \cdot \left(\frac{\mathbf{r}}{|\mathbf{r}|} \,|\boldsymbol{\ell}| \right) \\
&= \frac{1}{2\,|\boldsymbol{\ell}|} \left[\mathbf{x}_1 \cdot \dot{\mathbf{r}} - \left(\mathbf{x}_1 \cdot \frac{\mathbf{r}}{|\mathbf{r}|} \right) \left(\dot{\mathbf{r}} \cdot \frac{\mathbf{r}}{|\mathbf{r}|} \right) + \mathbf{x}_2 \cdot \dot{\mathbf{r}} - \left(\mathbf{x}_2 \cdot \frac{\mathbf{r}}{|\mathbf{r}|} \right) \left(\dot{\mathbf{r}} \cdot \frac{\mathbf{r}}{|\mathbf{r}|} \right) \right] - \frac{|\boldsymbol{\ell}|}{|\mathbf{r}|} \gamma \\
&= \frac{1}{2\,|\boldsymbol{\ell}|} \left[(\mathbf{x}_1 + \mathbf{x}_2) \cdot \dot{\mathbf{r}} - a_1 a_+ + a_2 a_+ \right] \\
&= -\frac{1}{2\,|\boldsymbol{\ell}|} a_- a_+,
\end{aligned} \tag{4.52}$$

and therefore

$$\sigma(t) = \sigma(0) - \frac{1}{2\,|\boldsymbol{\ell}|} a_- a_+ t = \frac{\sigma_0}{\rho_0} \left(\rho_0 + a_+ t \right) = -\frac{a_-}{2\,|\boldsymbol{\ell}|} \rho(t). \tag{4.53}$$

If $a_- = 0$, then the third term of (4.38) is identically zero and (4.47) yields the second claim of our proposition. If $a_- \neq 0$, then differentiating (4.51) yields

$$
\begin{aligned}
\dot{\bar{\mathbf{z}}} &= \dot{\sigma}\left(\frac{\mathbf{r}}{|\mathbf{r}|} \times \frac{\boldsymbol{\ell}}{|\boldsymbol{\ell}|}\right) + \sigma\left[\frac{d}{dt}\left(\frac{\mathbf{r}}{|\mathbf{r}|}\right) \times \frac{\boldsymbol{\ell}}{|\boldsymbol{\ell}|}\right] \\
&= -\frac{1}{2\,|\boldsymbol{\ell}|} a_- a_+ \left(\frac{\mathbf{r}}{|\mathbf{r}|} \times \frac{\boldsymbol{\ell}}{|\boldsymbol{\ell}|}\right) + \sigma\left[\frac{1}{\rho}\left(\frac{\mathbf{r}}{|\mathbf{r}|} \times \boldsymbol{\ell}\right) \times \frac{\boldsymbol{\ell}}{|\boldsymbol{\ell}|}\right] \\
&= -\frac{1}{2\,|\boldsymbol{\ell}|} a_- a_+ \left(\frac{1}{\sigma}\right)\left[\sigma\left(\frac{\mathbf{r}}{|\mathbf{r}|} \times \frac{\boldsymbol{\ell}}{|\boldsymbol{\ell}|}\right)\right] + \frac{\sigma}{\rho}\left[-\left(\frac{\boldsymbol{\ell}}{|\boldsymbol{\ell}|} \times \frac{\mathbf{r}}{|\mathbf{r}|}\right) \times \boldsymbol{\ell}\right] \\
&= \frac{a_+}{\rho}\left[\sigma\left(\frac{\mathbf{r}}{|\mathbf{r}|} \times \frac{\boldsymbol{\ell}}{|\boldsymbol{\ell}|}\right)\right] + \frac{1}{\rho}\left[\sigma\left(\frac{\mathbf{r}}{|\mathbf{r}|} \times \frac{\boldsymbol{\ell}}{|\boldsymbol{\ell}|}\right) \times \boldsymbol{\ell}\right] \\
&= \frac{1}{\rho}\left[a_+ \mathbb{1} - \hat{\boldsymbol{\ell}}\right] \bar{\mathbf{z}},
\end{aligned}
\tag{4.54}
$$

where we have made use of (4.9), (4.53) and the Jacobi identity. We recognize (4.54) as the same form as (4.29), and therefore have the analogous closed-form expression for $\bar{\mathbf{z}}$. The third and fourth claims of **Proposition 4** then follow from (4.48), (4.51), and (4.54), along with the fact that $\tilde{\mathbf{z}}(0) = \bar{\mathbf{z}}(0)$. Finally, if $\boldsymbol{\ell} = 0$, we have $\mathbf{x}_i(t) = \mathbf{x}_i^0$ (from (4.33)) and therefore $\dot{\bar{\mathbf{z}}}(t) = \frac{1}{2}\left(\mathbf{x}_1^0 + \mathbf{x}_2^0\right)$, establishing the first claim of the proposition. □

Remark 4.4.2 System behavior can be classified in terms of the initial conditions, parametrized by $\boldsymbol{\ell}$ and Θ, and the parameters a_+ and a_-. The sign and magnitude of $\boldsymbol{\ell}$ determine whether the baseline vector $\mathbf{r}$ will rotate ($\boldsymbol{\ell} \neq 0$) as well as the direction of rotation. Θ determines whether $\mathbf{r}, \mathbf{x}_1$ and $\mathbf{x}_2$ will evolve in a common plane. The parameter a_+ determines the rate of change of the inter-particle distance, and a_- determines if the center of mass will rotate. Figure 4.2 displays some of the possible system trajectories, including rectilinear and circling equilibria as well as an expanding spiral.

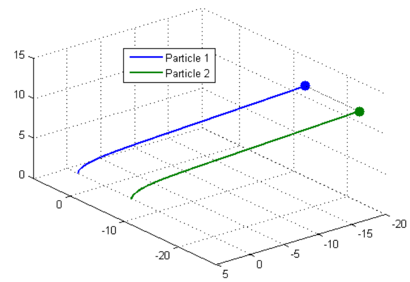

(a) Rectilinear equilibrium ($\boldsymbol{\ell} = 0$)

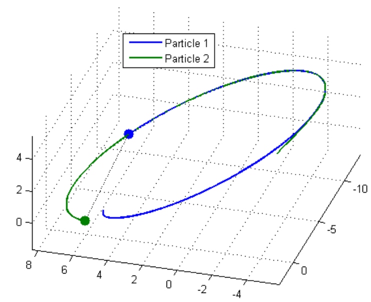

(b) Circling equilibrium ($\boldsymbol{\ell} \neq 0$; $a_- \neq 0$; $\Theta = 0$; $a_+ = 0$)

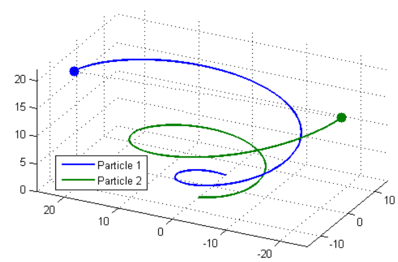

(c) Expanding spiral ($\boldsymbol{\ell}$, Θ, a_-, $a_+ \neq 0$)

Figure 4.2: These figures illustrate the various types of trajectories from **Proposition 4.4.1** in terms of initial conditions ($\boldsymbol{\ell}$ and Θ) and parameter values (a_+ and a_-).

4.5 Relative equilibria for the n-particle case

The analysis in [26] describes the possible types of relative equilibria for an n-particle system evolving according to (4.4) with $SE(3)$-invariant controls. These relative equilibria correspond to

1. rectilinear formations (i.e., all particles move in the same direction with arbi-

trary relative positions),

2. circling formations (i.e., all particles move on circular orbits with a common radius, in planes perpendicular to a common axis),

3. helical formations (i.e., all particles follow circular helices with the same radius, pitch, axis, and axial direction of motion).

As in [26], we can express our dynamics (4.4) in terms of group variables $g_1, g_2, \ldots, g_n \in G = SE(3)$ as the left-invariant system

$$\dot{g}_i = g_i \xi_i, \ i = 1, 2, \ldots, n, \tag{4.55}$$

where $\xi_i \in \mathfrak{g}$ = the Lie algebra of G. Then shape variables can be defined by

$$\tilde{g}_i = g_i^{-1} g_{i+1}, \ i = 1, 2, \ldots, n, \tag{4.56}$$

with corresponding dynamics

$$\dot{\tilde{g}}_i = \tilde{g}_i \tilde{\xi}_i, \ i = 1, 2, \ldots, n, \tag{4.57}$$

where $\tilde{\xi}_i = \xi_{i+1} - \mathrm{Ad}_{\tilde{g}_i^{-1}} \xi_i \in \mathfrak{g}$. Relative equilibria for the full dynamics are equilibria for the shape dynamics (4.57). In analogy to proposition (2.4.1) from the planar context, we present the following propositions concerning existence of relative equilibria for the general three-dimensional case.

Proposition 4.5.1. *Given $\{a_1, a_2, \ldots, a_n\}$, a relative equilibrium corresponding to rectilinear motion on $M_{CB(\mathbf{a})}$ under closed-loop cyclic CB pursuit dynamics (4.21) exists if and only if there exists a set of positive constants $\{\sigma_1, \sigma_2, \ldots, \sigma_n\}$ such that $\sum_{i=1}^{n} \sigma_i a_i = 0$.*

Proposition 4.5.2. *Given* $\{a_1, a_2, \ldots, a_n\}$*, define* $\{\alpha_1, \alpha_2, \ldots, \alpha_n\} \in (0, 2\pi)$ *by* $(\cos\alpha_i, \sin\alpha_i) = (-a_i, \sqrt{1-a_i^2})$*. Then a planar circling relative equilibrium on* $M_{CB(\mathbf{a})}$ *under closed-loop cyclic CB pursuit dynamics (4.21) exists if and only if*

$$i.\ a_i \neq \pm 1,\ i = 1, 2, \ldots, n; \quad ii.\ \sin\left(\sum_{i=1}^{n} \alpha_i\right) = 0. \tag{4.58}$$

Proof of Propositions 5 and 6. The proof for each proposition relies on **Proposition 2.4.1** and is sketched in appendix D. Note that the angle α_i as defined in **Proposition 4.5.2** matches the notation from the planar context, as discussed in section 4.3. (The choice of $\sin\alpha_i = \sqrt{1-a_i^2}$ corresponds to CCW circling equilibria, while choosing $\sin\alpha_i = -\sqrt{1-a_i^2}$ refers to CW circling equilibria.) Also, note that **Proposition 4.5.2** addresses the existence of circling equilibria on a common plane (rather than the more general definition of circling equilibria that permits multiple planes perpendicular to a common axis), and therefore the proof is simplified by assuming (without loss of generality) that the circling equilibrium evolves on the horizontal plane.

Remark 4.5.3 Observe that the constraint of **Proposition 4.5.1** is equivalent to requiring that either $a_i = 0,\ i = 1, 2, \ldots, n$ or that there exists $j, k \in [1, 2, \ldots, n]$ such that $a_j a_k < 0$. Also, observe that the condition in **Proposition 4.5.1** is not mutually exclusive with the conditions of **Proposition 4.5.2**, in contrast to the analogous planar propositions stated in chapter 2.

Chapter 5

Motion camouflage in a stochastic setting

5.1 Introduction and background

In chapters 2, 3 and 4, we have presented and analyzed a context in which pursuit interactions give rise to collective behavior which could be employed for cooperative maneuvering and control. In chapters 5 and 6, we turn to the more traditional setting in which pursuit is viewed as an adversarial (i.e. non-cooperative) phenomenon and the pursuee may employ evasive strategies. At the outset, we note that pursuit-evasion encounters do not always focus exclusively on the question of capture vs. escape. In fact, our analysis in both chapters 5 and 6 will focus on the *motion camouflage* pursuit strategy which attempts to maximize "stealth" and reduce pursuer "visibility" (in a sense that we will later make precise). Motion camouflage is a pursuit strategy observed in nature which relies on minimizing the perceived relative motion of the pursuer from the standpoint of the pursuee. This strategy is particularly suited to encounters in which the pursuee relies on optic flow sensing and does not typically detect looming cues, since the pursuer can conceal its approach by maneuvering so as to generate a trajectory which resembles that of a stationary object in the optic flow. Srinivasan and Davey were the first to postulate that an animal might use such a strategy to conceal its approach towards a pursuee[54], and they found empirical evidence to support the claim in their analysis of hoverfly flight data previously collected by Collett and Land[11]. The claim was bolstered by further research which demonstrated that dragonflies appear to use motion camouflage tactics in male-male territorial interactions[41]. Remarkably, it has also been shown (Ghose, Horiuchi, Krishnaprasad and Moss[19]) that bats use a strategy, known as *constant absolute target direction* (CATD), which is geometrically indistinguishable from motion camouflage. In this context, it is demonstrated that the pursuit strategy is nearly time-optimal in the sense that it minimizes time-to-intercept under a piecewise linear approximation.

A mathematical characterization of motion camouflage was presented by Glendinning in [20], in which the author derived differential equations for motion camouflage and described the pursuit curves for some basic examples. In [27], Justh and Krishnaprasad presented a biologically plausible feedback law for executing the motion camouflage pursuit strategy in the planar setting and proved a proposition concerning accessibility of the motion camouflage state in finite time. These results were subsequently extended to the three dimensional case[48] and also shown to hold when a sensorimotor delay was incorporated into the model[49]. Though this control law, known as the *motion camouflage proportional guidance* (MCPG) law, is rooted in biology, it has also been shown that there exist close parallels to certain proportional guidance schemes in the missile guidance literature[44, 51].

In chapter 5, we relate the previous deterministic work on motion camouflage in [27] to the stochastic setting, considering the impact of introducing evader controls driven by random processes[1]. This stochastic analysis is pertinent to the biological setting since there are many examples of organisms which appear to use stochastic control processes, such as the "run-and-tumble" movement exhibited in bacterial chemotaxis (see, e.g., [3]). Many species of bacteria use this type of stochastic steering control, which (as will be demonstrated in the sequel) can be modeled as a continuous time, finite state (CTFS) process driven by Poisson counters. In the vehicular setting, there may also be possible applications in adversarial encounters between unmanned vehicles in which one vehicle is equipped with an optical flow sensor and the other vehicle makes use of some type of stochastic evasive maneuver.

We proceed by providing a background discussion of some of the fundamentals of motion camouflage and the motion camouflage proportional guidance (MCPG) feedback law derived in [27]. We then move to the stochastic setting to address motion camouflage in the context of a stochastically steering evader, presenting the main result of this chapter in **Proposition 5.3.2**, which serves as a stochastic analogue to the motion camouflage accessibility result from the deterministic case (see Proposition 3.3 in [27]). In order to highlight the connections to the deterministic version, we present our analysis in terms of the full state dynamics (5.2) rather than the shape variable description developed in section 2.2.3. (In chapter 6 we will present a shape variable description of motion camouflage, which better suits our analysis for that particular context.) We end the chapter by presenting some

[1] This work was originally developed with Justh and Krishnaprasad and presented in [14].

specific forms of admissible stochastic controls (section 5.4) as well as simulation results (section 5.5).

5.2 Motion camouflage model

5.2.1 System dynamics

We base our model on the state dynamics presented in section 2.2.1, substituting the subscript p for the pursuer and e for the evader rather than the numbered indices used in the general model, by which we have the pursuer-evader dynamics

$$\begin{aligned} \dot{\mathbf{r}}_p &= \nu_p \mathbf{x}_p & \dot{\mathbf{r}}_e &= \nu_e \mathbf{x}_e \\ \dot{\mathbf{x}}_p &= \nu_p \mathbf{y}_p u_p & \dot{\mathbf{x}}_e &= \nu_e \mathbf{y}_e u_e \\ \dot{\mathbf{y}}_p &= -\nu_p \mathbf{x}_p u_p & \dot{\mathbf{y}}_e &= -\nu_e \mathbf{x}_e u_e. \end{aligned} \tag{5.1}$$

(The steering controls u_p and u_e may be given by feedback laws or prescribed.) By a straightforward rescaling of the time variable, we can always assume without loss of generality that the pursuer moves at unit speed and the evader moves at speed $\nu_e = \nu > 0$ (i.e., $\nu = \nu_e/\nu_p$ represents the ratio of the evader's speed to the pursuer's speed), and so our dynamics (5.1) can be represented as[2]

$$
\begin{aligned}
\dot{\mathbf{r}}_p &= \mathbf{x}_p & \dot{\mathbf{r}}_e &= \nu \mathbf{x}_e \\
\dot{\mathbf{x}}_p &= \mathbf{y}_p u_p & \dot{\mathbf{x}}_e &= \nu \mathbf{y}_e u_e \\
\dot{\mathbf{y}}_p &= -\mathbf{x}_p u_p & \dot{\mathbf{y}}_e &= -\nu \mathbf{x}_e u_e.
\end{aligned} \tag{5.2}
$$

In this chapter we will always assume that $\nu < 1$, i.e. the speed of the evader is strictly less than that of the pursuer.

5.2.2 Definition of motion camouflage

In this work we focus on "motion camouflage with respect to infinity", the strategy in which the pursuer maneuvers in such a way that, from the point of view of the evader, the pursuer always appears at the same bearing. This is described in [27] as

$$\mathbf{r}_p = \mathbf{r}_e + \lambda \mathbf{r}_\infty \tag{5.3}$$

where $\mathbf{r}_\infty$ is a fixed unit vector and λ is a time-dependent scalar. We define the "baseline vector" as the vector from the evader to the pursuer

$$\mathbf{r} = \mathbf{r}_p - \mathbf{r}_e, \tag{5.4}$$

and $|\mathbf{r}|$ denotes the baseline length. Since we have restricted ourselves to the non-collision case (i.e. $|\mathbf{r}| \neq 0$), we can define $\mathbf{w}$ as the vector component of $\dot{\mathbf{r}}$ which is

[2]This formulation matches the pursuer-evader dynamics presented in [27]. In chapter 6 we will present an alternative (but equivalent) formulation in which we assume the evader moves at unit speed, and the pursuer's speed is left to vary.

transverse to $\mathbf{r}$, i.e.

$$\mathbf{w} = \dot{\mathbf{r}} - \left(\frac{\mathbf{r}}{|\mathbf{r}|} \cdot \dot{\mathbf{r}} \right) \frac{\mathbf{r}}{|\mathbf{r}|}. \tag{5.5}$$

It was demonstrated in [27] that the pursuit-evasion system (5.2) is in a state of motion camouflage without collision on a given time interval iff $\mathbf{w} = 0$ on that interval.

5.2.3 Distance from motion camouflage

The function

$$\Gamma = \frac{\frac{d}{dt}|\mathbf{r}|}{|\frac{d\mathbf{r}}{dt}|} = \left(\frac{\mathbf{r}}{|\mathbf{r}|} \cdot \frac{\dot{\mathbf{r}}}{|\dot{\mathbf{r}}|} \right) \tag{5.6}$$

describes how far the pursuer-evader system is from a state of motion camouflage [27, 48]. The system is in a state of motion camouflage when $\Gamma = -1$, which corresponds to pure shortening of the baseline vector. (By contrast, $\Gamma = 0$ corresponds to pure rotation of the baseline vector, and $\Gamma = +1$ corresponds to pure lengthening of the baseline vector.) The difference $\Gamma - (-1) > 0$ is a measure of the distance of the pursuer-evader system from a state of motion camouflage.

For (5.6) to be well defined, we must have $|\mathbf{r}| > 0$ as well as $|\dot{\mathbf{r}}| > 0$. The former requirement is satisfied by assuming that $|\mathbf{r}| \neq 0$ initially, and then analyzing the engagement (for finite time) only until $|\mathbf{r}|$ reaches a value $r_0 > 0$ [27, 48]. The latter condition is ensured by the assumption that $0 < \nu < 1$, since $|\dot{\mathbf{r}}| \geq 1 - \nu$.

5.2.4 Feedback law for motion camouflage

When there is no delay associated with incorporating sensory information, we define our feedback law as

$$u_p = u_{MC} = -\mu_p \left(\frac{\mathbf{r}}{|\mathbf{r}|} \cdot \dot{\mathbf{r}}^{\perp} \right), \tag{5.7}$$

where $\mu_p > 0$ is a gain parameter [27, 48]. However, if there is a delay τ in the incorporation of sensory information, then we substitute $u_p(t-\tau)$ for u_p in equation (5.2), as described in [49]. (In this work, we only consider the delay-free case.)

Observe that (5.7) is well defined since, by the discussion in the previous subsection, $|\mathbf{r}| \neq 0$ during the duration of our analysis.

The key results for the deterministic motion camouflage feedback system are presented in [27, 48]. These results, particularly the planar result in [27], are the inspiration for the calculations below in Section 5.3.

5.3 Stochastic evader analysis

5.3.1 SDE for Γ

Let us now suppose that $u_p = u_{MC}$ as in (5.7) and u_e is not a deterministic function of time, but is instead driven by a stochastic process (in a way we will make precise later). Then $\mathbf{r}$ and $\dot{\mathbf{r}}$ are also stochastic processes, as is Γ given by (5.6). Analogous to the calculation of $\dot{\Gamma}$ given in [27], we can derive the following

SDE (Stochastic Differential Equation) for Γ (see **Remark 5.4.4**):

$$d\Gamma = \frac{|\dot{\mathbf{r}}|}{|\mathbf{r}|}\left[\frac{1}{|\dot{\mathbf{r}}|^2}\left(\frac{\mathbf{r}}{|\mathbf{r}|}\cdot\dot{\mathbf{r}}^{\perp}\right)^2\right]dt + \frac{1}{|\dot{\mathbf{r}}|}\left[\frac{1}{|\dot{\mathbf{r}}|^2}\left(\frac{\mathbf{r}}{|\mathbf{r}|}\cdot\dot{\mathbf{r}}^{\perp}\right)\right](1-\nu(\mathbf{x}_p\cdot\mathbf{x}_e))u_p dt$$
$$+\frac{1}{|\dot{\mathbf{r}}|}\left[\frac{1}{|\dot{\mathbf{r}}|^2}\left(\frac{\mathbf{r}}{|\mathbf{r}|}\cdot\dot{\mathbf{r}}^{\perp}\right)\right](\nu-(\mathbf{x}_p\cdot\mathbf{x}_e))\nu^2 u_e dt, \tag{5.8}$$

which is supplemented by the SDE version of (5.2), all of which should be interpreted as stochastic differential equations of the Itô type. Substituting (5.7) into (5.8) gives (c.f., [27])

$$d\Gamma = -\left[\frac{\mu_p}{|\dot{\mathbf{r}}|}(1-\nu(\mathbf{x}_p\cdot\mathbf{x}_e)) - \frac{|\dot{\mathbf{r}}|}{|\mathbf{r}|}\right]\left[\frac{1}{|\dot{\mathbf{r}}|^2}\left(\frac{\mathbf{r}}{|\mathbf{r}|}\cdot\dot{\mathbf{r}}^{\perp}\right)^2\right]dt$$
$$+\frac{1}{|\dot{\mathbf{r}}|}\left[\frac{1}{|\dot{\mathbf{r}}|^2}\left(\frac{\mathbf{r}}{|\mathbf{r}|}\cdot\dot{\mathbf{r}}^{\perp}\right)\right](\nu-(\mathbf{x}_p\cdot\mathbf{x}_e))\nu^2 u_e dt. \tag{5.9}$$

Noting that

$$\frac{1}{|\dot{\mathbf{r}}|^2}\left(\frac{\mathbf{r}}{|\mathbf{r}|}\cdot\dot{\mathbf{r}}^{\perp}\right)^2 = 1-\left(\frac{\mathbf{r}}{|\mathbf{r}|}\cdot\frac{\dot{\mathbf{r}}}{|\dot{\mathbf{r}}|}\right)^2 = 1-\Gamma^2, \tag{5.10}$$

and that $1-\Gamma^2 \geq 0$, we conclude that

$$d\Gamma \leq -(1-\Gamma^2)\left[\frac{\mu_p}{|\dot{\mathbf{r}}|}(1-\nu(\mathbf{x}_p\cdot\mathbf{x}_e)) - \frac{|\dot{\mathbf{r}}|}{|\mathbf{r}|}\right]dt$$
$$+\frac{1}{|\dot{\mathbf{r}}|^2}(\sqrt{1-\Gamma^2})\Big|(\nu-(\mathbf{x}_p\cdot\mathbf{x}_e))\nu^2 u_e\Big|dt. \tag{5.11}$$

Futhermore, as in the deterministic analysis in [27], we have the following inequalities:

$$|\mathbf{x}_p\cdot\mathbf{x}_e| \leq 1, \text{ and } 1-\nu \leq |\dot{\mathbf{r}}| \leq 1+\nu, \tag{5.12}$$

so that

$$d\Gamma \leq -(1-\Gamma^2)\left[\mu_p\left(\frac{1-\nu}{1+\nu}\right) - \frac{1+\nu}{|\mathbf{r}|}\right]dt + \frac{\nu^2(1+\nu)}{(1-\nu)^2}\left(\sqrt{1-\Gamma^2}\right)|u_e|dt. \tag{5.13}$$

For $\mu_p > 0$, we can define constants $r_0 > 0$ and $c_0 > 0$ such that

$$\mu_p = \left(\frac{1+\nu}{1-\nu}\right)\left(\frac{1+\nu}{r_0} + c_0\right), \tag{5.14}$$

and thus

$$\mu_p \geq \left(\frac{1+\nu}{1-\nu}\right)\left(\frac{1+\nu}{|\mathbf{r}|} + c_0\right), \quad \forall |\mathbf{r}| \geq r_0. \tag{5.15}$$

We thus have

$$d\Gamma \leq -(1-\Gamma^2)c_0 dt + \frac{\nu^2(1+\nu)}{(1-\nu)^2}\left(\sqrt{1-\Gamma^2}\right)\left|u_e\right|dt, \tag{5.16}$$

for all $|\mathbf{r}| \geq r_0$.

5.3.2 Bounds for $E[\Gamma]$

The next step is to take expected values of both sides of (5.16), which yields

$$\frac{d}{dt}E[\Gamma] \leq -c_0 E\left[1-\Gamma^2\right] + \frac{\nu^2(1+\nu)}{(1-\nu)^2}E\left[\left|u_e\right|\sqrt{1-\Gamma^2}\right], \tag{5.17}$$

provided $|\mathbf{r}| \geq r_0$. By the Cauchy-Schwartz Inequality,

$$\left|E\left[\left|u_e\right|\sqrt{1-\Gamma^2}\right]\right| \leq \sqrt{E\left[u_e^2\right]}\sqrt{E\left[1-\Gamma^2\right]}, \tag{5.18}$$

from which it follows that

$$\frac{d}{dt}E[\Gamma] \leq -c_0 E\left[1-\Gamma^2\right] + c_1\sqrt{E\left[1-\Gamma^2\right]}, \tag{5.19}$$

provided $|\mathbf{r}| > r_0$. Here we've assumed that u_e has a bounded second moment (i.e. $E[u_e^2] \leq u_{max}^2$ for some constant $u_{max} > 0$) and we've defined

$$c_1 = \frac{\nu^2(1+\nu)}{(1-\nu)^2}u_{max} > 0. \tag{5.20}$$

We can now show that, given $0 < \epsilon << 1$, we can choose c_0 (and hence μ_p) sufficiently large so as to ensure that $dE[\Gamma]/dt \leq 0$ for $E[1 - \Gamma^2] > \epsilon$ (provided $|\mathbf{r}| > r_0$). In particular, choose $c_0 > c_1/\sqrt{\epsilon}$. Then (5.19) becomes

$$\begin{aligned}
\frac{d}{dt}E[\Gamma] &\leq -E\left[1-\Gamma^2\right]\left(c_0 - \frac{c_1}{\sqrt{E\left[1-\Gamma^2\right]}}\right) \\
&\leq -E\left[1-\Gamma^2\right]\left(c_0 - \frac{c_1}{\sqrt{\epsilon}}\right) \\
&\leq -E\left[1-\Gamma^2\right]c_2 \\
&\leq -c_2\epsilon, \qquad (5.21)
\end{aligned}$$

where $c_2 = c_0 - c_1/\sqrt{\epsilon} > 0$, and provided $|\mathbf{r}| > r_0$. Now, (5.21) can be integrated with respect to time to give

$$E[\Gamma] \leq -c_2\epsilon t + E[\Gamma_0], \qquad (5.22)$$

as long as $E[1 - \Gamma^2] > \epsilon$, where $\Gamma_0 = \Gamma(0)$, and provided $|\mathbf{r}| > r_0$.

Because the initial positions $\mathbf{r}_p(0)$ and $\mathbf{r}_e(0)$ are assumed to be deterministic (even when u_e is stochastic), it follows that $|\mathbf{r}(0)|$ is deterministic. For $r_0 < |\mathbf{r}(0)|$, and using

$$|\mathbf{r}(t)| \geq |\mathbf{r}(0)| - (1+\nu)t, \qquad (5.23)$$

we can conclude that the interval $[0, T)$, where

$$T = \frac{|\mathbf{r}(0)| - r_0}{1+\nu} > 0, \qquad (5.24)$$

is an interval of time over which we can guarantee that $|\mathbf{r}| > r_0$ (regardless of the sample path of u_e).

From the form of (5.22), it is clear that by choosing c_2 sufficiently large, $E[\Gamma]$ can be driven to an arbitrary negative value at time T, but for the fact that (5.22) is only valid for $E[1-\Gamma^2] > \epsilon$. Indeed, for any $\eta > 0$ and

$$c_2 > \frac{1 + E[\Gamma_0]}{\epsilon T} + \eta, \tag{5.25}$$

by a contradiction argument, $E[1-\Gamma^2(t_1)] \leq \epsilon$ must hold for some $t_1 \in [0, T)$.

5.3.3 Statement of result

Analogously to [27], we define a notion of (finite-time) "accessibility" of the motion camouflage state for the stochastic setting:

Definition 5.3.1 Given the system (5.2), interpreted as SDEs driven by random processes u_p and u_e having (piecewise) continuous sample paths, we say that "motion camouflage is accessible in the mean in finite time" if for any $\epsilon > 0$ there exists a time t_1 such that $E[1-\Gamma^2(t_1)] \leq \epsilon$.

Proposition 5.3.2. *Consider the system (5.2), with control law (5.7), and* Γ *defined by (5.6), with the following hypotheses:*

(A1) $0 < \nu < 1$ *(and* ν *is constant),*

(A2) u_e *is a stochastic process with piecewise continuous sample paths and bounded first and second moments (i.e.* $\exists$ *constant* $0 < u_{max} < \infty$ *such that* $\forall t \geq 0$, $E[u_e^2] \leq u_{max}^2$ *and* $|E[u_e]| \leq u_{max}$*),*

(A3) u_e *is of a form such that the matrix* $X = [x_e \;\; y_e]$ *evolves on* $SO(2)$*,*

(A4) $E[1-\Gamma_0^2] > 0$, *where* $\Gamma_0 = \Gamma(0)$, *and*

(A5) $|\mathbf{r}(0)| > 0$.

Then motion camouflage is accessible in the mean in finite time using high-gain feedback (i.e., by choosing $\mu_p > 0$ sufficiently large.)

Proof. The proof is along the lines of the proof of Proposition 3.3 in [27] for the deterministic system.

Without loss of generality, we may assume that $E[1 - \Gamma_0^2] > \epsilon$.

Choose $r_0 > 0$ such that $r_0 < |\mathbf{r}(0)|$. Choose $c_2 > 0$ sufficiently large so as to satisfy

$$c_2 > \left(\frac{1+\nu}{|\mathbf{r}(0)| - r_0} \right) \left(\frac{1 + E[\Gamma_0]}{\epsilon} \right) + \eta, \tag{5.26}$$

where $\eta > 0$, and choose c_0 as

$$c_0 = c_2 + \frac{1}{\sqrt{\epsilon}} \left(\frac{\nu^2(1+\nu)}{(1-\nu)^2} u_{max} \right). \tag{5.27}$$

Then defining μ_p according to (5.14) ensures that $E[1 - \Gamma^2(t_1)] \le \epsilon$ for some $t_1 \in [0, T)$, where T is given by (5.24). □

Remark 5.3.3 Observe that **Definition 5.3.1** does not distinguish between motion camouflage with decreasing baseline distance (i.e., $\Gamma = -1$) and motion camouflage with increasing baseline distance (i.e., $\Gamma = +1$). By contrast, the definition of finite-time accessibility of motion camouflage given in [27] deals only with decreasing baseline distance.

Remark 5.3.4 Assumption (A3) equates to ensuring that the associated vector equation evolves on a circle. This is discussed in the following section.

5.4 Admissible stochastic controls

In considering the possible families of stochastic processes that could serve as controls for the evader, we can only select such controls that will cause the matrix $X = [x_e \;\; y_e]$ to evolve on $SO(2)$, the special orthogonal group in two dimensions. For a stochastic u_e, (5.2) provides the stochastic differential equation

$$dX_t = X_t \hat{A} u_e dt, \tag{5.28}$$

where $\hat{A}$ is the skew-symmetric matrix defined by

$$\hat{A} = \begin{pmatrix} 0 & -\nu \\ \nu & 0 \end{pmatrix}. \tag{5.29}$$

Let $x_0 \in \mathbb{R}^2$ and define x_t by $x_t^T = x_0^T X_t$. Then we have

$$dx_t^T = x_t^T \hat{A} u_e dt \Longrightarrow dx_t = \hat{A}^T x_t u_e dt. \tag{5.30}$$

It can be shown (see, e.g., [5]) that X_t evolves on $SO(2)$ if and only if (5.30) evolves on a circle.

Proposition 5.4.1. *Let the stochastic evader control u_e be defined as follows:*

$$\begin{aligned} dz &= \alpha(z,t)dt + \beta(z,t)dW, \;\; z(0) = z_0, \\ u_e &= z, \end{aligned} \tag{5.31}$$

where z is a scalar stochastic process, $W(\cdot)$ is standard Brownian motion, $\alpha : \mathbb{R} \times [0,\infty) \to \mathbb{R}$ and $\beta : \mathbb{R} \times [0,\infty) \to \mathbb{R}$ (and suitable technical hypotheses are met). Then (5.28) evolves on $SO(2)$.

Proof. Grouping (5.30) and (5.31) and dropping the time subscripts for simplicity, we have

$$d\begin{bmatrix} x \\ z \end{bmatrix} = \begin{bmatrix} \hat{A}^T xz \\ \alpha(z) \end{bmatrix} dt + \begin{bmatrix} 0 \\ \beta(z) \end{bmatrix} dW. \tag{5.32}$$

Let

$$y = \begin{bmatrix} x \\ z \end{bmatrix}, \quad f(y) = \begin{bmatrix} \hat{A}^T xz \\ \alpha(z) \end{bmatrix}, \text{ and } g(y) = \begin{bmatrix} 0 \\ \beta(z) \end{bmatrix}. \tag{5.33}$$

Then (5.32) becomes

$$dy = f(y)dt + g(y)dW. \tag{5.34}$$

Letting $\psi(y) = x^T x$ and using Itô's rule for differentiating, we have

$$\begin{aligned} d(x^T x) &= d\psi(y) \\ &= \left[\frac{\partial \psi}{\partial t} + \frac{\partial \psi}{\partial y} \cdot f + \frac{1}{2}\mathrm{tr}\left(\frac{\partial^2 \psi}{\partial y \partial y^T} g g^T\right)\right] dt + \left(\frac{\partial \psi}{\partial y} \cdot g\right) dW \\ &= \begin{bmatrix} 2x \\ 0 \end{bmatrix} \cdot \begin{bmatrix} \hat{A}^T xz \\ \alpha(z) \end{bmatrix} dt + \frac{1}{2}\mathrm{tr}\left(\begin{bmatrix} 2 & 0 \\ 0 & 0 \end{bmatrix} \begin{bmatrix} 0 & 0 \\ 0 & \beta^2(z) \end{bmatrix}\right) dt \\ &\quad + \begin{bmatrix} 2x \\ 0 \end{bmatrix} \cdot \begin{bmatrix} 0 \\ \beta(z) \end{bmatrix} dW \\ &= 2x^T \hat{A}^T xz dt \\ &= 0, \end{aligned} \tag{5.35}$$

where the last step follows from the skew-symmetry of $\hat{A}^T$. Equation (5.35) implies that $x^T x = x_0^T x_0$ for all times $t \geq 0$ (i.e., (5.30) evolves on a circle), and therefore (5.28) evolves on $SO(2)$. $\square$

Remark 5.4.2 A similar result can be proved for counter-driven stochastic controls of the form

$$\begin{aligned} dz &= \alpha(z,t)dt + \sum_{i=1}^{m} \beta_i(z,t)dN_i, \quad z(0) = z_0, \\ u_e &= z, \end{aligned} \tag{5.36}$$

where N_i, $i = 1, 2, ..., m$ are Poisson counters with rates λ_i. (Follow the previous proof and use Itô's rule for jump processes.)

We note the following specific possibilities for stochastic controls:

(a) Brownian motion. Letting $\alpha(z,t) = 0$ and $\beta(z,t) = 1$ in (5.31) results in

$$dz = dW, \quad z(0) = z_0, \quad u_e = z, \tag{5.37}$$

i.e., $u_e(\cdot) = W(\cdot)$. In this case, the steering control would be governed by sample paths of a Brownian motion process. However, this control does not satisfy assumption (A2) of **Proposition 5.3.2** and is therefore not admissible.

(b) Brownian motion with viscous damping. Let $\alpha(z,t) = -\delta z$ and $\beta(z,t) = \sigma$ for constants $\delta > 0$ and $\sigma \in \mathbb{R}$. Then (5.31) becomes

$$dz = -\delta z dt + \sigma dW, \quad z(0) = z_0, \quad u_e = z, \tag{5.38}$$

which is better known as the *Langevin equation*. This control satisfies both (A2) and (A3) and is therefore admissible.

(c) "Run-and-tumble" (bacterial chemotaxis). In (5.36) let $\alpha(z,t) = 0$ and define the Poisson counter rates and coefficients as follows:

$$
\begin{aligned}
\beta_1(z,t) &= \frac{1}{2}z(z-1), \\
\beta_2(z,t) &= -\frac{1}{2}z(z+1), \\
\beta_3(z,t) &= (z^2-1), \\
\beta_4(z,t) &= -(z^2-1), \\
\lambda_1 &= \lambda_2 = \lambda_H, \\
\lambda_3 &= \lambda_4 = \lambda_L.
\end{aligned} \tag{5.39}
$$

Then (5.36) becomes

$$
\begin{aligned}
dz &= \frac{1}{2}z(z-1)dN_1 - \frac{1}{2}z(z+1)dN_2 + (z^2-1)dN_3 - (z^2-1)dN_4, \\
z(0) &= z_0 \in \{-1, 0, 1\}, \\
u_e &= z,
\end{aligned} \tag{5.40}
$$

and u_e is a continuous time, finite state (CTFS) process taking values in the set $\{-1, 0, 1\}$. Hence u_e satisfies (A2) and (A3) and is admissible as a stochastic control for the evader. We can approximate bacterial chemotaxis, the "run-and-tumble" control used by certain types of bacteria to move towards food sources, by choosing $\lambda_H >> \lambda_L$. Under this open-loop control, the evader will move primarily in straight paths ($u_e = 0$), making occasional random short-duration turns whenever Poisson counter N_3 or N_4 fires. This could also be implemented as a closed-loop control by feeding state information (e.g. range to the pursuer) back to λ_H and λ_L.

Remark 5.4.3 Note that the control $u_e dt = dW$ (i.e., $u_e \approx$ "white noise") is not a permissible control for the evader, since a calculation similar to (5.35) yields

$$d(x^T x) = x^T \hat{A}\hat{A}^T x dt = \nu^2 x^T \begin{bmatrix} 0 & 1 \\ 1 & 0 \end{bmatrix} x dt, \tag{5.41}$$

which is not necessarily zero, and therefore $X = [x_e \;\; y_e]$ will not evolve on $SO(2)$.

Remark 5.4.4 Under assumptions (A2) and (A3) referred to above (we are specifically interested in u_e processes such as (5.38) and (5.40)), it follows that for each path of u_e, the random differential equations (5.2) with control (5.7), have well-defined local pathwise solutions away from collisional states $\mathbf{r}_p = \mathbf{r}_e$. Applying Itô's rule to the ensemble process (5.2),(5.7) gives us (5.8).

5.5 Simulation Results

The following simulation results demonstrate the effectiveness of the pursuit law (5.7) against an evader using a "run-and-tumble" steering control as described previously, confirming the analytical results presented in section 5.3. Each simulation is based on the same parameters but differs by the ratio of the Poisson counter rates λ_L and λ_H. (Note also that each simulation was run for approximately 250 time units in steps of .1 time units, and the ratio of evader's speed to pursuer's speed was fixed at $\nu = .9$.) Figure 5.1a shows the pursuer and evader trajectories for a simulation in which the ratio between the counter rates is very large ($\lambda_H = 40\lambda_L$) and therefore the evader makes fewer maneuvers. (The lighter lines connecting the pursuer and evader at regular time intervals indicate the evolution of the baseline vector $\mathbf{r}$. If the system (5.2) is in a state of motion camouflage, these lines will be parallel.) Figures 5.1b and 5.1c show the complete and transient behavior, respectively, of the cost function $\Gamma(t)$ given by (5.6). (Each graph shows the results for both a smaller pursuit feedback gain μ_p as well as the results for a gain three times larger.) Note that the cost function is driven close to the desired value of -1, with intermittent spikes which correspond to momentary deviations away from the motion camouflage state when the evader executes an abrupt turn.

The bottom row of 5.1 depicts results for a much smaller ratio of λ_H to λ_L (i.e. higher probability of evader maneuvering). As demonstrated in figure 5.1d, increased evader maneuvering induces more frequent steering requirements for the pursuer, indicating that, while such an evasive control may not prevent capture, it may introduce a high steering/attention cost on the pursuer. Note from figure 5.1e that the highly erratic evader steering control results in frequent deviations from motion camouflage. Figure 5.1f displays the initial transient behavior of $\Gamma(t)$. In the case of the larger value of μ_p, the initial behavior of $\Gamma(t)$ is similar to that of figure 5.1f since the pursuer is able to maneuver close to the motion camouflage state prior to the evader's first course change. For the smaller value of μ_p, the first evader maneuver occurs while $\Gamma(t)$ is still much larger than -1, thereby delaying convergence to the motion camouflage state.

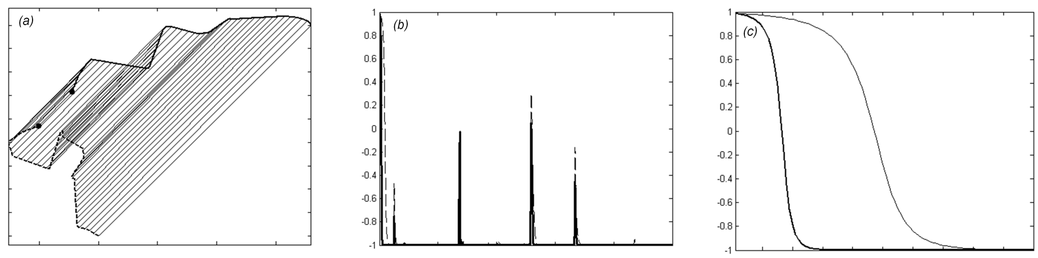

(a) (b) (c)

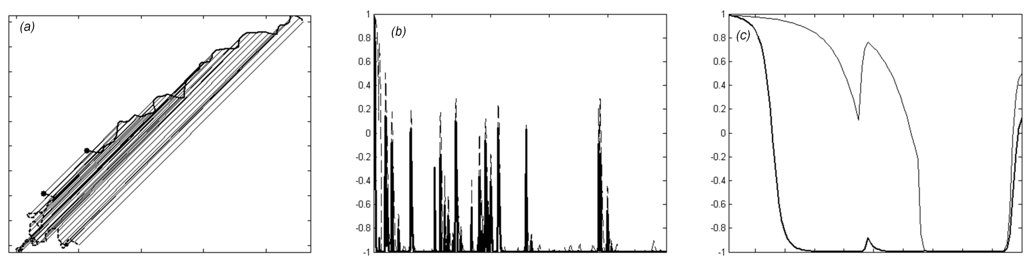

(d) (e) (f)

Figure 5.1: These figures depict the results of two motion camouflage pursuit scenarios in which the evader uses the counter-driven "run-and-tumble" steering control and the pursuer uses the feedback law given by (5.7). The top row of figures correspond to a large ratio between counter rates ($\lambda_H = 40\lambda_L$) for the stochastic evader steering process, while the bottom row of figures correspond to a much smaller ratio ($\lambda_H = 6.67\lambda_L$). The first figure in each row depicts the trajectories of the pursuer (solid dark line) and the evader (dashed dark line); the other figures depict respectively the long-term and transient behavior of the cost function $\Gamma(t)$. (The lighter dashed lines correspond to a small value of μ_p while the darker solid lines correspond to a value of μ_p which is three times larger.)

Chapter 6

A deterministic evasion strategy to counter motion camouflage pursuit

6.1 Introduction

In chapter 5, we introduced the motion camouflage pursuit strategy and associated pursuit law (5.7), and proved a result concerning finite-time accessibility of the motion camouflage state even in the case where the evader employs a stochastic steering process. Combined with the results of the deterministic analysis in [27], this analysis contributes to the evidence attesting to the effectiveness of the motion camouflage pursuit law for executing the desired MC pursuit strategy.

In this chapter, we return to the deterministic setting and consider the question of whether the evader can "defeat" the motion camouflage pursuit law by employing an appropriate feedback control. Rather than focusing on accessibility of the motion camouflage state for a high-gain pursuer (as in chapter 5), here we assume that the pursuer's control gain is finite, and for a family of evader feedback laws, we consider the existence of circling equilibria (which can be viewed as a "stand-off" condition and thus favorable to the evader). This chapter also lays the groundwork for a future game-theoretic study of pursuer-evader encounters which incorporate a payoff related to "visibility" of the pursuer.

We proceed by developing a shape variable formulation for motion camouflage and then deriving an evasion law (6.18) which aims to maximize a novel payoff function. (See section 6.4.) We then analyze the resultant closed-loop shape dynamics (the pursuer employing the motion camouflage pursuit law and the evader employing the evasion law (6.18)), first for the common speed case (section 6.5), and then for the more general case in which one of the agents possesses a speed advantage (section 6.6). We find that there exists a range of speed ratios and control gain ratios for which circling relative equilibria exist and are asymptotically stable (see **Propositions 6.6.1 and 6.6.4**), even in some cases where the pursuer has a speed advantage as well as a control gain advantage (see **Proposition 6.6.6**.)

6.2 Two-particle shape dynamics

As in section 5.2, we start with the pursuer-evader system dynamics presented in (5.1), but in a slight deviation[1] from the formulation in chapter 5, we choose to set $\nu_e \equiv 1$ and let $\nu_p = \bar{\nu} > 0$, so that $\bar{\nu}$ represents the ratio of the pursuer's speed to the evader's speed. (As discussed in section 5.2, this is equivalent to a scaling of

[1]In chapter 5, we found it important to match the notation from [27] in order to facilitate comparison of the results. Such a comparison is not required in this chapter, and notational clarity is enhanced in this context by referencing speeds and control gains in terms of the ratio of pursuer to evader. Therefore we have used $\bar{\nu}$, which is equivalent to $1/\nu$.

the time variable, and therefore we can proceed without loss of generality.) Then the pursuer-evader dynamics are given by

$$\begin{aligned} \dot{\mathbf{r}}_p &= \bar{\nu}\mathbf{x}_p & \dot{\mathbf{r}}_e &= \mathbf{x}_e \\ \dot{\mathbf{x}}_p &= \bar{\nu}\mathbf{y}_p u_p & \dot{\mathbf{x}}_e &= \mathbf{y}_e u_e \\ \dot{\mathbf{y}}_p &= -\bar{\nu}\mathbf{x}_p u_p & \dot{\mathbf{y}}_e &= -\mathbf{x}_e u_e, \end{aligned} \tag{6.1}$$

which hold for any $SE(2)$-invariant steering laws u_p and u_e.

While the analysis in chapter 5 was conducted exclusively in terms of the vector state variables (i.e. $\mathbf{r}_p, \mathbf{x}_p, \mathbf{y}_p$ and $\mathbf{r}_e, \mathbf{x}_e, \mathbf{y}_e$) in order to facilitate comparisons with previous work in [27], in the current chapter we find it helpful to work with the shape variable description. In a previous encounter with two-particle pursuit in section 3.2 of chapter 3, we have already demonstrated that the two-particle shape space can be parametrized without additional constraints in terms of κ_1, κ_2, and ρ, as defined in **Proposition 2.2.3** (with $\rho_1 = \rho_2 = \rho$). (Note that this result held for any $SE(2)$-invariant control u_i, not only for the CB pursuit law.) Though the original derivation of shape dynamics presented in section 2.2.4 was based on the unit speed assumption (i.e. $\nu_i = 1,\ i = 1, 2, \ldots, n$), it is not difficult to show that analogous calculations yield the following two-particle shape dynamics (again substituting the "p" and "e" notation for the numbered indices) corresponding to

(6.1):

$$\dot{\kappa}_p = -\bar{\nu} u_p + \frac{1}{\rho}\left[\bar{\nu}\sin(\kappa_p) + \sin(\kappa_e)\right],$$
$$\dot{\kappa}_e = -u_e + \frac{1}{\rho}\left[\bar{\nu}\sin(\kappa_p) + \sin(\kappa_e)\right],$$
$$\dot{\rho} = -\bar{\nu}\cos(\kappa_p) - \cos(\kappa_e), \tag{6.2}$$

subject only to $\rho > 0$.

It is of interest to relate the quantities $\bar{\nu}\sin(\kappa_p) + \sin(\kappa_e)$ and $-\bar{\nu}\cos(\kappa_p) - \cos(\kappa_e)$ back to the dynamics of the baseline vector $\mathbf{r} \triangleq \mathbf{r}_p - \mathbf{r}_e$. In particular, we note from (2.24) that

$$\cos(\kappa_p) = -\mathbf{x}_p \cdot \frac{\mathbf{r}}{|\mathbf{r}|}, \quad \sin(\kappa_p) = -\mathbf{y}_p \cdot \frac{\mathbf{r}}{|\mathbf{r}|},$$
$$\cos(\kappa_e) = \mathbf{x}_e \cdot \frac{\mathbf{r}}{|\mathbf{r}|}, \quad \sin(\kappa_e) = \mathbf{y}_e \cdot \frac{\mathbf{r}}{|\mathbf{r}|}, \tag{6.3}$$

and therefore

$$\bar{\nu}\sin(\kappa_p) + \sin(\kappa_e) = -\left(\bar{\nu}\mathbf{y}_p - \mathbf{y}_e\right) \cdot \frac{\mathbf{r}}{|\mathbf{r}|} = \left(\bar{\nu}\mathbf{x}_p - \mathbf{x}_e\right) \cdot \frac{\mathbf{r}}{|\mathbf{r}|}^{\perp} = \dot{\mathbf{r}} \cdot \frac{\mathbf{r}}{|\mathbf{r}|}^{\perp}, \tag{6.4}$$

and

$$-\bar{\nu}\cos(\kappa_p) - \cos(\kappa_e) = \left(\bar{\nu}\mathbf{x}_p - \mathbf{x}_e\right) \cdot \frac{\mathbf{r}}{|\mathbf{r}|} = \dot{\mathbf{r}} \cdot \frac{\mathbf{r}}{|\mathbf{r}|}. \tag{6.5}$$

Thus, defining

$$\omega \triangleq \bar{\nu}\sin(\kappa_p) + \sin(\kappa_e),$$
$$\eta \triangleq -\bar{\nu}\cos(\kappa_p) - \cos(\kappa_e), \tag{6.6}$$

we have the decomposition

$$\dot{\mathbf{r}} = \eta\frac{\mathbf{r}}{|\mathbf{r}|} + \omega\frac{\mathbf{r}}{|\mathbf{r}|}^{\perp}, \tag{6.7}$$

and our shape dynamics (6.2) can be expressed as

$$\begin{aligned}
\dot{\kappa}_p &= -\bar{\nu} u_p + \frac{\omega}{\rho}, \\
\dot{\kappa}_e &= -u_e + \frac{\omega}{\rho}, \\
\dot{\rho} &= \eta.
\end{aligned} \tag{6.8}$$

6.3 Motion camouflage in terms of shape variables

To describe motion camouflage in terms of the shape variables, we first recall from (5.6) the motion camouflage cost function given by

$$\Gamma = \frac{\mathbf{r}}{|\mathbf{r}|} \cdot \frac{\dot{\mathbf{r}}}{|\dot{\mathbf{r}}|}, \tag{6.9}$$

where $\Gamma = -1$ corresponds to attainment of the motion camouflage strategy. Then from (6.6) and (6.7), we have

$$|\dot{\mathbf{r}}| = \sqrt{\eta^2 + \omega^2} = \sqrt{\bar{\nu}^2 + 2\bar{\nu}\cos(\kappa_p - \kappa_e) + 1}, \tag{6.10}$$

and therefore

$$\Gamma = \frac{1}{|\dot{\mathbf{r}}|}\left(\dot{\mathbf{r}} \cdot \frac{\mathbf{r}}{|\mathbf{r}|}\right) = \frac{\eta}{\sqrt{\eta^2 + \omega^2}}. \tag{6.11}$$

Since Γ is the dot product of unit vectors, it takes values in the interval $[-1, 1]$, with

$$\Gamma = -1 \iff \omega = 0 \;\text{ and } \eta < 0. \tag{6.12}$$

The motion camouflage pursuit law for the pursuer, defined in (5.7), can then be expressed in terms of the shape variables by

$$u_p = u_{MC} \triangleq \mu_p \omega = \mu_p \left[\bar{\nu}\sin(\kappa_p) + \sin(\kappa_e)\right], \tag{6.13}$$

where $\mu_p > 0$ is a control gain.

6.4 An evasion strategy designed to counter MC pursuit

We are interested in strategies that an evader may employ to counter the motion camouflage pursuit law. Initially one may conjecture that the evader should attempt to maximize the motion camouflage cost function (6.11), i.e., drive Γ to $+1$. This strategy, best described as "motion camouflage evasion", corresponds to $\omega = 0$ (i.e. no rotation of the baseline vector) and $\eta > 0$ (i.e. increasing separation). While such a strategy may prove successful as a stealthy evasion strategy against pursuers which rely on relative motion for detection and tracking, numerical studies suggest that it fares poorly against the motion camouflage pursuit law, typically resulting in a tail-chase (and eventual capture for a slower evader). An evader may alternatively attempt to drive Γ to zero, corresponding to pure rotation of the baseline vector and a fixed pursuer-evader separation, but this strategy is not ideal because it does not even attempt to increase the distance from the pursuer.

We hypothesize that the evader should attempt to maximize the increase of pursuer-evader separation (i.e. drive η positive) while maximizing rotation of the baseline vector (i.e. maximizing the absolute value of ω). Maximizing the rotation of the baseline vector serves to both thwart the stealth aspect of the motion camouflage pursuit strategy (i.e. it increases the "visibility" of the pursuer from the perspective of the evader), and it may force additional costly steering for the pursuer. Such an evasion strategy can be defined as maximization of a payoff function of the form

$$L_\gamma = \eta + \gamma\omega^2 = -\Big(\bar{\nu}\cos(\kappa_p) + \cos(\kappa_e)\Big) + \gamma\Big(\bar{\nu}\sin(\kappa_p) + \sin(\kappa_e)\Big)^2, \qquad (6.14)$$

where $\gamma > 0$ determines the relative priority of opening distance and maximizing baseline vector rotation. We observe that L_γ has a global minimum value of $-(\bar{\nu}+1)$ at the point $\kappa_p = \kappa_e = 0$, i.e. a collision course. The gradient of L_γ is given by

$$\nabla L_\gamma = \left(\frac{\partial L_\gamma}{\partial \kappa_p}, \, \frac{\partial L_\gamma}{\partial \kappa_e} \right) = \Big(\bar{\nu} \left[\sin(\kappa_p) + 2\gamma\omega \cos(\kappa_p) \right], \, \sin(\kappa_e) + 2\gamma\omega \cos(\kappa_e) \Big), \tag{6.15}$$

by which one can show that if $\gamma \geq 1/2(\bar{\nu}+1)$, then L_γ reaches its maximum value of $\frac{1}{4\gamma}\Big(1 + 4\gamma^2(\bar{\nu}+1)^2\Big)$ at $\kappa_p = \kappa_e = \pm \cos^{-1}\Big(-\frac{1}{2\gamma(\bar{\nu}+1)}\Big)$. This corresponds to expanding spiral trajectories in the physical space if κ_p and κ_e are fixed at these values. If $\gamma < 1/2(\bar{\nu}+1)$, then the relative priority of escape (i.e. opening distance) over baseline vector rotation is high enough that the payoff L_γ is maximized by $\kappa_p = \kappa_e = \pi$, i.e. full retreat.

For simplicity, in this work we will choose $\gamma = 1$ and proceed with the payoff function

$$L_1 = \eta + \omega^2. \tag{6.16}$$

We consider the behavior of this payoff function for arbitrary $SE(2)$-invariant steering controls u_p and u_e, taking the derivative of (6.16) along trajectories of (6.8) to obtain

$$
\begin{aligned}
\dot{L}_1 &= \dot{\eta} + 2\omega\dot{\omega} \\
&= \bar{\nu}\dot{\kappa}_p \sin(\kappa_p) + \dot{\kappa}_e \sin(\kappa_e) + 2\omega \left[\bar{\nu}\dot{\kappa}_p \cos(\kappa_p) + \dot{\kappa}_e \cos(\kappa_e)\right] \\
&= \bar{\nu}\dot{\kappa}_p \left[\sin(\kappa_p) + 2\omega \cos(\kappa_p)\right] + \dot{\kappa}_e \left[\sin(\kappa_e) + 2\omega \cos(\kappa_e)\right] \\
&= \bar{\nu}\left(-\bar{\nu}u_p + \frac{\omega}{\rho}\right)\left[\sin(\kappa_p) + 2\omega \cos(\kappa_p)\right] + \left(-u_e + \frac{\omega}{\rho}\right)\left[\sin(\kappa_e) + 2\omega \cos(\kappa_e)\right] \\
&= -\bar{\nu}^2 u_p \left[\sin(\kappa_p) + 2\omega \cos(\kappa_p)\right] - u_e \left[\sin(\kappa_e) + 2\omega \cos(\kappa_e)\right] \\
&\qquad + \frac{\omega}{\rho}\left[\bar{\nu}\sin(\kappa_p) + 2\bar{\nu}\omega \cos(\kappa_p) + \sin(\kappa_e) + 2\omega \cos(\kappa_e)\right] \\
&= -\bar{\nu}^2 u_p \left[\sin(\kappa_p) + 2\omega \cos(\kappa_p)\right] - u_e \left[\sin(\kappa_e) + 2\omega \cos(\kappa_e)\right] + \frac{\omega}{\rho}\left(\omega - 2\omega\eta\right) \\
&= -\bar{\nu}^2 u_p \left[\sin(\kappa_p) + 2\omega \cos(\kappa_p)\right] - u_e \left[\sin(\kappa_e) + 2\omega \cos(\kappa_e)\right] + \frac{\omega^2}{\rho}\left(1 - 2\eta\right).
\end{aligned}
\tag{6.17}
$$

A game-theoretic study of pursuer-evader encounters with a pay-off function of the form L_γ is the subject of future research. In the current setting, we assume that the pursuer's steering is governed by a pre-determined control law (such as the motion camouflage pursuit law), and we choose u_e to maximize (6.17). From the form of (6.17), it seems apparent that no straightforward control law can be chosen to assure $\dot{L}_1 > 0$ (particularly because the $1/\rho$ factor makes the third term unbounded), but we proceed by choosing the relatively simple evasion law

$$
u_e = u_{AMC} = -\mu_e\Big(\sin(\kappa_e) + 2\omega\cos(\kappa_e)\Big), \tag{6.18}
$$

where $\mu_e > 0$ is a control gain. (We dub this the *Anti-MC Evasion Law*, as it is designed to counter the Motion Camouflage Pursuit Law (6.13).) Then substitution of (6.18) into (6.17) yields

$$\dot{L}_1 = -\bar{\nu}^2 u_p \left[\sin(\kappa_p) + 2\omega\cos(\kappa_p)\right] + \mu_e \left[\sin(\kappa_e) + 2\omega\cos(\kappa_e)\right]^2 + \frac{\omega^2}{\rho}\left(1 - 2\eta\right), \tag{6.19}$$

and the evader can employ high gain in an effort to increase $\dot{L}_1$.

Until now we have left the pursuer's control law unspecified. As we are particularly interested in the case in which the pursuer employs the Motion Camouflage Pursuit Law and the evader employs the Anti-MC Evasion Law, we substitute (6.13) and (6.18) into (6.8) to obtain the closed-loop pursuer-evader dynamics

$$\boxed{\begin{aligned} \dot{\kappa}_p &= \omega\left(-\mu_p\bar{\nu} + \frac{1}{\rho}\right), \\ \dot{\kappa}_e &= \mu_e \sin(\kappa_e) + \omega\left(2\mu_e\cos(\kappa_e) + \frac{1}{\rho}\right), \\ \dot{\rho} &= \eta. \end{aligned}} \tag{6.20}$$

While it is difficult to make conclusive statements regarding the evolution of the pay-off function L_1 under (6.20), numerical studies illustrated by figure 6.1 suggest the existence of interesting steady-state solutions such as rectilinear and circling relative equilibria. The rest of this chapter will be spent in characterizing existence conditions and stability properties for these relative equilibria, first for the common speed case $\bar{\nu} = 1$ and then for the general case.

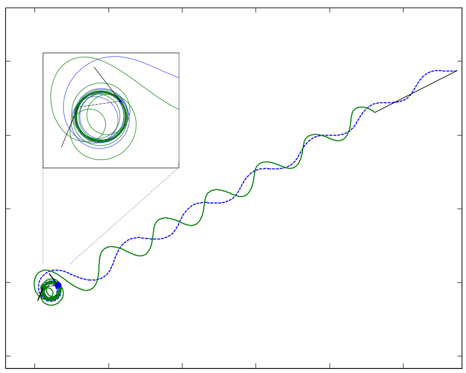

(a) Trajectories (pursuer is dashed line)

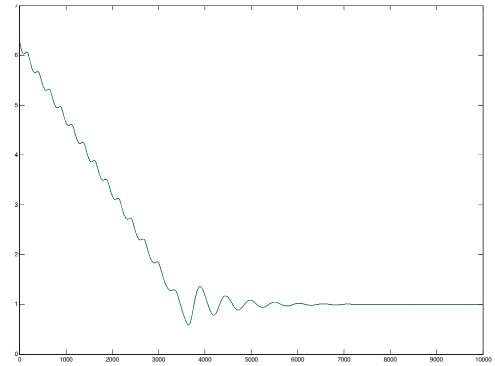

(b) Pursuer-evader separation (ρ)

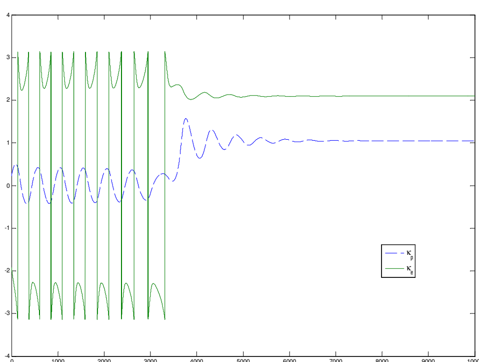

(c) κ_e (solid) and κ_p (dashed)

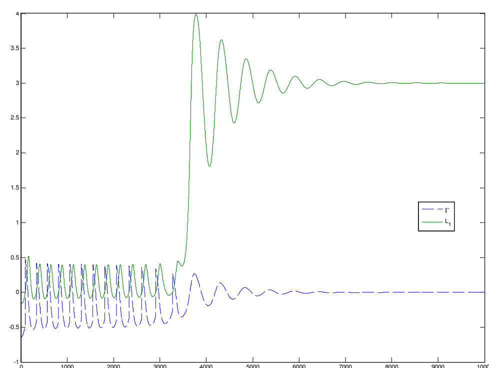

(d) Evader pay-off function L_1 (solid) and pursuer cost function Γ (dashed)

Figure 6.1: These graphs depict an engagement in which the pursuer employs the motion camouflage pursuit law (6.13) and the evader employs the anti-MC evasion law (6.18), resulting in an apparent circling equilibrium. Control gains are related by $\mu_p/\mu_e = .5$, and the speed ratio is $\bar{\nu} = 1$.

6.5 Relative equilibria for the common speed case $\bar{\nu} = 1$

6.5.1 Existence conditions for common speed relative equilibria

For $\bar{\nu} = 1$, a necessary condition for existence of relative equilibria is $\eta = 0$, or equivalently

$$\cos(\kappa_p) = -\cos(\kappa_e), \tag{6.21}$$

for which we require either $\kappa_p = \pi + \kappa_e$ or $\kappa_p = \pi - \kappa_e$. We'll begin by considering the first case.

If $\kappa_p = \pi + \kappa_e$, then by substitution into (6.6) we have

$$\omega = \sin(\kappa_p) + \sin(\kappa_e) = \sin(\pi + \kappa_e) + \sin(\kappa_e) = 0, \tag{6.22}$$

and our pursuer-evader shape dynamics (6.20) become

$$\begin{aligned}
\dot{\kappa}_p &= 0, \\
\dot{\kappa}_e &= \mu_e \sin(\kappa_e), \\
\dot{\rho} &= 0.
\end{aligned} \tag{6.23}$$

Therefore relative equilibria exist for the $\kappa_p = \pi + \kappa_e$ case if and only if $\sin(\kappa_e) = 0$, i.e. if and only if $(\kappa_p, \kappa_e) = (0, \pi)$ or $(\kappa_p, \kappa_e) = (\pi, 0)$. These rectilinear equilibria correspond to a "tail-chase" configuration with either the evader or the pursuer in the lead, and we refer to them respectively as *Type A rectilinear equilibria* and *Type B rectilinear equilibria*.

Turning to the second case, we observe that for $\kappa_p = \pi - \kappa_e$, substitution into (6.6) yields

$$\omega = \sin(\kappa_p) + \sin(\kappa_e) = \sin(\pi - \kappa_e) + \sin(\kappa_e) = 2\sin(\kappa_e), \tag{6.24}$$

and substituting into the $\dot{\kappa}_p$ equation from (6.20), we have

$$\begin{aligned} \dot{\kappa}_p &= \omega\left(-\mu_p + \frac{1}{\rho}\right) \\ &= 2\sin(\kappa_e)\left(-\mu_p + \frac{1}{\rho}\right). \end{aligned} \tag{6.25}$$

Note that if $\sin(\kappa_e) = 0$, then $\sin(\kappa_p) = \sin(\pi) = 0$ and we have the rectilinear equilibria previously analyzed. Therefore we assume $\sin(\kappa_e) \neq 0$, and hence it is a necessary condition for existence of relative equilibria (for this case) that

$$\rho = \frac{1}{\mu_p}. \tag{6.26}$$

Then substituting (6.24) and (6.26) into the $\dot{\kappa}_e$ equation from (6.20), we have

$$\begin{aligned} \dot{\kappa}_e &= \mu_e \sin(\kappa_e) + \omega\left(2\mu_e\cos(\kappa_e) + \frac{1}{\rho}\right) \\ &= \mu_e \sin(\kappa_e) + 2\sin(\kappa_e)\Big(2\mu_e\cos(\kappa_e) + \mu_p\Big) \\ &= \mu_e \sin(\kappa_e)\left(1 + 4\cos(\kappa_e) + 2\frac{\mu_p}{\mu_e}\right). \end{aligned} \tag{6.27}$$

Denoting

$$\bar{\mu} \triangleq \frac{\mu_p}{\mu_e}, \tag{6.28}$$

we observe that if a relative equilibrium exists, we must have

$$1 + 4\cos(\kappa_e) + 2\bar{\mu} = 0,$$

i.e.

$$\cos(\kappa_e) = -\frac{1}{4}(2\bar{\mu} + 1). \tag{6.29}$$

Since $\cos(\kappa_e)$ must take values in $[-1, 1]$,we note that (6.29) is only valid for values of $\bar{\mu}$ which satisfy

$$-1 \leq -\frac{1}{4}(2\bar{\mu} + 1) \leq 1. \tag{6.30}$$

The second inequality always holds since $\bar{\mu} > 0$, and the first inequality is satisfied if and only if $\bar{\mu} \leq \frac{3}{2}$. If equality holds (i.e. $\bar{\mu} = \frac{3}{2}$), then by (6.29) we have $\cos(\kappa_e) = -1$, which corresponds to the case $(\kappa_p, \kappa_e) = (0, \pi)$, which is the Type A rectilinear equilibrium we have previously analyzed. Thus we have shown that if $\bar{\mu} < \frac{3}{2}$ then a relative equilibrium exists and is described by

$$\begin{aligned}
\kappa_e &= \cos^{-1}\left(\frac{-2\bar{\mu} - 1}{4}\right), \\
\kappa_p &= \pi - \kappa_e, \\
\rho &= \frac{1}{\mu_p}.
\end{aligned} \tag{6.31}$$

By calculations analogous to those in the proof of **Proposition 2.4.1**, one can show that at this relative equilibrium we have

$$\mathbf{r}_p + \frac{\rho}{2\sin(\kappa_p)}\mathbf{x}_p^\perp = \mathbf{r}_e + \frac{\rho}{2\sin(\kappa_e)}\mathbf{x}_e^\perp, \tag{6.32}$$

and that the point

$$\mathbf{r}_{cc} = \mathbf{r}_p + \frac{\rho}{2\sin(\kappa_p)}\mathbf{x}_p^\perp = \mathbf{r}_e + \frac{\rho}{2\sin(\kappa_e)}\mathbf{x}_e^\perp \tag{6.33}$$

is equidistant from $\mathbf{r}_p$ and $\mathbf{r}_e$. Therefore this relative equilibrium is in fact a circling equilibrium, with radius r_c of the circumcircle given by

$$\begin{aligned} r_c &= \frac{1}{2}\left|\frac{\rho}{\sin(\kappa_e)}\right| \\ &= \frac{1}{2\mu_p}\left(\frac{1}{\sqrt{1-\cos^2(\kappa_e)}}\right) \\ &= \frac{1}{2\mu_p}\left(\frac{1}{\sqrt{1-\left(\frac{-2\bar{\mu}-1}{4}\right)^2}}\right) \\ &= \frac{1}{2\mu_p}\left(\frac{4}{\sqrt{16-(4\bar{\mu}^2+4\bar{\mu}+1)}}\right) \\ &= \frac{2}{\mu_p\sqrt{-4\bar{\mu}^2-4\bar{\mu}+15}}. \end{aligned} \tag{6.34}$$

We summarize the existence conditions for common speed relative equilibria with the following proposition.

Proposition 6.5.1. *For the common speed case ($\bar{\nu} = 1$), the existence of relative equilibria (i.e. equilibria for (6.20)) can be characterized as follows:*

1. *Rectilinear relative equilibria always exist, characterized by the equilibrium values*

$$\begin{aligned} (\hat{\kappa}_p, \hat{\kappa}_e) &= (0, \pi) \quad \textit{(Type A), and} \\ (\hat{\kappa}_p, \hat{\kappa}_e) &= (\pi, 0) \quad \textit{(Type B)}, \end{aligned} \tag{6.35}$$

with the inter-particle distance $\hat{\rho}$ arbitrary.

2. *Circling relative equilibria exist if and only if $\bar{\mu} < 3/2$, where $\bar{\mu} \triangleq \frac{\mu_p}{\mu_e}$. If they*

exist, circling equilibria are characterized by the equilibrium values

$$\hat{\kappa}_e = \cos^{-1}\left(\frac{-2\bar{\mu}-1}{4}\right),$$

$$\hat{\kappa}_p = \pi - \hat{\kappa}_e,$$

$$\hat{\rho} = \frac{1}{\mu_p}. \tag{6.36}$$

Proof. Follows from the previous discussion. □

Remark 6.5.2 Note from (6.36) that $\hat{\kappa}_e = \cos^{-1}\left(\frac{-2\bar{\mu}-1}{4}\right)$ always has two solutions, corresponding to CCW and CW circling equilibria.

Remark 6.5.3 It is of interest that the circling equilibria described by (6.36) have prescribed equilibrium values for the inter-particle separation $\rho = \hat{\rho}$ (and hence for the radius of the circling orbit), even though both the pursuit law (6.13) and the evasion law (6.18) involve only angular quantities. This can be contrasted with the cyclic CB pursuit case of chapters 2 and 3, for which there existed a *continuum* of circling equilibria without any prescribed equilibrium values for the ρ_i separations.

6.5.2 Stability properties of common speed relative equilibria

By calculations detailed in appendix D, we demonstrate that linearization of the shape dynamics (6.20) about a point $x = (\hat{\kappa}_p \ \hat{\kappa}_e \ \hat{\rho})^T$ yields the Jacobian matrix

$$\left(\frac{\partial f}{\partial x}\right) = \begin{bmatrix} \bar{\nu}\cos(\hat{\kappa}_p)\left(-\mu_p\bar{\nu} + \frac{1}{\hat{\rho}}\right) & \cos(\hat{\kappa}_e)\left(-\mu_p\bar{\nu} + \frac{1}{\hat{\rho}}\right) & -\frac{\omega}{\hat{\rho}^2} \\ \bar{\nu}\cos(\hat{\kappa}_p)\left(2\mu_e\cos(\hat{\kappa}_e) + \frac{1}{\hat{\rho}}\right) & \frac{\partial f_2}{\partial \kappa_e} & -\frac{\omega}{\hat{\rho}^2} \\ \bar{\nu}\sin(\hat{\kappa}_p) & \sin(\hat{\kappa}_e) & 0 \end{bmatrix}, \qquad (6.37)$$

where $\frac{\partial f_2}{\partial \kappa_e} = \mu_e\Big(\cos(\hat{\kappa}_e) + 2\cos^2(\hat{\kappa}_e) - 2\omega\sin(\hat{\kappa}_e)\Big) + \frac{\cos(\hat{\kappa}_e)}{\hat{\rho}}$ and $\omega = \bar{\nu}\sin(\hat{\kappa}_p) + \sin(\hat{\kappa}_e)$. Note that (6.37) represents the general case for which $\bar{\nu}$ is not necessarily 1. We now substitute $\bar{\nu} = 1$ and evaluate (6.37) at the relative equilibria of **Proposition 6.5.1**.

At a Type A rectilinear equilibrium, we have $(\hat{\kappa}_p, \hat{\kappa}_e) = (0, \pi)$ (and hence $\omega = 0$), and therefore substitution into the common speed version of (6.37) yields

$$\left(\frac{\partial f}{\partial x}\right)_A = \begin{bmatrix} -\mu_p + \frac{1}{\hat{\rho}} & -\left(-\mu_p + \frac{1}{\hat{\rho}}\right) & 0 \\ -2\mu_e + \frac{1}{\hat{\rho}} & \mu_e - \frac{1}{\hat{\rho}} & 0 \\ 0 & 0 & 0 \end{bmatrix}, \qquad (6.38)$$

where $\hat{\rho}$ is arbitrary. There is clearly one zero eigenvalue and two (possibly) non-zero eigenvalues associated with the two-by-two matrix in the upper left, which we will denote as A. We can use the familiar formula for the characteristic polynomial of a two-by-two matrix to obtain

$$\begin{aligned}P_A(\lambda) &= \lambda^2 - (\mu_e - \mu_p)\lambda + \left[\left(-\mu_p + \frac{1}{\hat{\rho}}\right)\left(\mu_e - \frac{1}{\hat{\rho}}\right) + \left(-\mu_p + \frac{1}{\hat{\rho}}\right)\left(-2\mu_e + \frac{1}{\hat{\rho}}\right)\right] \\ &= \lambda^2 - (\mu_e - \mu_p)\lambda - \mu_e\left(-\mu_p + \frac{1}{\hat{\rho}}\right), \qquad (6.39)\end{aligned}$$

and thus we have

$$\lambda = \frac{1}{2}\left\{\mu_e - \mu_p \pm \sqrt{(\mu_e - \mu_p)^2 + 4\mu_e\left(-\mu_p + \frac{1}{\hat{\rho}}\right)}\right\}. \qquad (6.40)$$

Observe that if $\mu_e > \mu_p$ (i.e. $\bar{\mu} < 1$) or if $-\mu_p + \frac{1}{\hat{\rho}} > 0$ (i.e. $\hat{\rho} < 1/\mu_p$) then at least one of the eigenvalues must have positive real part and the corresponding equilibrium is unstable. Numerical studies suggest that there also exists a range of $\bar{\mu}$ and $\hat{\rho}$ values for which the Type A rectilinear equilibria are asymptotically stable, and an analytical study of the stability properties is the subject of ongoing work.

To evaluate Type B rectilinear equilibria, we substitute $(\hat{\kappa}_p, \hat{\kappa}_e) = (\pi, 0)$ into the common speed version of (6.37) to obtain

$$\left(\frac{\partial f}{\partial x}\right)_B = \begin{bmatrix} -\left(-\mu_p + \frac{1}{\hat{\rho}}\right) & -\mu_p + \frac{1}{\hat{\rho}} & 0 \\ -\left(2\mu_e + \frac{1}{\hat{\rho}}\right) & 3\mu_e + \frac{1}{\hat{\rho}} & 0 \\ 0 & 0 & 0 \end{bmatrix}, \qquad (6.41)$$

where $\hat{\rho}$ is arbitrary. As before, there is one zero eigenvalue, and the characteristic polynomial for the two-by-two matrix in the upper left (which we designate as B) is given by

$$\begin{aligned}P_B(\lambda) &= \lambda^2 - (3\mu_e + \mu_p)\lambda + \left[-\left(-\mu_p + \frac{1}{\hat{\rho}}\right)\left(3\mu_e + \frac{1}{\hat{\rho}}\right) + \left(-\mu_p + \frac{1}{\hat{\rho}}\right)\left(2\mu_e + \frac{1}{\hat{\rho}}\right)\right] \\ &= \lambda^2 - (3\mu_e + \mu_p)\lambda - \mu_e\left(-\mu_p + \frac{1}{\hat{\rho}}\right). \qquad (6.42)\end{aligned}$$

Thus the non-zero eigenvalues of $\left(\frac{\partial f}{\partial x}\right)_B$ are given by

$$\lambda = \frac{1}{2}\left\{3\mu_e + \mu_p \pm \sqrt{(3\mu_e + \mu_p)^2 + 4\mu_e\left(-\mu_p + \frac{1}{\hat{\rho}}\right)}\right\}, \tag{6.43}$$

and since at least one of these eigenvalues must always be strictly positive, we conclude that Type B rectilinear equilibria are always unstable.

Finally, we evaluate the stability properties of our circling equilibria by first substituting $\hat{\kappa}_p = \pi - \hat{\kappa}_e$ and $\hat{\rho} = \frac{1}{\mu_p}$ into the common speed version of (6.37) to obtain

$$\left(\frac{\partial f}{\partial x}\right)_{circ} = \begin{bmatrix} 0 & 0 & -2\mu_p^2 \sin(\hat{\kappa}_e) \\ -\cos(\hat{\kappa}_e)\Big(2\mu_e \cos(\hat{\kappa}_e) + \mu_p\Big) & \frac{\partial f_2}{\partial \kappa_e} & -2\mu_p^2 \sin(\hat{\kappa}_e) \\ \sin(\hat{\kappa}_e) & \sin(\hat{\kappa}_e) & 0 \end{bmatrix}, \tag{6.44}$$

where $\hat{\kappa}_e$ is given by (6.36) and

$$\begin{aligned}
\frac{\partial f_2}{\partial \kappa_e} &= \mu_e\Big(\cos(\hat{\kappa}_e) + 2\cos^2(\hat{\kappa}_e) - 2\big(\sin(\pi - \hat{\kappa}_e) + \sin(\hat{\kappa}_e)\big)\sin(\hat{\kappa}_e)\Big) + \frac{\cos(\hat{\kappa}_e)}{\hat{\rho}} \\
&= \mu_e\Big(\cos(\hat{\kappa}_e) + 2\cos^2(\hat{\kappa}_e) - 4\sin^2(\hat{\kappa}_e)\Big) + \mu_p \cos(\hat{\kappa}_e) \\
&= 6\mu_e \cos^2(\hat{\kappa}_e) + (\mu_e + \mu_p)\cos(\hat{\kappa}_e) - 4\mu_e
\end{aligned} \tag{6.45}$$

The characteristic polynomial is defined by

$$P_{circ}(\lambda) = \det \begin{bmatrix} \lambda & 0 & 2\mu_p^2 \sin(\hat{\kappa}_e) \\ \cos(\hat{\kappa}_e)\left(2\mu_e \cos(\hat{\kappa}_e) + \mu_p\right) & \lambda - \frac{\partial f_2}{\partial \kappa_e} & 2\mu_p^2 \sin(\hat{\kappa}_e) \\ -\sin(\hat{\kappa}_e) & -\sin(\hat{\kappa}_e) & \lambda \end{bmatrix}, \tag{6.46}$$

and by cofactor expansion along the top row, we have

$$
\begin{aligned}
P_{circ}(\lambda) = \lambda & \left[\lambda^2 - \frac{\partial f_2}{\partial \kappa_e}\lambda + 2\mu_p^2 \sin^2(\hat{\kappa}_e)\right] \\
& + 2\mu_p^2 \sin(\hat{\kappa}_e)\Big[-\sin(\hat{\kappa}_e)\cos(\hat{\kappa}_e)\Big(2\mu_e \cos(\hat{\kappa}_e) + \mu_p\Big) \\
& \qquad + \sin(\hat{\kappa}_e)\lambda - \sin(\hat{\kappa}_e)\frac{\partial f_2}{\partial \kappa_e}\Big] \\
&= \lambda^3 - \frac{\partial f_2}{\partial \kappa_e}\lambda^2 + 4\mu_p^2 \sin^2(\hat{\kappa}_e)\lambda \\
& \quad - 2\mu_p^2 \sin^2(\hat{\kappa}_e)\left[\cos(\hat{\kappa}_e)\Big(2\mu_e \cos(\hat{\kappa}_e) + \mu_p\Big) + \frac{\partial f_2}{\partial \kappa_e}\right] \\
&= \lambda^3 - \Big(6\mu_e \cos^2(\hat{\kappa}_e) + (\mu_e + \mu_p)\cos(\hat{\kappa}_e) - 4\mu_e\Big)\lambda^2 + 4\mu_p^2 \sin^2(\hat{\kappa}_e)\lambda \\
& \quad - 2\mu_p^2 \sin^2(\hat{\kappa}_e)\Big(8\mu_e \cos^2(\hat{\kappa}_e) + (\mu_e + 2\mu_p)\cos(\hat{\kappa}_e) - 4\mu_e\Big) \\
&= \lambda^3 - \mu_e\Big(6\cos^2(\hat{\kappa}_e) + (1+\bar{\mu})\cos(\hat{\kappa}_e) - 4\Big)\lambda^2 + 4\mu_p^2 \sin^2(\hat{\kappa}_e)\lambda \\
& \quad - 4\mu_e\mu_p^2 \sin^2(\hat{\kappa}_e)\Big(4\cos^2(\hat{\kappa}_e) + \frac{1}{2}(1+2\bar{\mu})\cos(\hat{\kappa}_e) - 2\Big) \\
&= \lambda^3 - \mu_e\Omega\lambda^2 + 4\mu_p^2 \sin^2(\hat{\kappa}_e)\lambda - 4\mu_e\mu_p^2 \sin^2(\hat{\kappa}_e)\Phi,
\end{aligned} \tag{6.47}
$$

where

$$
\begin{aligned}
\Omega &= 6\cos^2(\hat{\kappa}_e) + (1+\bar{\mu})\cos(\hat{\kappa}_e) - 4, \\
\Phi &= 4\cos^2(\hat{\kappa}_e) + \frac{1}{2}(1+2\bar{\mu})\cos(\hat{\kappa}_e) - 2.
\end{aligned} \tag{6.48}
$$

Substitution of $\cos(\hat{\kappa}_e) = \frac{-2\bar{\mu}-1}{4}$ (from (6.36)), then yields

$$
\begin{aligned}
\Omega &= 6\left(\frac{-2\bar{\mu}-1}{4}\right)^2 + (1+\bar{\mu})\left(\frac{-2\bar{\mu}-1}{4}\right) - 4 \\
&= \frac{3}{8}\left(4\bar{\mu}^2 + 4\bar{\mu} + 1\right) + \frac{1}{4}\left(-2\bar{\mu}^2 - 3\bar{\mu} - 1\right) - 4 \\
&= \frac{1}{8}\Big(12\bar{\mu}^2 + 12\bar{\mu} + 3 - 4\bar{\mu}^2 - 6\bar{\mu} - 2 - 32\Big) \\
&= \frac{1}{8}\Big(8\bar{\mu}^2 + 6\bar{\mu} - 31\Big),
\end{aligned} \tag{6.49}
$$

and

$$\begin{aligned}\Phi &= 4\left(\frac{-2\bar{\mu}-1}{4}\right)^2 + \frac{1}{2}(1+2\bar{\mu})\left(\frac{-2\bar{\mu}-1}{4}\right) - 2\\ &= \frac{1}{4}\left(4\bar{\mu}^2+4\bar{\mu}+1\right) + \frac{1}{8}\left(-4\bar{\mu}^2-4\bar{\mu}-1\right) - 2\\ &= \frac{1}{8}\Big(4\bar{\mu}^2+4\bar{\mu}-15\Big)\\ &= \frac{1}{8}\Big(2\bar{\mu}-3\Big)\Big(2\bar{\mu}+5\Big), \end{aligned} \tag{6.50}$$

and one can confirm that for $\bar{\mu} < 3/2$ (which is required by **Proposition 6.5.1** for existence of circling equilibria), we have

$$\Omega < 0 \ \text{ and } \Phi < 0. \tag{6.51}$$

We also note that

$$\begin{aligned}\sin^2(\hat{\kappa}_e) = 1 - \cos^2(\hat{\kappa}_e) &= \frac{1}{16}\left(16 - (-2\bar{\mu}-1)^2\right)\\ &= -\frac{1}{16}\Big(4\bar{\mu}^2+4\bar{\mu}-15\Big)\\ &= -\frac{\Phi}{2}, \end{aligned} \tag{6.52}$$

and substitution into (6.47) yields

$$P_{circ}(\lambda) = \lambda^3 - \mu_e\Omega\lambda^2 - 2\mu_p^2\Phi\lambda + 2\mu_e\mu_p^2\Phi^2. \tag{6.53}$$

The Routh array associated with (6.53) is given by

$$\begin{array}{c|cc} \boldsymbol{\lambda^3} & 1 & -2\mu_p^2\Phi \\ \boldsymbol{\lambda^2} & -\mu_e\Omega & 2\mu_e\mu_p^2\Phi^2 \\ \boldsymbol{\lambda^1} & b & \\ \boldsymbol{\lambda^0} & 2\mu_e\mu_p^2\Phi^2 & \end{array}$$

where

$$b = -\left(\frac{1}{-\mu_e\Omega}\right)\left(2\mu_e\mu_p^2\Phi^2 - 2\mu_e\mu_p^2\Omega\Phi\right) = 2\mu_p^2\left(\frac{\Phi}{\Omega}\right)(\Phi - \Omega)\,. \tag{6.54}$$

Hence the first, second and fourth terms in the first column of the Routh array are strictly positive, and it remains to analyze the sign of b. Since Φ and Ω are both strictly negative, we have $\mathrm{sgn}(b) = \mathrm{sgn}(\Phi - \Omega)$. Observe that

$$\begin{aligned}\Phi - \Omega &= \frac{1}{8}\Big(2\bar{\mu} - 3\Big)\Big(2\bar{\mu} + 5\Big) - \frac{1}{8}\Big(8\bar{\mu}^2 + 6\bar{\mu} - 31\Big)\\ &= \frac{1}{8}\Big(\big(4\bar{\mu}^2 + 4\bar{\mu} - 15\big) - \big(8\bar{\mu}^2 + 6\bar{\mu} - 31\big)\Big)\\ &= -\frac{1}{8}\Big(4\bar{\mu}^2 + 2\bar{\mu} - 16\Big)\\ &> -\frac{1}{8}\left(4\left(\frac{3}{2}\right)^2 + 2\left(\frac{3}{2}\right) - 16\right)\\ &> 0,\end{aligned} \tag{6.55}$$

and hence $b > 0$. Thus there are no sign changes in the first column of the Routh array, and by the Routh-Hurwitz criterion we conclude that all the roots of (6.53) have non-positive real part. In what follows, we demonstrate that in fact the roots all have negative real parts, i.e. (6.44) does not have any pure imaginary eigenvalues.

Suppose $\lambda = j\gamma$ for some[2] $\gamma \neq 0 \in \mathbb{R}$. Then from (6.53) we have

$$P_{circ}(j\gamma) = -j\gamma^3 + \mu_e\Omega\gamma^2 - j2\mu_p^2\Phi\gamma + 2\mu_e\mu_p^2\Phi^2, \tag{6.56}$$

[2]Since the constant term in $P_{circ}(\lambda)$ is non-zero, we have already ruled out the possibility of zero eigenvalues.

and hence

$$
\begin{aligned}
P_{circ}(j\gamma) = 0 &\Longleftrightarrow \gamma^3 + 2\mu_p^2\Phi\gamma = 0 \quad \text{and} \quad \mu_e\Omega\gamma^2 + 2\mu_e\mu_p^2\Phi^2 = 0 \\
&\Longleftrightarrow \gamma^2 = -2\mu_p^2\Phi \quad \text{and} \quad \mu_e\Omega\gamma^2 + 2\mu_e\mu_p^2\Phi^2 = 0 \\
&\Longleftrightarrow \mu_e\Omega\left(-2\mu_p^2\Phi\right) + 2\mu_e\mu_p^2\Phi^2 = 0 \\
&\Longleftrightarrow 2\mu_e\mu_p^2\Phi\left(\Phi - \Omega\right) = 0. \qquad (6.57)
\end{aligned}
$$

However, by (6.51) and (6.55) we have $\Phi\left(\Phi - \Omega\right) \neq 0$, and therefore there are no pure imaginary eigenvalues.

We summarize all stability results (and recap the existence conditions) for the common speed case in the following proposition.

Proposition 6.5.4. *For the common speed ($\bar{\nu} = 1$) relative equilibria described in **Proposition 6.5.1**, the following stability properties hold:*

1. *For all values of $\bar{\mu} > 0$, Type A rectilinear equilibria exist.*
   - *If $\bar{\mu} < 1$, then all Type A rectilinear equilibria are unstable.*
   - *If $\hat{\rho} < \frac{1}{\mu_p}$, then the associated Type A rectilinear equilibrium is unstable.*
2. *For all values of $\bar{\mu} > 0$, Type B rectilinear equilibria exist and are unstable.*
3. *For $0 < \bar{\mu} < 3/2$, circling equilibria exist and are asymptotically stable.*

Proof. Follows from the previous discussion. □

6.6 Relative equilibria for the general case $\bar{\nu} \neq 1$

6.6.1 Existence conditions for relative equilibria in the general case

In this section, we assume $\bar{\nu} \neq 1$ and derive existence conditions and stability properties for relative equilibria. We first observe that a rectilinear equilibrium requires $|\dot{\mathbf{r}}| = 0$, and one can readily verify from (6.10) that this is possible if and only if $\bar{\nu} = 1$. Hence rectilinear equilibria do not exist for the $\bar{\nu} \neq 1$ case[3].

At a circling equilibrium we must have $\omega \neq 0$, and therefore from (6.20) we have

$$\dot{\kappa}_p = 0 \Longleftrightarrow \rho = \hat{\rho} = \frac{1}{\mu_p \bar{\nu}}. \tag{6.59}$$

Then by substitution back into (6.20) we obtain

$$\begin{aligned} \dot{\kappa}_e = 0 &\Longleftrightarrow \mu_e \sin(\kappa_e) + \omega\left(2\mu_e \cos(\kappa_e) + \mu_p \bar{\nu}\right) = 0 \\ &\Longleftrightarrow \sin(\kappa_e) + \omega\Big(2\cos(\kappa_e) + \bar{\mu}\bar{\nu}\Big) = 0 \\ &\Longleftrightarrow \sin(\kappa_e) + \Big(\bar{\nu}\sin(\kappa_p) + \sin(\kappa_e)\Big)\Big(2\cos(\kappa_e) + \bar{\mu}\bar{\nu}\Big) = 0 \end{aligned} \tag{6.60}$$

[3] Though rectilinear equilibria do not exist for the $\bar{\nu} \neq 1$ case, we note that the submanifold

$$M_{(0,\pi)} = \left\{ (\kappa_p, \kappa_e, \rho) \in M_{shape} \;\middle|\; \kappa_p = 0,\ \kappa_e = \pi \right\} \tag{6.58}$$

is invariant under the pursuer-evader dynamics (6.20), as are the related submanifolds $M_{(\pi,0)}$, $M_{(0,0)}$, and $M_{(\pi,\pi)}$, which are defined analogously. An analysis of the stability properties of these submanifolds is the subject of future work.

and

$$\dot{\rho} = 0 \Longleftrightarrow \bar{\nu}\cos(\kappa_p) + \cos(\kappa_e) = 0. \tag{6.61}$$

Therefore equilibrium values $\hat{\kappa}_p$ and $\hat{\kappa}_e$ can be determined (in terms of $\bar{\mu}$ and $\bar{\nu}$) by solving the set of equations

$$\bar{\nu}\cos(\hat{\kappa}_p) + \cos(\hat{\kappa}_e) = 0, \tag{6.62}$$

$$\sin(\hat{\kappa}_e) + \Big(\bar{\nu}\sin(\hat{\kappa}_p) + \sin(\hat{\kappa}_e)\Big)\Big(2\cos(\hat{\kappa}_e) + \bar{\mu}\bar{\nu}\Big) = 0. \tag{6.63}$$

A closed-form solution for these equations has proven elusive, so we proceed as follows.

We first note that **if $\boldsymbol{\sin(\hat{\kappa}_e) = 0}$**, then (6.63) simplifies to

$$\bar{\nu}\sin(\hat{\kappa}_p)\Big(2\cos(\hat{\kappa}_e) + \bar{\mu}\bar{\nu}\Big) = 0, \tag{6.64}$$

which holds if and only if $\sin(\hat{\kappa}_p) = 0$ or $\bar{\mu}\bar{\nu} = -2\cos(\hat{\kappa}_e)$. If $\sin(\hat{\kappa}_p) = 0$, then $\omega = 0$ and this can not be a circling equilibrium. Hence we assume $\sin(\hat{\kappa}_p) \neq 0$, and therefore (6.64) holds if and only if $\bar{\mu}\bar{\nu} = -2\cos(\hat{\kappa}_e)$, where $\cos(\hat{\kappa}_e)$ must be either 1 or -1 since $\sin(\hat{\kappa}_e) = 0$. Since $\bar{\mu}\bar{\nu} > 0$, we must have $\hat{\kappa}_e = \pi$ and $\bar{\mu}\bar{\nu} = 2$, and substitution into (6.62) yields $\cos(\hat{\kappa}_p) = 1/\bar{\nu}$, which is only valid for $\bar{\nu} > 1$. Hence for $\bar{\nu} > 1$ and $\bar{\mu}\bar{\nu} = 2$, there exists a circling equilibrium characterized by

$$\begin{aligned}
\hat{\kappa}_e &= \pi, \\
\hat{\kappa}_p &= \cos^{-1}\left(\frac{1}{\bar{\nu}}\right), \\
\hat{\rho} &= \frac{1}{\mu_p\bar{\nu}}.
\end{aligned} \tag{6.65}$$

Now **assume that $\sin(\hat{\kappa}_e) \neq 0$**. We define $\psi \in \mathbb{R} - \{0\}$ by

$$\psi \triangleq \frac{\sin(\hat{\kappa}_e)}{\omega} = \frac{\sin(\hat{\kappa}_e)}{\bar{\nu}\sin(\hat{\kappa}_p) + \sin(\hat{\kappa}_e)}, \tag{6.66}$$

and substituting $\bar{\nu}\sin(\hat{\kappa}_p) + \sin(\hat{\kappa}_e) = \sin(\hat{\kappa}_e)/\psi$ into (6.63), we have

$$\begin{aligned} 0 &= \sin(\hat{\kappa}_e) + \frac{1}{\psi}\sin(\hat{\kappa}_e)\Big(2\cos(\hat{\kappa}_e) + \bar{\mu}\bar{\nu}\Big) \\ &= \sin(\hat{\kappa}_e)\Big[1 + \frac{1}{\psi}\big(2\cos(\hat{\kappa}_e) + \bar{\mu}\bar{\nu}\big)\Big]. \end{aligned} \tag{6.67}$$

Observe that (6.67) holds if and only if

$$\cos(\hat{\kappa}_e) = -\frac{1}{2}\left(\psi + \bar{\mu}\bar{\nu}\right), \tag{6.68}$$

which is well-defined if and only if

$$-2 - \bar{\mu}\bar{\nu} \leq \psi \leq 2 - \bar{\mu}\bar{\nu}. \tag{6.69}$$

By (6.62) we then have

$$\cos(\hat{\kappa}_p) = -\frac{1}{\bar{\nu}}\cos(\hat{\kappa}_e) = \frac{1}{2\bar{\nu}}\left(\psi + \bar{\mu}\bar{\nu}\right), \tag{6.70}$$

and therefore we also require

$$-2\bar{\nu} - \bar{\mu}\bar{\nu} \leq \psi \leq 2\bar{\nu} - \bar{\mu}\bar{\nu}. \tag{6.71}$$

Combining (6.62), (6.66), and (6.68) yields the equilibrium equations

$$\bar{\nu}\cos(\hat{\kappa}_p) = -\cos(\hat{\kappa}_e) = \frac{1}{2}\left(\psi + \bar{\mu}\bar{\nu}\right), \tag{6.72}$$

$$\bar{\nu}\sin(\hat{\kappa}_p) = \left(\frac{1-\psi}{\psi}\right)\sin(\hat{\kappa}_e), \tag{6.73}$$

and we proceed by deriving conditions for existence of solutions $(\hat{\kappa}_p, \hat{\kappa}_e)$ for the system (6.72)-(6.73).

Observe (by squaring and summing (6.72) and (6.73)) that solutions for the system exist if and only if

$$\begin{aligned}
\bar{\nu}^2 &= \cos^2(\hat{\kappa}_e) + \left(\frac{1-\psi}{\psi}\right)^2 \sin^2(\hat{\kappa}_e) \\
&= \cos^2(\hat{\kappa}_e)\left(1 - \left(\frac{1-\psi}{\psi}\right)^2\right) + \left(\frac{1-\psi}{\psi}\right)^2 \\
&= \frac{1}{4}\left(\psi + \bar{\mu}\bar{\nu}\right)^2 \left(\frac{-1+2\psi}{\psi^2}\right) + \left(\frac{1-2\psi+\psi^2}{\psi^2}\right) \\
&= \frac{1}{4\psi^2}\Big[4\left(1-2\psi+\psi^2\right) + \left(\psi^2 + 2\bar{\mu}\bar{\nu}\psi + \bar{\mu}^2\bar{\nu}^2\right)(2\psi - 1)\Big] \\
&= \frac{1}{4\psi^2}\Big[2\psi^3 + (3+4\bar{\mu}\bar{\nu})\psi^2 + (2\bar{\mu}^2\bar{\nu}^2 - 2\bar{\mu}\bar{\nu} - 8)\psi + (4 - \bar{\mu}^2\bar{\nu}^2)\Big],
\end{aligned} \tag{6.74}$$

which holds if and only if

$$0 = 2\psi^3 + (3 + 4\bar{\mu}\bar{\nu} - 4\bar{\nu}^2)\psi^2 + 2(\bar{\mu}^2\bar{\nu}^2 - \bar{\mu}\bar{\nu} - 4)\psi + (4 - \bar{\mu}^2\bar{\nu}^2). \tag{6.75}$$

Therefore solutions to the system (6.72)-(6.73) exist (and therefore circling equilibria exist) if and only if a non-zero real-valued root of the polynomial

$$F(\psi) = 2\psi^3 + (3 + 4\bar{\mu}\bar{\nu} - 4\bar{\nu}^2)\psi^2 + 2(\bar{\mu}^2\bar{\nu}^2 - \bar{\mu}\bar{\nu} - 4)\psi + (4 - \bar{\mu}^2\bar{\nu}^2) \tag{6.76}$$

satisfies (6.69) and (6.71), i.e.

$$-2 - \bar{\mu}\bar{\nu} \leq \psi \leq 2 - \bar{\mu}\bar{\nu}, \quad \text{and} \tag{6.77}$$

$$-2\bar{\nu} - \bar{\mu}\bar{\nu} \leq \psi \leq 2\bar{\nu} - \bar{\mu}\bar{\nu}. \tag{6.78}$$

It is straightforward to show that the constraints in (6.77) are active for $\bar{\nu} > 1$, and the constraints in (6.78) are active for $\bar{\nu} < 1$. (For $\bar{\nu} = 1$, the constraints in (6.77) and (6.78) are equivalent.)

We summarize the existence conditions for circling equilibria in the following proposition.

Proposition 6.6.1. *For the general case (i.e. $\bar{\nu}$ not necessarily equal to 1), circling relative equlibria for the system (6.20) exist if and only if one of the following conditions holds.*

1. *There exists a non-zero real-valued root $\psi = \psi^*$ of the polynomial*

$$F(\psi) = 2\psi^3 + (3 + 4\bar{\mu}\bar{\nu} - 4\bar{\nu}^2)\psi^2 + 2(\bar{\mu}^2\bar{\nu}^2 - \bar{\mu}\bar{\nu} - 4)\psi + (4 - \bar{\mu}^2\bar{\nu}^2) \quad (6.79)$$

which satisfies the constraints

$$-2 - \bar{\mu}\bar{\nu} \leq \psi^* \leq 2 - \bar{\mu}\bar{\nu}, \quad \textit{for } \bar{\nu} > 1, \textit{ and} \quad (6.80)$$

$$-2\bar{\nu} - \bar{\mu}\bar{\nu} \leq \psi^* \leq 2\bar{\nu} - \bar{\mu}\bar{\nu}, \quad \textit{for } 0 < \bar{\nu} < 1. \quad (6.81)$$

For every ψ^* which satisfies the requirements above, the equilibrium values for the corresponding pair of circling equilibria are characterized by

$$\cos(\hat{\kappa}_e) = -\frac{1}{2}\left(\psi^* + \bar{\mu}\bar{\nu}\right), \quad (6.82)$$

$$\cos(\hat{\kappa}_p) = \frac{1}{2\bar{\nu}}\left(\psi^* + \bar{\mu}\bar{\nu}\right); \quad \sin(\hat{\kappa}_p) = \left(\frac{1 - \psi^*}{\bar{\nu}\psi^*}\right)\sin(\hat{\kappa}_e), \quad (6.83)$$

$$\rho = \frac{1}{\mu_p\bar{\nu}}. \quad (6.84)$$

Observe that (6.82) specifies two possible equilibrium values for $\hat{\kappa}_e$ (corresponding to CW and CCW circling equilibria), and (6.83) specifies exactly one corresponding value for $\hat{\kappa}_p$ in each case.

2. The parameters $\bar{\mu}$ and $\bar{\nu}$ satisfy $\bar{\mu}\bar{\nu} = 2$ and $\bar{\nu} > 1$. In this case, there exists a pair of circling relative equilibria with equilibrium values given by

$$\begin{aligned}
\hat{\kappa}_e &= \pi, \\
\hat{\kappa}_p &= \pm \cos^{-1}\left(\frac{1}{\bar{\nu}}\right), \\
\rho &= \frac{1}{\mu_p \bar{\nu}}.
\end{aligned} \tag{6.85}$$

Proof. Follows from the previous discussion. □

Remark 6.6.2 Note that condition 1 and condition 2 of **Proposition 6.6.1** are not mutually exclusive. In fact, one can show that if $\bar{\mu}$ and $\bar{\nu}$ satisfy condition 2, then there always exists ψ^* which satisfies condition 1, i.e., there exists two pairs of circling equilibria, one pair described by (6.82)-(6.84) and the other by (6.85).

Remark 6.6.3 We can demonstrate that the common speed case $\bar{\nu} = 1$ (discussed in section 6.5) in fact specializes from **Proposition 6.6.1**. For $\bar{\nu} = 1$, we observe that (6.79) simplifies to

$$\begin{aligned}
F(\psi) &= 2\psi^3 + (4\bar{\mu} - 1)\psi^2 + 2(\bar{\mu}^2 - \bar{\mu} - 4)\psi + (4 - \bar{\mu}^2) \\
&= (2\psi - 1)\left(\psi^2 + 2\bar{\mu}\psi + (\bar{\mu}^2 - 4)\right) \\
&= 2\left(\psi - 1/2\right)\Big(\psi + (\bar{\mu} + 2)\Big)\Big(\psi + (\bar{\mu} - 2)\Big),
\end{aligned} \tag{6.86}$$

and (6.80) and (6.81) require $-2-\bar{\mu} \leq \psi^* \leq 2-\bar{\mu}$. Then (6.86) has three roots given by $\psi^* = 1/2, -2 - \bar{\mu}, 2 - \bar{\mu}$, the first of which satisfies (6.80) if and only if $\bar{\mu} \leq 3/2$, and the second two which always satisfy (6.80). (The case $\bar{\mu} = 3/2,\ \psi^* = -\frac{7}{2}, \frac{1}{2}$

corresponds to the two rectilinear equilibria.) Substituting $\bar{\nu} = 1$ and either $\psi^* = -2 - \bar{\mu}$ or $\psi^* = 2 - \bar{\mu}$ into (6.82)-(6.84) yields the rectilinear equilibria described by (6.35), and substituting $\bar{\nu} = 1$ and $\psi^* = 1/2$ into (6.82)-(6.84) yields the circling equilibria described by (6.36).

6.6.2 Stability of circling relative equilibria for the general case

Suppose condition 1 of **Proposition 6.6.1** is satisfied, and therefore there exists a circling equilibrium described by (6.82)-(6.84). As in the common speed case, we analyze stability properties of this circling equilibrium by linearization of the dynamics (6.20), starting from the general form of the Jacobian given by (6.37) (as derived in appendix D). To evaluate (6.37) at the equilibrium values given by (6.82)-(6.84), we first note that at equilibrium,

$$\omega = \bar{\nu}\sin(\hat{\kappa}_p) + \sin(\hat{\kappa}_e) = \left[\left(\frac{1-\psi^*}{\psi^*}\right) + 1\right]\sin(\hat{\kappa}_e) = \frac{1}{\psi^*}\sin(\hat{\kappa}_e). \tag{6.87}$$

Substitution of equilibrium values into the first element of the second row of (6.37) yields

$$\begin{aligned}
\bar{\nu}\cos(\hat{\kappa}_p)\left(2\mu_e\cos(\hat{\kappa}_e) + \frac{1}{\hat{\rho}}\right) &= -\cos(\hat{\kappa}_e)\left(2\mu_e\cos(\hat{\kappa}_e) + \mu_p\bar{\nu}\right) \\
&= -\mu_e\cos(\hat{\kappa}_e)\left(2\cos(\hat{\kappa}_e) + \bar{\mu}\bar{\nu}\right) \\
&= -\frac{\mu_e}{2}\left(\psi^* + \bar{\mu}\bar{\nu}\right)\psi^*, \qquad (6.88)
\end{aligned}$$

and therefore we have

$$\left(\frac{\partial f}{\partial x}\right)_{circ} = \begin{bmatrix} 0 & 0 & -\frac{\mu_e^2}{\psi^*}\bar{\mu}^2\bar{\nu}^2\sin(\hat{\kappa}_e) \\ -\frac{\mu_e}{2}\left(\psi^* + \bar{\mu}\bar{\nu}\right)\psi^* & \frac{\partial f_2}{\partial \kappa_e} & -\frac{\mu_e^2}{\psi^*}\bar{\mu}^2\bar{\nu}^2\sin(\hat{\kappa}_e) \\ \left(\frac{1-\psi^*}{\psi^*}\right)\sin(\hat{\kappa}_e) & \sin(\hat{\kappa}_e) & 0 \end{bmatrix}, \tag{6.89}$$

where

$$\begin{aligned} \frac{\partial f_2}{\partial \kappa_e} &= \mu_e\Big(\cos(\hat{\kappa}_e) + 2\cos^2(\hat{\kappa}_e) - 2\omega\sin(\hat{\kappa}_e)\Big) + \frac{\cos(\hat{\kappa}_e)}{\hat{\rho}} \\ &= \mu_e\Big(\cos(\hat{\kappa}_e)(1+\bar{\mu}\bar{\nu}) + 2\cos^2(\hat{\kappa}_e) - 2(1/\psi^*)\sin^2(\hat{\kappa}_e)\Big) \\ &= \frac{\mu_e}{\psi^*}\Big(\cos(\hat{\kappa}_e)(1+\bar{\mu}\bar{\nu})\psi^* + 2\cos^2(\hat{\kappa}_e)(\psi^*+1) - 2\Big) \\ &= \frac{\mu_e}{\psi^*}\left(-\frac{1}{2}\left(\psi^* + \bar{\mu}\bar{\nu}\right)(1+\bar{\mu}\bar{\nu})\psi^* + \frac{1}{2}\left(\psi^* + \bar{\mu}\bar{\nu}\right)^2(\psi^*+1) - 2\right) \\ &= \frac{\mu_e}{2\psi^*}\left(-(1+\bar{\mu}\bar{\nu}){\psi^*}^2 - \bar{\mu}\bar{\nu}(1+\bar{\mu}\bar{\nu})\psi^* + \left({\psi^*}^2 + 2\bar{\mu}\bar{\nu}\psi^* + \bar{\mu}^2\bar{\nu}^2\right)(\psi^*+1) - 4\right) \\ &= \frac{\mu_e}{2\psi^*}\left({\psi^*}^3 + \bar{\mu}\bar{\nu}{\psi^*}^2 + \bar{\mu}\bar{\nu}\psi^* + \bar{\mu}^2\bar{\nu}^2 - 4\right). \end{aligned} \tag{6.90}$$

The characteristic polynomial is given by

$$P_{circ}(\lambda) = \det\begin{bmatrix} \lambda & 0 & \frac{\mu_e^2}{\psi^*}\bar{\mu}^2\bar{\nu}^2\sin(\hat{\kappa}_e) \\ \frac{\mu_e}{2}\left(\psi^* + \bar{\mu}\bar{\nu}\right)\psi^* & \lambda - \frac{\partial f_2}{\partial \kappa_e} & \frac{\mu_e^2}{\psi^*}\bar{\mu}^2\bar{\nu}^2\sin(\hat{\kappa}_e) \\ -\left(\frac{1-\psi^*}{\psi^*}\right)\sin(\hat{\kappa}_e) & -\sin(\hat{\kappa}_e) & \lambda \end{bmatrix}, \tag{6.91}$$

and by cofactor expansion along the top row, we have

$$
\begin{aligned}
P_{circ}(\lambda) &= \lambda\left(\lambda^2 - \frac{\partial f_2}{\partial \kappa_e}\lambda + \frac{\mu_e^2}{\psi^*}\bar{\mu}^2\bar{\nu}^2\sin^2(\hat{\kappa}_e)\right) \\
&\quad + \frac{\mu_e^2}{\psi^*}\bar{\mu}^2\bar{\nu}^2\sin(\hat{\kappa}_e)\Bigg[-\frac{\mu_e}{2}\left(\psi^* + \bar{\mu}\bar{\nu}\right)\psi^*\sin(\hat{\kappa}_e) \\
&\qquad\qquad + \left(\frac{1-\psi^*}{\psi^*}\right)\sin(\hat{\kappa}_e)\lambda - \left(\frac{1-\psi^*}{\psi^*}\right)\frac{\partial f_2}{\partial \kappa_e}\sin(\hat{\kappa}_e)\Bigg] \\
&= \left(\lambda^3 - \frac{\partial f_2}{\partial \kappa_e}\lambda^2 + \frac{\mu_e^2}{\psi^*}\bar{\mu}^2\bar{\nu}^2\sin^2(\hat{\kappa}_e)\lambda\right) + \frac{\mu_e^2}{\psi^*}\bar{\mu}^2\bar{\nu}^2\left(\frac{1-\psi^*}{\psi^*}\right)\sin^2(\hat{\kappa}_e)\lambda \\
&\quad + \frac{\mu_e^2}{\psi^*}\bar{\mu}^2\bar{\nu}^2\sin(\hat{\kappa}_e)\left(\frac{-\sin(\hat{\kappa}_e)}{\psi^*}\right)\left[\frac{\mu_e}{2}\left(\psi^* + \bar{\mu}\bar{\nu}\right){\psi^*}^2 + (1-\psi^*)\frac{\partial f_2}{\partial \kappa_e}\right].
\end{aligned}
\tag{6.92}
$$

Then substituting (6.90), we obtain

$$
\begin{aligned}
P_{circ}(\lambda) &= \lambda^3 - \frac{\mu_e}{2\psi^*}\left({\psi^*}^3 + \bar{\mu}\bar{\nu}{\psi^*}^2 + \bar{\mu}\bar{\nu}\psi^* + \bar{\mu}^2\bar{\nu}^2 - 4\right)\lambda^2 + \frac{\mu_e^2}{{\psi^*}^2}\bar{\mu}^2\bar{\nu}^2\sin^2(\hat{\kappa}_e)\lambda \\
&\quad - \frac{\mu_e^2}{{\psi^*}^2}\bar{\mu}^2\bar{\nu}^2\sin^2(\hat{\kappa}_e)\Bigg[\frac{\mu_e}{2}\left(\psi^* + \bar{\mu}\bar{\nu}\right){\psi^*}^2 \\
&\qquad\qquad + \frac{\mu_e\left(1-\psi^*\right)}{2\psi^*}\left({\psi^*}^3 + \bar{\mu}\bar{\nu}{\psi^*}^2 + \bar{\mu}\bar{\nu}\psi^* + \bar{\mu}^2\bar{\nu}^2 - 4\right)\Bigg] \\
&= \lambda^3 - \frac{\mu_e}{2\psi^*}\left({\psi^*}^3 + \bar{\mu}\bar{\nu}{\psi^*}^2 + \bar{\mu}\bar{\nu}\psi^* + \bar{\mu}^2\bar{\nu}^2 - 4\right)\lambda^2 + \frac{\mu_e^2}{{\psi^*}^2}\bar{\mu}^2\bar{\nu}^2\sin^2(\hat{\kappa}_e)\lambda \\
&\quad - \frac{\mu_e^3}{2{\psi^*}^3}\bar{\mu}^2\bar{\nu}^2\sin^2(\hat{\kappa}_e)\Big[{\psi^*}^4 + \bar{\mu}\bar{\nu}{\psi^*}^3 \\
&\qquad\qquad + (1-\psi^*)\left({\psi^*}^3 + \bar{\mu}\bar{\nu}{\psi^*}^2 + \bar{\mu}\bar{\nu}\psi^* + \bar{\mu}^2\bar{\nu}^2 - 4\right)\Big] \\
&= \lambda^3 - \frac{\mu_e}{2\psi^*}\Omega\lambda^2 + \frac{\mu_e^2}{{\psi^*}^2}\bar{\mu}^2\bar{\nu}^2\sin^2(\hat{\kappa}_e)\lambda - \frac{\mu_e^3}{2{\psi^*}^3}\bar{\mu}^2\bar{\nu}^2\sin^2(\hat{\kappa}_e)\Phi,
\end{aligned}
\tag{6.93}
$$

where

$$
\begin{aligned}
\Omega &\triangleq {\psi^*}^3 + \bar{\mu}\bar{\nu}{\psi^*}^2 + \bar{\mu}\bar{\nu}\psi^* + \bar{\mu}^2\bar{\nu}^2 - 4, \\
\Phi &\triangleq {\psi^*}^3 + (4 + \bar{\mu}\bar{\nu} - \bar{\mu}^2\bar{\nu}^2)\psi^* + \bar{\mu}^2\bar{\nu}^2 - 4,
\end{aligned}
\tag{6.94}
$$

and $\sin^2(\hat{\kappa}_e) \neq 0$ can be expressed explicitly in terms of $\bar{\mu}, \bar{\nu}$, and ψ^* by (6.82).

If we let

$$\tilde{\lambda} \triangleq \left(\frac{\psi^*}{\mu_e}\right)\lambda, \tag{6.95}$$

then we have

$$P_{circ}(\tilde{\lambda}) = \left(\frac{\mu_e}{\psi^*}\right)^3 \left\{\tilde{\lambda}^3 - \frac{1}{2}\Omega\tilde{\lambda}^2 + \bar{\mu}^2\bar{\nu}^2\sin^2(\hat{\kappa}_e)\tilde{\lambda} - \frac{1}{2}\bar{\mu}^2\bar{\nu}^2\sin^2(\hat{\kappa}_e)\Phi\right\}, \tag{6.96}$$

and since $\mu_e > 0$, we need only concern ourselves with the polynomial inside the braces. Note that the cubic coefficient and the first order coefficient are always positive, and therefore we make the initial observation that if $\Phi > 0$, then by Descartes' sign rule we must have at least one positive real eigenvalue. Therefore we conclude that $\Phi \leq 0$ is a necessary condition for stability.

We proceed by considering the Routh array associated with (6.96), given by

$$\begin{array}{c|cc}
\tilde{\lambda}^{\mathbf{3}} & 1 & \bar{\mu}^2\bar{\nu}^2\sin^2(\hat{\kappa}_e) \\
\tilde{\lambda}^{\mathbf{2}} & -\frac{1}{2}\Omega & -\frac{1}{2}\bar{\mu}^2\bar{\nu}^2\sin^2(\hat{\kappa}_e)\Phi \\
\tilde{\lambda}^{\mathbf{1}} & b & \\
\tilde{\lambda}^{\mathbf{0}} & -\frac{1}{2}\bar{\mu}^2\bar{\nu}^2\sin^2(\hat{\kappa}_e)\Phi &
\end{array}$$

where

$$\begin{aligned}
b &= -\left(\frac{1}{-\frac{1}{2}\Omega}\right)\left(-\frac{1}{2}\bar{\mu}^2\bar{\nu}^2\sin^2(\hat{\kappa}_e)\Phi + \frac{1}{2}\Omega\bar{\mu}^2\bar{\nu}^2\sin^2(\hat{\kappa}_e)\right) \\
&= \bar{\mu}^2\bar{\nu}^2\sin^2(\hat{\kappa}_e)\left(\frac{1}{\Omega}\right)(\Omega - \Phi).
\end{aligned} \tag{6.97}$$

We have already stated that $\Phi \leq 0$ is a necessary condition for stability, i.e. it is necessary that the last term in the first column of the Routh array must be non-negative. From (6.95) we note that $\operatorname{sgn}(\operatorname{Re}(\lambda)) = \operatorname{sgn}(\psi^*)\operatorname{sgn}(\operatorname{Re}(\tilde{\lambda}))$, and hence stability requires $\psi^* > 0$ and no sign changes[4] in the first column of the Routh array, i.e. $\Omega \le 0$, $b \ge 0$ (which requires $\Omega - \Phi \le 0$), and $\Phi \le 0$. In fact, if $\Phi \le 0$ and $\Omega - \Phi \le 0$, then it necessarily follows that $\Omega \le 0$, and therefore we have

$$\mathrm{Re}(\lambda) \le 0 \Longleftrightarrow \psi^* > 0,\ \Phi \le 0,\ \text{and } \Omega - \Phi \le 0. \tag{6.98}$$

We first note from (6.80) that $\bar{\mu}\bar{\nu} < 2$ is a necessary condition for $\psi^* > 0$, and therefore it is a necessary condition for $\mathrm{Re}(\lambda) \le 0$. From (6.94), we have

$$\begin{aligned}\Omega - \Phi &= \Big(\psi^{*^3} + \bar{\mu}\bar{\nu}\psi^{*^2} + \bar{\mu}\bar{\nu}\psi^* + \bar{\mu}^2\bar{\nu}^2 - 4\Big) - \Big(\psi^{*^3} + (4 + \bar{\mu}\bar{\nu} - \bar{\mu}^2\bar{\nu}^2)\psi^* + \bar{\mu}^2\bar{\nu}^2 - 4\Big)\\ &= \psi^*\Big(\bar{\mu}\bar{\nu}\psi^* + (\bar{\mu}\bar{\nu} + 2)(\bar{\mu}\bar{\nu} - 2)\Big).\end{aligned} \tag{6.99}$$

Again making use of (6.80) we substitute $0 < \psi^* \le 2 - \bar{\mu}\bar{\nu}$ into (6.99) to obtain

$$\Omega - \Phi \le \psi^*\Big(\bar{\mu}\bar{\nu}(2 - \bar{\mu}\bar{\nu}) + (\bar{\mu}\bar{\nu} + 2)(\bar{\mu}\bar{\nu} - 2)\Big) \le -2\psi^*(2 - \bar{\mu}\bar{\nu}), \tag{6.100}$$

and thus $\bar{\mu}\bar{\nu} < 2$ is sufficient to ensure $\Omega - \Phi < 0$.

We can therefore summarize our stability characterization as follows.

Proposition 6.6.4. *Suppose condition 1 of **Proposition 6.6.1** is satisfied, i.e. there exists $\psi^* \neq 0$ such that*

$$F(\psi^*) = 2\psi^{*^3} + (3 + 4\bar{\mu}\bar{\nu} - 4\bar{\nu}^2)\psi^{*^2} + 2(\bar{\mu}^2\bar{\nu}^2 - \bar{\mu}\bar{\nu} - 4)\psi^* + (4 - \bar{\mu}^2\bar{\nu}^2) = 0, \tag{6.101}$$

[4] If $\psi^* < 0$, then $\mathrm{sgn}(\mathrm{Re}(\lambda)) = -\,\mathrm{sgn}(\mathrm{Re}(\tilde{\lambda}))$, and stability would require three sign changes in the first column of the Routh array (i.e. positive real parts for all $\tilde{\lambda}$). However, this is not possible, since the first and last terms in the first column of the Routh array are positive.

and

$$-2 - \bar{\mu}\bar{\nu} \leq \psi^* \leq 2 - \bar{\mu}\bar{\nu}, \quad \textit{for } \bar{\nu} > 1, \textit{ and}$$

$$-2\bar{\nu} - \bar{\mu}\bar{\nu} \leq \psi^* \leq 2\bar{\nu} - \bar{\mu}\bar{\nu}, \quad \textit{for } 0 < \bar{\nu} < 1.$$

Then the stability properties of the corresponding pair of circling equilibria described by (6.82)-(6.84) can be characterized in terms of

$$\Phi(\psi^*) \triangleq {\psi^*}^3 + (4 + \bar{\mu}\bar{\nu} - \bar{\mu}^2\bar{\nu}^2)\psi^* + \bar{\mu}^2\bar{\nu}^2 - 4 \tag{6.102}$$

as follows:

1. *If* $\bar{\mu}\bar{\nu} \geq 2$*, the corresponding circling equilibria are unstable.*

2. *If* $\bar{\mu}\bar{\nu} < 2$*, and* $\psi^* < 0$ *or* $\Phi(\psi^*) > 0$*, the corresponding circling equilibria are unstable.*

3. *If* $\bar{\mu}\bar{\nu} < 2$*,* $\psi^* > 0$ *and* $\Phi(\psi^*) < 0$*, the corresponding circling equilibria are asymptotically stable.*

Proof. The instability claims follow directly from the previous discussion, and therefore it remains to demonstrate asymptotic stability for the $\Phi < 0$ case. By the analysis presented in the section leading up to **Proposition 6.6.4**, we have already established that if $\bar{\mu}\bar{\nu} < 2$, $\psi^* > 0$, and $\Phi < 0$, then there are no sign changes in the first column of the Routh array and therefore all eigenvalues of (6.96) have non-positive real parts. It remains to demonstrate that our assumptions also imply that (6.96) has no pure imaginary eigenvalues. Observe from (6.96) that

$$\begin{aligned} P_{circ}(j\omega) &= \left(\frac{\mu_e}{\psi^*}\right)^3 \left\{(j\omega)^3 - \frac{1}{2}\Omega(j\omega)^2 + \bar{\mu}^2\bar{\nu}^2\sin^2(\hat{\kappa}_e)(j\omega) - \frac{1}{2}\bar{\mu}^2\bar{\nu}^2\sin^2(\hat{\kappa}_e)\Phi\right\} \\ &= \left(\frac{\mu_e}{\psi^*}\right)^3 \left\{-j\omega^3 + \frac{1}{2}\Omega\omega^2 + \bar{\mu}^2\bar{\nu}^2\sin^2(\hat{\kappa}_e)(j\omega) - \frac{1}{2}\bar{\mu}^2\bar{\nu}^2\sin^2(\hat{\kappa}_e)\Phi\right\} \\ &= \left(\frac{\mu_e}{\psi^*}\right)^3 \left\{\frac{1}{2}\Omega\omega^2 - \frac{1}{2}\bar{\mu}^2\bar{\nu}^2\sin^2(\hat{\kappa}_e)\Phi - j\omega\Big(\omega^2 - \bar{\mu}^2\bar{\nu}^2\sin^2(\hat{\kappa}_e)\Big)\right\}, \end{aligned} \tag{6.103}$$

and therefore

$$\begin{aligned} P_{circ}(j\omega) = 0 &\Longleftrightarrow \omega^2 - \bar{\mu}^2\bar{\nu}^2\sin^2(\hat{\kappa}_e) = 0 \ \text{ and } \frac{1}{2}\Omega\omega^2 - \frac{1}{2}\bar{\mu}^2\bar{\nu}^2\sin^2(\hat{\kappa}_e)\Phi = 0 \\ &\Longleftrightarrow \omega^2 = \bar{\mu}^2\bar{\nu}^2\sin^2(\hat{\kappa}_e) \ \text{ and } \Omega = \Phi. \end{aligned} \tag{6.104}$$

However, this is not possible since $\Omega - \Phi < 0$ (by (6.100) and the assumption $\bar{\mu}\bar{\nu} < 2$), and therefore (6.96) has no pure imaginary eigenvalues, i.e. the corresponding circling equilibria are asymptotically stable. □

Remark 6.6.5 The Jacobian matrix associated with the circling equilibria corresponding to condition 2 of **Proposition 6.6.1** has one strictly negative eigenvalue and two pure imaginary eigenvalues. Stability analysis for these type of circling equilibria is the subject of ongoing research.

6.6.3 Analysis of the special case $\bar{\nu} > 1$, $\bar{\mu}\bar{\nu} = 3/2$

Here we consider the particular case $\bar{\nu} > 1$ and $\bar{\mu}\bar{\nu} = 3/2$, applying **Propositions 6.6.1 and 6.6.4** to prove the existence of asymptotically stable circling equlibria. (In **Remark 6.6.7**, we explain why this case is of interest.) Substituting

$\bar{\nu} > 1$ and $\bar{\mu}\bar{\nu} = 3/2$ into (6.79) yields

$$F(\psi) = \frac{1}{4}\Big(8\psi^3 + 4(9 - 4\bar{\nu}^2)\psi^2 - 26\psi + 7\Big), \tag{6.105}$$

and by **Proposition 6.6.1**, circling equilibria exist if and only if there exists a real root $\psi = \psi^*$ in the interval given by (6.80), i.e.

$$-7/2 \leq \psi^* \leq 1/2. \tag{6.106}$$

One method for determining the existence of polynomial roots in a particular interval is provided by Sturm's Theorem. (See, for instance, [18].) To employ Sturm's Theorem, we let $a = 9 - 4\bar{\nu}^2$ and construct the *Sturm sequence* of polynomials $p_0(\psi), p_1(\psi), p_2(\psi), p_3(\psi)$ as follows:

$$\begin{aligned}
p_0(\psi) &= 4F(\psi) = 8\psi^3 + 4a\psi^2 - 26\psi + 7, \\
p_1(\psi) &= 4F'(\psi) = 24\psi^2 + 8a\psi - 26, \\
p_2(\psi) &= -\mathrm{rem}(p_0(\psi), p_1(\psi)) = \frac{1}{9}\Big(156 + 4a^2\Big)\psi - \frac{1}{9}\Big(63 + 13a\Big), \\
p_3(\psi) &= -\mathrm{rem}(p_1(\psi), p_2(\psi)) = \left(\frac{9}{2\left(39 + a^2\right)^2}\right)\Big(5 - a\Big)\Big(28a^2 - 29a + 1493\Big),
\end{aligned} \tag{6.107}$$

where $\mathrm{rem}(f, g)$ denotes the remainder resulting from polynomial division of f by g. Then letting $\mathcal{V}(\xi)$ denote the number of sign changes in the Sturm sequence evaluated at $\psi = \xi$, Sturm's Theorem states that the number of distinct roots of $F(\psi)$ contained in the interval (c, d), for $c < d \in \mathbb{R}$, is given by $\mathcal{V}(c) - \mathcal{V}(d)$. In our case we are interested in the number of distinct roots of $F(\psi)$ in the intervals $(-7/2, 0)$ and $(0, 1/2)$, and by substitution into (6.107) we have the evaluated Sturm sequence

(read left to right)

ψ	$p_0(\psi)$	$p_1(\psi)$	$p_2(\psi)$	$p_3(\psi)$
$-7/2$	$-196(\bar{\nu}^2-1)$	$16\,(7\bar{\nu}^2+1)$	$-\frac{4}{9}\,(56\bar{\nu}^4-265\bar{\nu}^2+465)$	p_3
0	7	-26	$\frac{4}{9}\,(13\bar{\nu}^2-45)$	p_3
$1/2$	$-4(\bar{\nu}^2-1)$	$-16\,(\bar{\nu}^2-1)$	$\frac{4}{9}\,(\bar{\nu}^2-1)\,(8\bar{\nu}^2-15)$	p_3

where $p_3(-7/2) = p_3(0) = p_3(1/2) = p_3 > 0$, since $5-a = 4(\bar{\nu}^2-1)$ and $28a^2-29a+1493 > 0$ for any $a \in \mathbb{R}$. Since $\bar{\nu} > 1$, we have sign-definiteness on all terms except for $p_2(0)$ and $p_2(1/2)$, and we summarize the sign variations in the following table:

ψ	$p_0(\psi)$	$p_1(\psi)$	$p_2(\psi)$	$p_3(\psi)$	$\mathcal{V}(\psi)$
$-7/2$	$-$	$+$	$-$	$+$	3
0	$+$	$-$	?	$+$	2
$1/2$	$-$	$-$	?	$+$	1

Reading the number of sign variations from left to right, we obtain the values for $\mathcal{V}(\psi)$ listed in the last column. (Note that we can determine the number of sign variations despite the sign ambiguity on $p_2(0)$ and $p_2(1/2)$.) Since $\mathcal{V}(-7/2)-\mathcal{V}(0) = 1$ and $\mathcal{V}(0)-\mathcal{V}(1/2) = 1$, we have demonstrated that under the constraints $\bar{\nu} > 1$ and $\bar{\mu}\bar{\nu} = 3/2$, (6.105) always has exactly one root in the interval $-7/2 < \psi^* < 0$ and exactly one root in the interval $0 < \psi^* < 1/2$.

We summarize the existence and stability of circling equilibria for the $\bar{\nu} > 1$, $\bar{\mu}\bar{\nu} = 3/2$ case in the following proposition.

Proposition 6.6.6. *For any $\bar{\mu}$ and $\bar{\nu}$ satisfying $\bar{\nu} > 1$ and $\bar{\mu}\bar{\nu} = 3/2$, there exists a unique $\psi_1^* \in (-7/2, 0)$ and a unique $\psi_2^* \in (0, 1/2)$ which satisfy condition 1 from* ***Proposition 6.6.1****. The pair of circling equilibria associated with ψ_1^* are unstable, and the pair of circling equilibria associated with ψ_2^* are asymptotically stable.*

Proof. The fact that ψ_1^* and ψ_2^* exist and satisfy condition 1 of **Proposition 6.6.1** follows from the previous discussion based on Sturm's theorem. To demonstrate the stability properties of these circling equilibria, we apply the results of **Proposition 6.6.4**. That the circling equilibria associated with ψ_1^* are unstable follows direcly from the fact that ψ_1^* is negative. To determine the stability properties of the circling equlibria associated with ψ_2^*, we substitute $\bar{\mu}\bar{\nu} = 3/2$ into (6.102) to obtain

$$\begin{aligned} \Phi\left(\psi_2^*\right) &= {\psi_2^*}^3 + \frac{13}{4}\psi_2^* - \frac{7}{4} \\ &= \frac{1}{4}\left(2\psi_2^* - 1\right)\left(2{\psi_2^*}^2 + \psi_2^* + 7\right). \end{aligned} \tag{6.108}$$

Hence, since $0 < \psi_2^* < 1/2$, it follows that $\Phi < 0$ and therefore the associated circling equilibria are asymptotically stable. □

Remark 6.6.7 Observe that **Proposition 6.6.6** demonstrates the existence and asymptotic stability of particular circling equilibria (a "stand-off" condition) even in cases for which the pursuer has both a speed advantage (i.e. $\bar{\nu} > 1$) and a control gain advantage (i.e. $\bar{\mu} > 1$), so long as the speed ratio $\bar{\nu}$ and control gain ratio $\bar{\mu}$ satisfy $\bar{\mu}\bar{\nu} = 3/2$. (For instance, $\bar{\nu} = 5/4$ and $\bar{\mu} = 6/5$ would satisfy the constraints.) Hence, there exists a set of initial conditions in a neighborhood of these equilibrium values such that a (moderately) disadvantaged evader can still force the circling equilibrium stand-off condition. However, from (6.84) we note that the separation at equilibrium is given by $\rho = \frac{1}{\mu_p \bar{\nu}}$, and therefore the pursuer can drive the separation arbitrarily small by using high gain. Hence this evasion law may be most effective when used against a pursuer whose control gain μ_p is bounded and relatively small.

Chapter 7

Conclusions and directions for future research

The main point of this work has been to demonstrate that relatively simple dyadic pursuit interactions can give rise to a diverse array of collective behaviors. In chapter 2 we analyzed planar cyclic CB pursuit systems and characterized existence of relative equilibria and pure shape equilibria. In chapter 3 we considered two low-dimensional planar cases, deriving explicit trajectory solutions in the mutual pursuit case, and providing an extensive stability analysis for the three-particle system. The insight gained from analysis of these low-dimensional systems provides a glimpse into the remarkable variety of collective behaviors attainable by cyclic CB pursuit, and serves as a primary contribution of this work. In chapter 4 we developed the three-dimensional version of CB pursuit, deriving a novel control law and considering the closed-loop cyclic CB pursuit dynamics, primarily for the mutual pursuit case.

Throughout our analysis of cyclic CB pursuit, we have regarded the CB pursuit parameters (α_i in the planar setting; a_i in the 3-D case) as fixed constants, and the most interesting direction for future research involves time-dependent variation of the CB pursuit parameters, either in a scheduled (i.e. open-loop) fashion or by means of feedback. Such time-variation of the pursuit parameters would introduce transient behaviors as the collective converges to the “new” CB pursuit manifold, but the effects of these transient behaviors could be minimized by varying the CB parameters slowly, so that the CB pursuit manifold evolves on a slow time-scale. We also hypothesize that periodic forcing of the CB parameters (and the induced periodic shape changes for the collective) could possibly achieve a prescribed direction of motion with respect to a fixed reference frame. Alternatively, feedback control of the CB parameters could be used to stabilize a particular desired shape (e.g. a circling equilibrium of a specified radius), which could be useful for applications such as surveillance or environmental sensing, which require coverage of a particular area. Such an approach is taken for a different type of model in [46], where the authors define a feedback policy for the CB parameters which (under certain assumptions on the initial conditions) ensures that the agents trace out a desired spiral formation.

In addition to varying the pursuit parameters, it would be interesting to consider a dynamic pursuit graph which models reassignment of pursuit targets. Such a pursuit graph could remain cyclic but occasionally prescribe a permuted agent order for cyclic pursuit. In regards to 3-D cyclic CB pursuit, future work will focus on determining stability properties of the three-particle case, and existence conditions for non-planar relative equilibria in the n-particle setting, such as helices and “stacked” circling equilibria.

In chapters 5 and 6 we considered the motion camouflage pursuit strategy and analyzed possible evader strategies. While the stochastic steering strategy of chapter 5 proved unsuccessful in countering the MC pursuit strategy in the face of speed domination by the pursuer, the (deterministic) evasion law introduced in chapter 6 was capable of forcing a circling equilibrium (stand-off scenario) under certain conditions. Future work includes stability analysis of the submanifolds referred to in (6.58), derivation of a 3-D version of the planar Anti-MC Evasion Law (6.18), and a game-theoretic study with regards to the pay-off function (6.16).

Appendix A

Proof of rotation matrix identities

Proof of (1.8):

(i) $\Longrightarrow$ (ii)

Nontriviality of the null space of $[R(2\theta) - I]$ implies that $\exists \mathbf{v} \neq \mathbf{0} \in \mathbb{R}^2$ such that $[R(2\theta) - I]\,\mathbf{v} = \mathbf{0}$, i.e. the matrix $[R(2\theta) - I]$ must be singular. Since

$$\begin{aligned} det|R(2\theta) - I| &= det\left|\begin{pmatrix} \cos(2\theta) & -\sin(2\theta) \\ \sin(2\theta) & \cos(2\theta) \end{pmatrix} - \begin{pmatrix} 1 & 0 \\ 0 & 1 \end{pmatrix}\right| \\ &= det\begin{vmatrix} \cos(2\theta) - 1 & -\sin(2\theta) \\ \sin(2\theta) & \cos(2\theta) - 1 \end{vmatrix} \\ &= \Big(\cos(2\theta) - 1\Big)^2 + \Big(\sin(2\theta)\Big)^2, \end{aligned}$$

we note that

$$det|R(2\theta) - I| = 0 \Longrightarrow \cos(2\theta) = 1 \text{ and } \sin(2\theta) = 0,$$

from which (ii) follows.

(ii) $\Longrightarrow$ (iii)

$$\begin{aligned}R(2\theta) = I &\Longrightarrow \cos(2\theta) = 1 \text{ and } \sin(2\theta) = 0\\ &\Longrightarrow \cos^2(\theta) - \sin^2(\theta) = 1 \text{ and } 2\sin(\theta)\cos(\theta) = 0\\ &\Longrightarrow \sin(\theta) = 0.\end{aligned}$$

(iii) $\Longrightarrow$ (i)

$$\begin{aligned}\sin(\theta) = 0 &\Longrightarrow \sin^2(\theta) = 0\\ &\Longrightarrow \cos^2(\theta) = 1\\ &\Longrightarrow \cos^2(\theta) - \sin^2(\theta) = 1 \text{ and } 2\sin(\theta)\cos(\theta) = 0\\ &\Longrightarrow \cos(2\theta) = 1 \text{ and } \sin(2\theta) = 0\\ &\Longrightarrow [R(2\theta) - I] = 0_{2\times 2}\\ &\Longrightarrow \mathcal{N}ull\,\{[R(2\theta) - I]\} = \mathbb{R}^2.\end{aligned}$$

$\square$

Proof of (1.13): We establish this identity by mathematical induction, first noting that

$$\prod_{i=1}^{2} h_i = \begin{pmatrix} B_1 & \mathbf{q}_1 \\ 0\,0 & 1 \end{pmatrix} \begin{pmatrix} B_2 & \mathbf{q}_2 \\ 0\,0 & 1 \end{pmatrix} = \begin{pmatrix} B_1 B_2 & \mathbf{q}_1 + B_1 \mathbf{q}_2 \\ 0\,0 & 1 \end{pmatrix}, \tag{A.1}$$

which corresponds with (1.13). Then assuming that (1.13) holds for k, we observe that

$$
\begin{aligned}
\prod_{i=1}^{k+1} h_i &= \left(\prod_{i=1}^{k} h_i\right) h_{k+1} \\
&= \begin{pmatrix} \prod_{j=1}^{k} B_j & \mathbf{q}_1 + \sum_{i=1}^{k-1} \left(\prod_{j=1}^{i} B_j\right) \mathbf{q}_{i+1} \\ 0 \quad 0 & 1 \end{pmatrix} \begin{pmatrix} B_{k+1} & \mathbf{q}_{k+1} \\ 0\,0 & 1 \end{pmatrix} \\
&= \begin{pmatrix} \prod_{j=1}^{k+1} B_j & \left(\prod_{j=1}^{k} B_j\right) \mathbf{q}_{k+1} + \mathbf{q}_1 + \sum_{i=1}^{k-1} \left(\prod_{j=1}^{i} B_j\right) \mathbf{q}_{i+1} \\ 0 \quad 0 & 1 \end{pmatrix} \\
&= \begin{pmatrix} \prod_{j=1}^{k+1} B_j & \mathbf{q}_1 + \sum_{i=1}^{k} \left(\prod_{j=1}^{i} B_j\right) \mathbf{q}_{i+1} \\ 0 \quad 0 & 1 \end{pmatrix}, \qquad \text{(A.2)}
\end{aligned}
$$

which completes the induction argument. □

Appendix B

Supplemental calculations for the proof of Proposition 2.4.1

Proof of (2.79): To establish (2.79), we must demonstrate that

$$\left[\mathbf{r}_{i-1} + \frac{\rho_{i-1}}{2\sin(\alpha_{i-1})}\mathbf{x}_{i-1}^{\perp}\right] - \left[\mathbf{r}_i + \frac{\rho_i}{2\sin(\alpha_i)}\mathbf{x}_i^{\perp}\right] = 0,\ i = 1, 2, \ldots, n. \tag{B.1}$$

First, by (2.35) (with $\kappa_i \equiv \alpha_i$) and (2.36), we have

$$\mathbf{x}_{i-1} = -\frac{1}{\rho_{i-1}} R(-\alpha_{i-1})(\mathbf{r}_{i-1} - \mathbf{r}_i),\ i = 1, 2, \ldots, n, \tag{B.2}$$

and

$$\mathbf{x}_i = \frac{1}{\rho_{i-1}} R(-\theta_i)(\mathbf{r}_{i-1} - \mathbf{r}_i),\ i = 1, 2, \ldots, n, \tag{B.3}$$

and substitution into the left-hand side of (B.1) yields

$$\begin{aligned}
&\left[\mathbf{r}_{i-1} + \frac{\rho_{i-1}}{2\sin(\alpha_{i-1})}\mathbf{x}_{i-1}^{\perp}\right] - \left[\mathbf{r}_i + \frac{\rho_i}{2\sin(\alpha_i)}\mathbf{x}_i^{\perp}\right] \\
&\quad = \left[\mathbf{r}_{i-1} + \frac{\rho_{i-1}}{2\sin(\alpha_{i-1})} R\left(\frac{\pi}{2}\right)\left(-\frac{1}{\rho_{i-1}} R(-\alpha_{i-1})(\mathbf{r}_{i-1} - \mathbf{r}_i)\right)\right] \\
&\qquad\qquad - \left[\mathbf{r}_i + \frac{\rho_i}{2\sin(\alpha_i)} R\left(\frac{\pi}{2}\right)\left(\frac{1}{\rho_{i-1}} R(-\theta_i)(\mathbf{r}_{i-1} - \mathbf{r}_i)\right)\right] \\
&\quad = (\mathbf{r}_{i-1} - \mathbf{r}_i) - \frac{1}{2\sin(\alpha_{i-1})} R\left(\frac{\pi}{2} - \alpha_{i-1}\right)(\mathbf{r}_{i-1} - \mathbf{r}_i) \\
&\qquad\qquad - \left(\frac{\rho_i}{\rho_{i-1}}\right)\frac{1}{2\sin(\alpha_i)} R\left(\frac{\pi}{2} - \theta_i\right)(\mathbf{r}_{i-1} - \mathbf{r}_i).
\end{aligned} \tag{B.4}$$

Then by substituting the equilibrium values for θ_i and $\frac{\rho_i}{\rho_{i-1}}$ given by the second case of (2.77), we can further simplify (B.4) to

$$\begin{aligned}
&\left\{\mathbb{1} - \frac{1}{2\sin(\alpha_{i-1})} R\left(\frac{\pi}{2} - \alpha_{i-1}\right)\right. \\
&\qquad \left. - \left(\frac{\sin(\alpha_i)}{\sin(\alpha_{i-1})}\right)\frac{1}{2\sin(\alpha_i)} R\left(\frac{\pi}{2} - (\pi - \alpha_{i-1})\right)\right\}(\mathbf{r}_{i-1} - \mathbf{r}_i)
\end{aligned} \tag{B.5}$$

which yields

$$\left\{\mathbb{1} - \frac{1}{2\sin(\alpha_{i-1})}\left[R\left(\frac{\pi}{2} - \alpha_{i-1}\right) + R\left(-\frac{\pi}{2} + \alpha_{i-1}\right)\right]\right\}(\mathbf{r}_{i-1} - \mathbf{r}_i). \tag{B.6}$$

By employing (1.7) we simplify (B.6) to

$$\left\{\mathbb{1} - \frac{1}{2\sin(\alpha_{i-1})} 2\cos\left(\frac{\pi}{2} - \alpha_{i-1}\right)\mathbb{1}\right\}(\mathbf{r}_{i-1} - \mathbf{r}_i), \tag{B.7}$$

and application of the trigonometric identity $\cos\left(\frac{\pi}{2} - \phi\right) = \sin(\phi)$ then establishes (B.1). $\square$

Proof of (2.89): Since

$$\sin(\alpha_n)\mathbb{1} + \sum_{i=1}^{n-1} \sin(\alpha_i) R\left(\sum_{j=1}^{i} (\alpha_j + \alpha_{j-1})\right) =$$

$$\sin(\alpha_n)\mathbb{1} + \sum_{i=1}^{n-1} \sin(\alpha_i) \begin{pmatrix} \cos\left(\sum_{j=1}^{i} (\alpha_j + \alpha_{j-1})\right) & -\sin\left(\sum_{j=1}^{i} (\alpha_j + \alpha_{j-1})\right) \\ \sin\left(\sum_{j=1}^{i} (\alpha_j + \alpha_{j-1})\right) & \cos\left(\sum_{j=1}^{i} (\alpha_j + \alpha_{j-1})\right) \end{pmatrix} \tag{B.8}$$

we will establish (2.89) by proving that

$$\begin{aligned} \sum_{i=1}^{n-1} \sin(\alpha_i) \sin\left(\sum_{j=1}^{i} (\alpha_j + \alpha_{j-1})\right) &= \sin\left(\sum_{i=1}^{n} \alpha_i\right) \sin\left(\sum_{i=1}^{n-1} \alpha_i\right), \\ \sin(\alpha_n) + \sum_{i=1}^{n-1} \sin(\alpha_i) \cos\left(\sum_{j=1}^{i} (\alpha_j + \alpha_{j-1})\right) &= \sin\left(\sum_{i=1}^{n} \alpha_i\right) \cos\left(\sum_{i=1}^{n-1} \alpha_i\right). \end{aligned} \tag{B.9}$$

Our main strategy in dealing with the $\sin\left(\sum_{j=1}^{i} (\alpha_j + \alpha_{j-1})\right)$ terms (and related cosine terms) is to factor out $\sin\left(\sum_{i=1}^{n} \alpha_i\right)$ and $\cos\left(\sum_{i=1}^{n} \alpha_i\right)$ and then use trigonometric identities to simplify. As a first step, one can verify that

$$\sum_{j=1}^{i} (\alpha_j + \alpha_{j-1}) = \begin{cases} \sum_{j=1}^{n} \alpha_j - \sum_{k=i+1}^{n-1} \alpha_k, & \text{for } i = 1 \\ \sum_{j=1}^{n} \alpha_j + \sum_{\ell=1}^{i-1} \alpha_\ell - \sum_{k=i+1}^{n-1} \alpha_k, & \text{for } 2 \le i \le n-2 \\ \sum_{j=1}^{n} \alpha_j + \sum_{\ell=1}^{i-1} \alpha_\ell, & \text{for } i = n-1. \end{cases} \tag{B.10}$$

Making use of (B.10) and appropriate trigonometric identities, we have

$$
\begin{aligned}
&\sum_{i=1}^{n-1} \sin(\alpha_i) \sin\left(\sum_{j=1}^{i} (\alpha_j + \alpha_{j-1})\right) = \\
&\qquad \sin(\alpha_1) \left[\sin\left(\sum_{j=1}^{n} \alpha_j\right) \cos\left(\sum_{k=2}^{n-1} \alpha_k\right) - \cos\left(\sum_{j=1}^{n} \alpha_j\right) \sin\left(\sum_{k=2}^{n-1} \alpha_k\right)\right] \\
&\qquad + \sum_{i=2}^{n-2} \sin(\alpha_i) \Bigg[\sin\left(\sum_{j=1}^{n} \alpha_j\right) \cos\left(\sum_{\ell=1}^{i-1} \alpha_\ell - \sum_{k=i+1}^{n-1} \alpha_k\right) \\
&\qquad\qquad + \cos\left(\sum_{j=1}^{n} \alpha_j\right) \sin\left(\sum_{\ell=1}^{i-1} \alpha_\ell - \sum_{k=i+1}^{n-1} \alpha_k\right)\Bigg] \\
&\qquad + \sin(\alpha_{n-1}) \left[\sin\left(\sum_{j=1}^{n} \alpha_j\right) \cos\left(\sum_{\ell=1}^{n-2} \alpha_\ell\right) + \cos\left(\sum_{j=1}^{n} \alpha_j\right) \sin\left(\sum_{\ell=1}^{n-2} \alpha_\ell\right)\right],
\end{aligned}
$$

and by factoring out $\sin\left(\sum_{i=1}^{n} \alpha_i\right)$ and $\cos\left(\sum_{i=1}^{n} \alpha_i\right)$, we are left with

$$
\begin{aligned}
&\sin\left(\sum_{j=1}^{n} \alpha_j\right) \Bigg[\sin(\alpha_1) \cos\left(\sum_{k=2}^{n-1} \alpha_k\right) + \sum_{i=2}^{n-2} \sin(\alpha_i) \cos\left(\sum_{\ell=1}^{i-1} \alpha_\ell - \sum_{k=i+1}^{n-1} \alpha_k\right) \\
&\qquad + \sin(\alpha_{n-1}) \cos\left(\sum_{\ell=1}^{n-2} \alpha_\ell\right)\Bigg] \\
&+ \cos\left(\sum_{j=1}^{n} \alpha_j\right) \Bigg[- \sin(\alpha_1) \sin\left(\sum_{k=2}^{n-1} \alpha_k\right) + \sum_{i=2}^{n-2} \sin(\alpha_i) \sin\left(\sum_{\ell=1}^{i-1} \alpha_\ell - \sum_{k=i+1}^{n-1} \alpha_k\right) \\
&\qquad + \sin(\alpha_{n-1}) \sin\left(\sum_{\ell=1}^{n-2} \alpha_\ell\right)\Bigg].
\end{aligned}
\tag{B.11}
$$

By application of the trigonometric product-to-sum identities

$$
\begin{aligned}
\sin(\theta) \cos(\phi) &= \frac{1}{2} \left[\sin(\theta - \phi) + \sin(\theta + \phi)\right], \\
\sin(\theta) \sin(\phi) &= \frac{1}{2} \left[\cos(\theta - \phi) - \cos(\theta + \phi)\right],
\end{aligned}
\tag{B.12}
$$

we can express (B.11) as

$$
\begin{aligned}
&\frac{1}{2}\sin\left(\sum_{j=1}^{n}\alpha_j\right)\Bigg\{\sin\left(\alpha_1-\sum_{k=2}^{n-1}\alpha_k\right)+\sin\left(\sum_{k=1}^{n-1}\alpha_k\right)\\
&\qquad+\sum_{i=2}^{n-2}\left[\sin\left(-\sum_{\ell=1}^{i-1}\alpha_\ell+\sum_{k=i}^{n-1}\alpha_k\right)+\sin\left(\sum_{\ell=1}^{i}\alpha_\ell-\sum_{k=i+1}^{n-1}\alpha_k\right)\right]\\
&\qquad\qquad+\sin\left(\alpha_{n-1}-\sum_{\ell=1}^{n-2}\alpha_\ell\right)+\sin\left(\sum_{\ell=1}^{n-1}\alpha_\ell\right)\Bigg\}\\
&+\frac{1}{2}\cos\left(\sum_{j=1}^{n}\alpha_j\right)\Bigg\{-\cos\left(\alpha_1-\sum_{k=2}^{n-1}\alpha_k\right)+\cos\left(\sum_{k=1}^{n-1}\alpha_k\right)\\
&\qquad+\sum_{i=2}^{n-2}\left[\cos\left(-\sum_{\ell=1}^{i-1}\alpha_\ell+\sum_{k=i}^{n-1}\alpha_k\right)-\cos\left(\sum_{\ell=1}^{i}\alpha_\ell-\sum_{k=i+1}^{n-1}\alpha_k\right)\right]\\
&\qquad\qquad+\cos\left(\alpha_{n-1}-\sum_{\ell=1}^{n-2}\alpha_\ell\right)-\cos\left(\sum_{\ell=1}^{n-1}\alpha_\ell\right)\Bigg\},
\end{aligned}
\tag{B.13}
$$

and since $\cos(-\phi)=\cos(\phi)$ and $\sin(-\phi)=-\sin(\phi)$, the interior summation (in each case) reduces to two terms. This gives us

$$
\begin{aligned}
&\frac{1}{2}\sin\left(\sum_{j=1}^{n}\alpha_j\right)\Bigg\{\sin\left(\alpha_1-\sum_{k=2}^{n-1}\alpha_k\right)+\sin\left(\sum_{k=1}^{n-1}\alpha_k\right)+\sin\left(-\alpha_1+\sum_{k=2}^{n-1}\alpha_k\right)\\
&\qquad+\sin\left(-\alpha_{n-1}+\sum_{\ell=1}^{n-2}\alpha_\ell\right)+\sin\left(\alpha_{n-1}-\sum_{\ell=1}^{n-2}\alpha_\ell\right)+\sin\left(\sum_{\ell=1}^{n-1}\alpha_\ell\right)\Bigg\}\\
&+\frac{1}{2}\cos\left(\sum_{j=1}^{n}\alpha_j\right)\Bigg\{-\cos\left(\alpha_1-\sum_{k=2}^{n-1}\alpha_k\right)+\cos\left(\sum_{k=1}^{n-1}\alpha_k\right)+\cos\left(-\alpha_1+\sum_{k=2}^{n-1}\alpha_k\right)\\
&\qquad-\cos\left(-\alpha_{n-1}+\sum_{\ell=1}^{n-2}\alpha_\ell\right)+\cos\left(\alpha_{n-1}-\sum_{\ell=1}^{n-2}\alpha_\ell\right)-\cos\left(\sum_{\ell=1}^{n-1}\alpha_\ell\right)\Bigg\},
\end{aligned}
\tag{B.14}
$$

and since the term enclosed in the second pair of braces sums to zero, our final expression is

$$
\sin\left(\sum_{i=1}^{n}\alpha_i\right)\sin\left(\sum_{i=1}^{n-1}\alpha_i\right). \tag{B.15}
$$

To establish the second equality in (B.9), we begin with

$$
\begin{aligned}
&\sum_{i=1}^{n-1} \sin(\alpha_i) \cos\left(\sum_{j=1}^{i} (\alpha_j + \alpha_{j-1})\right) = \\
&\qquad \sin(\alpha_1) \left[\cos\left(\sum_{j=1}^{n} \alpha_j\right) \cos\left(\sum_{k=2}^{n-1} \alpha_k\right) + \sin\left(\sum_{j=1}^{n} \alpha_j\right) \sin\left(\sum_{k=2}^{n-1} \alpha_k\right)\right] \\
&\qquad + \sum_{i=2}^{n-2} \sin(\alpha_i) \left[\cos\left(\sum_{j=1}^{n} \alpha_j\right) \cos\left(\sum_{\ell=1}^{i-1} \alpha_\ell - \sum_{k=i+1}^{n-1} \alpha_k\right) \right. \\
&\qquad\qquad \left. - \sin\left(\sum_{j=1}^{n} \alpha_j\right) \sin\left(\sum_{\ell=1}^{i-1} \alpha_\ell - \sum_{k=i+1}^{n-1} \alpha_k\right)\right] \\
&\qquad + \sin(\alpha_{n-1}) \left[\cos\left(\sum_{j=1}^{n} \alpha_j\right) \cos\left(\sum_{\ell=1}^{n-2} \alpha_\ell\right) - \sin\left(\sum_{j=1}^{n} \alpha_j\right) \sin\left(\sum_{\ell=1}^{n-2} \alpha_\ell\right)\right],
\end{aligned}
$$

which yields

$$
\begin{aligned}
&\sin\left(\sum_{j=1}^{n} \alpha_j\right) \left[\sin(\alpha_1) \sin\left(\sum_{k=2}^{n-1} \alpha_k\right) - \sum_{i=2}^{n-2} \sin(\alpha_i) \sin\left(\sum_{\ell=1}^{i-1} \alpha_\ell - \sum_{k=i+1}^{n-1} \alpha_k\right) \right. \\
&\qquad\qquad \left. - \sin(\alpha_{n-1}) \sin\left(\sum_{\ell=1}^{n-2} \alpha_\ell\right)\right] \\
&\quad + \cos\left(\sum_{j=1}^{n} \alpha_j\right) \left[\sin(\alpha_1) \cos\left(\sum_{k=2}^{n-1} \alpha_k\right) + \sum_{i=2}^{n-2} \sin(\alpha_i) \cos\left(\sum_{\ell=1}^{i-1} \alpha_\ell - \sum_{k=i+1}^{n-1} \alpha_k\right) \right. \\
&\qquad\qquad \left. + \sin(\alpha_{n-1}) \cos\left(\sum_{\ell=1}^{n-2} \alpha_\ell\right)\right].
\end{aligned} \tag{B.16}
$$

Observe that the bracketed terms are the same (with the exception of a sign change in the first term) as those in (B.11), and therefore we can use the previously established results to express (B.16) as

$$
\cos\left(\sum_{i=1}^{n} \alpha_i\right) \sin\left(\sum_{i=1}^{n-1} \alpha_i\right). \tag{B.17}
$$

The second equality in (B.9) is then established by

$$
\begin{aligned}
\sin(\alpha_n) &+ \sum_{i=1}^{n-1} \sin(\alpha_i) \cos\left(\sum_{j=1}^{i} (\alpha_j + \alpha_{j-1})\right) \\
&= \sin(\alpha_n) + \cos\left(\sum_{i=1}^{n} \alpha_i\right) \sin\left(-\alpha_n + \sum_{i=1}^{n} \alpha_i\right) \\
&= \sin(\alpha_n) + \cos\left(\sum_{i=1}^{n} \alpha_i\right) \left[\sin\left(\sum_{i=1}^{n} \alpha_i\right) \cos(\alpha_n) - \cos\left(\sum_{i=1}^{n} \alpha_i\right) \sin(\alpha_n)\right] \\
&= \sin(\alpha_n) \left[1 - \cos^2\left(\sum_{i=1}^{n} \alpha_i\right)\right] + \cos(\alpha_n) \cos\left(\sum_{i=1}^{n} \alpha_i\right) \sin\left(\sum_{i=1}^{n} \alpha_i\right) \\
&= \sin(\alpha_n) \sin^2\left(\sum_{i=1}^{n} \alpha_i\right) + \cos(\alpha_n) \cos\left(\sum_{i=1}^{n} \alpha_i\right) \sin\left(\sum_{i=1}^{n} \alpha_i\right) \\
&= \sin\left(\sum_{i=1}^{n} \alpha_i\right) \left[\sin(\alpha_n) \sin\left(\sum_{i=1}^{n} \alpha_i\right) + \cos(\alpha_n) \cos\left(\sum_{i=1}^{n} \alpha_i\right)\right] \\
&= \sin\left(\sum_{i=1}^{n} \alpha_i\right) \cos\left(\sum_{i=1}^{n-1} \alpha_i\right). \qquad \text{(B.18)}
\end{aligned}
$$

$\square$

Proof of (2.137): To establish the equivalence between (2.136) and (2.137), we must demonstrate that for n odd,

$$
\begin{aligned}
\sum_{i=1}^{n-1} \cos(\alpha_i) \sin\left(\sum_{j=1}^{i} (\pi + \alpha_j + \alpha_{j-1})\right) &= \cos\left(\sum_{i=1}^{n} \alpha_i\right) \sin\left(\sum_{i=1}^{n-1} \alpha_i\right), \\
\cos(\alpha_n) + \sum_{i=1}^{n-1} \cos(\alpha_i) \cos\left(\sum_{j=1}^{i} (\pi + \alpha_j + \alpha_{j-1})\right) &= \cos\left(\sum_{i=1}^{n} \alpha_i\right) \cos\left(\sum_{i=1}^{n-1} \alpha_i\right),
\end{aligned}
\qquad \text{(B.19)}
$$

and for n even,

$$\sum_{i=1}^{n-1} \cos(\alpha_i) \sin\left(\sum_{j=1}^{i} (\pi + \alpha_j + \alpha_{j-1})\right) = -\sin\left(\sum_{i=1}^{n} \alpha_i\right) \sin\left(\frac{\pi}{2} + \sum_{i=1}^{n-1} \alpha_i\right),$$
$$\cos(\alpha_n) + \sum_{i=1}^{n-1} \cos(\alpha_i) \cos\left(\sum_{j=1}^{i} (\pi + \alpha_j + \alpha_{j-1})\right) = -\sin\left(\sum_{i=1}^{n} \alpha_i\right) \cos\left(\frac{\pi}{2} + \sum_{i=1}^{n-1} \alpha_i\right). \tag{B.20}$$

Our strategy follows the same lines as the previous proof, and we begin by expressing the summation argument as

$$\sum_{j=1}^{i} (\pi + \alpha_j + \alpha_{j-1}) = \begin{cases} \pi + \sum_{j=1}^{n} \alpha_j - \sum_{k=i+1}^{n-1} \alpha_k, & \text{for } i = 1 \\ i\pi + \sum_{j=1}^{n} \alpha_j + \sum_{\ell=1}^{i-1} \alpha_\ell - \sum_{k=i+1}^{n-1} \alpha_k, & \text{for } 2 \le i \le n-2 \\ (n-1)\pi + \sum_{j=1}^{n} \alpha_j + \sum_{\ell=1}^{i-1} \alpha_\ell, & \text{for } i = n-1. \end{cases} \tag{B.21}$$

Then

$$\begin{aligned}
&\sum_{i=1}^{n-1} \cos(\alpha_i) \sin\left(\sum_{j=1}^{i} (\pi + \alpha_j + \alpha_{j-1})\right) = \\
&\quad \cos(\alpha_1)\left[\sin\left(\sum_{j=1}^{n} \alpha_j\right) \cos\left(\pi - \sum_{k=2}^{n-1} \alpha_k\right) + \cos\left(\sum_{j=1}^{n} \alpha_j\right) \sin\left(\pi - \sum_{k=2}^{n-1} \alpha_k\right)\right] \\
&\qquad + \sum_{i=2}^{n-2} \cos(\alpha_i)\left[\sin\left(\sum_{j=1}^{n} \alpha_j\right) \cos\left(i\pi + \sum_{\ell=1}^{i-1} \alpha_\ell - \sum_{k=i+1}^{n-1} \alpha_k\right)\right. \\
&\qquad\qquad \left. + \cos\left(\sum_{j=1}^{n} \alpha_j\right) \sin\left(i\pi + \sum_{\ell=1}^{i-1} \alpha_\ell - \sum_{k=i+1}^{n-1} \alpha_k\right)\right] \\
&\qquad + \cos(\alpha_{n-1})\left[\sin\left(\sum_{j=1}^{n} \alpha_j\right) \cos\left((n-1)\pi + \sum_{\ell=1}^{n-2} \alpha_\ell\right)\right. \\
&\qquad\qquad \left. + \cos\left(\sum_{j=1}^{n} \alpha_j\right) \sin\left((n-1)\pi + \sum_{\ell=1}^{n-2} \alpha_\ell\right)\right],
\end{aligned}$$

and by factoring out $\sin\left(\sum_{i=1}^{n}\alpha_i\right)$ and $\cos\left(\sum_{i=1}^{n}\alpha_i\right)$, we are left with

$$\begin{aligned}\sin\left(\sum_{j=1}^{n}\alpha_j\right)\Bigg[&\cos(\alpha_1)\cos\left(\pi-\sum_{k=2}^{n-1}\alpha_k\right)\\&+\sum_{i=2}^{n-2}\cos(\alpha_i)\cos\left(i\pi+\sum_{\ell=1}^{i-1}\alpha_\ell-\sum_{k=i+1}^{n-1}\alpha_k\right)\\&+\cos(\alpha_{n-1})\cos\left((n-1)\pi+\sum_{\ell=1}^{n-2}\alpha_\ell\right)\Bigg]\\+\cos\left(\sum_{j=1}^{n}\alpha_j\right)\Bigg[&\cos(\alpha_1)\sin\left(\pi-\sum_{k=2}^{n-1}\alpha_k\right)\\&+\sum_{i=2}^{n-2}\cos(\alpha_i)\sin\left(i\pi+\sum_{\ell=1}^{i-1}\alpha_\ell-\sum_{k=i+1}^{n-1}\alpha_k\right)\\&+\cos(\alpha_{n-1})\sin\left((n-1)\pi+\sum_{\ell=1}^{n-2}\alpha_\ell\right)\Bigg].\end{aligned}\tag{B.22}$$

Here we apply the trigonometric product-to-sum identities

$$\begin{aligned}\cos(\theta)\cos(\phi)&=\frac{1}{2}\left[\cos(\theta+\phi)+\cos(\theta-\phi)\right],\\\cos(\theta)\sin(\phi)&=\frac{1}{2}\left[\sin(\theta+\phi)-\sin(\theta-\phi)\right],\end{aligned}\tag{B.23}$$

to arrive at

$$
\begin{aligned}
&\frac{1}{2}\sin\left(\sum_{j=1}^{n}\alpha_j\right)\Bigg\{\cos\left(\pi+\alpha_1-\sum_{k=2}^{n-1}\alpha_k\right)+\cos\left(-\pi+\sum_{k=1}^{n-1}\alpha_k\right)\\
&\quad+\sum_{i=2}^{n-2}\left[\cos\left(i\pi+\sum_{\ell=1}^{i}\alpha_\ell-\sum_{k=i+1}^{n-1}\alpha_k\right)+\cos\left(-i\pi-\sum_{\ell=1}^{i-1}\alpha_\ell+\sum_{k=i}^{n-1}\alpha_k\right)\right]\\
&\qquad\qquad+\cos\left((n-1)\pi+\sum_{\ell=1}^{n-1}\alpha_\ell\right)+\cos\left(\alpha_{n-1}-(n-1)\pi-\sum_{\ell=1}^{n-2}\alpha_\ell\right)\Bigg\}\\
&+\frac{1}{2}\cos\left(\sum_{j=1}^{n}\alpha_j\right)\Bigg\{\sin\left(\pi+\alpha_1-\sum_{k=2}^{n-1}\alpha_k\right)-\sin\left(-\pi+\sum_{k=1}^{n-1}\alpha_k\right)\\
&\quad+\sum_{i=2}^{n-2}\left[\sin\left(i\pi+\sum_{\ell=1}^{i}\alpha_\ell-\sum_{k=i+1}^{n-1}\alpha_k\right)-\sin\left(-i\pi-\sum_{\ell=1}^{i-1}\alpha_\ell+\sum_{k=i}^{n-1}\alpha_k\right)\right]\\
&\qquad\qquad+\sin\left((n-1)\pi+\sum_{\ell=1}^{n-1}\alpha_\ell\right)-\sin\left(\alpha_{n-1}-(n-1)\pi-\sum_{\ell=1}^{n-2}\alpha_\ell\right)\Bigg\},
\end{aligned}
\tag{B.24}
$$

or the equivalent expression

$$
\begin{aligned}
&\frac{1}{2}\sin\left(\sum_{j=1}^{n}\alpha_j\right)\Bigg\{-\cos\left(\alpha_1-\sum_{k=2}^{n-1}\alpha_k\right)-\cos\left(\sum_{k=1}^{n-1}\alpha_k\right)\\
&\quad+\sum_{i=2}^{n-2}\left[(-1)^i\cos\left(\sum_{\ell=1}^{i}\alpha_\ell-\sum_{k=i+1}^{n-1}\alpha_k\right)+(-1)^i\cos\left(\sum_{\ell=1}^{i-1}\alpha_\ell-\sum_{k=i}^{n-1}\alpha_k\right)\right]\\
&\qquad\qquad+(-1)^{n-1}\cos\left(\sum_{\ell=1}^{n-1}\alpha_\ell\right)+(-1)^{n-1}\cos\left(\alpha_{n-1}-\sum_{\ell=1}^{n-2}\alpha_\ell\right)\Bigg\}\\
&+\frac{1}{2}\cos\left(\sum_{j=1}^{n}\alpha_j\right)\Bigg\{-\sin\left(\alpha_1-\sum_{k=2}^{n-1}\alpha_k\right)+\sin\left(\sum_{k=1}^{n-1}\alpha_k\right)\\
&\quad+\sum_{i=2}^{n-2}\left[(-1)^i\sin\left(\sum_{\ell=1}^{i}\alpha_\ell-\sum_{k=i+1}^{n-1}\alpha_k\right)+(-1)^i\sin\left(\sum_{\ell=1}^{i-1}\alpha_\ell-\sum_{k=i}^{n-1}\alpha_k\right)\right]\\
&\qquad\qquad+(-1)^{n-1}\sin\left(\sum_{\ell=1}^{n-1}\alpha_\ell\right)+(-1)^{n-1}\sin\left(-\alpha_{n-1}+\sum_{\ell=1}^{n-2}\alpha_\ell\right)\Bigg\}.
\end{aligned}
\tag{B.25}
$$

As before, the terms in brackets cancel pairwise yielding

$$\begin{aligned}
&\frac{1}{2}\sin\left(\sum_{j=1}^{n}\alpha_j\right)\Bigg\{-\cos\left(\alpha_1-\sum_{k=2}^{n-1}\alpha_k\right)-\cos\left(\sum_{k=1}^{n-1}\alpha_k\right)+(-1)^{n-2}\cos\left(-\alpha_{n-1}+\sum_{\ell=1}^{n-2}\alpha_\ell\right)\\
&\qquad+\cos\left(\alpha_1-\sum_{k=2}^{n-1}\alpha_k\right)+(-1)^{n-1}\cos\left(\sum_{\ell=1}^{n-1}\alpha_\ell\right)+(-1)^{n-1}\cos\left(\alpha_{n-1}-\sum_{\ell=1}^{n-2}\alpha_\ell\right)\Bigg\}\\
&+\frac{1}{2}\cos\left(\sum_{j=1}^{n}\alpha_j\right)\Bigg\{-\sin\left(\alpha_1-\sum_{k=2}^{n-1}\alpha_k\right)+\sin\left(\sum_{k=1}^{n-1}\alpha_k\right)+(-1)^{n-2}\sin\left(-\alpha_{n-1}+\sum_{\ell=1}^{n-2}\alpha_\ell\right)\\
&\qquad+\sin\left(\alpha_1-\sum_{k=2}^{n-1}\alpha_k\right)+(-1)^{n-1}\sin\left(\sum_{\ell=1}^{n-1}\alpha_\ell\right)+(-1)^{n-1}\sin\left(-\alpha_{n-1}+\sum_{\ell=1}^{n-2}\alpha_\ell\right)\Bigg\},
\end{aligned} \tag{B.26}$$

and consequently

$$\sum_{i=1}^{n-1}\cos(\alpha_i)\sin\left(\sum_{j=1}^{i}(\pi+\alpha_j+\alpha_{j-1})\right)=\begin{cases}\cos\left(\sum_{i=1}^{n}\alpha_i\right)\sin\left(\sum_{i=1}^{n-1}\alpha_i\right), & \text{for } n \text{ odd}\\ -\sin\left(\sum_{i=1}^{n}\alpha_i\right)\cos\left(\sum_{i=1}^{n-1}\alpha_i\right), & \text{for } n \text{ even.}\end{cases} \tag{B.27}$$

Turning to the second equality in (B.19) and (B.20), we begin with

$$\begin{aligned}
&\sum_{i=1}^{n-1}\cos(\alpha_i)\cos\left(\sum_{j=1}^{i}(\pi+\alpha_j+\alpha_{j-1})\right)=\\
&\quad\cos(\alpha_1)\left[\cos\left(\sum_{j=1}^{n}\alpha_j\right)\cos\left(\pi-\sum_{k=2}^{n-1}\alpha_k\right)-\sin\left(\sum_{j=1}^{n}\alpha_j\right)\sin\left(\pi-\sum_{k=2}^{n-1}\alpha_k\right)\right]\\
&\quad+\sum_{i=2}^{n-2}\cos(\alpha_i)\Bigg[\cos\left(\sum_{j=1}^{n}\alpha_j\right)\cos\left(i\pi+\sum_{\ell=1}^{i-1}\alpha_\ell-\sum_{k=i+1}^{n-1}\alpha_k\right)\\
&\qquad\qquad-\sin\left(\sum_{j=1}^{n}\alpha_j\right)\sin\left(i\pi+\sum_{\ell=1}^{i-1}\alpha_\ell-\sum_{k=i+1}^{n-1}\alpha_k\right)\Bigg]\\
&\quad+\cos(\alpha_{n-1})\Bigg[\cos\left(\sum_{j=1}^{n}\alpha_j\right)\cos\left((n-1)\pi+\sum_{\ell=1}^{n-2}\alpha_\ell\right)\\
&\qquad\qquad-\sin\left(\sum_{j=1}^{n}\alpha_j\right)\sin\left((n-1)\pi+\sum_{\ell=1}^{n-2}\alpha_\ell\right)\Bigg]
\end{aligned}$$

and factor out $\sin\left(\sum_{i=1}^{n}\alpha_i\right)$ and $\cos\left(\sum_{i=1}^{n}\alpha_i\right)$ to obtain

$$\begin{aligned}
\sin\left(\sum_{j=1}^{n}\alpha_j\right)\Bigg[&-\cos(\alpha_1)\sin\left(\pi-\sum_{k=2}^{n-1}\alpha_k\right)\\
&-\sum_{i=2}^{n-2}\cos(\alpha_i)\sin\left(i\pi+\sum_{\ell=1}^{i-1}\alpha_\ell-\sum_{k=i+1}^{n-1}\alpha_k\right)\\
&-\cos(\alpha_{n-1})\sin\left((n-1)\pi+\sum_{\ell=1}^{n-2}\alpha_\ell\right)\Bigg]\\
+\cos\left(\sum_{j=1}^{n}\alpha_j\right)\Bigg[&\cos(\alpha_1)\cos\left(\pi-\sum_{k=2}^{n-1}\alpha_k\right)\\
&+\sum_{i=2}^{n-2}\cos(\alpha_i)\cos\left(i\pi+\sum_{\ell=1}^{i-1}\alpha_\ell-\sum_{k=i+1}^{n-1}\alpha_k\right)\\
&+\cos(\alpha_{n-1})\cos\left((n-1)\pi+\sum_{\ell=1}^{n-2}\alpha_\ell\right)\Bigg].
\end{aligned}\tag{B.28}$$

Again, the terms in brackets are familiar from (B.22), and we can make use of previous results to obtain

$$\sum_{i=1}^{n-1}\cos(\alpha_i)\cos\left(\sum_{j=1}^{i}(\pi+\alpha_j+\alpha_{j-1})\right)=\begin{cases}-\sin\left(\sum_{i=1}^{n}\alpha_i\right)\sin\left(\sum_{i=1}^{n-1}\alpha_i\right), & \text{for } n \text{ odd}\\ -\cos\left(\sum_{i=1}^{n}\alpha_i\right)\cos\left(\sum_{i=1}^{n-1}\alpha_i\right), & \text{for } n \text{ even.}\end{cases}\tag{B.29}$$

Noting that, for n odd,

$$\begin{aligned}
&\cos(\alpha_n) + \sum_{i=1}^{n-1} \cos(\alpha_i) \cos\left(\sum_{j=1}^{i} (\pi + \alpha_j + \alpha_{j-1})\right) \\
&\quad = \cos(\alpha_n) - \sin\left(\sum_{i=1}^{n} \alpha_i\right) \sin\left(-\alpha_n + \sum_{i=1}^{n} \alpha_i\right) \\
&\quad = \cos(\alpha_n) - \sin\left(\sum_{i=1}^{n} \alpha_i\right) \left[\sin\left(\sum_{i=1}^{n} \alpha_i\right) \cos(\alpha_n) - \cos\left(\sum_{i=1}^{n} \alpha_i\right) \sin(\alpha_n)\right] \\
&\quad = \cos(\alpha_n) \left[1 - \sin^2\left(\sum_{i=1}^{n} \alpha_i\right)\right] + \sin(\alpha_n) \cos\left(\sum_{i=1}^{n} \alpha_i\right) \sin\left(\sum_{i=1}^{n} \alpha_i\right) \\
&\quad = \cos(\alpha_n) \cos^2\left(\sum_{i=1}^{n} \alpha_i\right) + \sin(\alpha_n) \cos\left(\sum_{i=1}^{n} \alpha_i\right) \sin\left(\sum_{i=1}^{n} \alpha_i\right) \\
&\quad = \cos\left(\sum_{i=1}^{n} \alpha_i\right) \left[\cos(\alpha_n) \cos\left(\sum_{i=1}^{n} \alpha_i\right) + \sin(\alpha_n) \sin\left(\sum_{i=1}^{n} \alpha_i\right)\right] \\
&\quad = \cos\left(\sum_{i=1}^{n} \alpha_i\right) \cos\left(\sum_{i=1}^{n-1} \alpha_i\right), \qquad \text{(B.30)}
\end{aligned}$$

and for n even,

$$\begin{aligned}
&\cos(\alpha_n) + \sum_{i=1}^{n-1} \cos(\alpha_i) \cos\left(\sum_{j=1}^{i} (\pi + \alpha_j + \alpha_{j-1})\right) \\
&\quad = \cos(\alpha_n) - \cos\left(\sum_{i=1}^{n} \alpha_i\right) \cos\left(-\alpha_n + \sum_{i=1}^{n} \alpha_i\right) \\
&\quad = \cos(\alpha_n) - \cos\left(\sum_{i=1}^{n} \alpha_i\right) \left[\cos\left(\sum_{i=1}^{n} \alpha_i\right) \cos(\alpha_n) + \sin\left(\sum_{i=1}^{n} \alpha_i\right) \sin(\alpha_n)\right] \\
&\quad = \cos(\alpha_n) \left[1 - \cos^2\left(\sum_{i=1}^{n} \alpha_i\right)\right] - \sin(\alpha_n) \cos\left(\sum_{i=1}^{n} \alpha_i\right) \sin\left(\sum_{i=1}^{n} \alpha_i\right) \\
&\quad = \cos(\alpha_n) \sin^2\left(\sum_{i=1}^{n} \alpha_i\right) - \sin(\alpha_n) \cos\left(\sum_{i=1}^{n} \alpha_i\right) \sin\left(\sum_{i=1}^{n} \alpha_i\right) \\
&\quad = \sin\left(\sum_{i=1}^{n} \alpha_i\right) \left[\cos(\alpha_n) \sin\left(\sum_{i=1}^{n} \alpha_i\right) - \sin(\alpha_n) \cos\left(\sum_{i=1}^{n} \alpha_i\right)\right] \\
&\quad = \sin\left(\sum_{i=1}^{n} \alpha_i\right) \sin\left(\sum_{i=1}^{n-1} \alpha_i\right), \qquad \text{(B.31)}
\end{aligned}$$

we have (B.19) and (B.20) by application of trigonometric identities. □

Appendix C

Supplemental calculations for three-particle planar cyclic CB pursuit analysis

Derivation of the elements for the general Jacobian matrix (3.64), (3.65), (3.66) and (3.67):

Making use of 3.61, we calculate as follows:

$$\begin{aligned}
\frac{\partial g_1}{\partial \theta_2} &= \frac{\partial P}{\partial \theta_2}\Big(e^{\tilde{\lambda}}\left[\sin(\alpha_1)+\sin(\theta_2)\right]-\sin(\alpha_2)\Big)+Pe^{\tilde{\lambda}}\cos(\theta_2)-\cos(\theta_2-\alpha_2-\alpha_3)\\
&= \frac{e^{\tilde{\lambda}}}{P}\sin(\theta_2-\alpha_2)\Big(e^{\tilde{\lambda}}\left[\sin(\alpha_1)+\sin(\theta_2)\right]-\sin(\alpha_2)\Big)\\
&\qquad + Pe^{\tilde{\lambda}}\cos(\theta_2)-\cos(\theta_2-\alpha_2-\alpha_3)\\
&= \frac{1}{P}\Big\{e^{2\tilde{\lambda}}\sin(\theta_2-\alpha_2)\left[\sin(\alpha_1)+\sin(\theta_2)\right]-e^{\tilde{\lambda}}\sin(\theta_2-\alpha_2)\sin(\alpha_2)\\
&\qquad + P^2e^{\tilde{\lambda}}\cos(\theta_2)-P\cos(\theta_2-\alpha_2-\alpha_3)\Big\}\\
&= \frac{1}{P}\Big\{e^{2\tilde{\lambda}}\sin(\theta_2-\alpha_2)\left[\sin(\alpha_1)+\sin(\theta_2)\right]-e^{\tilde{\lambda}}\sin(\theta_2-\alpha_2)\sin(\alpha_2)\\
&\qquad + \Big[e^{2\tilde{\lambda}}-2e^{\tilde{\lambda}}\cos(\theta_2-\alpha_2)+1\Big]e^{\tilde{\lambda}}\cos(\theta_2)-P\cos(\theta_2-\alpha_2-\alpha_3)\Big\}\\
&= \frac{1}{P}\Big\{e^{3\tilde{\lambda}}\cos(\theta_2)+e^{2\tilde{\lambda}}\Big(\sin(\theta_2-\alpha_2)\left[\sin(\alpha_1)+\sin(\theta_2)\right]-2\cos(\theta_2-\alpha_2)\cos(\theta_2)\Big)\\
&\qquad + e^{\tilde{\lambda}}\Big(\cos(\theta_2)-\sin(\theta_2-\alpha_2)\sin(\alpha_2)\Big)-P\cos(\theta_2-\alpha_2-\alpha_3)\Big\}, \quad \text{(C.1)}
\end{aligned}$$

$$
\begin{aligned}
\frac{\partial g_1}{\partial \tilde{\lambda}} &= \frac{\partial P}{\partial \tilde{\lambda}}\Big(e^{\tilde{\lambda}}\left[\sin(\alpha_1)+\sin(\theta_2)\right]-\sin(\alpha_2)\Big)+Pe^{\tilde{\lambda}}\left[\sin(\alpha_1)+\sin(\theta_2)\right]-e^{\tilde{\lambda}}\sin(\alpha_3)\\
&= \frac{e^{\tilde{\lambda}}}{P}\Big(e^{\tilde{\lambda}}-\cos(\theta_2-\alpha_2)\Big)\Big(e^{\tilde{\lambda}}\left[\sin(\alpha_1)+\sin(\theta_2)\right]-\sin(\alpha_2)\Big)\\
&\qquad\qquad +Pe^{\tilde{\lambda}}\left[\sin(\alpha_1)+\sin(\theta_2)\right]-e^{\tilde{\lambda}}\sin(\alpha_3)\\
&= \frac{e^{\tilde{\lambda}}}{P}\Big\{e^{2\tilde{\lambda}}\left[\sin(\alpha_1)+\sin(\theta_2)\right]-e^{\tilde{\lambda}}\Big(\sin(\alpha_2)+\cos(\theta_2-\alpha_2)\left[\sin(\alpha_1)+\sin(\theta_2)\right]\Big)\\
&\qquad\qquad +\cos(\theta_2-\alpha_2)\sin(\alpha_2)+P^2\left[\sin(\alpha_1)+\sin(\theta_2)\right]-P\sin(\alpha_3)\Big\}\\
&= \frac{e^{\tilde{\lambda}}}{P}\Big\{e^{2\tilde{\lambda}}\left[\sin(\alpha_1)+\sin(\theta_2)\right]-e^{\tilde{\lambda}}\Big(\sin(\alpha_2)+\cos(\theta_2-\alpha_2)\left[\sin(\alpha_1)+\sin(\theta_2)\right]\Big)\\
&\qquad\qquad +\cos(\theta_2-\alpha_2)\sin(\alpha_2)\\
&\qquad\qquad\quad +\Big[e^{2\tilde{\lambda}}-2e^{\tilde{\lambda}}\cos(\theta_2-\alpha_2)+1\Big]\left[\sin(\alpha_1)+\sin(\theta_2)\right]-P\sin(\alpha_3)\Big\}\\
&= \frac{e^{\tilde{\lambda}}}{P}\Big\{2e^{2\tilde{\lambda}}\left[\sin(\alpha_1)+\sin(\theta_2)\right]-e^{\tilde{\lambda}}\Big(\sin(\alpha_2)+3\cos(\theta_2-\alpha_2)\left[\sin(\alpha_1)+\sin(\theta_2)\right]\Big)\\
&\qquad\qquad +\cos(\theta_2-\alpha_2)\sin(\alpha_2)+\left[\sin(\alpha_1)+\sin(\theta_2)\right]-P\sin(\alpha_3)\Big\},
\end{aligned}
\tag{C.2}
$$

$$
\begin{aligned}
\frac{\partial g_2}{\partial \theta_2} &= \frac{\partial P}{\partial \theta_2}\Big(e^{\tilde{\lambda}}\left[\cos(\alpha_1)+\cos(\theta_2)\right]-\cos(\alpha_2)\Big)-Pe^{\tilde{\lambda}}\sin(\theta_2)-\sin(\theta_2-\alpha_2-\alpha_3)\\
&= \frac{e^{\tilde{\lambda}}}{P}\sin(\theta_2-\alpha_2)\Big(e^{\tilde{\lambda}}\left[\cos(\alpha_1)+\cos(\theta_2)\right]-\cos(\alpha_2)\Big)\\
&\qquad\qquad -Pe^{\tilde{\lambda}}\sin(\theta_2)-\sin(\theta_2-\alpha_2-\alpha_3)\\
&= \frac{1}{P}\Big\{e^{2\tilde{\lambda}}\sin(\theta_2-\alpha_2)\left[\cos(\alpha_1)+\cos(\theta_2)\right]-e^{\tilde{\lambda}}\sin(\theta_2-\alpha_2)\cos(\alpha_2)\\
&\qquad\qquad -P^2e^{\tilde{\lambda}}\sin(\theta_2)-P\sin(\theta_2-\alpha_2-\alpha_3)\Big\}\\
&= \frac{1}{P}\Big\{e^{2\tilde{\lambda}}\sin(\theta_2-\alpha_2)\left[\cos(\alpha_1)+\cos(\theta_2)\right]-e^{\tilde{\lambda}}\sin(\theta_2-\alpha_2)\cos(\alpha_2)\\
&\qquad\qquad -\Big[e^{2\tilde{\lambda}}-2e^{\tilde{\lambda}}\cos(\theta_2-\alpha_2)+1\Big]e^{\tilde{\lambda}}\sin(\theta_2)-P\sin(\theta_2-\alpha_2-\alpha_3)\Big\}\\
&= \frac{1}{P}\Big\{-e^{3\tilde{\lambda}}\sin(\theta_2)+e^{2\tilde{\lambda}}\Big(\sin(\theta_2-\alpha_2)\left[\cos(\alpha_1)+\cos(\theta_2)\right]+2\cos(\theta_2-\alpha_2)\sin(\theta_2)\Big)\\
&\qquad\qquad -e^{\tilde{\lambda}}\Big(\sin(\theta_2)+\sin(\theta_2-\alpha_2)\cos(\alpha_2)\Big)-P\sin(\theta_2-\alpha_2-\alpha_3)\Big\},
\end{aligned}
\tag{C.3}
$$

$$
\begin{aligned}
\frac{\partial g_2}{\partial \tilde{\lambda}} &= \frac{\partial P}{\partial \tilde{\lambda}}\Big(e^{\tilde{\lambda}}\left[\cos(\alpha_1)+\cos(\theta_2)\right]-\cos(\alpha_2)\Big)+Pe^{\tilde{\lambda}}\left[\cos(\alpha_1)+\cos(\theta_2)\right]-e^{\tilde{\lambda}}\cos(\alpha_3)\\
&= \frac{e^{\tilde{\lambda}}}{P}\Big(e^{\tilde{\lambda}}-\cos(\theta_2-\alpha_2)\Big)\Big(e^{\tilde{\lambda}}\left[\cos(\alpha_1)+\cos(\theta_2)\right]-\cos(\alpha_2)\Big)\\
&\qquad\quad +Pe^{\tilde{\lambda}}\left[\cos(\alpha_1)+\cos(\theta_2)\right]-e^{\tilde{\lambda}}\cos(\alpha_3)\\
&= \frac{e^{\tilde{\lambda}}}{P}\Big\{e^{2\tilde{\lambda}}\left[\cos(\alpha_1)+\cos(\theta_2)\right]-e^{\tilde{\lambda}}\Big(\cos(\alpha_2)+\cos(\theta_2-\alpha_2)\left[\cos(\alpha_1)+\cos(\theta_2)\right]\Big)\\
&\qquad\quad +\cos(\theta_2-\alpha_2)\cos(\alpha_2)+P^2\left[\cos(\alpha_1)+\cos(\theta_2)\right]-P\cos(\alpha_3)\Big\}\\
&= \frac{e^{\tilde{\lambda}}}{P}\Big\{e^{2\tilde{\lambda}}\left[\cos(\alpha_1)+\cos(\theta_2)\right]-e^{\tilde{\lambda}}\Big(\cos(\alpha_2)+\cos(\theta_2-\alpha_2)\left[\cos(\alpha_1)+\cos(\theta_2)\right]\Big)\\
&\qquad\quad +\cos(\theta_2-\alpha_2)\cos(\alpha_2)\\
&\qquad\qquad +\Big[e^{2\tilde{\lambda}}-2e^{\tilde{\lambda}}\cos(\theta_2-\alpha_2)+1\Big]\left[\cos(\alpha_1)+\cos(\theta_2)\right]-P\cos(\alpha_3)\Big\}\\
&= \frac{e^{\tilde{\lambda}}}{P}\Big\{2e^{2\tilde{\lambda}}\left[\cos(\alpha_1)+\cos(\theta_2)\right]-e^{\tilde{\lambda}}\Big(\cos(\alpha_2)+3\cos(\theta_2-\alpha_2)\left[\cos(\alpha_1)+\cos(\theta_2)\right]\Big)\\
&\qquad\quad +\cos(\theta_2-\alpha_2)\cos(\alpha_2)+\left[\cos(\alpha_1)+\cos(\theta_2)\right]-P\cos(\alpha_3)\Big\}. \qquad \text{(C.4)}
\end{aligned}
$$

Derivation of the Type 2 rectilinear equilibrium Jacobian matrix (3.79):

By (3.49), (3.51) and **Proposition 3.5.1**, the equilibrium values for $\theta_2, e^{\tilde{\lambda}}$, and P (at a Type 2 rectilinear equilibrium) are given by

$$
\theta_2=\pi+\alpha_1,\quad e^{\tilde{\lambda}}=\frac{\sin(\alpha_3-\alpha_1)}{\sin(\alpha_2-\alpha_3)},\quad P=\frac{\sin(\alpha_1-\alpha_2)}{\sin(\alpha_2-\alpha_3)}. \qquad \text{(C.5)}
$$

In anticipation of substituting these equilibrium values into the Jacobian matrix, we evaluate the following frequently appearing terms:

$$
\begin{aligned}
&\sin(\theta_2) = \sin(\pi + \alpha_1) = -\sin(\alpha_1),\\
&\cos(\theta_2) = \cos(\pi + \alpha_1) = -\cos(\alpha_1),\\
&\sin(\theta_2 - \alpha_2) = \sin(\pi + \alpha_1 - \alpha_2) = -\sin(\alpha_1 - \alpha_2),\\
&\cos(\theta_2 - \alpha_2) = \cos(\pi + \alpha_1 - \alpha_2) = -\cos(\alpha_1 - \alpha_2),\\
&\sin(\theta_2 - \alpha_2 - \alpha_3) = \sin(\pi + \alpha_1 - \alpha_2 - \alpha_3) = -\sin(\alpha_1 - \alpha_2 - \alpha_3),\\
&\cos(\theta_2 - \alpha_2 - \alpha_3) = \cos(\pi + \alpha_1 - \alpha_2 - \alpha_3) = -\cos(\alpha_1 - \alpha_2 - \alpha_3),\\
&\sin(\alpha_1) + \sin(\theta_2) = 0, \qquad \cos(\alpha_1) + \cos(\theta_2) = 0.
\end{aligned} \tag{C.6}
$$

We also note the following simplification:

$$
\begin{aligned}
&\sin^2(\alpha_3 - \alpha_1) + 2\sin(\alpha_3 - \alpha_1)\sin(\alpha_2 - \alpha_3)\cos(\alpha_1 - \alpha_2) + \sin^2(\alpha_2 - \alpha_3)\\
&\quad = \sin^2(\alpha_3 - \alpha_1) + 2\sin(\alpha_3 - \alpha_1)\sin(\alpha_2 - \alpha_3)\cos(\alpha_2 - \alpha_3 + \alpha_3 - \alpha_1) + \sin^2(\alpha_2 - \alpha_3)\\
&\quad = \sin^2(\alpha_3 - \alpha_1) + 2\sin(\alpha_3 - \alpha_1)\sin(\alpha_2 - \alpha_3)\cos(\alpha_2 - \alpha_3)\cos(\alpha_3 - \alpha_1)\\
&\qquad\qquad - 2\sin^2(\alpha_3 - \alpha_1)\sin^2(\alpha_2 - \alpha_3) + \sin^2(\alpha_2 - \alpha_3)\\
&\quad = \sin^2(\alpha_3 - \alpha_1)\left(1 - \sin^2(\alpha_2 - \alpha_3)\right) + \sin^2(\alpha_2 - \alpha_3)\left(1 - \sin^2(\alpha_3 - \alpha_1)\right)\\
&\qquad\qquad + 2\sin(\alpha_3 - \alpha_1)\sin(\alpha_2 - \alpha_3)\cos(\alpha_2 - \alpha_3)\cos(\alpha_3 - \alpha_1)\\
&\quad = \sin^2(\alpha_3 - \alpha_1)\cos^2(\alpha_2 - \alpha_3)) + \sin^2(\alpha_2 - \alpha_3)\cos^2(\alpha_3 - \alpha_1)\\
&\qquad\qquad\qquad\qquad + 2\sin(\alpha_3 - \alpha_1)\sin(\alpha_2 - \alpha_3)\cos(\alpha_2 - \alpha_3)\cos(\alpha_3 - \alpha_1\\
&\quad = \Big(\sin(\alpha_3 - \alpha_1)\cos(\alpha_2 - \alpha_3) + \sin(\alpha_2 - \alpha_3)(\alpha_3 - \alpha_1)\Big)^2\\
&\quad = \sin^2(\alpha_1 - \alpha_2).
\end{aligned} \tag{C.7}
$$

Then substituting into the elements of our Jacobian matrix, starting with (3.64),

we have

$$
\begin{aligned}
\frac{\partial g_1}{\partial \theta_2} &= \left(\frac{\sin(\alpha_2-\alpha_3)}{\sin(\alpha_1-\alpha_2)}\right)\Bigg\{\left(\frac{\sin(\alpha_3-\alpha_1)}{\sin(\alpha_2-\alpha_3)}\right)^3(-\cos(\alpha_1)) \\
&\quad + \left(\frac{\sin(\alpha_3-\alpha_1)}{\sin(\alpha_2-\alpha_3)}\right)^2\Big(-2\cos(\alpha_1)\cos(\alpha_1-\alpha_2)\Big) \\
&\quad + \left(\frac{\sin(\alpha_3-\alpha_1)}{\sin(\alpha_2-\alpha_3)}\right)\Big(-\cos(\alpha_1)+\sin(\alpha_1-\alpha_2)\sin(\alpha_2)\Big) \\
&\quad + \left(\frac{\sin(\alpha_1-\alpha_2)}{\sin(\alpha_2-\alpha_3)}\right)\cos(\alpha_1-\alpha_2-\alpha_3)\Bigg\} \\
&= \frac{1}{\sin(\alpha_1-\alpha_2)\sin^2(\alpha_2-\alpha_3)}\Bigg\{-\cos(\alpha_1)\sin^3(\alpha_3-\alpha_1) \\
&\quad - 2\sin^2(\alpha_3-\alpha_1)\sin(\alpha_2-\alpha_3)\cos(\alpha_1)\cos(\alpha_1-\alpha_2) \\
&\quad + \sin(\alpha_3-\alpha_1)\sin^2(\alpha_2-\alpha_3)\Big(-\cos(\alpha_1)+\sin(\alpha_1-\alpha_2)\sin(\alpha_2)\Big) \\
&\quad + \sin(\alpha_1-\alpha_2)\sin^2(\alpha_2-\alpha_3)\cos(\alpha_1-\alpha_2-\alpha_3)\Bigg\} \\
&= \frac{1}{\sin(\alpha_1-\alpha_2)\sin^2(\alpha_2-\alpha_3)}\Bigg\{-\cos(\alpha_1)\sin(\alpha_3-\alpha_1)\Big[\sin^2(\alpha_3-\alpha_1) \\
&\quad + 2\sin(\alpha_3-\alpha_1)\sin(\alpha_2-\alpha_3)\cos(\alpha_1-\alpha_2)+\sin^2(\alpha_2-\alpha_3)\Big] \\
&\quad + \sin(\alpha_1-\alpha_2)\sin^2(\alpha_2-\alpha_3)\Big[\sin(\alpha_3-\alpha_1)\sin(\alpha_2)+\cos(\alpha_2+\alpha_3-\alpha_1)\Big]\Bigg\} \\
&= \frac{1}{\sin(\alpha_1-\alpha_2)\sin^2(\alpha_2-\alpha_3)}\Bigg\{-\cos(\alpha_1)\sin(\alpha_3-\alpha_1)\sin^2(\alpha_1-\alpha_2) \\
&\quad + \sin(\alpha_1-\alpha_2)\sin^2(\alpha_2-\alpha_3)\Big[\sin(\alpha_3-\alpha_1)\sin(\alpha_2)+\cos(\alpha_2)\cos(\alpha_3-\alpha_1) \\
&\quad - \sin(\alpha_2)\sin(\alpha_3-\alpha_1)\Big]\Bigg\} \\
&= \frac{1}{\sin(\alpha_1-\alpha_2)\sin^2(\alpha_2-\alpha_3)}\Bigg\{-\cos(\alpha_1)\sin(\alpha_3-\alpha_1)\sin^2(\alpha_1-\alpha_2) \\
&\quad + \sin(\alpha_1-\alpha_2)\sin^2(\alpha_2-\alpha_3)\cos(\alpha_2)\cos(\alpha_3-\alpha_1)\Bigg\} \\
&= \frac{1}{\sin^2(\alpha_2-\alpha_3)}\Bigg\{-\cos(\alpha_1)\sin(\alpha_3-\alpha_1)\sin(\alpha_1-\alpha_2)
\end{aligned}
$$

$$+\cos(\alpha_2)\sin^2(\alpha_2-\alpha_3)\cos(\alpha_3-\alpha_1)\Bigg\}. \tag{C.8}$$

Likewise, we substitute into (3.65) and simplify by

$$\begin{aligned}
\frac{\partial g_1}{\partial\tilde{\lambda}} &= \left(\frac{\sin(\alpha_3-\alpha_1)}{\sin(\alpha_1-\alpha_2)}\right)\Bigg\{-\left(\frac{\sin(\alpha_3-\alpha_1)}{\sin(\alpha_2-\alpha_3)}\right)\sin(\alpha_2)-\cos(\alpha_1-\alpha_2)\sin(\alpha_2)\\
&\qquad -\left(\frac{\sin(\alpha_1-\alpha_2)}{\sin(\alpha_2-\alpha_3)}\right)\sin(\alpha_3)\Bigg\}\\
&= \frac{-\sin(\alpha_3-\alpha_1)}{\sin(\alpha_1-\alpha_2)\sin(\alpha_2-\alpha_3)}\Bigg\{\sin(\alpha_3-\alpha_1)\sin(\alpha_2)\\
&\qquad +\sin(\alpha_2-\alpha_3)\cos(\alpha_1-\alpha_2)\sin(\alpha_2)+\sin(\alpha_1-\alpha_2)\sin(\alpha_3)\Bigg\}\\
&= \frac{-\sin(\alpha_3-\alpha_1)}{\sin(\alpha_1-\alpha_2)\sin(\alpha_2-\alpha_3)}\Bigg\{\sin(\alpha_2)\Big[\sin(\alpha_3)\cos(\alpha_1)-\cos(\alpha_3)\sin(\alpha_1)\Big]\\
&\qquad +\sin(\alpha_3)\Big[\sin(\alpha_1)\cos(\alpha_2)-\cos(\alpha_1)\sin(\alpha_2)\Big]\\
&\qquad\quad +\sin(\alpha_2-\alpha_3)\cos(\alpha_1-\alpha_2)\sin(\alpha_2)\Bigg\}\\
&= \frac{-\sin(\alpha_3-\alpha_1)}{\sin(\alpha_1-\alpha_2)\sin(\alpha_2-\alpha_3)}\Bigg\{-\sin(\alpha_1)\Big[\sin(\alpha_2)\cos(\alpha_3)-\cos(\alpha_2)\sin(\alpha_3)\Big]\\
&\qquad +\sin(\alpha_2-\alpha_3)\cos(\alpha_1-\alpha_2)\sin(\alpha_2)\Bigg\}\\
&= \frac{\sin(\alpha_3-\alpha_1)}{\sin(\alpha_1-\alpha_2)}\Bigg\{\sin(\alpha_1)-\cos(\alpha_1-\alpha_2)\sin(\alpha_2)\Bigg\}\\
&= \frac{\sin(\alpha_3-\alpha_1)}{\sin(\alpha_1-\alpha_2)}\Bigg\{\sin(\alpha_1)-\cos(\alpha_1)\cos(\alpha_2)\sin(\alpha_2)-\sin(\alpha_1)\sin^2(\alpha_2)\Bigg\}\\
&= \frac{\sin(\alpha_3-\alpha_1)}{\sin(\alpha_1-\alpha_2)}\Bigg\{\sin(\alpha_1)\cos^2(\alpha_2)-\cos(\alpha_1)\cos(\alpha_2)\sin(\alpha_2)\Bigg\}\\
&= \frac{\sin(\alpha_3-\alpha_1)}{\sin(\alpha_1-\alpha_2)}\Bigg\{\cos(\alpha_2)\Big[\sin(\alpha_1)\cos(\alpha_2)-\cos(\alpha_1)\sin(\alpha_2)\Big]\Bigg\}\\
&= \cos(\alpha_2)\sin(\alpha_3-\alpha_1).
\end{aligned} \tag{C.9}$$

Once again making use of (C.7), we can express $\frac{\partial g_2}{\partial\theta_2}$ as

$$\frac{\partial g_2}{\partial\theta_2} = \left(\frac{\sin(\alpha_2-\alpha_3)}{\sin(\alpha_1-\alpha_2)}\right)\Bigg\{\left(\frac{\sin(\alpha_3-\alpha_1)}{\sin(\alpha_2-\alpha_3)}\right)^3\sin(\alpha_1)$$

$$+ 2\left(\frac{\sin(\alpha_3-\alpha_1)}{\sin(\alpha_2-\alpha_3)}\right)^2 \sin(\alpha_1)\cos(\alpha_1-\alpha_2)$$
$$+ \left(\frac{\sin(\alpha_3-\alpha_1)}{\sin(\alpha_2-\alpha_3)}\right)\Big(\sin(\alpha_1)+\sin(\alpha_1-\alpha_2)\cos(\alpha_2)\Big)$$
$$+ \left(\frac{\sin(\alpha_1-\alpha_2)}{\sin(\alpha_2-\alpha_3)}\right)\sin(\alpha_1-\alpha_2-\alpha_3)\Bigg\}$$
$$= \frac{1}{\sin(\alpha_1-\alpha_2)\sin^2(\alpha_2-\alpha_3)}\Bigg\{\sin(\alpha_1)\sin^3(\alpha_3-\alpha_1)$$
$$+ 2\sin^2(\alpha_3-\alpha_1)\sin(\alpha_2-\alpha_3)\sin(\alpha_1)\cos(\alpha_1-\alpha_2)$$
$$+ \sin(\alpha_3-\alpha_1)\sin^2(\alpha_2-\alpha_3)\Big(\sin(\alpha_1)+\sin(\alpha_1-\alpha_2)\cos(\alpha_2)\Big)$$
$$+ \sin(\alpha_1-\alpha_2)\sin^2(\alpha_2-\alpha_3)\sin(\alpha_1-\alpha_2-\alpha_3)\Bigg\}$$
$$= \frac{1}{\sin(\alpha_1-\alpha_2)\sin^2(\alpha_2-\alpha_3)}\Bigg\{\sin(\alpha_1)\sin(\alpha_3-\alpha_1)\Big[\sin^2(\alpha_3-\alpha_1)$$
$$+ 2\sin(\alpha_3-\alpha_1)\sin(\alpha_2-\alpha_3)\cos(\alpha_1-\alpha_2)+\sin^2(\alpha_2-\alpha_3)\Big]$$
$$+ \sin(\alpha_1-\alpha_2)\sin^2(\alpha_2-\alpha_3)\Big[\sin(\alpha_3-\alpha_1)\cos(\alpha_2)+\sin(\alpha_1-\alpha_3-\alpha_2)\Big]\Bigg\}$$
$$= \frac{1}{\sin(\alpha_1-\alpha_2)\sin^2(\alpha_2-\alpha_3)}\Bigg\{\sin(\alpha_1)\sin(\alpha_3-\alpha_1)\sin^2(\alpha_1-\alpha_2)$$
$$+ \sin(\alpha_1-\alpha_2)\sin^2(\alpha_2-\alpha_3)\Big[\sin(\alpha_3-\alpha_1)\cos(\alpha_2)$$
$$+ \sin(\alpha_1-\alpha_3)\cos(\alpha_2)-\cos(\alpha_1-\alpha_3)\sin(\alpha_2)\Big]\Bigg\}$$
$$= \frac{1}{\sin^2(\alpha_2-\alpha_3)}\Bigg\{\sin(\alpha_1)\sin(\alpha_3-\alpha_1)\sin(\alpha_1-\alpha_2)$$
$$- \sin(\alpha_2)\sin^2(\alpha_2-\alpha_3)\cos(\alpha_3-\alpha_1)\Bigg\}. \tag{C.10}$$

Lastly, we have

$$\frac{\partial g_2}{\partial\tilde{\lambda}} = \left(\frac{\sin(\alpha_3-\alpha_1)}{\sin(\alpha_1-\alpha_2)}\right)\Bigg\{-\left(\frac{\sin(\alpha_3-\alpha_1)}{\sin(\alpha_2-\alpha_3)}\right)\cos(\alpha_2)-\cos(\alpha_1-\alpha_2)\cos(\alpha_2)$$
$$- \left(\frac{\sin(\alpha_1-\alpha_2)}{\sin(\alpha_2-\alpha_3)}\right)\cos(\alpha_3)\Bigg\}$$

$$
\begin{aligned}
&= \frac{-\sin(\alpha_3-\alpha_1)}{\sin(\alpha_1-\alpha_2)\sin(\alpha_2-\alpha_3)}\Big\{\sin(\alpha_3-\alpha_1)\cos(\alpha_2) \\
&\quad + \sin(\alpha_2-\alpha_3)\cos(\alpha_1-\alpha_2)\cos(\alpha_2) + \sin(\alpha_1-\alpha_2)\cos(\alpha_3)\Big\} \\
&= \frac{-\sin(\alpha_3-\alpha_1)}{\sin(\alpha_1-\alpha_2)\sin(\alpha_2-\alpha_3)}\Big\{\cos(\alpha_2)\Big[\sin(\alpha_3)\cos(\alpha_1) - \cos(\alpha_3)\sin(\alpha_1)\Big] \\
&\quad + \cos(\alpha_3)\Big[\sin(\alpha_1)\cos(\alpha_2) - \cos(\alpha_1)\sin(\alpha_2)\Big] \\
&\qquad + \sin(\alpha_2-\alpha_3)\cos(\alpha_1-\alpha_2)\cos(\alpha_2)\Big\} \\
&= \frac{-\sin(\alpha_3-\alpha_1)}{\sin(\alpha_1-\alpha_2)\sin(\alpha_2-\alpha_3)}\Big\{-\cos(\alpha_1)\Big[\sin(\alpha_2)\cos(\alpha_3) - \cos(\alpha_2)\sin(\alpha_3)\Big] \\
&\quad + \sin(\alpha_2-\alpha_3)\cos(\alpha_1-\alpha_2)\cos(\alpha_2)\Big\} \\
&= \frac{\sin(\alpha_3-\alpha_1)}{\sin(\alpha_1-\alpha_2)}\Big\{\cos(\alpha_1) - \cos(\alpha_1-\alpha_2)\cos(\alpha_2)\Big\} \\
&= \frac{\sin(\alpha_3-\alpha_1)}{\sin(\alpha_1-\alpha_2)}\Big\{\cos(\alpha_1) - \cos(\alpha_1)\cos^2(\alpha_2) - \sin(\alpha_1)\sin(\alpha_2)\cos(\alpha_2)\Big\} \\
&= \frac{\sin(\alpha_3-\alpha_1)}{\sin(\alpha_1-\alpha_2)}\Big\{\cos(\alpha_1)\sin^2(\alpha_2) - \sin(\alpha_1)\sin(\alpha_2)\cos(\alpha_2)\Big\} \\
&= \frac{\sin(\alpha_3-\alpha_1)}{\sin(\alpha_1-\alpha_2)}\Big\{-\sin(\alpha_2)\Big[\sin(\alpha_1)\cos(\alpha_2) - \cos(\alpha_1)\sin(\alpha_2)\Big]\Big\} \\
&= -\sin(\alpha_2)\sin(\alpha_3-\alpha_1). \qquad \text{(C.11)}
\end{aligned}
$$

Proof of **Proposition 3.5.7**:

Proof. For notational simplicity, we denote $\tilde{\rho} \triangleq e^{\tilde{\lambda}}$ and

$$
\begin{aligned}
h_1(\alpha,\phi) &\triangleq \sin(\phi+\alpha) - \sin(\alpha), \\
h_2(\alpha,\phi) &\triangleq \cos(\phi+\alpha) - \cos(\alpha), \qquad \text{(C.12)}
\end{aligned}
$$

so that (3.105) can be expressed as

$$g_1(\alpha,\phi,\tilde{\rho}) = -P\left[h_1(\alpha,\phi)\tilde{\rho} + \sin(\alpha)\right] + \left[\tilde{\rho}\sin(\alpha) - \sin(\phi-\alpha)\right],$$

$$g_2(\alpha,\phi,\tilde{\rho}) = -P\left[h_2(\alpha,\phi)\tilde{\rho} + \cos(\alpha)\right] + \left[\tilde{\rho}\cos(\alpha) + \cos(\phi-\alpha)\right]. \tag{C.13}$$

We then proceed by analyzing the related quantities

$$\begin{aligned}
G_1(\alpha,\phi,\tilde{\rho}) &= g_1(\alpha,\phi,\tilde{\rho})\left(-P\left[h_1(\alpha,\phi)\tilde{\rho} + \sin(\alpha)\right] - \left[\tilde{\rho}\sin(\alpha) - \sin(\phi-\alpha)\right]\right) \\
&= \left(-P\left[h_1(\alpha,\phi)\tilde{\rho} + \sin(\alpha)\right] + \left[\tilde{\rho}\sin(\alpha) - \sin(\phi-\alpha)\right]\right) \times \\
&\qquad \left(-P\left[h_1(\alpha,\phi)\tilde{\rho} + \sin(\alpha)\right] - \left[\tilde{\rho}\sin(\alpha) - \sin(\phi-\alpha)\right]\right) \\
&= P^2\left[h_1(\alpha,\phi)\tilde{\rho} + \sin(\alpha)\right]^2 - \left[\tilde{\rho}\sin(\alpha) - \sin(\phi-\alpha)\right]^2 \\
&= \left(\tilde{\rho}^2 + 2\cos(\phi)\tilde{\rho} + 1\right)\left[\tilde{\rho}^2 h_1^2(\alpha,\phi) + 2\tilde{\rho}\sin(\alpha)h_1(\alpha,\phi) + \sin^2(\alpha)\right] \\
&\qquad - \left(\tilde{\rho}^2\sin^2(\alpha) - 2\tilde{\rho}\sin(\alpha)\sin(\phi-\alpha) + \sin^2(\phi-\alpha)\right) \\
&= \tilde{\rho}^4 h_1^2(\alpha,\phi) + \tilde{\rho}^3\left[2\sin(\alpha)h_1(\alpha,\phi) + 2\cos(\phi)h_1^2(\alpha,\phi)\right] \\
&\quad + \tilde{\rho}^2\left[\sin^2(\alpha) + h_1^2(\alpha,\phi) + 4\sin(\alpha)\cos(\phi)h_1(\alpha,\phi)\right] \\
&\qquad + \tilde{\rho}\left[2\sin^2(\alpha)\cos(\phi) + 2\sin(\alpha)h_1(\alpha,\phi)\right] \\
&\qquad\quad + \sin^2(\alpha) - \left(\tilde{\rho}^2\sin^2(\alpha) - 2\tilde{\rho}\sin(\alpha)\sin(\phi-\alpha) + \sin^2(\phi-\alpha)\right) \\
&= \tilde{\rho}^4 h_1^2(\alpha,\phi) + \tilde{\rho}^3\left[2\sin(\alpha)h_1(\alpha,\phi) + 2\cos(\phi)h_1^2(\alpha,\phi)\right] \\
&\quad + \tilde{\rho}^2\left[h_1^2(\alpha,\phi) + 4\sin(\alpha)\cos(\phi)h_1(\alpha,\phi)\right] \\
&\qquad + \tilde{\rho}\left[2\sin^2(\alpha)\cos(\phi) + 2\sin(\alpha)h_1(\alpha,\phi) + 2\sin(\alpha)\sin(\phi-\alpha)\right] \\
&\qquad\quad + \left[\sin^2(\alpha) - \sin^2(\phi-\alpha)\right] \\
&= \tilde{\rho}^4 h_1^2(\alpha,\phi) + 2\tilde{\rho}^3 h_1(\alpha,\phi)\left[\sin(\alpha) + \cos(\phi)h_1(\alpha,\phi)\right] \\
&\quad + \tilde{\rho}^2 h_1(\alpha,\phi)\left[h_1(\alpha,\phi) + 4\sin(\alpha)\cos(\phi)\right]
\end{aligned}$$

$$+ 2\tilde{\rho}\sin(\alpha)\left[\sin(\alpha)\cos(\phi) + h_1(\alpha,\phi) + \sin(\phi-\alpha)\right]$$

$$+ \left[\sin^2(\alpha) - \sin^2(\phi-\alpha)\right], \tag{C.14}$$

and

$$\begin{aligned}
G_2(\alpha,\phi,\tilde{\rho}) &= g_2(\alpha,\phi,\tilde{\rho})\left(-P\left[h_2(\alpha,\phi)\tilde{\rho} + \cos(\alpha)\right] - \left[\tilde{\rho}\cos(\alpha) + \cos(\phi-\alpha)\right]\right) \\
&= \left(-P\left[h_2(\alpha,\phi)\tilde{\rho} + \cos(\alpha)\right] + \left[\tilde{\rho}\cos(\alpha) + \cos(\phi-\alpha)\right]\right) \times \\
&\quad \left(-P\left[h_2(\alpha,\phi)\tilde{\rho} + \cos(\alpha)\right] - \left[\tilde{\rho}\cos(\alpha) + \cos(\phi-\alpha)\right]\right) \\
&= P^2\left[h_2(\alpha,\phi)\tilde{\rho} + \cos(\alpha)\right]^2 - \left[\tilde{\rho}\cos(\alpha) + \cos(\phi-\alpha)\right]^2 \\
&= \left(\tilde{\rho}^2 + 2\cos(\phi)\tilde{\rho} + 1\right)\left[\tilde{\rho}^2 h_2^2(\alpha,\phi) + 2\tilde{\rho}\cos(\alpha)h_2(\alpha,\phi) + \cos^2(\alpha)\right] \\
&\quad - \left(\tilde{\rho}^2\cos^2(\alpha) + 2\tilde{\rho}\cos(\alpha)\cos(\phi-\alpha) + \cos^2(\phi-\alpha)\right) \\
&= \tilde{\rho}^4 h_2^2(\alpha,\phi) + \tilde{\rho}^3\left[2\cos(\alpha)h_2(\alpha,\phi) + 2\cos(\phi)h_2^2(\alpha,\phi)\right] \\
&\quad + \tilde{\rho}^2\left[\cos^2(\alpha) + h_2^2(\alpha,\phi) + 4\cos(\alpha)\cos(\phi)h_2(\alpha,\phi)\right] \\
&\quad + \tilde{\rho}\left[2\cos^2(\alpha)\cos(\phi) + 2\cos(\alpha)h_2(\alpha,\phi)\right] \\
&\quad + \cos^2(\alpha) - \left(\tilde{\rho}^2\cos^2(\alpha) + 2\tilde{\rho}\cos(\alpha)\cos(\phi-\alpha) + \cos^2(\phi-\alpha)\right) \\
&= \tilde{\rho}^4 h_2^2(\alpha,\phi) + \tilde{\rho}^3\left[2\cos(\alpha)h_2(\alpha,\phi) + 2\cos(\phi)h_2^2(\alpha,\phi)\right] \\
&\quad + \tilde{\rho}^2\left[h_2^2(\alpha,\phi) + 4\cos(\alpha)\cos(\phi)h_2(\alpha,\phi)\right] \\
&\quad + \tilde{\rho}\left[2\cos^2(\alpha)\cos(\phi) + 2\cos(\alpha)h_2(\alpha,\phi) - 2\cos(\alpha)\cos(\phi-\alpha)\right] \\
&\quad + \left[\cos^2(\alpha) - \cos^2(\phi-\alpha)\right] \\
&= \tilde{\rho}^4 h_2^2(\alpha,\phi) + 2\tilde{\rho}^3 h_2(\alpha,\phi)\left[\cos(\alpha) + \cos(\phi)h_2(\alpha,\phi)\right] \\
&\quad + \tilde{\rho}^2 h_2(\alpha,\phi)\left[h_2(\alpha,\phi) + 4\cos(\alpha)\cos(\phi)\right] \\
&\quad + 2\tilde{\rho}\cos(\alpha)\left[\cos(\alpha)\cos(\phi) + h_2(\alpha,\phi) - \cos(\phi-\alpha)\right]
\end{aligned}$$

$$+\left[\cos^2(\alpha) - \cos^2(\phi-\alpha)\right]. \quad \text{(C.15)}$$

Viewing $G_1(\alpha,\phi,\tilde{\rho})$ and $G_2(\alpha,\phi,\tilde{\rho})$ as polynomials in $\tilde{\rho}$, we have

$$G_1(\alpha,\phi,\tilde{\rho}) = a_4(\alpha,\phi)\tilde{\rho}^4 + a_3(\alpha,\phi)\tilde{\rho}^3 + a_2(\alpha,\phi)\tilde{\rho}^2 + a_1(\alpha,\phi)\tilde{\rho} + a_0(\alpha,\phi), \quad \text{(C.16)}$$

where

$$\begin{aligned}
a_4(\alpha,\phi) &= h_1^2(\alpha,\phi),\\
a_3(\alpha,\phi) &= 2h_1(\alpha,\phi)\left[\sin(\alpha) + \cos(\phi)h_1(\alpha,\phi)\right],\\
a_2(\alpha,\phi) &= h_1(\alpha,\phi)\left[h_1(\alpha,\phi) + 4\sin(\alpha)\cos(\phi)\right],\\
a_1(\alpha,\phi) &= 2\sin(\alpha)\left[\sin(\alpha)\cos(\phi) + h_1(\alpha,\phi) + \sin(\phi-\alpha)\right],\\
a_0(\alpha,\phi) &= \sin^2(\alpha) - \sin^2(\phi-\alpha),
\end{aligned} \quad \text{(C.17)}$$

as well as

$$G_2(\alpha,\phi,\tilde{\rho}) = b_4(\alpha,\phi)\tilde{\rho}^4 + b_3(\alpha,\phi)\tilde{\rho}^3 + b_2(\alpha,\phi)\tilde{\rho}^2 + b_1(\alpha,\phi)\tilde{\rho} + b_0(\alpha,\phi), \quad \text{(C.18)}$$

where

$$\begin{aligned}
b_4(\alpha,\phi) &= h_2^2(\alpha,\phi),\\
b_3(\alpha,\phi) &= 2h_2(\alpha,\phi)\left[\cos(\alpha) + \cos(\phi)h_2(\alpha,\phi)\right],\\
b_2(\alpha,\phi) &= h_2(\alpha,\phi)\left[h_2(\alpha,\phi) + 4\cos(\alpha)\cos(\phi)\right],\\
b_1(\alpha,\phi) &= 2\cos(\alpha)\left[\cos(\alpha)\cos(\phi) + h_2(\alpha,\phi) - \cos(\phi-\alpha)\right],\\
b_0(\alpha,\phi) &= \cos^2(\alpha) - \cos^2(\phi-\alpha).
\end{aligned} \quad \text{(C.19)}$$

The proof proceeds by analyzing the sign of each of the $a_i(\alpha, \phi)$ and $b_i(\alpha, \phi)$ coefficient functions on $\Omega^+_{\alpha^+}$ and $\Omega^-_{\alpha^+}$ so that we can apply Descartes' sign rule to both G_1 and G_2.

Since on the interval $[0, \pi/2]$ the sine function is monotone increasing and the cosine function is monotone decreasing, we have

$$\begin{aligned} &\text{On } \Omega^+_{\alpha^+}: \quad h_1(\alpha, \phi) > 0,\ h_2(\alpha, \phi) > 0, \\ &\text{On } \Omega^-_{\alpha^+}: \quad h_1(\alpha, \phi) < 0,\ h_2(\alpha, \phi) > 0. \end{aligned} \tag{C.20}$$

Clearly $a_4(\alpha, \phi) > 0$ and $b_4(\alpha, \phi) > 0$ on both $\Omega^+_{\alpha^+}$ and $\Omega^-_{\alpha^+}$, and therefore we proceed by considering the remaining coefficients.

- $a_3(\alpha, \phi)$:
  - On $\Omega^+_{\alpha^+}$ we have $\sin(\alpha) > 0$, $\cos(\phi) > 0$ and $h_1(\alpha, \phi) > 0$, and therefore $a_3(\alpha, \phi) > 0$.
  - For the analysis on $\Omega^-_{\alpha^+}$, we express

    $$a_3(\alpha, \phi) = 2h_1(\alpha, \phi)\big\{\sin(\alpha) + \cos(\phi)\,[\sin(\phi + \alpha) - \sin(\alpha)]\big\} \tag{C.21}$$

    and then consider the term in braces. Making use of the various bounds applicable on $\Omega^-_{\alpha^+}$, we have

$$\begin{aligned}
&\sin(\alpha) + \cos(\phi)\left[\sin(\phi+\alpha) - \sin(\alpha)\right] \\
&\qquad = \sin(\alpha) + \cos(\phi)\left[\sin(\phi)\cos(\alpha) + \cos(\phi)\sin(\alpha) - \sin(\alpha)\right] \\
&\qquad = \sin(\alpha)\left[1 + \cos^2(\phi) - \cos(\phi)\right] + \cos(\phi)\sin(\phi)\cos(\alpha) \\
&\qquad \geq \sin(\alpha)\left[1 + \cos^2(\phi) - \cos(\phi)\right] - \cos(\phi)\sin(\alpha)\cos(\alpha) \\
&\qquad \geq \sin(\alpha)\left[1 + \cos^2(\phi) - \cos(\phi)\right] + \cos(\phi)\sin(\alpha)(-\cos(\phi)) \\
&\qquad \geq \sin(\alpha)\left[1 - \cos(\phi)\right] \\
&\qquad \geq 0,
\end{aligned} \tag{C.22}$$

and therefore since $h_1(\alpha,\phi) < 0$ on $\Omega^-_{\alpha^+}$, we have $a_3(\alpha,\phi) \leq 0$.

- $a_2(\alpha,\phi)$:
  - On $\Omega^+_{\alpha^+}$ we have $\sin(\alpha) > 0$, $\cos(\phi) > 0$ and $h_1(\alpha,\phi) > 0$, and therefore $a_2(\alpha,\phi) > 0$.
  - On $\Omega^-_{\alpha^+}$, we have

$$\begin{aligned}
h_1(\alpha,\phi) + 4\sin(\alpha)\cos(\phi) &= \sin(\phi+\alpha) - \sin(\alpha) + 4\sin(\alpha)\cos(\phi) \\
&= \sin(\phi)\cos(\alpha) - \sin(\alpha) + 5\sin(\alpha)\cos(\phi) \\
&\geq -\sin(\alpha)\cos(\alpha) - \sin(\alpha) + 5\sin(\alpha)\cos(\alpha) \\
&\geq \sin(\alpha)\left[4\cos(\alpha) - 1\right],
\end{aligned} \tag{C.23}$$

and

$$\begin{aligned}
h_1(\alpha,\phi) + 4\sin(\alpha)\cos(\phi) &= \sin(\phi)\cos(\alpha) - \sin(\alpha) + 5\sin(\alpha)\cos(\phi) \\
&\geq -\cos^2(\alpha) - \sin(\alpha) + 5\sin^2(\alpha) \\
&\geq (\sin^2(\alpha) - 1) - \sin(\alpha) + 5\sin^2(\alpha) \\
&\geq (2\sin(\alpha) - 1)(3\sin(\alpha) + 1)\,. \qquad \text{(C.24)}
\end{aligned}$$

Since (C.23) is positive for $\cos(\alpha) > 1/4$ and (C.24) is positive for $\sin(\alpha) > 1/2$, one can verify that $h_1(\alpha,\phi) + 4\sin(\alpha)\cos(\phi) \geq 0$ for $0 < \alpha < \pi/2$. Therefore $a_2(\alpha,\phi) \leq 0$ on $\Omega^-_{\alpha^+}$.

- $a_1(\alpha,\phi)$: First, observe that

$$\begin{aligned}
a_1(\alpha,\phi) &= 2\sin(\alpha)\left[\sin(\alpha)\cos(\phi) + h_1(\alpha,\phi) + \sin(\phi-\alpha)\right] \\
&= 2\sin(\alpha)\left[\sin(\alpha)\cos(\phi) - \sin(\alpha) + \sin(\phi+\alpha) + \sin(\phi-\alpha)\right] \\
&= 2\sin(\alpha)\big[\sin(\alpha)\cos(\phi) - \sin(\alpha) + \sin(\phi)\cos(\alpha) + \cos(\phi)\sin(\alpha) \\
&\qquad + \sin(\phi)\cos(\alpha) - \cos(\phi)\sin(\alpha)\big] \\
&= 2\sin(\alpha)\left[\sin(\alpha)\cos(\phi) - \sin(\alpha) + 2\sin(\phi)\cos(\alpha)\right]. \qquad \text{(C.25)}
\end{aligned}$$

– On $\Omega^+_{\alpha^+}$, we have

$$\begin{aligned}
a_1(\alpha,\phi) &= 2\sin(\alpha)\left[\sin(\alpha)\cos(\phi) - \sin(\alpha) + 2\sin(\phi)\cos(\alpha)\right] \\
&\geq 2\sin(\alpha)\left[\sin(\alpha)\cos(\phi) - \sin(\alpha) + 2\sin^2(\phi)\right] \\
&\geq 2\sin(\alpha)\left[\sin(\alpha)\cos(\phi) - \sin(\alpha) + 2 - 2\cos^2(\phi)\right] \\
&\geq 2\sin(\alpha)\Big(1-\cos(\phi)\Big)\Big(2-\sin(\alpha)+2\cos(\phi)\Big) \\
&\geq 2\sin(\alpha)\Big(1-\cos(\phi)\Big)\Big(2+\sin(\alpha)\Big) \\
&\geq 0. \qquad \text{(C.26)}
\end{aligned}$$

– On $\Omega^-_{\alpha^+}$ we have $\sin(\alpha) > 0$, $\cos(\alpha) > 0$, $\sin(\phi) < 0$, and $\cos(\phi) < 1$, and therefore $a_1(\alpha,\phi) < 0$.

- $a_0(\alpha,\phi)$: Since

$$\begin{aligned}
a_0(\alpha,\phi) &= \sin^2(\alpha) - \sin^2(\phi-\alpha) \\
&= \sin^2(\alpha) - \sin^2(\alpha-\phi) \qquad \text{(C.27)}
\end{aligned}$$

and $\sin^2(\cdot)$ is monotone increasing on the interval $[0,\pi/2]$, it holds that $a_0(\alpha,\phi) > 0$ on $\Omega^+_{\alpha^+}$ and $a_0(\alpha,\phi) < 0$ on $\Omega^-_{\alpha^+}$.

Similarly, we have the following for the coefficients listed in (C.19).

- $b_3(\alpha,\phi)$:

– On $\Omega^-_{\alpha^+}$ we have $\cos(\alpha) > 0$, $\cos(\phi) > 0$ and $h_2(\alpha,\phi) > 0$, and therefore $b_3(\alpha,\phi) > 0$.

- For the analysis on $\Omega^+_{\alpha^+}$, we express

$$b_3(\alpha,\phi) = 2h_2(\alpha,\phi)\big\{\cos(\alpha) + \cos(\phi)\left[\cos(\phi+\alpha) - \cos(\alpha)\right]\big\} \qquad \text{(C.28)}$$

  and then consider the term in braces. Making use of the various bounds applicable on $\Omega^+_{\alpha^+}$, we have

$$\begin{aligned}
&\cos(\alpha) + \cos(\phi)\left[\cos(\phi+\alpha) - \cos(\alpha)\right] \\
&\quad = \cos(\alpha) + \cos(\phi)\left[\cos(\phi)\cos(\alpha) - \sin(\phi)\sin(\alpha) - \cos(\alpha)\right] \\
&\quad = \cos(\alpha)\left[1 + \cos^2(\phi) - \cos(\phi)\right] + \cos(\phi)\sin(\alpha)(-\sin(\phi)) \\
&\quad \geq \cos(\alpha)\left[1 + \cos^2(\phi) - \cos(\phi)\right] + \cos(\phi)\sin(\alpha)(-\cos(\alpha)) \\
&\quad \geq \cos(\alpha)\left[1 + \cos^2(\phi) - \cos(\phi)\right] + \cos(\phi)(-\cos(\phi))\cos(\alpha) \\
&\quad \geq \cos(\alpha)\left[1 - \cos(\phi)\right] \\
&\quad \geq 0,
\end{aligned} \qquad \text{(C.29)}$$

  and therefore since $h_2(\alpha,\phi) < 0$ on $\Omega^+_{\alpha^+}$, we have $b_3(\alpha,\phi) \leq 0$.

- $b_2(\alpha,\phi)$:

  - On $\Omega^-_{\alpha^+}$ we have $\cos(\alpha) > 0$, $\cos(\phi) > 0$ and $h_2(\alpha,\phi) > 0$, and therefore $b_2(\alpha,\phi) > 0$.

  - On $\Omega^+_{\alpha^+}$, we have

$$\begin{aligned}
h_2(\alpha,\phi) + 4\cos(\alpha)\cos(\phi) &= \cos(\phi+\alpha) - \cos(\alpha) + 4\cos(\alpha)\cos(\phi) \\
&= 5\cos(\alpha)\cos(\phi) - \sin(\alpha)\sin(\phi) - \cos(\alpha) \\
&\geq 5\cos(\alpha)\sin(\alpha) - \sin(\alpha)\cos(\alpha) - \cos(\alpha) \\
&\geq \cos(\alpha)\left[4\sin(\alpha) - 1\right],
\end{aligned} \qquad \text{(C.30)}$$

and

$$
\begin{aligned}
h_2(\alpha,\phi) + 4\cos(\alpha)\cos(\phi) &= \cos(\phi+\alpha) - \cos(\alpha) + 4\cos(\alpha)\cos(\phi) \\
&\geq 5\cos^2(\alpha) - \sin^2(\alpha) - \cos(\alpha) \\
&\geq 5\cos^2(\alpha) - (1-\cos^2(\alpha)) - \cos(\alpha) \\
&\geq (2\cos(\alpha)-1)(3\cos(\alpha)+1). \qquad \text{(C.31)}
\end{aligned}
$$

Since (C.30) is positive for $\sin(\alpha) > 1/4$ and (C.31) is positive for $\cos(\alpha) > 1/2$, one can verify that $h_2(\alpha,\phi) + 4\cos(\alpha)\cos(\phi) \geq 0$ for $0 < \alpha < \pi/2$. Therefore $b_2(\alpha,\phi) \leq 0$ on $\Omega^+_{\alpha^+}$.

- $b_1(\alpha,\phi)$: First, observe that

$$
\begin{aligned}
b_1(\alpha,\phi) &= 2\cos(\alpha)\left[\cos(\alpha)\cos(\phi) + h_2(\alpha,\phi) - \cos(\phi-\alpha)\right] \\
&= 2\cos(\alpha)\left[\cos(\alpha)\cos(\phi) - \cos(\alpha) + \cos(\phi+\alpha) - \cos(\phi-\alpha)\right] \\
&= 2\cos(\alpha)\big[\cos(\alpha)\cos(\phi) - \cos(\alpha) + \cos(\alpha)\cos(\phi) - \sin(\alpha)\sin(\phi) \\
&\qquad - \cos(\alpha)\cos(\phi) - \sin(\alpha)\sin(\phi)\big] \\
&= 2\cos(\alpha)\left[\cos(\alpha)\cos(\phi) - \cos(\alpha) - 2\sin(\alpha)\sin(\phi)\right]. \qquad \text{(C.32)}
\end{aligned}
$$

  - On $\Omega^-_{\alpha^+}$, we have $-2\sin(\phi) > 0$ and $\sin(\alpha) \geq -\sin(\phi)$, and therefore $-2\sin(\phi)\sin(\alpha) \geq -2\sin(\phi)(-\sin(\phi)) = 2\sin^2(\phi)$. Applying this bound to (C.32), we have

$$\begin{aligned}
b_1(\alpha,\phi) &\geq 2\cos(\alpha)\left[\cos(\alpha)\cos(\phi) - \cos(\alpha) + 2\sin^2(\phi)\right] \\
&\geq 2\cos(\alpha)\left[\cos(\alpha)\cos(\phi) - \cos(\alpha) + 2 - 2\cos^2(\phi)\right] \\
&\geq 2\cos(\alpha)\Big(1-\cos(\phi)\Big)\Big(2-\cos(\alpha)+2\cos(\phi)\Big) \\
&\geq 2\cos(\alpha)\Big(1-\cos(\phi)\Big)\Big(2+\cos(\alpha)\Big) \\
&\geq 0. \qquad \text{(C.33)}
\end{aligned}$$

– On $\Omega^+_{\alpha^+}$, we have $\cos(\alpha) > 0$, $\cos(\phi) < 1$, $\sin(\alpha) > 0$, and $\sin(\phi) > 0$, and therefore $b_1(\alpha,\phi) < 0$.

- $b_0(\alpha,\phi)$: Since

$$\begin{aligned}
b_0(\alpha,\phi) &= \cos^2(\alpha) - \cos^2(\phi-\alpha) \\
&= \cos^2(\alpha) - \cos^2(\alpha-\phi) \qquad \text{(C.34)}
\end{aligned}$$

and $\cos^2(\cdot)$ is monotone decreasing on the interval $[0,\pi/2]$, it holds that $b_0(\alpha,\phi) > 0$ on $\Omega^-_{\alpha^+}$ and $b_0(\alpha,\phi) < 0$ on $\Omega^+_{\alpha^+}$.

We can now apply Descartes' sign rule to both G_1 and G_2 restricted to the sets $\Omega^+_{\alpha^+}$ and $\Omega^-_{\alpha^+}$.

- On $\Omega^+_{\alpha^+}$:
  – All $a_i(\alpha,\phi)$ coefficients are positive or zero, i.e. there are no sign variations between consecutive coefficients. Then according to the sign rule, G_1 (viewed as a polynomial in $\tilde{\rho}$) does not have any positive real roots on $\Omega^+_{\alpha^+}$. Therefore $G_1(\alpha,\phi,\tilde{\rho}) \neq 0$ at all points $(\alpha,\phi,\tilde{\rho}) \in \Omega^+_{\alpha^+}$.

– All $b_i(\alpha, \phi)$ coefficients (with the exception of $b_4(\alpha, \phi)$) are negative or zero, i.e. there is exactly one sign variation between consecutive coefficients. Then according to the sign rule, G_2 may have at most one positive real root on $\Omega^+_{\alpha^+}$. However, since G_2 is a fourth-order polynomial with all real coefficients, any complex roots must occur in complex conjugate pairs and therefore there must be an even number of real roots. Therefore G_2 does not have any positive real roots on $\Omega^+_{\alpha^+}$, i.e. $G_2(\alpha, \phi, \tilde{\rho}) \neq 0$ at all points $(\alpha, \phi, \tilde{\rho}) \in \Omega^+_{\alpha^+}$.

- On $\Omega^-_{\alpha^+}$:

  – All $a_i(\alpha, \phi)$ coefficients (with the exception of $a_4(\alpha, \phi)$) are negative or zero, and by the same reasoning used above, we have $G_1(\alpha, \phi, \tilde{\rho}) \neq 0$ at all points $(\alpha, \phi, \tilde{\rho}) \in \Omega^-_{\alpha^+}$.

  – All $b_i(\alpha, \phi)$ coefficients are positive or zero, i.e. $G_2(\alpha, \phi, \tilde{\rho}) \neq 0$ at all points $(\alpha, \phi, \tilde{\rho}) \in \Omega^-_{\alpha^+}$.

Recalling from (C.14) and (C.15) that $g_1(\alpha, \phi, \tilde{\rho})$ is a factor of $G_1(\alpha, \phi, \tilde{\rho})$ and $g_2(\alpha, \phi, \tilde{\rho})$ is a factor of $G_2(\alpha, \phi, \tilde{\rho})$, we observe that the previous results must apply to $g_1(\alpha, \phi, \tilde{\rho})$ and $g_2(\alpha, \phi, \tilde{\rho})$ as well, i.e.

$$g_1(\alpha, \phi, \tilde{\rho}) \neq 0 \text{ and } g_2(\alpha, \phi, \tilde{\rho}) \neq 0 \text{ at all points } (\alpha, \phi, \tilde{\rho}) \in \Omega^+_{\alpha^+} \cup \Omega^-_{\alpha^+}. \tag{C.35}$$

Finally, we note that $\Omega^+_{\alpha^+}$ and $\Omega^-_{\alpha^+}$ can each be viewed as connected subsets of $\mathbb{R}^3$, and therefore they each have the Intermediate Value Property, i.e. any continuous function $f : \Omega^+_{\alpha^+} \longrightarrow \mathbb{R}$ (or $f : \Omega^-_{\alpha^+} \longrightarrow \mathbb{R}$) has an interval as its image. Since g_i

(for $i = 1, 2$) is continuous on both $\Omega^+_{\alpha^+}$ and $\Omega^-_{\alpha^+}$, the image of $g_i : \Omega^+_{\alpha^+} \longrightarrow \mathbb{R}$ and the image of $g_i : \Omega^-_{\alpha^+} \longrightarrow \mathbb{R}$ are both intervals *which do not include the value 0* (by the result of (C.35)). Therefore in each case the image is either entirely positive or entirely negative. One can resolve the sign ambiguity by evaluating g_i at any point $(\alpha, \phi, \tilde{\rho})$ in the respective sets $\Omega^+_{\alpha^+}$ and $\Omega^-_{\alpha^+}$. For example, we can evaluate g_1 at the point $(\pi/4, \pi/12, 1) \in \Omega^+_{\alpha^+}$ to get

$$\begin{aligned} g_1(\pi/4, \pi/12, 1) &= -\sqrt{2 + 2\cos(\pi/12)}\sin(\pi/12 + \pi/4) + [\sin(\pi/4) - \sin(\pi/12 - \pi/4)] \\ &= -\sqrt{2 + 2\cos(\pi/12)}\sin(\pi/3) + \sin(\pi/4) - \sin(-\pi/6) \\ &= -\sqrt{2 + 2\cos(\pi/12)}(\sqrt{3}/2) + (\sqrt{2}/2) + (1/2) \\ &= (1/2)\left(-\sqrt{6 + 6\cos(\pi/12)} + \sqrt{2} + 1\right) \\ &< 0, \end{aligned} \tag{C.36}$$

establishing that $g_1(\alpha, \phi, \tilde{\rho}) < 0$ on $\Omega^+_{\alpha^+}$. By analogous calculations, one can verify the remaining claims of the proposition. □

Derivation of (3.120):

Note that

$$\frac{\partial P}{\partial \tilde{\lambda}} = \frac{1}{2P}(2e^{2\tilde{\lambda}} + 2\delta e^{\tilde{\lambda}}) = \frac{e^{\tilde{\lambda}}}{P}\left(e^{\tilde{\lambda}} + \delta\right), \tag{C.37}$$

and therefore

$$\begin{aligned} \frac{d^2\delta}{d\tilde{\lambda}^2} = \frac{-1}{\left(Pe^{\tilde{\lambda}} + 1\right)^2}\Bigg\{ &\left(\frac{\partial P}{\partial \tilde{\lambda}}(e^{\tilde{\lambda}} - \delta e^{\tilde{\lambda}} - 1) + P(e^{\tilde{\lambda}} - \delta e^{\tilde{\lambda}}) + e^{\tilde{\lambda}}\right)\left(Pe^{\tilde{\lambda}} + 1\right) \\ &+ \left(P(e^{\tilde{\lambda}} - \delta e^{\tilde{\lambda}} - 1) + (e^{\tilde{\lambda}} + \delta)\right)\left(\frac{\partial P}{\partial \tilde{\lambda}}e^{\tilde{\lambda}} + Pe^{\tilde{\lambda}}\right)\Bigg\} \end{aligned}$$

$$
\begin{aligned}
&= \frac{-1}{\left(Pe^{\tilde{\lambda}}+1\right)^2}\Bigg\{\left(\frac{e^{\tilde{\lambda}}}{P}\left(e^{\tilde{\lambda}}+\delta\right)\left(e^{\tilde{\lambda}}-\delta e^{\tilde{\lambda}}-1\right)+Pe^{\tilde{\lambda}}(1-\delta)+e^{\tilde{\lambda}}\right)\left(Pe^{\tilde{\lambda}}+1\right) \\
&\qquad -\left(P\left(e^{\tilde{\lambda}}-\delta e^{\tilde{\lambda}}-1\right)+\left(e^{\tilde{\lambda}}+\delta\right)\right)\left(\frac{e^{\tilde{\lambda}}}{P}\left(e^{\tilde{\lambda}}+\delta\right)e^{\tilde{\lambda}}+Pe^{\tilde{\lambda}}\right)\Bigg\} \\
&= \frac{-e^{\tilde{\lambda}}}{P\left(Pe^{\tilde{\lambda}}+1\right)^2}\Bigg\{\left(\left(e^{\tilde{\lambda}}+\delta\right)\left(e^{\tilde{\lambda}}-\delta e^{\tilde{\lambda}}-1\right)+P^2(1-\delta)+P\right)\left(Pe^{\tilde{\lambda}}+1\right) \\
&\qquad -\left(P\left(e^{\tilde{\lambda}}-\delta e^{\tilde{\lambda}}-1\right)+\left(e^{\tilde{\lambda}}+\delta\right)\right)\left(e^{\tilde{\lambda}}\left(e^{\tilde{\lambda}}+\delta\right)+P^2\right)\Bigg\} \\
&= \frac{-e^{\tilde{\lambda}}}{P\left(Pe^{\tilde{\lambda}}+1\right)^2}\Bigg\{\left(e^{\tilde{\lambda}}+\delta\right)\left(e^{\tilde{\lambda}}-\delta e^{\tilde{\lambda}}-1\right)+P^3e^{\tilde{\lambda}}(1-\delta)+P^2\left(1-\delta+e^{\tilde{\lambda}}\right) \\
&\qquad +P\left(1+e^{\tilde{\lambda}}\left(e^{\tilde{\lambda}}+\delta\right)\left(e^{\tilde{\lambda}}-\delta e^{\tilde{\lambda}}-1\right)\right) \\
&\qquad\quad -\Bigg(P^3\left(e^{\tilde{\lambda}}-\delta e^{\tilde{\lambda}}-1\right)+P^2\left(e^{\tilde{\lambda}}+\delta\right) \\
&\qquad\qquad +Pe^{\tilde{\lambda}}\left(e^{\tilde{\lambda}}+\delta\right)\left(e^{\tilde{\lambda}}-\delta e^{\tilde{\lambda}}-1\right)+e^{\tilde{\lambda}}\left(e^{\tilde{\lambda}}+\delta\right)^2\Bigg)\Bigg\} \\
&= \frac{-e^{\tilde{\lambda}}}{P\left(Pe^{\tilde{\lambda}}+1\right)^2}\Bigg\{P^3+P^2\left(1-2\delta\right)+P \\
&\qquad +\left(e^{\tilde{\lambda}}+\delta\right)\left(e^{\tilde{\lambda}}-\delta e^{\tilde{\lambda}}-1\right)-e^{\tilde{\lambda}}\left(e^{\tilde{\lambda}}+\delta\right)^2\Bigg\} \\
&= \frac{-e^{\tilde{\lambda}}}{P\left(Pe^{\tilde{\lambda}}+1\right)^2}\Bigg\{\left(e^{2\tilde{\lambda}}+2\delta e^{\tilde{\lambda}}+1\right)\left(P+1-2\delta\right)+P \\
&\qquad +\left(e^{\tilde{\lambda}}+\delta\right)\left(-e^{2\tilde{\lambda}}+(1-2\delta)e^{\tilde{\lambda}}-1\right)\Bigg\} \\
&= \frac{-e^{\tilde{\lambda}}}{P\left(Pe^{\tilde{\lambda}}+1\right)^2}\Bigg\{P\left(e^{2\tilde{\lambda}}+2\delta e^{\tilde{\lambda}}+2\right)+\left(e^{2\tilde{\lambda}}+2\delta e^{\tilde{\lambda}}+1\right)\left(1-2\delta\right) \\
&\qquad -e^{3\tilde{\lambda}}+e^{2\tilde{\lambda}}(1-3\delta)+e^{\tilde{\lambda}}(-2\delta^2+\delta-1)-\delta\Bigg\} \\
&= \frac{-e^{\tilde{\lambda}}}{P\left(Pe^{\tilde{\lambda}}+1\right)^2}\Bigg\{P\left(e^{2\tilde{\lambda}}+2\delta e^{\tilde{\lambda}}+2\right)-e^{3\tilde{\lambda}}+e^{2\tilde{\lambda}}(2-5\delta) \\
&\qquad +e^{\tilde{\lambda}}(-6\delta^2+3\delta-1)+(1-3\delta)\Bigg\}. \qquad\qquad (C.38)
\end{aligned}
$$

Proof of **Proposition 3.5.11**:

Proof. Define the term in the braces from (3.120) as $b : D_{\delta,\tilde{\lambda}} \longrightarrow \mathbb{R}$,

$$b(\delta,\tilde{\lambda}) = P\left(e^{2\tilde{\lambda}} + 2\delta e^{\tilde{\lambda}} + 2\right) - e^{3\tilde{\lambda}} + e^{2\tilde{\lambda}}(2-5\delta) + e^{\tilde{\lambda}}(-6\delta^2 + 3\delta - 1) + (1-3\delta), \tag{C.39}$$

so that

$$\frac{d^2\delta}{d\tilde{\lambda}^2} = \frac{-e^{\tilde{\lambda}}}{P\left(Pe^{\tilde{\lambda}}+1\right)^2} b(\delta,\tilde{\lambda}). \tag{C.40}$$

We prove the proposition by demonstrating that $b(\delta,\tilde{\lambda}) > 0$ on the set $\Big\{(\delta,\tilde{\lambda}) \in D_{\delta,\tilde{\lambda}} \;\Big|\; \delta \in [1/25, 1)\Big\}$. To simplify notation in the ensuing analysis, we denote $\tilde{\rho} \triangleq e^{\tilde{\lambda}}$ so that

$$b(\delta,\tilde{\rho}) = P\left(\tilde{\rho}^2 + 2\delta\tilde{\rho} + 2\right) + \Big(-\tilde{\rho}^3 + \tilde{\rho}^2(2-5\delta) + \tilde{\rho}(-6\delta^2 + 3\delta - 1) + (1-3\delta)\Big), \tag{C.41}$$

i.e. b maps $D_{\delta,\tilde{\rho}} \longrightarrow \mathbb{R}$ where

$$D_{\delta,\tilde{\rho}} = \left\{[-1,1] \times \mathbb{R}^+\right\} - \{(-1,1)\}. \tag{C.42}$$

We proceed by analyzing the related expression

$$\begin{aligned} B(\delta,\tilde{\rho}) = b(\delta,\tilde{\rho})\Big[&P\left(\tilde{\rho}^2 + 2\delta\tilde{\rho} + 2\right) \\ &- \Big(-\tilde{\rho}^3 + \tilde{\rho}^2(2-5\delta) + \tilde{\rho}(-6\delta^2 + 3\delta - 1) + (1-3\delta)\Big)\Big] \\ = \Big[&P\left(\tilde{\rho}^2 + 2\delta\tilde{\rho} + 2\right) + \Big(-\tilde{\rho}^3 + \tilde{\rho}^2(2-5\delta) + \tilde{\rho}(-6\delta^2 + 3\delta - 1) + (1-3\delta)\Big)\Big] \times \\ &\Big[P\left(\tilde{\rho}^2 + 2\delta\tilde{\rho} + 2\right) - \Big(-\tilde{\rho}^3 + \tilde{\rho}^2(2-5\delta) + \tilde{\rho}(-6\delta^2 + 3\delta - 1) + (1-3\delta)\Big)\Big] \\ = P^2&\left(\tilde{\rho}^2 + 2\delta\tilde{\rho} + 2\right)^2 - \Big(-\tilde{\rho}^3 + \tilde{\rho}^2(2-5\delta) + \tilde{\rho}(-6\delta^2 + 3\delta - 1) + (1-3\delta)\Big)^2. \end{aligned} \tag{C.43}$$

Upon substitution of $P = \sqrt{(\tilde{\rho}^2 + 2\delta\tilde{\rho} + 1)}$, the first term simplifies to

$$\begin{aligned}
&\left(\tilde{\rho}^2 + 2\delta\tilde{\rho} + 1\right)\left(\tilde{\rho}^4 + 4\delta\tilde{\rho}^3 + 4\left(1+\delta^2\right)\tilde{\rho}^2 + 8\delta\tilde{\rho} + 4\right) \\
&\quad = \tilde{\rho}^6 + 6\delta\tilde{\rho}^5 + (12\delta^2+5)\tilde{\rho}^4 + (8\delta^3+20\delta)\tilde{\rho}^3 + (20\delta^2+8)\tilde{\rho}^2 + 16\delta\tilde{\rho} + 4, \quad \text{(C.44)}
\end{aligned}$$

and the second term of (C.43) simplifies to

$$\begin{aligned}
-\Big(&\tilde{\rho}^6 + (10\delta-4)\tilde{\rho}^5 + (37\delta^2 - 26\delta + 6)\tilde{\rho}^4 + (60\delta^3 - 54\delta^2 + 28\delta - 6)\tilde{\rho}^3 \\
&+ (36\delta^4 - 36\delta^3 + 51\delta^2 - 28\delta + 5)\tilde{\rho}^2 \\
&\quad + (36\delta^3 - 30\delta^2 + 12\delta - 2)\tilde{\rho} + (9\delta^2 - 6\delta + 1)\Big). \qquad \text{(C.45)}
\end{aligned}$$

Therefore we can express (C.43) as

$$\begin{aligned}
B(\delta,\tilde{\rho}) &= -(4\delta-4)\tilde{\rho}^5 - (25\delta^2 - 26\delta + 1)\tilde{\rho}^4 - (52\delta^3 - 54\delta^2 + 8\delta - 6)\tilde{\rho}^3 \\
&\qquad - (36\delta^4 - 36\delta^3 + 31\delta^2 - 28\delta - 3)\tilde{\rho}^2 - (36\delta^3 - 30\delta^2 - 4\delta - 2)\tilde{\rho} \\
&\qquad\quad - (9\delta^2 - 6\delta - 3) \\
&= (1-\delta)\Big\{4\tilde{\rho}^5 + (25\delta - 1)\tilde{\rho}^4 + (52\delta^2 - 2\delta + 6)\tilde{\rho}^3 \\
&\qquad + (36\delta^3 + 31\delta + 3)\tilde{\rho}^2 + (36\delta^2 + 6\delta + 2)\tilde{\rho} + (9\delta + 3)\Big\}. \qquad \text{(C.46)}
\end{aligned}$$

Considering the quantity in (C.46) as a polynomial in $\tilde{\rho}$ with coefficients parametrized by δ, one can verify that for $\delta \in [1/25, 1)$ all the coefficients are non-negative and therefore (by Descartes' sign rule) the parametrized polynomial has no positive real roots. Since any pair $(\delta, \tilde{\rho})$ satisfying $b(\delta,\tilde{\rho}) = 0$ must also satisfy $B(\delta,\tilde{\rho}) = 0$, we conclude that $b(\delta,\tilde{\rho}) \neq 0$ on the set $\left\{(\delta,\tilde{\rho}) \in D_{\delta,\tilde{\rho}} \;\middle|\; \delta \in [1/25, 1)\right\}$. Note that b is a continuous function on a connected subset of $\mathbb{R}^2$, and therefore the Intermediate Value Theorem applies (i.e. the image of b is an interval). We have already demonstrated that zero is not included in the image when b is restricted to the smaller subset $[1/25, 1) \times \mathbb{R}^+$, and therefore the image must be an interval that is entirely positive or entirely negative. We resolve the ambiguity by testing a particular point such as $(\delta = 1/2, \tilde{\rho} = 1)$, demonstrating that $b(1/2, 1) = 4\sqrt{3} - 3 > 0$. Therefore $b > 0$ (and hence $\frac{d^2\delta}{d\tilde{\lambda}^2} < 0$) on the entire set $\left\{(\delta, \tilde{\rho}) \in D_{\delta,\tilde{\rho}} \;\middle|\; \delta \in [1/25, 1)\right\}$. $\square$

Derivation of the circling equilibrium Jacobian matrix (3.148): This can be derived directly by substituting (2.75) into the Jacobian matrix elements and then simplifying through a sequence of trigonometric manipulations, analogous to the calculations for the pure shape equilibrium linearization (3.156) detailed next in this appendix. Since the calculations are similar, we will instead establish (3.148) by demonstrating that it follows from (3.156) under the circling equilibrium existence conditions.

If a circling equilibrium exists for the three-particle case, then $\{\alpha_1, \alpha_2, \alpha_3\}$ must satisfy $\sin\left(\sum_{i=1}^3 \alpha_i\right) = 0$ and $\sin(\alpha_{i-1})\sin(\alpha_i) > 0,\ i = 1, 2, 3$. Since $\alpha_i \in [0, 2\pi],\ i = 1, 2, 3$, this is only possible if one of the following four cases holds:

- $\alpha_i \in (0, \pi),\ i = 1, 2, 3$, and $\sum_{i=1}^3 \alpha_i = \pi$,
- $\alpha_i \in (0, \pi),\ i = 1, 2, 3$, and $\sum_{i=1}^3 \alpha_i = 2\pi$,
- $\alpha_i \in (\pi, 2\pi),\ i = 1, 2, 3$, and $\sum_{i=1}^3 \alpha_i = 4\pi$,
- $\alpha_i \in (\pi, 2\pi),\ i = 1, 2, 3$, and $\sum_{i=1}^3 \alpha_i = 5\pi$.

From **Remark 2.4.5**, we note that circling equilibria are a special case of pure shape equilibria for which $\sin(\tau_k) = 0$, and therefore if a three-particle circling equilibrium exists, then there must exist $\hat{k} \in \{1, 2\}$ such that $\sin(\tau_{\hat{k}}) = 0$, where

$\tau_{\hat{k}} = -\frac{\hat{k}\pi}{3} + \frac{1}{3}\sum_{i=1}^{3}\alpha_i$. In the following table, we identify the value of $\hat{k}$ for each of the cases listed above:

	$\sum_{i=1}^{3}\alpha_i$	$\hat{k}$	$\tau_{\hat{k}}$	$\cos(\hat{k}\pi)$	$\cos(\tau_{\hat{k}})$	$\cos\left(\sum_{i=1}^{3}\alpha_i\right)$
$\alpha_i \in (0,\pi),\ i=1,2,3$	π	1	0	-1	1	-1
$\alpha_i \in (0,\pi),\ i=1,2,3$	2π	2	0	1	1	1
$\alpha_i \in (\pi,2\pi),\ i=1,2,3$	4π	1	π	-1	-1	1
$\alpha_i \in (\pi,2\pi),\ i=1,2,3$	5π	2	π	1	-1	-1

The most significant observation here is that in every case $\cos(\hat{k}\pi)/\cos(\tau_{\hat{k}}) = \cos\left(\sum_{i=1}^{3}\alpha_i\right)$, and therefore we can substitute $\cos\left(\sum_{i=1}^{3}\alpha_i\right)$ as appropriate into the elements of (3.156). Then since substitution of either $\tau_k = 0$ or $\tau_k = \pi$ into (3.157) yields

$$\begin{aligned}
S_1 &= \sin(\alpha_1+\alpha_2) + \sin(\alpha_1)\cos(\alpha_2),\\
S_2 &= \sin(\alpha_1+\alpha_2) + \sin(\alpha_2)\cos(\alpha_1),\\
C &= \sin(\alpha_1)\sin(\alpha_2),\\
D &= \sin^2(\alpha_1+\alpha_2) - \sin(\alpha_1)\sin(\alpha_2)\cos(\alpha_1)\cos(\alpha_2),
\end{aligned} \tag{C.47}$$

it is apparent that (3.148) follows from (3.156).

Derivation of the pure shape equilibrium Jacobian matrix (3.156): By **Proposition 2.4.2** and (3.51), the equilibrium values for θ_2 and $e^{\tilde{\lambda}}$ (at a pure shape equilibrium) are given by

$$\theta_2 = \pi - \alpha_1 + 2\tau_k, \quad e^{\tilde{\lambda}} = \frac{\sin(\alpha_2 - \tau_k)}{\sin(\alpha_1 - \tau_k)}, \tag{C.48}$$

and by (3.49) and **Proposition 2.4.2**, we have[1]

$$\begin{aligned} P &= \frac{\sin(\alpha_3 - \tau_k)}{\sin(\alpha_1 - \tau_k)} \\ &= \frac{\sin\big((\alpha_3 - 3\tau_k) + 2\tau_k\big)}{\sin(\alpha_1 - \tau_k)} \\ &= \frac{\sin\big((k\pi - \alpha_1 - \alpha_2\big) + 2\tau_k)}{\sin(\alpha_1 - \tau_k)} \\ &= \frac{-\cos(k\pi)\sin(\alpha_1 + \alpha_2 - 2\tau_k)}{\sin(\alpha_1 - \tau_k)}. \end{aligned} \tag{C.49}$$

where

$$\tau_k = -\frac{k\pi}{3} + \sum_{i=1}^{3} \frac{\alpha_i}{3}. \tag{C.50}$$

We also note the following useful simplification:

$$\begin{aligned} &\sin^2(\alpha_2 - \tau_k) + 2\cos(\alpha_1 + \alpha_2 - 2\tau_k)\sin(\alpha_1 - \tau_k)\sin(\alpha_2 - \tau_k) + \sin^2(\alpha_1 - \tau_k) \\ &= \sin^2(\alpha_2 - \tau_k) + 2\cos(\alpha_1 - \tau_k)\cos(\alpha_2 - \tau_k)\sin(\alpha_1 - \tau_k)\sin(\alpha_2 - \tau_k) \\ &\qquad - 2\sin^2(\alpha_1 - \tau_k)\sin^2(\alpha_2 - \tau_k) + \sin^2(\alpha_1 - \tau_k) \\ &= \sin^2(\alpha_2 - \tau_k)\big(1 - \sin^2(\alpha_1 - \tau_k)\big) + \sin^2(\alpha_1 - \tau_k)\big(1 - \sin^2(\alpha_2 - \tau_k)\big) \\ &\qquad + 2\cos(\alpha_1 - \tau_k)\cos(\alpha_2 - \tau_k)\sin(\alpha_1 - \tau_k)\sin(\alpha_2 - \tau_k) \\ &= \sin^2(\alpha_2 - \tau_k)\cos^2(\alpha_1 - \tau_k) + \sin^2(\alpha_1 - \tau_k)\cos^2(\alpha_2 - \tau_k) \\ &\qquad + 2\cos(\alpha_1 - \tau_k)\cos(\alpha_2 - \tau_k)\sin(\alpha_1 - \tau_k)\sin(\alpha_2 - \tau_k) \\ &= \big(\sin(\alpha_1 - \tau_k)\cos(\alpha_2 - \tau_k) + \cos(\alpha_1 - \tau_k)\sin(\alpha_2 - \tau_k)\big)^2 \\ &= \sin^2(\alpha_1 + \alpha_2 - 2\tau_k). \end{aligned} \tag{C.51}$$

[1] This can also be derived by direct substitution of (C.48) into (3.52).

In anticipation of substituting (C.48) and (C.49) into the Jacobian matrix, we note that the equilibrium values satisfy

$$
\begin{aligned}
&\sin(\theta_2) = \sin(\pi - \alpha_1 + 2\tau_k) = \sin(\alpha_1 - 2\tau_k),\\
&\cos(\theta_2) = \cos(\pi - \alpha_1 + 2\tau_k) = -\cos(\alpha_1 - 2\tau_k),\\
&\sin(\theta_2 - \alpha_2) = \sin(\pi - \alpha_1 + 2\tau_k - \alpha_2) = \sin(\alpha_1 + \alpha_2 - 2\tau_k),\\
&\cos(\theta_2 - \alpha_2) = \cos(\pi - \alpha_1 + 2\tau_k - \alpha_2) = -\cos(\alpha_1 + \alpha_2 - 2\tau_k),\\
&\alpha_3 - \tau_k = (\alpha_3 - 3\tau_k) + 2\tau_k = \left(\alpha_3 + k\pi - \sum_{i=1}^{3}\alpha_i\right) + 2\tau_k = k\pi - \alpha_1 - \alpha_2 + 2\tau_k,\\
&\theta_2 - \alpha_2 - \alpha_3 = \pi + 2\tau_k - \sum_{i=1}^{3}\alpha_i = \left(\pi + 3\tau_k - \sum_{i=1}^{3}\alpha_i\right) - \tau_k = \pi(1-k) - \tau_k,
\end{aligned}
\tag{C.52}
$$

from which it follows that

$$
\begin{aligned}
\sin(\alpha_1) + \sin(\theta_2) &= \sin\big((\alpha_1 - \tau_k) + \tau_k\big) + \sin(\alpha_1 - \tau_k)\cos(\tau_k) - \cos(\alpha_1 - \tau_k)\sin(\tau_k)\\
&= 2\sin(\alpha_1 - \tau_k)\cos(\tau_k),\\
\cos(\alpha_1) + \cos(\theta_2) &= \cos\big((\alpha_1 - \tau_k) + \tau_k\big) - \cos(\alpha_1 - \tau_k)\cos(\tau_k) - \sin(\alpha_1 - \tau_k)\sin(\tau_k)\\
&= -2\sin(\alpha_1 - \tau_k)\sin(\tau_k),\\
\sin(\alpha_3 - \tau_k) &= \sin(k\pi - \alpha_1 - \alpha_2 + 2\tau_k) = -\cos(k\pi)\sin(\alpha_1 + \alpha_2 - 2\tau_k),\\
\cos(\alpha_3 - \tau_k) &= \cos(k\pi - \alpha_1 - \alpha_2 + 2\tau_k) = \cos(k\pi)\cos(\alpha_1 + \alpha_2 - 2\tau_k),\\
\sin(\theta_2 - \alpha_2 - \alpha_3) &= \sin\big(\pi(1-k) - \tau_k\big) = -\cos\big(\pi(1-k)\big)\sin(\tau_k) = \cos(k\pi)\sin(\tau_k),\\
\cos(\theta_2 - \alpha_2 - \alpha_3) &= \cos\big(\pi(1-k) - \tau_k\big) = \cos\big(\pi(1-k)\big)\cos(\tau_k) = -\cos(k\pi)\cos(\tau_k).
\end{aligned}
\tag{C.53}
$$

We then substitute into the elements of our Jacobian matrix, starting with

(3.64), to obtain

$$
\begin{aligned}
\frac{\partial g_1}{\partial \theta_2} = K\Bigg\{ &- \left(\frac{\sin(\alpha_2 - \tau_k)}{\sin(\alpha_1 - \tau_k)}\right)^3 \cos(\alpha_1 - 2\tau_k) \\
&+ \left(\frac{\sin(\alpha_2 - \tau_k)}{\sin(\alpha_1 - \tau_k)}\right)^2 \Big[2\cos(\tau_k)\sin(\alpha_1 - \tau_k)\sin(\alpha_1 + \alpha_2 - 2\tau_k) \\
&\qquad - 2\cos(\alpha_1 + \alpha_2 - 2\tau_k)\cos(\alpha_1 - 2\tau_k)\Big] \\
&\quad + \left(\frac{\sin(\alpha_2 - \tau_k)}{\sin(\alpha_1 - \tau_k)}\right)\Big[-\cos(\alpha_1 - 2\tau_k) - \sin(\alpha_2)\sin(\alpha_1 + \alpha_2 - 2\tau_k)\Big] \\
&\qquad - \left(\frac{\cos(k\pi)\sin(\alpha_1 + \alpha_2 - 2\tau_k)}{\sin(\alpha_1 - \tau_k)}\right)\cos(k\pi)\cos(\tau_k)\Bigg\},
\end{aligned}
\tag{C.54}
$$

where

$$
K = \frac{1}{P} = \frac{-\sin(\alpha_1 - \tau_k)}{\cos(k\pi)\sin(\alpha_1 + \alpha_2 - 2\tau_k)}. \tag{C.55}
$$

Then factoring out $\frac{-1}{\sin^3(\alpha_1 - \tau_k)}$ from the term in braces, and letting

$$
K_1 = \left(\frac{1}{P}\right)\left(\frac{-1}{\sin^3(\alpha_1 - \tau_k)}\right) = \frac{1}{\cos(k\pi)\sin^2(\alpha_1 - \tau_k)\sin(\alpha_1 + \alpha_2 - 2\tau_k)}, \tag{C.56}
$$

we have

$$
\begin{aligned}
\frac{\partial g_1}{\partial \theta_2} = K_1\Bigg\{ &\underline{\sin^3(\alpha_2 - \tau_k)\cos(\alpha_1 - 2\tau_k)} \\
&- 2\cos(\tau_k)\sin^2(\alpha_1 - \tau_k)\sin^2(\alpha_2 - \tau_k)\sin(\alpha_1 + \alpha_2 - 2\tau_k) \\
&+ \underline{2\sin(\alpha_1 - \tau_k)\sin^2(\alpha_2 - \tau_k)\cos(\alpha_1 + \alpha_2 - 2\tau_k)\cos(\alpha_1 - 2\tau_k)} \\
&+ \underline{\sin^2(\alpha_1 - \tau_k)\sin(\alpha_2 - \tau_k)\cos(\alpha_1 - 2\tau_k)} \\
&+ \sin^2(\alpha_1 - \tau_k)\sin(\alpha_2 - \tau_k)\sin(\alpha_2 - \tau_k + \tau_k)\sin(\alpha_1 + \alpha_2 - 2\tau_k) \\
&+ \sin^2(\alpha_1 - \tau_k)\cos(\tau_k)\sin(\alpha_1 + \alpha_2 - 2\tau_k)\Bigg\} \\
= K_1\Bigg\{ &\underline{\sin(\alpha_2 - \tau_k)\cos(\alpha_1 - 2\tau_k)\Big[\sin^2(\alpha_2 - \tau_k) + \sin^2(\alpha_1 - \tau_k)}
\end{aligned}
$$

$$\underline{+2\sin(\alpha_1-\tau_k)\sin(\alpha_2-\tau_k)\cos(\alpha_1+\alpha_2-2\tau_k)\Big]}$$

$$+\sin^2(\alpha_1-\tau_k)\sin(\alpha_1+\alpha_2-2\tau_k)\Big[-2\cos(\tau_k)\sin^2(\alpha_2-\tau_k)+\cos(\tau_k)$$

$$+\sin(\alpha_2-\tau_k)\Big(\sin(\alpha_2-\tau_k)\cos(\tau_k)+\cos(\alpha_2-\tau_k)\sin(\tau_k)\Big)\Big]\Bigg\},$$

$$\tag{C.57}$$

where we have used underlining to indicate terms which were grouped and simplified in proceeding from the first equality to the second equality. We can apply (C.51) to the term in the first set of brackets, and the second set of brackets simplifies to

$$\begin{aligned}
&-\cos(\tau_k)\sin^2(\alpha_2-\tau_k)+\cos(\tau_k)+\sin(\alpha_2-\tau_k)\cos(\alpha_2-\tau_k)\sin(\tau_k)\\
&=\cos(\tau_k)\cos^2(\alpha_2-\tau_k)+\sin(\alpha_2-\tau_k)\cos(\alpha_2-\tau_k)\sin(\tau_k)\\
&=\cos(\alpha_2-\tau_k)\Big(\cos(\alpha_2-\tau_k)\cos(\tau_k)+\sin(\alpha_2-\tau_k)\sin(\tau_k)\Big),
\end{aligned}\tag{C.58}$$

and hence (C.57) simplifies to

$$\begin{aligned}
\frac{\partial g_1}{\partial \theta_2}=K_2\Bigg\{&\sin(\alpha_2-\tau_k)\cos(\alpha_1-2\tau_k)\sin(\alpha_1+\alpha_2-2\tau_k)\\
&+\sin^2(\alpha_1-\tau_k)\cos(\alpha_2-\tau_k)\Big(\cos(\alpha_2-\tau_k)\cos(\tau_k)+\sin(\alpha_2-\tau_k)\sin(\tau_k)\Big)\Bigg\},
\end{aligned}\tag{C.59}$$

where we have factored out $\sin(\alpha_1+\alpha_2-2\tau_k)$ and defined

$$K_2=\sin(\alpha_1+\alpha_2-2\tau_k)K_1=\frac{1}{\cos(k\pi)\sin^2(\alpha_1-\tau_k)}.\tag{C.60}$$

We further simplify (C.59) by expanding $\cos(\alpha_1-2\tau_k)$ and grouping coefficients of

$\cos(\tau_k)$ and $\sin(\tau_k)$, arriving at

$$\begin{aligned}
\frac{\partial g_1}{\partial \theta_2} &= K_2\Bigg\{\sin(\alpha_2-\tau_k)\sin(\alpha_1+\alpha_2-2\tau_k)\Big(\cos(\alpha_1-\tau_k)\cos(\tau_k)+\sin(\alpha_1-\tau_k)\sin(\tau_k)\Big)\\
&\qquad + \sin^2(\alpha_1-\tau_k)\cos(\alpha_2-\tau_k)\Big(\cos(\alpha_2-\tau_k)\cos(\tau_k)+\sin(\alpha_2-\tau_k)\sin(\tau_k)\Big)\Bigg\}\\
&= K_2\Bigg\{\cos(\tau_k)\Big[\sin(\alpha_1+\alpha_2-2\tau_k)\sin(\alpha_2-\tau_k)\cos(\alpha_1-\tau_k)\\
&\qquad\qquad + \sin^2(\alpha_1-\tau_k)\cos^2(\alpha_2-\tau_k)\Big]\\
&\qquad + \sin(\tau_k)\sin(\alpha_1-\tau_k)\sin(\alpha_2-\tau_k)\Big[\sin(\alpha_1+\alpha_2-2\tau_k)\\
&\qquad\qquad + \sin(\alpha_1-\tau_k)\cos(\alpha_2-\tau_k)\Big]\Bigg\}\\
&= K_2\Bigg\{\cos(\tau_k)\Big[\sin^2(\alpha_2-\tau_k)\cos^2(\alpha_1-\tau_k)+\sin^2(\alpha_1-\tau_k)\cos^2(\alpha_2-\tau_k)\\
&\qquad\qquad + \sin(\alpha_1-\tau_k)\sin(\alpha_2-\tau_k)\cos(\alpha_1-\tau_k)\cos(\alpha_2-\tau_k)\Big]\\
&\qquad + \sin(\tau_k)\sin(\alpha_1-\tau_k)\sin(\alpha_2-\tau_k)\Big[\sin(\alpha_1+\alpha_2-2\tau_k)\\
&\qquad\qquad + \sin(\alpha_1-\tau_k)\cos(\alpha_2-\tau_k)\Big]\Bigg\},
\end{aligned} \tag{C.61}$$

where we have progressed from the second to the third equality in (C.61) by expanding $\sin(\alpha_1+\alpha_2-2\tau_k)$ and multiplying out. Then applying[2] (C.51) to the first bracket term and defining

$$\begin{aligned}
D &= \sin^2(\alpha_1+\alpha_2-2\tau_k)-\sin(\alpha_1-\tau_k)\sin(\alpha_2-\tau_k)\cos(\alpha_1-\tau_k)\cos(\alpha_2-\tau_k),\\
C &= \sin(\alpha_1-\tau_k)\sin(\alpha_2-\tau_k),\\
S_1 &= \sin(\alpha_1+\alpha_2-2\tau_k)+\sin(\alpha_1-\tau_k)\cos(\alpha_2-\tau_k),
\end{aligned} \tag{C.62}$$

[2]This step is made clear by comparing the third equality in (C.51) with the first bracket term of (C.61).

we have

$$\frac{\partial g_1}{\partial \theta_2} = \frac{\cos(\tau_k)D + \sin(\tau_k)CS_1}{\cos(k\pi)\sin^2(\alpha_1 - \tau_k)}. \tag{C.63}$$

Now to derive the $(1, 2)$ element of the Jacobian matrix, we substitute (C.48), (C.49), and the simplifying terms (C.52) and (C.53) into (3.65) to obtain

$$\begin{aligned}
\frac{\partial g_1}{\partial \tilde{\lambda}} = L\Bigg\{ & 4\left(\frac{\sin(\alpha_2 - \tau_k)}{\sin(\alpha_1 - \tau_k)}\right)^2 \cos(\tau_k)\sin(\alpha_1 - \tau_k) \\
& - \left(\frac{\sin(\alpha_2 - \tau_k)}{\sin(\alpha_1 - \tau_k)}\right)\Big[\sin(\alpha_2) - 6\cos(\tau_k)\sin(\alpha_1 - \tau_k)\cos(\alpha_1 + \alpha_2 - 2\tau_k)\Big] \\
& - \sin(\alpha_2)\cos(\alpha_1 + \alpha_2 - 2\tau_k) + 2\cos(\tau_k)\sin(\alpha_1 - \tau_k) \\
& + \left(\frac{\cos(k\pi)\sin(\alpha_1 + \alpha_2 - 2\tau_k)}{\sin(\alpha_1 - \tau_k)}\right)\sin(\alpha_3)\Bigg\} \\
= \frac{L}{\sin(\alpha_1 - \tau_k)}\Bigg\{ & 4\sin^2(\alpha_2 - \tau_k)\cos(\tau_k) \\
& - \sin(\alpha_2 - \tau_k)\Big[\sin(\alpha_2) - 6\cos(\tau_k)\sin(\alpha_1 - \tau_k)\cos(\alpha_1 + \alpha_2 - 2\tau_k)\Big] \\
& - \sin(\alpha_2)\sin(\alpha_1 - \tau_k)\cos(\alpha_1 + \alpha_2 - 2\tau_k) + 2\cos(\tau_k)\sin^2(\alpha_1 - \tau_k) \\
& + \cos(k\pi)\sin(\alpha_1 + \alpha_2 - 2\tau_k)\sin(\alpha_3)\Bigg\},
\end{aligned} \tag{C.64}$$

where

$$L = \frac{e^{\tilde{\lambda}}}{P} = \frac{-\sin(\alpha_2 - \tau_k)}{\cos(k\pi)\sin(\alpha_1 + \alpha_2 - 2\tau_k)}. \tag{C.65}$$

Then using the expansion

$$\sin(\alpha_i) = \sin\big((\alpha_i - \tau_k) + \tau_k\big) = \sin(\alpha_i - \tau_k)\cos(\tau_k) + \cos(\alpha_i - \tau_k)\sin(\tau_k) \tag{C.66}$$

for $\sin(\alpha_2)$ and $\sin(\alpha_3)$, we have

$$
\begin{aligned}
\frac{\partial g_1}{\partial \tilde{\lambda}} &= \frac{L}{\sin(\alpha_1-\tau_k)}\Bigg\{4\sin^2(\alpha_2-\tau_k)\cos(\tau_k)+2\cos(\tau_k)\sin^2(\alpha_1-\tau_k) \\
&\quad -\sin(\alpha_2-\tau_k)\Big[\sin(\alpha_2-\tau_k)\cos(\tau_k)+\cos(\alpha_2-\tau_k)\sin(\tau_k)\Big] \\
&\quad +6\cos(\tau_k)\sin(\alpha_1-\tau_k)\sin(\alpha_2-\tau_k)\cos(\alpha_1+\alpha_2-2\tau_k) \\
&\quad -\sin(\alpha_1-\tau_k)\cos(\alpha_1+\alpha_2-2\tau_k)\Big[\sin(\alpha_2-\tau_k)\cos(\tau_k)+\cos(\alpha_2-\tau_k)\sin(\tau_k)\Big] \\
&\quad +\cos(k\pi)\sin(\alpha_1+\alpha_2-2\tau_k)\Big[\sin(\alpha_3-\tau_k)\cos(\tau_k)+\cos(\alpha_3-\tau_k)\sin(\tau_k)\Big]\Bigg\} \\
&= \frac{L}{\sin(\alpha_1-\tau_k)}\Bigg\{3\sin^2(\alpha_2-\tau_k)\cos(\tau_k)+2\cos(\tau_k)\sin^2(\alpha_1-\tau_k) \\
&\quad -\sin(\alpha_2-\tau_k)\cos(\alpha_2-\tau_k)\sin(\tau_k) \\
&\quad +5\cos(\tau_k)\sin(\alpha_1-\tau_k)\sin(\alpha_2-\tau_k)\cos(\alpha_1+\alpha_2-2\tau_k) \\
&\quad -\sin(\alpha_1-\tau_k)\cos(\alpha_1+\alpha_2-2\tau_k)\cos(\alpha_2-\tau_k)\sin(\tau_k) \\
&\quad -\sin^2(\alpha_1+\alpha_2-2\tau_k)\cos(\tau_k)+\sin(\alpha_1+\alpha_2-2\tau_k)\cos(\alpha_1+\alpha_2-2\tau_k)\sin(\tau_k)\Bigg\},
\end{aligned}
\tag{C.67}
$$

where we have used the expanded forms of $\sin(\alpha_3-\tau_k)$ and $\cos(\alpha_3-\tau_k)$ from (C.53). We proceed by first grouping coefficients of $\cos(\tau_k)$ and $\sin(\tau_k)$ and then expanding $\cos(\alpha_1+\alpha_2-2\tau_k)$ terms, as follows:

$$
\begin{aligned}
\frac{\partial g_1}{\partial \tilde{\lambda}} &= \frac{L}{\sin(\alpha_1-\tau_k)}\Bigg\{\cos(\tau_k)\Big[3\sin^2(\alpha_2-\tau_k)+2\sin^2(\alpha_1-\tau_k) \\
&\qquad -\sin^2(\alpha_1+\alpha_2-2\tau_k)+5\sin(\alpha_1-\tau_k)\sin(\alpha_2-\tau_k)\cos(\alpha_1+\alpha_2-2\tau_k)\Big] \\
&\quad -\sin(\tau_k)\Big[\sin(\alpha_2-\tau_k)\cos(\alpha_2-\tau_k)-\sin(\alpha_1+\alpha_2-2\tau_k)\cos(\alpha_1+\alpha_2-2\tau_k) \\
&\qquad +\cos(\alpha_2-\tau_k)\sin(\alpha_1-\tau_k)\cos(\alpha_1+\alpha_2-2\tau_k)\Big]\Bigg\}
\end{aligned}
$$

$$
\begin{aligned}
&= \frac{L}{\sin(\alpha_1-\tau_k)}\Bigg\{\cos(\tau_k)\Bigg[\bigg(3\sin^2(\alpha_2-\tau_k)+2\sin^2(\alpha_1-\tau_k)\\
&\quad -\sin^2(\alpha_1+\alpha_2-2\tau_k)-5\sin^2(\alpha_1-\tau_k)\sin^2(\alpha_2-\tau_k)\\
&\quad +5\sin(\alpha_1-\tau_k)\sin(\alpha_2-\tau_k)\cos(\alpha_1-\tau_k)\cos(\alpha_2-\tau_k)\bigg)\Bigg]\\
&\quad -\sin(\tau_k)\Big[\sin(\alpha_2-\tau_k)\cos(\alpha_2-\tau_k)-\sin(\alpha_1+\alpha_2-2\tau_k)\cos(\alpha_1+\alpha_2-2\tau_k)\\
&\quad +\cos^2(\alpha_2-\tau_k)\cos(\alpha_1-\tau_k)\sin(\alpha_1-\tau_k)\\
&\quad -\cos(\alpha_2-\tau_k)\sin^2(\alpha_1-\tau_k)\sin(\alpha_2-\tau_k)\Big]\Bigg\}\\
&= \frac{L}{\sin(\alpha_1-\tau_k)}\Bigg\{\cos(\tau_k)\Big[\underline{3\sin^2(\alpha_2-\tau_k)\cos^2(\alpha_1-\tau_k)+2\sin^2(\alpha_1-\tau_k)\cos^2(\alpha_2-\tau_k)}\\
&\quad \underline{+5\sin(\alpha_1-\tau_k)\sin(\alpha_2-\tau_k)\cos(\alpha_1-\tau_k)\cos(\alpha_2-\tau_k)}-\sin^2(\alpha_1+\alpha_2-2\tau_k)\Big]\\
&\quad -\sin(\tau_k)\Big[-\sin(\alpha_1+\alpha_2-2\tau_k)\cos(\alpha_1+\alpha_2-2\tau_k)\\
&\quad +\underline{\cos^2(\alpha_2-\tau_k)\cos(\alpha_1-\tau_k)\sin(\alpha_1-\tau_k)}\\
&\quad \underline{+\cos(\alpha_2-\tau_k)\cos^2(\alpha_1-\tau_k)\sin(\alpha_2-\tau_k)}\Big]\Bigg\}. \qquad \text{(C.68)}
\end{aligned}
$$

Then noting that the first underlined term simplifies to

$$
\begin{aligned}
&\Big[\sin(\alpha_2-\tau_k)\cos(\alpha_1-\tau_k)+\sin(\alpha_1-\tau_k)\cos(\alpha_2-\tau_k)\Big]\times\\
&\quad\Big[3\sin(\alpha_2-\tau_k)\cos(\alpha_1-\tau_k)+2\sin(\alpha_1-\tau_k)\cos(\alpha_2-\tau_k)\Big]\\
&= \sin(\alpha_1+\alpha_2-2\tau_k)\Big[2\sin(\alpha_1+\alpha_2-2\tau_k)+\sin(\alpha_2-\tau_k)\cos(\alpha_1-\tau_k)\Big] \qquad \text{(C.69)}
\end{aligned}
$$

and the second underlined term simplifies to

$$
\begin{aligned}
&\cos(\alpha_1-\tau_k)\cos(\alpha_2-\tau_k)\Big[\sin(\alpha_1-\tau_k)\cos(\alpha_2-\tau_k)+\sin(\alpha_2-\tau_k)\cos(\alpha_1-\tau_k)\Big]\\
&= \cos(\alpha_1-\tau_k)\cos(\alpha_2-\tau_k)\sin(\alpha_1+\alpha_2-2\tau_k), \qquad \text{(C.70)}
\end{aligned}
$$

we have

$$
\begin{aligned}
\frac{\partial g_1}{\partial \tilde{\lambda}} &= \frac{L}{\sin(\alpha_1-\tau_k)}\Bigg\{\cos(\tau_k)\sin(\alpha_1+\alpha_2-2\tau_k)\Big[\sin(\alpha_1+\alpha_2-2\tau_k) \\
&\qquad\quad + \sin(\alpha_2-\tau_k)\cos(\alpha_1-\tau_k)\Big] \\
&\quad - \sin(\tau_k)\Big[-\sin(\alpha_1+\alpha_2-2\tau_k)\cos(\alpha_1+\alpha_2-2\tau_k) \\
&\qquad\quad + \cos(\alpha_1-\tau_k)\cos(\alpha_2-\tau_k)\sin(\alpha_1+\alpha_2-2\tau_k)\Big]\Bigg\} \\
&= \frac{L\sin(\alpha_1+\alpha_2-2\tau_k)}{\sin(\alpha_1-\tau_k)}\Bigg\{\cos(\tau_k)\Big[\sin(\alpha_1+\alpha_2-2\tau_k)+\sin(\alpha_2-\tau_k)\cos(\alpha_1-\tau_k)\Big] \\
&\quad + \sin(\tau_k)\Big[\cos(\alpha_1+\alpha_2-2\tau_k)-\cos(\alpha_1-\tau_k)\cos(\alpha_2-\tau_k)\Big]\Bigg\} \\
&= \frac{-\sin(\alpha_2-\tau_k)}{\cos(k\pi)\sin(\alpha_1-\tau_k)}\Big(\cos(\tau_k)S_2-\sin(\tau_k)C\Big), \qquad \text{(C.71)}
\end{aligned}
$$

where

$$
S_2 = \sin(\alpha_1+\alpha_2-2\tau_k)+\sin(\alpha_2-\tau_k)\cos(\alpha_1-\tau_k), \qquad \text{(C.72)}
$$

and C is as defined in (C.62).

Substituting equilibrium values into the $(2,1)$ element of the Jacobian matrix, given by (3.66), yields

$$
\begin{aligned}
\frac{\partial g_2}{\partial \theta_2} &= K\Bigg\{-\left(\frac{\sin(\alpha_2-\tau_k)}{\sin(\alpha_1-\tau_k)}\right)^3\sin(\alpha_1-2\tau_k) \\
&\quad + \left(\frac{\sin(\alpha_2-\tau_k)}{\sin(\alpha_1-\tau_k)}\right)^2\Big[-2\sin(\tau_k)\sin(\alpha_1-\tau_k)\sin(\alpha_1+\alpha_2-2\tau_k) \\
&\qquad - 2\cos(\alpha_1+\alpha_2-2\tau_k)\sin(\alpha_1-2\tau_k)\Big] \\
&\qquad - \left(\frac{\sin(\alpha_2-\tau_k)}{\sin(\alpha_1-\tau_k)}\right)\Big[\sin(\alpha_1-2\tau_k)+\cos(\alpha_2)\sin(\alpha_1+\alpha_2-2\tau_k)\Big]
\end{aligned}
$$

$$+\left(\frac{\cos(k\pi)\sin(\alpha_1+\alpha_2-2\tau_k)}{\sin(\alpha_1-\tau_k)}\right)\cos(k\pi)\sin(\tau_k)\Bigg\}, \tag{C.73}$$

where K is as defined by (C.55). Then factoring out $\frac{-1}{\sin^3(\alpha_1-\tau_k)}$ from the term in braces, and defining K_1 as in (C.56), we have

$$\begin{aligned}
\frac{\partial g_2}{\partial \theta_2} = K_1\Bigg\{ & \underline{\sin^3(\alpha_2-\tau_k)\sin(\alpha_1-2\tau_k)} \\
& + 2\sin(\tau_k)\sin^2(\alpha_1-\tau_k)\sin^2(\alpha_2-\tau_k)\sin(\alpha_1+\alpha_2-2\tau_k) \\
& + \underline{2\sin(\alpha_1-\tau_k)\sin^2(\alpha_2-\tau_k)\cos(\alpha_1+\alpha_2-2\tau_k)\sin(\alpha_1-2\tau_k)} \\
& + \underline{\sin^2(\alpha_1-\tau_k)\sin(\alpha_2-\tau_k)\sin(\alpha_1-2\tau_k)} \\
& + \sin^2(\alpha_1-\tau_k)\sin(\alpha_2-\tau_k)\cos(\alpha_2-\tau_k+\tau_k)\sin(\alpha_1+\alpha_2-2\tau_k) \\
& - \sin^2(\alpha_1-\tau_k)\sin(\tau_k)\sin(\alpha_1+\alpha_2-2\tau_k)\Bigg\} \\
= K_1\Bigg\{ & \underline{\sin(\alpha_2-\tau_k)\sin(\alpha_1-2\tau_k)\Big[\sin^2(\alpha_2-\tau_k)+\sin^2(\alpha_1-\tau_k)} \\
& \underline{+2\sin(\alpha_1-\tau_k)\sin(\alpha_2-\tau_k)\cos(\alpha_1+\alpha_2-2\tau_k)\Big]} \\
& + \sin^2(\alpha_1-\tau_k)\sin(\alpha_1+\alpha_2-2\tau_k)\Big[2\sin(\tau_k)\sin^2(\alpha_2-\tau_k)-\sin(\tau_k) \\
& + \sin(\alpha_2-\tau_k)\Big(\cos(\alpha_2-\tau_k)\cos(\tau_k)-\sin(\alpha_2-\tau_k)\sin(\tau_k)\Big)\Big]\Bigg\}.
\end{aligned} \tag{C.74}$$

The term in the first set of brackets simplifies by application of (C.51), and the second set of brackets simplifies to

$$\begin{aligned}
& \sin(\tau_k)\sin^2(\alpha_2-\tau_k)-\sin(\tau_k)+\sin(\alpha_2-\tau_k)\cos(\alpha_2-\tau_k)\cos(\tau_k) \\
& = -\sin(\tau_k)\cos^2(\alpha_2-\tau_k)+\sin(\alpha_2-\tau_k)\cos(\alpha_2-\tau_k)\cos(\tau_k) \\
& = \cos(\alpha_2-\tau_k)\Big(-\cos(\alpha_2-\tau_k)\sin(\tau_k)+\sin(\alpha_2-\tau_k)\cos(\tau_k)\Big),
\end{aligned} \tag{C.75}$$

and hence (C.74) simplifies to

$$\frac{\partial g_2}{\partial \theta_2} = K_2 \Bigg\{ \sin(\alpha_2 - \tau_k)\sin(\alpha_1 - 2\tau_k)\sin(\alpha_1 + \alpha_2 - 2\tau_k) + \sin^2(\alpha_1 - \tau_k)\cos(\alpha_2 - \tau_k)\Big(-\cos(\alpha_2 - \tau_k)\sin(\tau_k) + \sin(\alpha_2 - \tau_k)\cos(\tau_k)\Big)\Bigg\}, \tag{C.76}$$

where we have factored out $\sin(\alpha_1 + \alpha_2 - 2\tau_k)$ and defined K_2 as in (C.60). Then expanding the $\sin(\alpha_1 - 2\tau_k)$ term and grouping coefficients of $\cos(\tau_k)$ and $\sin(\tau_k)$, we have

$$\begin{aligned}\frac{\partial g_2}{\partial \theta_2} &= K_2 \Bigg\{ \sin(\alpha_2 - \tau_k)\sin(\alpha_1 + \alpha_2 - 2\tau_k)\Big(\sin(\alpha_1 - \tau_k)\cos(\tau_k) - \cos(\alpha_1 - \tau_k)\sin(\tau_k)\Big) \\ &\quad + \sin^2(\alpha_1 - \tau_k)\cos(\alpha_2 - \tau_k)\Big(-\cos(\alpha_2 - \tau_k)\sin(\tau_k) + \sin(\alpha_2 - \tau_k)\cos(\tau_k)\Big)\Bigg\} \\ &= K_2 \Bigg\{ \cos(\tau_k)\sin(\alpha_1 - \tau_k)\sin(\alpha_2 - \tau_k)\Big[\sin(\alpha_1 + \alpha_2 - 2\tau_k) \\ &\qquad + \sin(\alpha_1 - \tau_k)\cos(\alpha_2 - \tau_k)\Big] \\ &\quad - \sin(\tau_k)\Big[\sin(\alpha_1 + \alpha_2 - 2\tau_k)\sin(\alpha_2 - \tau_k)\cos(\alpha_1 - \tau_k) \\ &\qquad + \sin^2(\alpha_1 - \tau_k)\cos^2(\alpha_2 - \tau_k)\Big]\Bigg\},\end{aligned} \tag{C.77}$$

and by comparison with the second equality in (C.61), we see that

$$\frac{\partial g_2}{\partial \theta_2} = \frac{\cos(\tau_k) C S_1 - \sin(\tau_k) D}{\cos(k\pi)\sin^2(\alpha_1 - \tau_k)}. \tag{C.78}$$

We complete our Jacobian calculation by evaluating the $(2, 2)$ element, given by (3.67). Substituting (C.48), (C.49), and the simplifying terms (C.52) and (C.53) into (3.67), we have

$$\begin{aligned}
\frac{\partial g_2}{\partial \tilde{\lambda}} &= L\Bigg\{-4\left(\frac{\sin(\alpha_2-\tau_k)}{\sin(\alpha_1-\tau_k)}\right)^2 \sin(\tau_k)\sin(\alpha_1-\tau_k) \\
&\qquad -\left(\frac{\sin(\alpha_2-\tau_k)}{\sin(\alpha_1-\tau_k)}\right)\Big[\cos(\alpha_2)+6\sin(\tau_k)\sin(\alpha_1-\tau_k)\cos(\alpha_1+\alpha_2-2\tau_k)\Big] \\
&\qquad -\cos(\alpha_2)\cos(\alpha_1+\alpha_2-2\tau_k)-2\sin(\tau_k)\sin(\alpha_1-\tau_k) \\
&\qquad +\left(\frac{\cos(k\pi)\sin(\alpha_1+\alpha_2-2\tau_k)}{\sin(\alpha_1-\tau_k)}\right)\cos(\alpha_3)\Bigg\} \\
&= \frac{-L}{\sin(\alpha_1-\tau_k)}\Bigg\{4\sin^2(\alpha_2-\tau_k)\sin(\tau_k) \\
&\qquad +\sin(\alpha_2-\tau_k)\Big[\cos(\alpha_2)+6\sin(\tau_k)\sin(\alpha_1-\tau_k)\cos(\alpha_1+\alpha_2-2\tau_k)\Big] \\
&\qquad +\cos(\alpha_2)\sin(\alpha_1-\tau_k)\cos(\alpha_1+\alpha_2-2\tau_k)+2\sin(\tau_k)\sin^2(\alpha_1-\tau_k) \\
&\qquad -\cos(k\pi)\sin(\alpha_1+\alpha_2-2\tau_k)\cos(\alpha_3)\Bigg\},
\end{aligned} \tag{C.79}$$

where L is defined by (C.65). Applying the expansion

$$\cos(\alpha_i)=\cos\big((\alpha_i-\tau_k)+\tau_k\big)=\cos(\alpha_i-\tau_k)\cos(\tau_k)-\sin(\alpha_i-\tau_k)\sin(\tau_k) \tag{C.80}$$

to $\cos(\alpha_2)$ and $\cos(\alpha_3)$, we have

$$\begin{aligned}
\frac{\partial g_2}{\partial \tilde{\lambda}} &= \frac{-L}{\sin(\alpha_1-\tau_k)}\Bigg\{4\sin^2(\alpha_2-\tau_k)\sin(\tau_k)+2\sin(\tau_k)\sin^2(\alpha_1-\tau_k) \\
&\quad +\sin(\alpha_2-\tau_k)\Big[\cos(\alpha_2-\tau_k)\cos(\tau_k)-\sin(\alpha_2-\tau_k)\sin(\tau_k)\Big] \\
&\quad +6\sin(\tau_k)\sin(\alpha_1-\tau_k)\sin(\alpha_2-\tau_k)\cos(\alpha_1+\alpha_2-2\tau_k) \\
&\quad +\sin(\alpha_1-\tau_k)\cos(\alpha_1+\alpha_2-2\tau_k)\Big[\cos(\alpha_2-\tau_k)\cos(\tau_k)-\sin(\alpha_2-\tau_k)\sin(\tau_k)\Big] \\
&\quad -\cos(k\pi)\sin(\alpha_1+\alpha_2-2\tau_k)\Big[\cos(\alpha_3-\tau_k)\cos(\tau_k)-\sin(\alpha_3-\tau_k)\sin(\tau_k)\Big]\Bigg\} \\
&= \frac{-L}{\sin(\alpha_1-\tau_k)}\Bigg\{3\sin^2(\alpha_2-\tau_k)\sin(\tau_k)+2\sin(\tau_k)\sin^2(\alpha_1-\tau_k)
\end{aligned}$$

$$
\begin{aligned}
&+\sin(\alpha_2-\tau_k)\cos(\alpha_2-\tau_k)\cos(\tau_k)\\
&+5\sin(\tau_k)\sin(\alpha_1-\tau_k)\sin(\alpha_2-\tau_k)\cos(\alpha_1+\alpha_2-2\tau_k)\\
&+\sin(\alpha_1-\tau_k)\cos(\alpha_1+\alpha_2-2\tau_k)\cos(\alpha_2-\tau_k)\cos(\tau_k)\\
&-\sin(\alpha_1+\alpha_2-2\tau_k)\cos(\alpha_1+\alpha_2-2\tau_k)\cos(\tau_k)-\sin^2(\alpha_1+\alpha_2-2\tau_k)\sin(\tau_k)\Bigg\},
\end{aligned}
\tag{C.81}
$$

where we have used the expanded forms of $\sin(\alpha_3-\tau_k)$ and $\cos(\alpha_3-\tau_k)$ from (C.53).

Grouping coefficients of $\cos(\tau_k)$ and $\sin(\tau_k)$, we have

$$
\begin{aligned}
\frac{\partial g_2}{\partial\tilde{\lambda}}=\frac{-L}{\sin(\alpha_1-\tau_k)}\Bigg\{&\sin(\tau_k)\Big[3\sin^2(\alpha_2-\tau_k)+2\sin^2(\alpha_1-\tau_k)\\
&+5\sin(\alpha_1-\tau_k)\sin(\alpha_2-\tau_k)\cos(\alpha_1+\alpha_2-2\tau_k)-\sin^2(\alpha_1+\alpha_2-2\tau_k)\Big]\\
&+\cos(\tau_k)\Big[\sin(\alpha_2-\tau_k)\cos(\alpha_2-\tau_k)-\sin(\alpha_1+\alpha_2-2\tau_k)\cos(\alpha_1+\alpha_2-2\tau_k)\\
&+\sin(\alpha_1-\tau_k)\cos(\alpha_1+\alpha_2-2\tau_k)\cos(\alpha_2-\tau_k)\Big]\Bigg\},
\end{aligned}
\tag{C.82}
$$

and by comparison with the first equality in (C.68), it follows by analogy that

$$
\frac{\partial g_2}{\partial\tilde{\lambda}}=\frac{\sin(\alpha_2-\tau_k)}{\cos(k\pi)\sin(\alpha_1-\tau_k)}\Big(\cos(\tau_k)C+\sin(\tau_k)S_2\Big).
\tag{C.83}
$$

Appendix D

Supplemental calculations for chapter 4 analysis of relative equilibria

Proof of Proposition 4.5.1:

Proof. ($\Rightarrow$) At a rectilinear relative equilibrium on $M_{CB(\mathbf{a})}$ we have ρ_i constant, $i = 1, 2, ..., n$, and therefore we can make the assignment $\sigma_i = \rho_i = |\mathbf{r}_{i,i+1}|$. Furthermore, by definition of a rectilinear relative equilibrium, there exists a unit vector $\mathbf{x}_{com}$ such that $\mathbf{x}_1 = \mathbf{x}_2 = \ldots = \mathbf{x}_n = \mathbf{x}_{com}$.

Note that the closure constraint

$$\sum_{i=1}^{n} \mathbf{r}_{i,i+1} = \mathbf{0} \tag{D.1}$$

always holds, implying that

$$0 = \mathbf{x}_{com} \cdot \sum_{i=1}^{n} \mathbf{r}_{i,i+1} = \sum_{i=1}^{n} \mathbf{x}_i \cdot \mathbf{r}_{i,i+1} = \sum_{i=1}^{n} |\mathbf{r}_{i,i+1}| \left(\mathbf{x}_i \cdot \frac{\mathbf{r}_{i,i+1}}{|\mathbf{r}_{i,i+1}|} \right) = \sum_{i=1}^{n} \sigma_i \; a_i, \tag{D.2}$$

where the last equality follows from the definition of $M_{CB(\mathbf{a})}$.

($\Leftarrow$) Assume that there exists a set of constants $\{\sigma_1, \sigma_2, \ldots, \sigma_n\}$ which satisfy the conditions of **Proposition 4.5.1**. Then a rectilinear relative equilibrium can be constructed as follows:

1. Place $\mathbf{r}_1$ at the origin with the frame $\{\mathbf{x}_1, \mathbf{y}_1, \mathbf{z}_1\}$ aligned with the coordinate frame.

2. Assign the positions and velocities of the remaining $n-1$ particles in an iterative fashion by

$$\mathbf{x}_i = \mathbf{x}_1, \ i = 2, 3, \ldots, n, \tag{D.3}$$

$$\mathbf{r}_{i+1} = \mathbf{r}_i + \sigma_i R_z(\alpha_i)\mathbf{x}_i, \ i = 1, 2, \ldots, n-1, \tag{D.4}$$

   where α_i is defined by $(\cos\alpha_i, \sin\alpha_i) = (-a_i, \sqrt{1-a_i^2})$ and $R_z(\alpha_i)$ is defined by

$$R_z(\alpha_i) = \begin{pmatrix} \cos(\alpha_i) & -\sin(\alpha_i) & 0 \\ \sin(\alpha_i) & \cos(\alpha_i) & 0 \\ 0 & 0 & 1 \end{pmatrix}. \tag{D.5}$$

We must show that our constructed state is on $M_{CB(\mathbf{a})}$ by demonstrating that $\mathbf{x}_i \cdot \frac{\mathbf{r}_{i,i+1}}{|\mathbf{r}_{i,i+1}|} = a_i, \ i = 1, 2, \ldots, n$. Using (D.4), we compute

$$\begin{aligned} \mathbf{x}_i \cdot \frac{\mathbf{r}_{i,i+1}}{|\mathbf{r}_{i,i+1}|} &= \mathbf{x}_i \cdot \frac{-\sigma_i R_z(\alpha_i)\mathbf{x}_i}{|\sigma_i R_z(\alpha_i)\mathbf{x}_i|} \\ &= -\mathbf{x}_i \cdot R_z(\alpha_i)\mathbf{x}_i \\ &= a_i, \ i = 1, 2, \ldots, n-1. \end{aligned} \tag{D.6}$$

This shows that the first $n-1$ particles are on $M_{CB(\mathbf{a})}$, and we must now show that $\mathbf{x}_n \cdot \frac{\mathbf{r}_{n,1}}{|\mathbf{r}_{n,1}|} = a_n$ also.

Summing up expressions (D.4), and substituting $\mathbf{x}_i = \mathbf{x}_1$ per (D.3), we have

$$\mathbf{r}_n = \left(\sum_{i=1}^{n-1} \sigma_i R_z(\alpha_i) \right) \mathbf{x}_1. \tag{D.7}$$

Since $\mathbf{r}_1$ is at the origin, we have

$$\mathbf{x}_n \cdot \frac{\mathbf{r}_{n,1}}{|\mathbf{r}_{n,1}|} = \mathbf{x}_n \cdot \frac{\mathbf{r}_n}{|\mathbf{r}_n|} = \mathbf{x}_1 \cdot \left(\frac{1}{\sigma_n} \sum_{i=1}^{n-1} \sigma_i R_z(\alpha_i) \right) \mathbf{x}_1 = \frac{1}{\sigma_n} \sum_{i=1}^{n-1} (-\sigma_i a_i) = a_n, \tag{D.8}$$

where the last step follows from the assumptions of the proposition. Therefore we conclude that the state lies in $M_{CB(\mathbf{a})}$, and since $\mathbf{x}_i = \mathbf{x}_1,\ i = 1, 2, \ldots, n$ implies that the state is at a rectilinear equilibrium, the proof is complete. □

Proof of Proposition 4.5.2:

Proof. (⇒) Suppose a circling equilibrium exists on $M_{CB(\mathbf{a})}$ and is restricted to a plane. By definition of $M_{CB(\mathbf{a})}$ we have $\mathbf{x}_i \cdot \frac{\mathbf{r}_{i,i+1}}{|\mathbf{r}_{i,i+1}|} = a_i,\ i = 1, 2, \ldots, n$, and without loss of generality, we assume that the circling equilibrium evolves in the horizontal plane. In **Remark 4.3.4** we demonstrated the relationship between the planar CB strategy (defined in section 2.3) and the 3-D CB pursuit strategy (**Definition 4.3.2**) restricted to the plane. In particular, we showed that for $i = 1, 2, \ldots, n$, if $\mathbf{x}_i \cdot \frac{\mathbf{r}_{i,i+1}}{|\mathbf{r}_{i,i+1}|} = a_i$ in the plane, then there exists α_i such that $\big(\cos(\alpha_i), \sin(\alpha_i)\big) = \left(-a_i, \pm\sqrt{1 - a_i^2}\right)$ and $R_z(\alpha_i)\mathbf{x}_i \cdot \frac{\mathbf{r}_{i,i+1}}{|\mathbf{r}_{i,i+1}|} = -1$. As discussed in **Remark 4.3.4**, the 3-D CB strategy does not prescribe a particular sign for the $\sin(\alpha_i)$, i.e., there are two discrete possibilities for each $\sin(\alpha_i)$. However, our previous analysis of *planar* circling equilibria in **Proposition 2.4.1** demonstrates that all the $\sin(\alpha_i)$ terms must have the same sign (i.e. $\sin(\alpha_i) = \sqrt{1 - a_i^2},\ i = 1, 2, \ldots, n$, or $\sin(\alpha_i) = -\sqrt{1 - a_i^2},\ i = 1, 2, \ldots, n$), must all be nonzero (i.e. $a_i \neq \pm 1$), and must satisfy $\sin\left(\sum_{i=1}^{n} \alpha_i\right) = 0$.

($\Leftarrow$) First, we observe that if all the vectors $\mathbf{x}_i, \mathbf{y}_i, \frac{\mathbf{r}_{i,i+1}}{|\mathbf{r}_{i,i+1}|},\ i = 1, 2, \ldots, n$ are coplanar on $M_{CB(\mathbf{a})}$, then they remain coplanar. This follows from (4.21), since

$$\begin{aligned}
\dot{\mathbf{z}}_i &= \frac{-1}{|\mathbf{r}_{i,i+1}|}\left[\mathbf{y}_i \cdot \left(\dot{\mathbf{r}}_{i,i+1} \times \frac{\mathbf{r}_{i,i+1}}{|\mathbf{r}_{i,i+1}|}\right)\right]\mathbf{x}_i \\
&= \frac{-1}{|\mathbf{r}_{i,i+1}|}\left[\mathbf{y}_i \cdot \left(\left(\mathbf{x}_i - \mathbf{x}_{i+1}\right) \times \frac{\mathbf{r}_{i,i+1}}{|\mathbf{r}_{i,i+1}|}\right)\right]\mathbf{x}_i \\
&= 0
\end{aligned} \tag{D.9}$$

if $\mathbf{x}_i, \mathbf{y}_i, \frac{\mathbf{r}_{i,i+1}}{|\mathbf{r}_{i,i+1}|},\ i = 1, 2, \ldots, n$ are all coplanar. Therefore, given $\{a_1, a_2, \ldots, a_n\}$ satisfying the conditions of the proposition, we define α_i as in the statement of the proposition and construct our circling equilibrium in the horizontal plane as follows:

1. Place $\mathbf{r}_1$ on the horizontal axis with $|\mathbf{r}_1| = r_{com} > 0$ and assign the positions of the remaining $n-1$ particles by

$$\mathbf{r}_i = R_z\left(2\sum_{k=1}^{i-1} \alpha_k\right)\mathbf{r}_1,\ i = 2, 3, \ldots, n. \tag{D.10}$$

2. Specify the velocities by

$$\mathbf{x}_i = R_z\left(\frac{\pi}{2}\right)\frac{\mathbf{r}_i}{|\mathbf{r}_i|},\ i = 1, 2, \ldots, n. \tag{D.11}$$

Then by calculations analogous to the planar analysis already presented, one can readily demonstrate that this represents a planar circling equilibrium. $\square$

Appendix E

Supplemental calculations for chapter 6 analysis of relative equilibria

Derivation of (6.37): We first note that straightforward calculation yields

$$\frac{\partial\omega}{\partial\kappa_p} = \bar{\nu}\cos(\kappa_p), \quad \frac{\partial\omega}{\partial\kappa_e} = \cos(\kappa_e), \quad \frac{\partial\omega}{\partial\rho} = 0$$
$$\frac{\partial\eta}{\partial\kappa_p} = \bar{\nu}\sin(\kappa_p), \quad \frac{\partial\eta}{\partial\kappa_e} = \sin(\kappa_e), \quad \frac{\partial\eta}{\partial\rho} = 0. \tag{E.1}$$

Then defining

$$f_1(\kappa_p,\kappa_e,\rho) \triangleq \dot{\kappa}_p = \omega\left(-\mu_p\bar{\nu} + \frac{1}{\rho}\right),$$
$$f_2(\kappa_p,\kappa_e,\rho) \triangleq \dot{\kappa}_e = \mu_e\sin(\kappa_e) + \omega\left(2\mu_e\cos(\kappa_e) + \frac{1}{\rho}\right),$$
$$f_3(\kappa_p,\kappa_e,\rho) \triangleq \dot{\rho} = \eta, \tag{E.2}$$

we have

$$\frac{\partial f_1}{\partial\kappa_p} = \left(\frac{\partial\omega}{\partial\kappa_p}\right)\left(-\mu_p\bar{\nu} + \frac{1}{\rho}\right) = \bar{\nu}\cos(\kappa_p)\left(-\mu_p\bar{\nu} + \frac{1}{\rho}\right),$$
$$\frac{\partial f_1}{\partial\kappa_e} = \left(\frac{\partial\omega}{\partial\kappa_e}\right)\left(-\mu_p\bar{\nu} + \frac{1}{\rho}\right) = \cos(\kappa_e)\left(-\mu_p\bar{\nu} + \frac{1}{\rho}\right),$$
$$\frac{\partial f_1}{\partial\rho} = -\frac{\omega}{\rho^2},$$

$$\tag{E.3}$$

as well as

$$\begin{aligned}
\frac{\partial f_2}{\partial \kappa_p} &= \left(\frac{\partial \omega}{\partial \kappa_p}\right)\left(2\mu_e \cos(\kappa_e) + \frac{1}{\rho}\right) = \bar{\nu}\cos(\kappa_p)\left(2\mu_e \cos(\kappa_e) + \frac{1}{\rho}\right), \\
\frac{\partial f_2}{\partial \kappa_e} &= \mu_e \cos(\kappa_e) + \left(\frac{\partial \omega}{\partial \kappa_e}\right)\left(2\mu_e \cos(\kappa_e) + \frac{1}{\rho}\right) + \omega\left(-2\mu_e \sin(\kappa_e)\right) \\
&= \mu_e \cos(\kappa_e) + \cos(\kappa_e)\left(2\mu_e \cos(\kappa_e) + \frac{1}{\rho}\right) - 2\mu_e \omega \sin(\kappa_e) \\
&= \mu_e\Big(\cos(\kappa_e) + 2\cos^2(\kappa_e) - 2\omega\sin(\kappa_e)\Big) + \frac{\cos(\kappa_e)}{\rho} \\
\frac{\partial f_2}{\partial \rho} &= -\frac{\omega}{\rho^2},
\end{aligned} \tag{E.4}$$

and

$$\begin{aligned}
\frac{\partial f_3}{\partial \kappa_p} &= \left(\frac{\partial \eta}{\partial \kappa_p}\right) = \bar{\nu}\sin(\kappa_p), \\
\frac{\partial f_3}{\partial \kappa_e} &= \left(\frac{\partial \eta}{\partial \kappa_e}\right) = \sin(\kappa_e), \\
\frac{\partial f_3}{\partial \rho} &= 0.
\end{aligned} \tag{E.5}$$

Thus the Jacobian matrix associated with the linearization of (6.20) is given by

$$\left(\frac{\partial f}{\partial x}\right) = \begin{bmatrix} \bar{\nu}\cos(\kappa_p)\left(-\mu_p\bar{\nu} + \frac{1}{\rho}\right) & \cos(\kappa_e)\left(-\mu_p\bar{\nu} + \frac{1}{\rho}\right) & -\frac{\omega}{\rho^2} \\ \bar{\nu}\cos(\kappa_p)\left(2\mu_e\cos(\kappa_e) + \frac{1}{\rho}\right) & \frac{\partial f_2}{\partial \kappa_e} & -\frac{\omega}{\rho^2} \\ \bar{\nu}\sin(\kappa_p) & \sin(\kappa_e) & 0 \end{bmatrix}, \tag{E.6}$$

where $\frac{\partial f_2}{\partial \kappa_e} = \mu_e\Big(\cos(\kappa_e) + 2\cos^2(\kappa_e) - 2\omega\sin(\kappa_e)\Big) + \frac{\cos(\kappa_e)}{\rho}$.

Bibliography

[1] U. Alon. Network motifs: theory and experimental approaches. *Nature*, 8:450–461, 2007.

[2] R.C. Archibald and H.P. Manning. Remarks and historical notes [on the pursuit problem]. *Amer. Math. Monthly*, 28:91–93, 1921.

[3] H.C. Berg and D.A. Brown. Chemotaxis in *Escherichia coli* analyzed by three-dimensional tracking. *Nature*, 239:500–504, 1972.

[4] G. D. Birkhoff. The restricted problem of three bodies. *Rendi. Circ. Mat. Palermo*, 39:265–334, 1915.

[5] R.W. Brockett. *Lie algebras and Lie groups in control theory*, pages 43–82. in D. Q. Mayne and R. W. Brockett, Eds., Geometric Methods in System Theory. Reidel, Dordrecht, Holland, 1973.

[6] Roger Broucke, Antonio Elipe, and Andrés Riaguas. On the figure-8 periodic solutions in the three-body problem. *Chaos, Solitons and Fractals*, 30:513–520, 2006.

[7] A.M. Bruckstein. Why the ant trails look so straight and nice. *The Mathematical Intelligencer*, 15(2):59–62, 1993.

[8] A.M. Bruckstein, N. Cohen, and A. Efrat. Ants, crickets and frogs in cyclic pursuit. CIS Report #9105, Technion - Israel Institute of Technology, July 1991.

[9] J. Buhl, D.J.T. Sumpter, I.D. Couzin, J.J. Hale, E. Despland, E.R. Miller, and S.J. Simpson. From disorder to order in marching locusts. *Science*, 312:1402–1406, 2006.

[10] Alain Chenciner and Richard Montgomery. A remarkable periodic solution of the three-body problem in the case of equal masses. *Annals of Mathematics*, 152:881–901, 2000.

[11] T.S. Collett and M.F. Land. Visual control of flight behaviour in the hoverfly, *Syritta pipiens. J. comp. Physiol.*, 99:1–66, 1975.

[12] M.B. Elowitz and S. Leibler. A synthetic oscillatory network of transcriptional regulators. *Nature*, 403:335–338, 2000.

[13] M. Ballerini et al. Interaction ruling animal collective behavior depends on topological rather than metric distance: Evidence from a field study. *Proc. Natl Acad. Sci.*, 105:1232–1237, 2008.

[14] K.S. Galloway, E.W. Justh, and P.S. Krishnaprasad. Motion camouflage in a stochastic setting. *Proc. 46th IEEE Conf. Decision and Control*, pages 1652–1659, 2007.

[15] K.S. Galloway, E.W. Justh, and P.S. Krishnaprasad. Geometry of cyclic pursuit. *Proc. 48th IEEE Conf. Decision and Control*, pages 7485–7490, 2009. (See also extended version at http://www.isr.umd.edu/Labs/ISL/PURSUIT).

[16] K.S. Galloway, E.W. Justh, and P.S. Krishnaprasad. Cyclic pursuit in three dimensions. *Proc. 49th IEEE Conf. Decision and Control*, pages 7141–7146, 2010.

[17] K.S. Galloway, E.W. Justh, and P.S. Krishnaprasad. Portraits of cyclic pursuit. *to appear, Proc. 50th IEEE Conf. Decision and Control*, 2011.

[18] F.R. Gantmacher. *The theory of matrices, vol. 2*. Chelsea, New York, 1960.

[19] K. Ghose, T. Horiuchi, P.S. Krishnaprasad, and C. Moss. Echolocating bats use a nearly time-optimal strategy to intercept prey. *PLoS Biology*, 4(5):865–873, e108, 2006.

[20] P. Glendinning. The mathematics of motion camouflage. *Proc. Roy. Soc. Lond. B*, 271(1538):477–481, 2004.

[21] D. Husemoller. *Fibre Bundles*. Springer-Verlag, New York, 1975.

[22] Piers Ingram, Michael Stumpf, and Jaroslav Stark. Network motifs: structure does not determine function. *BMC Genomics*, 7:108, 2006.

[23] R. Isaacs. *Differential Games*. John Wiley and Sons, New York, 1965.

[24] A. Jadbabaie, J. Lin, and A.S. Morse. Coordination of groups of mobile autonomous agents using nearest neighbor rules. *IEEE Trans. Automat. Control*, 48(6):988–1001, 2003.

[25] E.W. Justh and P.S. Krishnaprasad. Equilibria and steering laws for planar formations. *Systems & Control Letters*, 52:25–38, 2004.

[26] E.W. Justh and P.S. Krishnaprasad. Natural frames and interacting particles in three dimensions. *Proc. 44th IEEE Conf. Decision and Control*, pages 2841–2846, 2005. (see also arXiv:math.OC/0503390v1).

[27] E.W. Justh and P.S. Krishnaprasad. Steering laws for motion camouflage. *Proc. R. Soc. A*, 462:3629–3643, 2006.

[28] D.G. Kendall. Shape manifolds, procrustean metrics, and complex projective spaces. *Bulletin of London Math. Society*, 16(2):81–121, 1984.

[29] H. K. Khalil. *Nonlinear Systems*. Prentice-Hall, New Jersey, third edition, 2002.

[30] M.S. Klamkin and D.J. Newman. Cyclic pursuit or "the three bugs problem". *The American Mathematical Monthly*, 78(6):631–639, 1971.

[31] P.S. Krishnaprasad and D.P. Tsakiris. Nonholonomic kinematic chains on lie groups. *Proc. 33rd IEEE Conf. Decision and Control*, pages 2955–2960, 1994.

[32] N.E. Leonard and E. Fiorelli. Virtual leaders, artificial potentials and coordinated control of groups. *Proc. 40th IEEE Conf. Decision and Control*, pages 2968–2973, 2001.

[33] Z. Lin, M.E. Broucke, and B.A. Francis. Local control strategies for groups of mobile autonomous agents. *IEEE Trans. Automat. Control*, 49(4):622–629, 2004.

[34] J. W. Lorimer. Curved paths in raptor flight: Deterministic models. *J. Theor. Biol.*, 242:880–889, 2006.

[35] J.E. Marsden and T.S. Ratiu. *Introduction to mechanics and symmetry.* Springer, New York, second edition, 1999.

[36] J.A. Marshall, M.E. Broucke, and B.A. Francis. Formations of vehicles in cyclic pursuit. *IEEE Trans. Automat. Control*, 49(11):1963–1974, 2004.

[37] J.A. Marshall, M.E. Broucke, and B.A. Francis. Pursuit formations of unicycles. *Automatica*, 42(1):3–12, 2006.

[38] R. Milo, S. Shen-Orr, S. Itzkovitz, N. Kashtan, D. Chklovskii, and U. Alon. Network motifs: simple building blocks of complex networks. *Science*, 298:824–827, 2002.

[39] M. Mischiati and P.S. Krishnaprasad. The dynamics of mutual motion camouflage. *submitted for publication*, 2011.

[40] M. Mischiati and P.S. Krishnaprasad. Mutual motion camouflage in 3D. *Proc. of the 18th IFAC World Congress, Part 1*, pages 4483–4488, 2011. (See also extended version at http://www.isr.umd.edu/Labs/ISL/PURSUIT).

[41] A.K. Mizutani, J.S. Chahl, and M.V. Srinivasan. Motion camouflage in dragonflies. *Nature*, 423:604, 2003.

[42] Richard Montgomery. A new solution to the three-body problem. *Notices Am. Math. Soc.*, 48:471–481, 2001.

[43] Richard M. Murray. Recent research in cooperative control of multivehicle systems. *J. Dyn. Sys., Meas., Control*, 129:571–583, 2007. doi:10.1115/1.2766721.

[44] J.H. Oh and I.J. Ha. Capturability of the 3-dimensional pure PNG law. *IEEE Trans. Aerospace. Electr. Syst.*, 35(2):491–503, 1999.

[45] Julia K. Parrish, Steven V. Viscido, and Daniel Grunbaum. Self-organized fish schools: an examination of emergent properties. *Biol. Bull.*, 202:296–305, 2002.

[46] M. Pavone and E. Frazzoli. Decentralized policies for geometric pattern formation and path coverage. *J. Dyn. Sys., Meas., Control*, 129(5):633–643, 2007. doi:10.1115/1.2767658.

[47] J. Ramirez-Riberos, M. Pavone, E. Frazzoli, and D. W. Miller. Distributed control of spacecraft formations via cyclic pursuit: theory and experiments. *Journal of Guidance, Control, and Dynamics*, 33(5):1655–1669, 2010.

[48] P.V. Reddy, E.W. Justh, and P.S. Krishnaprasad. Motion camouflage in three dimensions. *Proc. 45th IEEE Conf. Decision and Control*, pages 3327–3332, 2006. (see also arXiv:math.OC/0603176).

[49] P.V. Reddy, E.W. Justh, and P.S. Krishnaprasad. Motion camouflage with sensorimotor delay. *Proc. 46th IEEE Conf. Decision and Control*, pages 1660–1665, 2007.

[50] T.J. Richardson. Non-mutual captures in cyclic pursuit. *Annals of Mathematics and Artificial Intelligence*, 31:127–146, 2001.

[51] N.A. Shneydor. *Missile Guidance and Pursuit.* Horwood, Chichester, 1998.

[52] A. Sinha and D. Ghose. Generalization of nonlinear cyclic pursuit. *Automatica*, 43:1954–1960, 2007.

[53] S.L. Smith, M.E. Broucke, and B.A. Francis. A hierarchical cyclic pursuit scheme for vehicle networks. *Automatica*, 41(6):1045–1053, 2005.

[54] M.V. Srinivasan and M. Davey. Strategies for active camouflage of motion. *Proc. Roy. Soc. Lond. B*, 259(1354):19–25, 1995.

[55] V.A. Tucker, A.E. Tucker, K. Akers, and J.H. Enderson. Curved flight paths and sideways vision in peregrine falcons (*Falco peregrinus*). *J Exp Biol*, 203(24):3755–3763, 2000.

[56] L.S. Wang. *Geometry, Dynamics, and Control of Coupled Systems.* PhD thesis, University of Maryland, College Park, 1990.

[57] E. Wei, E.W. Justh, and P.S. Krishnaprasad. Pursuit and an evolutionary game. *Proc. R. Soc. A*, 465:1539–1559, 2009. First published online Feb.25, 2009, doi:10.1098/rspa.2008.0480.

[58] D.M. Wolf and A.P. Arkin. Motifs, modules and games in bacteria. *Current Opinion in Microbiology*, 6:125–134, 2003.

[59] Fumin Zhang. *Geometric Cooperative Control of Formations.* PhD thesis, University of Maryland, College Park, 2004.